



United States  
Department of  
Agriculture

Forest  
Service

Rocky Mountain  
Research  
Station

1221 S. Main Street  
Moscow, ID 83843

---

June 25, 1997

Dear LISA user:

We are happy to enclose a copy of the LISA and DLISA slope stability software you requested.

If you write a paper with more than a passing reference to either LISA or DLISA, we would appreciate your sending us the citation and a short description, and, if possible, a copy of the paper. We also would be happy to review any such papers before publication to ensure accuracy regarding LISA and DLISA.

In your publications, please reference the *software* as:

*Level I Stability Analysis Ver. 2.0* (LISA 2.0). January 1991. Moscow, ID: U.S. Department of Agriculture, Forest Service, Intermountain Research Station, Engineering Technology. Computer software.

*Deterministic Level I Stability Analysis Ver. 1.02* (DLISA 1.02). May 1991. Moscow, ID: U.S. Department of Agriculture, Forest Service, Intermountain Research Station, Engineering Technology. Computer software.

and the *manual* as:

Hammond, C.; Hall, D.; Miller, S.; Swetik, P. 1992. *Level I Stability Analysis (LISA) documentation for version 2.0*. Gen. Tech. Rep. INT-285. Ogden, UT: U.S. Department of Agriculture, Forest Service, Intermountain Research Station. 190 p.

If you have questions about LISA, please contact me:

David Hall, Programmer-Analyst  
U.S. Forest Service  
Rocky Mountain Research Station  
1221 South Main Street  
Moscow, ID 83843-4211 USA  
Internet: [dhall@forest.moscowfs1.wsu.edu](mailto:dhall@forest.moscowfs1.wsu.edu)  
FS Openmail: david hall/int,moscow

or check our web site:

<http://forest.moscowfs1.wsu.edu>  
<http://forest.moscowfs1.wsu.edu/4702/slope0.html>

If you distribute copies of LISA, please request that the new users notify us that they are using LISA so that we can notify them of updates or other important information.



Caring for the Land and Serving People

# *Level I Stability Analysis (LISA) documentation for version 2.0*

## **Hammond, Hall, Miller, Swetik**

---

### **Errata and clarifications sheet**

---

#### **Preliminaries**

- p. 3.-- "Level I stability analysis" under "LISA" should read "Level I Stability Analysis program"
- p. 4.-- "Stability analysis for road access" under "SARA" should read "Stability Analysis for Road Access program"
- p. 5.--  $\gamma$ -m,  $\gamma$ -d, and  $\gamma$ -max should be  $\gamma$ -sub-m,  $\gamma$ -sub-d, and  $\gamma$ -sub-max.
- 

#### **Part 1--Reference Manual**

- p. 22.-- The equation for the computed standard deviation of the logarithms of the values of X ( $\hat{\sigma}_l$ ) is incorrect. The x-squared term should be  $\bar{x}$ -squared.
- p. 31.-- In text of figure 3.1, the definition for  $\gamma$ -sub-d should be removed.
- p. 40.-- Paragraph 2, line 7: "This method produces correlation coefficient..." should read "This method produces a correlation coefficient..."
- p. 64.-- Section 5.3.5.2, paragraph 1, last line: "Bjerrum and Bjerrum 1960" should be "Bishop and Bjerrum 1961".
- p. 69.\*-- Section 5.3.5.2.2, last line: "Hammond and Hardcastle 1991" is actually "Hardcastle and Hammond 1991".
- p. 69.-- Section 5.3.5.3.1: "Bjerrum and Simons (1960)" should be "Bjerrum and Simons (1961)".
- p. 93.-- Table 6.2, polygon 5D: Pf range for natural state should be .08-.09 for a moderate hazard.
- p. 97.-- "Bjerrum, A.W.; Bjerrum, L. 1960." is actually "Bishop, A.W.; Bjerrum, L. 1961."
- p. 97.-- "Bjerrum, L.; Simons, N.E. 1960." should be "Bjerrum, L.; Simons, N.E. 1961."
- p. 99.\*-- "Hammond, C.J.; Hardcastle, J.H. 1992." may actually be "Hardcastle, J.H.; Hammond, C.J. 1991." 6 p. [or is it the big one?]
- p. 105.-- Tsukamoto & Kusakabe 1984: Should read "Vegetative influences...", not "Vegetation influences..."; publisher information should be "Honolulu, HI: Environment and Policy Institute, East-West Center".
- p. 105.-- Wu, McKinnell & Swanston 1979: Should be "landslides on Prince of Wales" not "landslides of Prince of

Wales"

- p. 109.-- Tsukamoto & Kusakabe 1984: Should read "Vegetative influences...", not "Vegetation influences..."; publisher information should be "Honolulu, HI: Environment and Policy Institute, East-West Center".
- p. 110.-- Wu, McKinnell & Swanston 1979: Should be "landslides on Prince of Wales" not "landslides of Prince of Wales"
- p. 110.-- "Bjerrum, A.W.; Bjerrum, L. 1960." is actually "Bishop, A.W.; Bjerrum, L. 1961."
- p. 110.-- "Bjerrum, L.; Simons, N.E. 1960." should be "Bjerrum, L.; Simons, N.E. 1961".
- p. 111.-- "Hammond, C.J.; Hardcastle, J.H. 1992." may actually be "Hardcastle, J.H.; Hammond, C.J. 1991." 6 p. [or is it the big one?]

---

### Part 2--Program Operation

- p. 144.-- Section 3.9: "Delete drive:\datapath\filename (y/N)?" should be "Erase drive:\datapath\filename? (y/N)"
- p. 185.-- Appendix B: Our software has not been referenced in the Software Reference Center.
- p. 186.-- Appendix C: It has been recommended that "D", not "d", should be used for soil depth in the equations on this page. A capital "D" is used elsewhere in the manual for soil depth, and the placement of a lower-case "d" following a gamma can lead to confusion ("Is that moist unit weight times soil depth, or dry unit weight?"). Change 10 occurrences of "gamma d" to "gamma D".

---

Web page contact: /s=d.hall/ou1=s22L04a@mhs-fswa.attmail.com  
File date: 5/8/95

United States  
Department  
of Agriculture

Forest Service

Intermountain  
Research Station

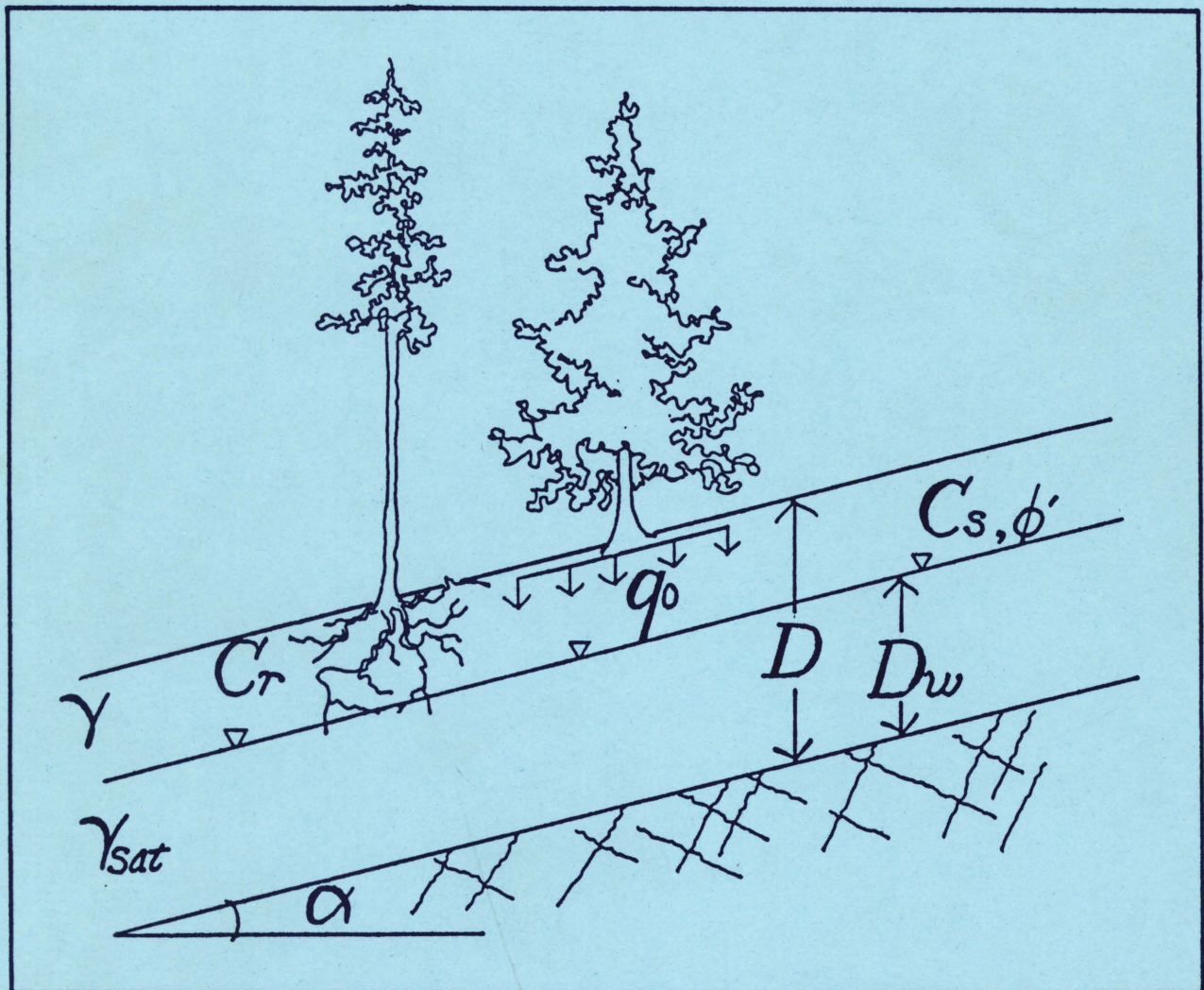
General Technical  
Report INT-285

April 1992



# Level I Stability Analysis (LISA) Documentation for Version 2.0

Carol Hammond  
David Hall  
Stanley Miller  
Paul Swetik



## THE AUTHORS

CAROL HAMMOND is a research engineer with the Intermountain Research Station, Forest Service, U.S. Department of Agriculture, Ogden, UT, located at the Forestry Sciences Laboratory, Moscow, ID.

DAVID HALL is a computer programmer analyst with the Intermountain Research Station, located at the Forestry Sciences Laboratory, Moscow, ID.

STANLEY MILLER is an associate professor, Department of Geology and Geological Engineering, University of Idaho, Moscow.

PAUL SWETIK is a systems analyst with the Intermountain Research Station, located at the Forestry Sciences Laboratory, Moscow, ID.

## DISCLAIMERS

The authors of LISA assume no liability or responsibility for the use of LISA, the interpretation of LISA results, or the consequences of management decisions that are based upon LISA results. In no event shall the authors be liable for any damages whatsoever arising out of the use of or inability to use LISA, even if the authors have been advised of the possibility of such damages or of problems with the software.

Efforts have been made to see that LISA is reliable, but it is a model of reality, not reality itself. The user should have a thorough understanding of the model and should compare results to actual field conditions.

No person, whether an individual or an employee of the Federal Government or any outside agency or corporation, may sell the LISA program for profit. The LISA program may be distributed as it is received, and a reasonable distribution fee may be charged for transferring the copy.

The use of trade or firm names in this publication is for reader information and does not imply endorsement by the U.S. Department of Agriculture of any product or service.

## ACKNOWLEDGMENTS

The development of LISA has been a team effort with many participants. Rod Prellwitz (Intermountain Research Station) recognized the need for and conceived the idea of a probabilistic Level I landslide hazard analysis using the infinite slope stability model. He played an integral role throughout the LISA program development. Gordon Booth (Intermountain Research Station) initially suggested the Monte Carlo approach to us. Dr. Terry Howard and Dr. Clarence Potratz (University of Idaho) and Dr. Henry Shovic (Gallatin National Forest) were involved in early LISA development. Several of our users, in particular the Gifford Pinchot National Forest geotechnical group, have contributed greatly by their efforts in applying LISA to field situations and effectively communicating the results to land managers. Their feedback to us during the development process has been enormously helpful and is much appreciated. We also appreciate the drafting of figure 5.7 by Karl Anderson, Gifford Pinchot National Forest.

## A CAVEAT

LISA is a *tool* to be used by investigators who have some knowledge and experience concerning landslide behavior and geotechnical properties of soils. It requires engineering judgment and common sense, both in developing input distributions and interpreting the results. It does not give a unique "right" answer. It is a tool to help the user understand slope stability processes, quantify observations and judgments, and document and communicate those observations and judgments to other geotechnical specialists and to land managers. Do not rely on LISA alone, but add it to your existing toolbox. Any answer that one desires can be obtained by altering the input data. Without rationally justifying the input used, and without correctly understanding and interpreting the output, LISA becomes little more than a game of numbers.

Furthermore, LISA does not provide a complete risk analysis. The consequences of slope failures (such as the potential for damage to timber and fisheries resources, roads or structures, or the potential for injury or loss of life) should be assessed by users.

## RESEARCH SUMMARY

The Level I Stability Analysis (LISA) computer program is a *tool* to help estimate the relative stability of natural slopes or landforms. LISA results are intended to support management decisions at the multi-project or resource allocation level of planning. The primary use of the probability of failure estimated using LISA is to make qualitative, relative comparisons between the stability of landforms, and to identify areas that should be targeted for additional analysis. LISA also can be used to estimate the relative decrease in stability of a landform after timber harvest due to a potential reduction in estimated tree root strength and an increase in groundwater levels. The probability of failure also can be used quantitatively in a risk analysis, such as an expected monetary value (EMV) decision analysis.

LISA uses the infinite slope stability model to compute the factor of safety against failure for a given set of *in situ* conditions. The factor of safety ( $FS$ ) is the ratio of the forces resisting a slope failure (tree root strength and soil shear strength) to the forces driving the failure (gravity). A slope with an  $FS$  greater than 1 is expected to be stable; a slope with an  $FS$  less than 1, unstable. The calculation of an  $FS$  with a single set of input values is called a *deterministic analysis*. However, it is recognized that there are variability in *in situ* conditions on a given slope or landform and many uncertainties in estimating input values for the variables in the

infinite slope equation. Therefore, LISA uses Monte Carlo simulation to estimate the *probability* of slope failure rather than a single  $FS$  value. Monte Carlo simulation is useful for modeling an attribute that cannot be sampled or measured directly. The  $FS$  is such an attribute. A large number of Monte Carlo passes (say 1,000) is made with repeated random samplings of possible input values and the calculation of a factor of safety for each pass. The end result is a histogram of the calculated factors of safety and the probability of failure. LISA calculates the probability of failure by dividing the total number of passes into the number of factors of safety less than or equal to 1.

It is common to view the probability of an event as the likelihood of the event occurring. This meaning does not work well for the probability of failure in a large, variable landform. Viewing the probability of failure as the relative frequency of failure events is more realistic. For purposes of estimating the consequences of failure, the probability of failure also can be thought of as the portion of the land area in, or potentially in, a failed state during the period appropriate to the analysis. However, this meaning should be used with caution. The validity of the meaning depends on the scale of the analysis and should be checked with a landslide inventory. LISA does not simulate the actual number of failures, nor the size or location of individual failures. LISA provides the hazard, but the potential consequences still must be evaluated by the user.

# CONTENTS

	Page
Introduction . . . . .	1
List of Symbols . . . . .	2
<b>PART 1—REFERENCE MANUAL</b>	
<b>Chapter 1—Concepts in Probabilistic Slope Stability Analysis</b>	
1.1 Applicability of LISA . . . . .	7
1.2 What Is a Probabilistic Analysis? (Deterministic vs. Probabilistic Analysis) . . . . .	7
1.3 How to Perform a Probabilistic Analysis—Monte Carlo Simulation . . . . .	8
1.4 Meaning of the Probability of Failure Estimated by LISA . . . . .	9
1.5 Use of the Probability of Failure . . . . .	10
1.6 Limitations of the LISA Analysis (What LISA Does Not Do) . . . . .	11
1.7 How Factor of Safety Relates to Probability of Failure . . . . .	11
<b>Chapter 2—Probability Theory Review</b>	
2.1 Definitions and Relationships . . . . .	14
2.2 Probability Distributions . . . . .	20
2.2.1 Uniform Distribution . . . . .	20
2.2.2 Triangular Distribution . . . . .	20
2.2.3 Normal Distribution . . . . .	20
2.2.4 Lognormal Distribution . . . . .	22
2.2.5 Beta Distribution . . . . .	23
2.2.6 Relative-Frequency Histogram Distribution . . . . .	25
2.2.7 Bivariate Normal Distribution . . . . .	28
<b>Chapter 3—The Infinite Slope Model</b>	
3.1 Description . . . . .	30
3.2 Assumptions . . . . .	30
3.3 Sensitivity to Input Values . . . . .	32
<b>Chapter 4—How the LISA Program Works (The Inside Nuts and Bolts)</b>	
4.1 Overview . . . . .	39
4.2 Correlation Between Variables . . . . .	39
4.3 Simulating Groundwater Values . . . . .	44
4.4 Reproducibility of the Probability of Failure . . . . .	44
<b>Chapter 5—Applying LISA</b>	
5.1 Getting Started . . . . .	47
5.1.1 General . . . . .	47
5.1.2 Delineating Polygons . . . . .	47
5.1.3 Using LISA for Level II Analyses . . . . .	47
5.1.4 Data Files and Map Unit Subdirectories . . . . .	48
5.2 Selecting Input Distributions—General Comments and Helpful Hints . . . . .	48
5.3 Estimating Input Values and Selecting Distributions for Each Variable . . . . .	50
5.3.1 Ground Slope . . . . .	51
5.3.2 Soil Depth . . . . .	51
5.3.3 Tree Surcharge . . . . .	53
5.3.4 Root Strength . . . . .	54
5.3.4.1 Values of Root Strength Measured . . . . .	56
5.3.4.2 Effect of Root Morphology and Suggested Probability Distributions . . . . .	56
5.3.4.3 Effect of Timber Harvest on Root Strength . . . . .	58
5.3.5 Soil Shear Strength and Unit Weight . . . . .	59
5.3.5.1 Distributions Reported in the Literature . . . . .	62

5.3.5.2	Shear Strength of Sands and Gravels . . . . .	64
5.3.5.2.1	Typical Strength Values and PDF's for $C'_s$ and $\phi'$ . . . . .	67
5.3.5.2.2	Typical Values for Unit Weight . . . . .	69
5.3.5.3	Shear Strength and Unit Weight of Clays . . . . .	69
5.3.5.3.1	Normally Consolidated Clays . . . . .	69
5.3.5.3.2	Overconsolidated Clays . . . . .	74
5.3.5.3.3	Unit Weight . . . . .	77
5.3.5.4	Residual Shear Strength of Sands and Clays . . . . .	77
5.3.5.4.1	Background . . . . .	77
5.3.5.4.2	Suggested Values and PDF's . . . . .	78
5.3.5.5	Apparent Cohesion . . . . .	78
5.3.5.6	Obtaining Values for Correlation Coefficient ( $r$ ) . . . . .	80
5.3.6	Moisture Content . . . . .	81
5.3.7	Groundwater . . . . .	82
5.3.7.1	Effects of Timber Harvest on Groundwater Levels . . . . .	84
<b>Chapter 6—Example Application: Dark 3 Planning Area, Gifford Pinchot National Forest</b>		
6.1	Introduction . . . . .	87
6.2	Geology, Soils, and Topography . . . . .	87
6.3	Polygon Delineation and Distribution Selection—Level I . . . . .	89
6.4	Level I Results . . . . .	89
6.5	Polygon Delineation and Distribution Selection—Level II . . . . .	89
6.6	Level II Results . . . . .	94
References by Author . . . . .		97
References by Subject		
	General Slope Stability . . . . .	106
	Probability and Monte Carlo Sampling . . . . .	107
	Root Strength . . . . .	108
	Soil Shear Strength . . . . .	110
	Groundwater . . . . .	113
	Timber Harvest Effects on Groundwater Levels . . . . .	114
Appendix A—Derivation of the Infinite Slope Equation . . . . .		116
Appendix B—Root Strength: A Detailed Literature Review . . . . .		118
Appendix C—Rationale for Selecting Root Strength PDF's . . . . .		122
Appendix D—Using Infiltration Event Return Periods With Probabilities of Failure From LISA . . . . .		125
Index . . . . .		128
<b>PART 2—PROGRAM OPERATION</b>		
<b>Chapter 1—Installation Instructions</b>		
1.1	Hardware Requirements . . . . .	131
1.2	LISA Installation . . . . .	131
1.2.1	Data File Location . . . . .	132
1.2.2	Running LISA From Any Subdirectory . . . . .	132
1.2.3	Running LISA From Windows 3.0 . . . . .	132
1.2.4	Customizing LISA With Environment Variables . . . . .	132
1.2.4.1	Specifying Your Own File Viewer . . . . .	132
1.2.4.2	Specifying IBM Graphics Characters . . . . .	133
1.3	LISA Program Files . . . . .	133
<b>Chapter 2—General Execution Instructions</b>		
2.1	Screen Structure of LISA . . . . .	134

2.2	Data File Structure . . . . .	134
2.3	General Principles . . . . .	134
Chapter 3—Detailed Execution Instructions		
3.1	Executing LISA . . . . .	137
3.2	Selecting Colors . . . . .	137
3.3	Entering a User Name . . . . .	138
3.4	Selecting the Path to Data (Map Unit) Subdirectories . . . . .	139
3.5	Selecting an Existing Map Unit . . . . .	141
3.6	Creating a New Map Unit . . . . .	143
3.7	Deleting an Existing Map Unit . . . . .	144
3.8	Selecting Existing Data Files . . . . .	144
3.9	Deleting an Existing Data File . . . . .	144
3.10	Entering or Editing Data . . . . .	144
3.10.1	Constant Value . . . . .	147
3.10.2	Uniform Distribution . . . . .	147
3.10.3	Normal Distribution . . . . .	147
3.10.4	Lognormal Distribution . . . . .	149
3.10.5	Triangular Distribution . . . . .	150
3.10.6	Beta Distribution . . . . .	150
3.10.7	Histogram Distribution . . . . .	151
3.10.8	Bivariate Normal Distribution . . . . .	152
3.11	Plotting Distributions . . . . .	155
3.12	Modifying Distributions While Plotting . . . . .	156
3.13	Saving Data Files . . . . .	159
3.14	Saving Simulated Values . . . . .	159
3.15	Entering a Descriptive Comment (“ID”) . . . . .	160
3.16	Changing the Random Seed . . . . .	161
3.17	Entering the Number of Iterations . . . . .	161
3.18	Starting the Simulation . . . . .	162
3.19	Viewing and Modifying the Factor of Safety Histogram . . . . .	164
3.20	Viewing Scatter Plots and Variable Histograms . . . . .	164
3.21	Viewing, Saving, and Printing the Output Files . . . . .	167
3.22	Exiting LISA . . . . .	171
Chapter 4—DLISA Execution Instructions		
4.1	Introduction . . . . .	175
4.2	Installation . . . . .	175
4.3	Starting DLISA . . . . .	175
4.4	Data Entry . . . . .	178
4.5	Entering Values . . . . .	178
4.6	Execution . . . . .	179
4.7	Back-Calculation Error . . . . .	180
4.8	Leaving DLISA . . . . .	181
Reference . . . . .		183
Appendix A—Downloading from the DG . . . . .		183
Appendix B—Using the Software Reference Center . . . . .		185
Appendix C—DLISA Equations . . . . .		186
Appendix D—Error and Warning Messages		
	LISA . . . . .	187
	DLISA . . . . .	187
Index . . . . .		189

# Level I Stability Analysis (LISA) Documentation for Version 2.0

**Carol Hammond**  
**David Hall**  
**Stanley Miller**  
**Paul Swetik**

## Introduction

This report provides comprehensive information required to use LISA intelligently. The goal was to give the user a sufficient reference manual for understanding and obtaining input distributions, understanding the concepts and methods LISA uses, and interpreting LISA results, and to be a guide for program operation. This report, therefore, has been divided into two parts: part 1 is the reference manual and part 2, the program operations guide. *Important points throughout this report are set in italic and marked by a block in the outside margin.*

It is *essential* that the user understands the fundamentals and concepts presented in part 1, or meaningless or misleading results might be obtained using LISA. However, understanding part 1 may be made easier for the uninitiated user if one first becomes familiar with LISA by running the demonstration exercise in part 2, chapter 3.

The Research Summary explains what LISA does and what the program results mean. It can be included, along with user additions, in reports of LISA results to help land managers understand the methods that have been applied.

The detailed Table of Contents functions as a reference device, assisting the reader in locating subjects by page number. The numeric system used to identify section and subsection headings assists the reader in locating cross-referenced sections. A list of symbols can be found after this introduction.

Part 1 of this report consists of six chapters and four appendices. Chapter 1 introduces the philosophy behind probabilistic slope stability analysis. Chapter 2 reviews probability and statistics fundamentals. Chapter 3 describes the infinite slope equation and its sensitivity to various input parameters. Chapter 4 describes details of the methods used in the LISA program and interpretation of results. Chapter 5 discusses how to select input distributions and values describing those distributions, both in general and for each variable in the infinite slope equation. Chapter 6 contains two examples of the range of uses to which LISA can be applied. References cited in part 1 are given after chapter 6.

Appendix A shows the derivation of the infinite slope equation with a phreatic surface parallel to the slope. Appendix B gives a detailed literature review of root strength. Appendix C discusses the rationale for selecting the suggested PDF's for root strength. Appendix D discusses using rain or rain-on-snow return periods with LISA probabilities of failure to arrive at an estimate of the likelihood of failure events occurring.

Part 2 contains four chapters and four appendices. Chapter 1 gives installation instructions. Chapter 2 gives general principles on how to run LISA. Chapters 1 and 2 generally will be all that are needed to get the user started. Chapter 3 describes in detail LISA operation, including screen prompts and error

messages and a demonstration exercise. Chapter 4 describes use of DLISA, the deterministic version of LISA. The reference cited in part 2 is given after chapter 4.

Appendix A describes how to download LISA and DLISA from the Data General computer at Moscow, ID. Appendix B describes how to use the Software Reference Center on the Data General computer in the Washington, DC, office to obtain information on the latest program revision. Appendix C lists the equations used in DLISA. Appendix D is a list of error messages from both LISA and DLISA with cross references into chapters 3 and 4.

Documented source code (Hall and Kendall 1992) is available separately by special request made to the authors. Additional examples of LISA applications have been described by Hammond and others (1992) and Hammond and others (1988).

## List of Symbols

$A$	Angular grain shape
$A$	Area of soil in a root count sample
$a$	Minimum value specified for a uniform, triangular, or beta PDF
$a_i$	Root cross-sectional area for the $i$ th size class
$A_R$	Total cross-sectional area of all roots in a root count
$b$	Maximum value specified for a uniform or beta PDF, and apex of a triangular PDF; also width of slice in infinite slope derivation
$B[a, b, P, Q]$	Notation specifying a beta PDF
bf	Board foot = 12 by 12 by 1 inches
$BN[\bar{x}, s, r]$	Notation specifying a bivariate normal PDF
$c$	Maximum value specified for a triangular distribution
$C'_a$	Apparent soil cohesion caused by interpretation of a curved Mohr-Coulomb failure envelope
$C_{app}$	Apparent soil cohesion caused by capillary suction
CDF	Cumulative distribution function
CH	USC designation for fat clay
CL	USC designation for lean clay
$c_v$	Sample coefficient of variation = $s/\bar{x}$
$C_v$	Population coefficient of variation = $\sigma_X/\mu_X$
$cov[X, Y]$	Sample covariance between $X$ and $Y = rs_Xs_Y$
$Cov[X, Y]$	Population covariance between $X$ and $Y = \rho\sigma_X\sigma_Y$
$C_r$	Additional shear strength caused by tree roots
$C'_s$	Effective soil cohesion
$D$	Soil depth measured vertically
$D_{ac}$	Apparent soil depth measured along a cutslope face

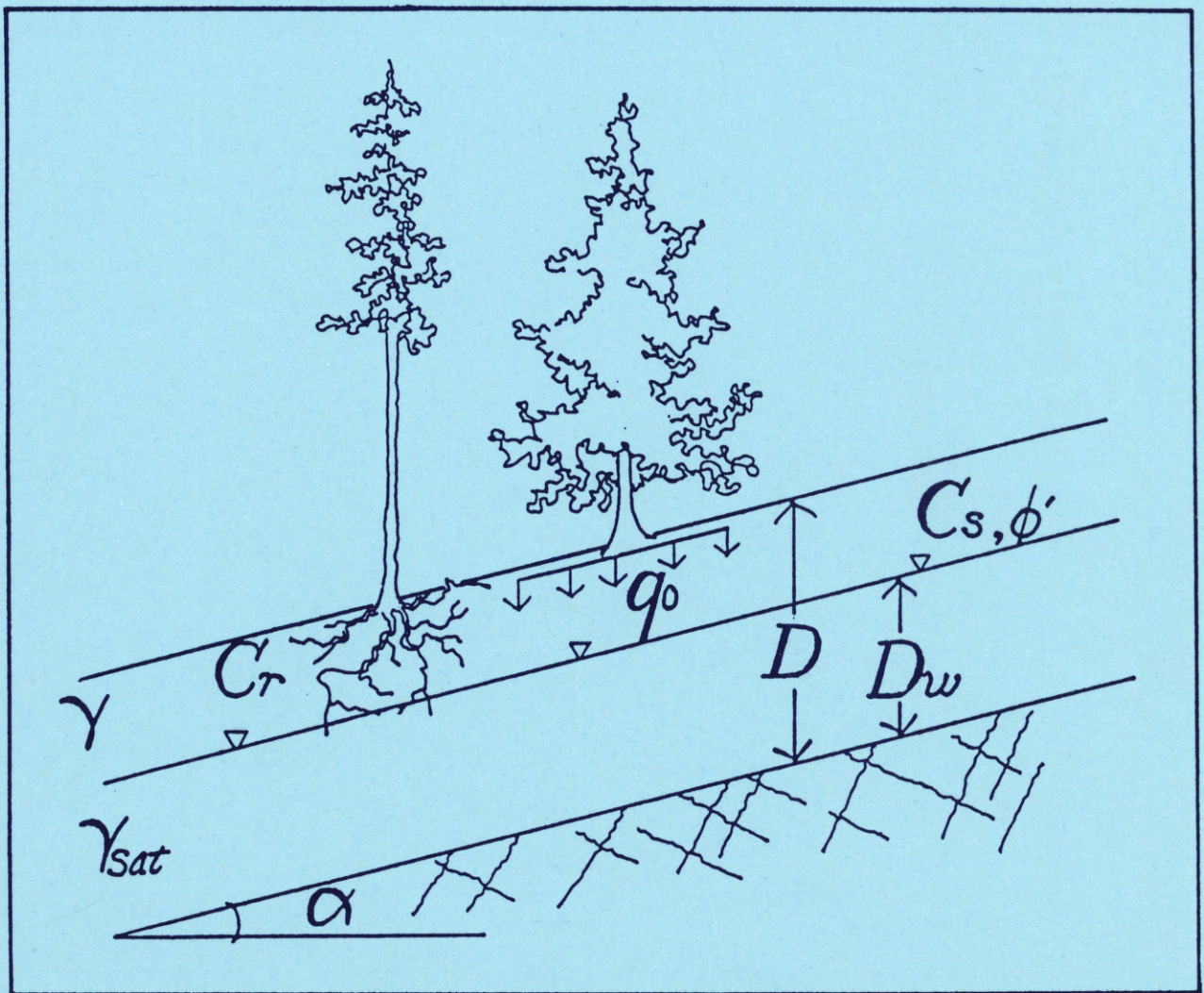
$D_{as}$	Soil depth measured using seismic refraction; depth is measured perpendicular to the refractor surface
$D_b$	Bulk density of minus 2mm fraction of soil
$D_m$	Vertical height of soil above the phreatic surface = $D - D_w$
$D_r$	Relative density of soil
$D_R$	Diameter of a root
$D_w$	Vertical height of phreatic surface
$E[X]$	Expected value of a random variable $X$
$\text{Var}[X]$	Variance of a random variable $X = \sigma_X^2$
$E_R$	Longitudinal stiffness modulus of a root
$FS$	Factor of safety
$F_i$	Average resisting tensile force of roots in the $i$ th size class; also fraction of observations in the $i$ th class of a histogram PDF
ft or ' "	Foot
$f(\mathbf{x})$	Function of $\mathbf{x}$ that describes the $Y$ -ordinate of a PDF curve
GC	USC designation for clayey gravel
GM	USC designation for silty gravel
GP	USC designation for poorly graded gravel
GRC	Geologic resources and conditions data base
GRI	Geologic resource inventory
$G_w$	Specific gravity of solids
GW	USC designation for well-graded gravel
$H[k, f_1, \dots, f_n]$	Notation for histogram PDF with $k$ classes and $f_n$ percent in each class
$h_p$	Vertical height of equipotential line
in or " "	Inch
$k$	Number of classes in a histogram PDF
$k_{\phi 1}, k_{\phi 2}$	Empirical coefficients to estimate angle of internal friction from $D_r$
lb	Pound
LISA	Level I stability analysis
$L[\mathbf{x}, \mathbf{s}]$	Notation specifying a lognormal PDF
LSI	Land systems inventory
MH	USC designation for plastic silt
ML	USC designation for non plastic silt
N	Number of years

$N$	Normal force at the base of the slice in the infinite slope derivation
$N'$	Effective normal force
$n$	Number of data values or observations in a sample
$N[\bar{x}; s]$	Notation for a normal PDF with mean $\bar{x}$ , and standard deviation $s$
$n_i$	Number of roots in size class $i$
$OC$	Organic carbon content of soil
OCR	Overconsolidation ratio
$P$	One of two shape parameters for a beta PDF
pcf	Pounds per cubic foot
PDF	Probability density function
PI	Plasticity index
psf	Pounds per square foot
$P[A \cap B]$	The occurrence of event $B$ given that event $A$ has occurred = $P[A]P[B \setminus A]$
$P[B]$	The probability that event $B$ will occur
$P[\bar{B}]$	The probability that event $B$ will not occur = $1 - P[B]$
$P[B \setminus A]$	The probability that event $B$ will occur given that event $A$ has occurred. This is called a conditional probability and is used when the probability of event $B$ depends on the occurrence of event $A$ .
$P[FS \leq 1]$ or $P_f$	The probability of $FS$ being less than or equal to 1, or the probability of slope failure
$Q$	One of two shape parameters for a beta PDF
$q_0$	Tree surcharge
$r$	Sample correlation coefficient
$r^2$	Coefficient of determination
R	Rounded grain shape
$R_{pi}$	Return period of event $i$
$r.v.$	Random variable
$s$	Standard deviation of sample data
$S$	Soil shear strength
SA	Subangular grain shape
SARA	Stability analysis for road access (Level II)
SC	USC designation for clayey sand
SM	USC designation for silty sand
SP	USC designation for poorly graded sand

SPT	Standard penetration test (ASTM D-1586)
SR	Subrounded grain shape
SRI	Soil resource inventory
$s_X$	Standard deviation of sample data for random variable $X$
$T$	Shear force acting on the base of a slice in the infinite slope derivation
$T_i$	Average tensile strength per foot cross-sectional area for the $i$ th class
$T_n$	Normal component of root tensile resistance
$T_r$	Tensile strength of individual roots
$T_R$	Weighted average root tensile strength per average root cross-sectional area of all size classes
$t_R$	Average tensile root strength per unit soil area
$T_s$	Tangential component of root tensile resistance
$T[a, b, c]$	Notation for a triangular PDF
T-99	ASHTO test designation for the standard Proctor test
$u$ or $u_w$	Pore-water pressure
$u_a$	Pore-air pressure
$U$	Uplift force on the base of a slice in the infinite slope derivation caused by pore-water pressure, $u$
USC	Unified Soil Classification system (ASTM D-2487-85 and D-2488-84)
$U[a, b]$	Notation for a uniform PDF
$\text{Var}[X]$	Variance of a random variable $X = \sigma_X^2$
$w$	Gravimetric moisture content = weight of water/weight of solids x 100%
$W_T$	Total weight of a soil slice in the infinite slope derivation
$\bar{x}$	Mean of sample data set
$X$	Random variable $X$
$Y$	Random variable $Y$
$z$	Thickness of the shear zone
$\alpha$	Natural slope angle, in percentage or degrees in DLISA; in percentage in LISA
$\beta$	Artificial slope angle in degrees or ratio
$\gamma$ or $\gamma_m$	Moist soil unit weight
$\gamma_d$	Dry soil unit weight
$\gamma_{\max}$	Maximum unit weight obtained with a standard laboratory test such as standard (T-99) or modified (T-180) Proctor test

$\gamma_{\text{sat}}$	Saturated soil unit weight
$\gamma_w$	Unit weight of water = 62.5 pcf
$\theta$	Angle of root shear distortion
$\mu_l$	Mean of the logarithm of data values
$\mu_X$ or $\mu$	Mean of random variable $X$
$\rho$	Population correlation coefficient
$\sigma'$ or $\sigma'_n$	Effective normal stress
$\sigma_l$	Standard deviation of the logarithm of data values
$\sigma_R$	Tensile stress developed in the root at the shear plane
$\sigma_X$ or $\sigma$	Standard deviation of random variable $X$
$\tau$	Soil shear strength; also shear stress
$\tau_R$	Skin friction stress along a root
$\phi'$	Effective angle of internal friction
$\phi'_a$	Apparent effective angle of internal friction caused by interpretation of a curved Mohr-Coulomb failure envelope
$\phi^b$	Slope of the line relating capillary suction and apparent soil cohesion
$\phi'_r$	Residual angle of internal friction
$\phi'_p$	Peak angle of internal friction
$\phi'_{\text{ult}}$	Ultimate angle of internal friction, equivalent to $\phi'_r$
$\phi_\mu$	Particle-to-particle friction angle
$\hat{\phantom{x}}$	Estimation of a population (true) parameter from sample data (e.g., $\hat{\mu}$ or $\hat{\sigma}$ )

# Part 1—Reference Manual



# CHAPTER 1—CONCEPTS IN PROBABILISTIC SLOPE STABILITY ANALYSIS

## 1.1 Applicability of LISA

LISA is a probabilistic model intended to be used primarily for relative landslide hazard evaluation for resource allocation, forest planning (land management plans), timber sale allocation, environmental assessment reports (EARs), and transportation planning (Prellwitz and others 1983). LISA can delineate areas susceptible to broad-scale landslides to alert land managers as to where the hazard is greatest. LISA also can be useful for project planning (Level II) to evaluate the stability of natural slopes in cutting units and the effects of timber harvest on stability.

LISA is a *tool* to be used by investigators who have some knowledge and experience concerning landslide behavior and geotechnical properties of soils. It requires engineering judgment and common sense, both in developing input distributions and interpreting the results. It does not give a unique “right” answer. It is a tool to help the user understand slope stability processes, quantify observations and judgments, and document and communicate those observations and judgments to other geotechnical specialists and to land managers. Do not rely on LISA alone, but add it to your existing toolbox. Any answer that one may desire can be obtained by altering the input data. Without rationally justifying the input used, and without correctly understanding and interpreting the output, LISA becomes little more than a game of numbers.

LISA does *not* provide a complete risk analysis; the impact or consequence of potential failures needs to be evaluated by the user. For example, the user may want to assess the potential for damage to timber and fisheries resources or to roads or structures, or the potential for injury or loss of life resulting from slope failures.

## 1.2 What Is a Probabilistic Analysis? (Deterministic vs. Probabilistic Analysis)

Typically in day-to-day engineering work, slope stability analyses are performed using limit equilibrium equations to obtain a calculated factor of safety against failure. A slope with a factor of safety greater than 1 is expected to be stable, whereas a slope with a factor of safety less than or equal to 1 is expected to be unstable. This calculation of a single factor of safety, given a single set of input values, is a deterministic analysis. However, it is recognized that there are many uncertainties in estimating input values for an analysis. Variability and uncertainty in soil shear strength parameters are due both to variation in soil properties across the site and to measurement errors in field and laboratory testing. Groundwater levels vary spatially and temporally. There are uncertainty and variability in the other factors as well, all of which yield uncertainty as to the precise meaning of the factor of safety value. That is, it is recognized that a slope with a calculated factor of safety of 0.9 may not fail, and one with a calculated factor of safety of 1.1 might fail. Thus, design factors of safety of 1.2 to 1.5 often are used to give the engineer a conservative buffer against uncertainty and spatial variability.

A probabilistic analysis provides an estimate of the probability of slope failure, rather than the factor of safety, by using probabilistic models to quantify the uncertainty and variability associated with the prediction of slope stability. The primary advantage of a probabilistic analysis is that it logically and

systematically accounts for uncertainty and variability in the stability analysis and communicates to all concerned that uncertainty and variability have been considered. With a probabilistic analysis, a single value for each input parameter is no longer required. Rather than modeling a site as homogeneous, we can deal with the site's variable factors.

A probabilistic analysis also provides results that can serve as input for a decision making analysis in the light of recognized uncertainty. Such analyses require a probability of failure (in other words, hazard) and the consequences of failure in order to evaluate risk. In a risk analysis, the hazard and its consequences associated with various decision alternatives are evaluated to aid in decision making. In the context of the following discussion, *hazard* is defined as the calculated probability of slope failure, and *risk* is defined as a measure of the socioeconomic consequences of slope failure (susceptibility to losses). Two slopes may have the same estimated probability of slope failure and therefore the same hazard (as estimated by LISA). However, if a bridge or an anadromous fisheries stream lies below one of the slopes and not the other, the risks associated with failure of the first slope are much greater than are those associated with the other slope. Comprehensive risk analysis is beyond the scope of this manual.

### **1.3 How to Perform a Probabilistic Analysis—Monte Carlo Simulation**

Most probabilistic methods described in the literature focus on the analysis of individual slopes and consider only the variability of soil cohesion, angle of internal friction, or groundwater, or a combination of these. A closed-form solution is derived for the mean and standard deviation of the factor of safety, which has an assumed probability distribution (usually normal, lognormal, or beta), and then a probability of failure is calculated (Chowdhury and Tang 1987). One problem with these methods is that the variabilities of other important factors, such as slope and soil depth, are not considered. One reason all factors are not considered as stochastic variables is that the calculus needed to evaluate the integrals resulting from the derivation of the probability distribution of the factors of safety would not be tractable. However, when analyzing large areas, as in resource planning, all of the input factors have sufficient spatial variability and measurement uncertainty to warrant treatment as stochastic variables.

An alternative method used to evaluate landslide hazard is Monte Carlo simulation. Monte Carlo simulation is useful for modeling an attribute that cannot be sampled or measured directly but can be expressed as a mathematical function of properties that can be sampled or described. Factor of safety is such an attribute. Monte Carlo simulation is the method used in LISA because of its capability to incorporate the variabilities of many input parameters, as is required for a stability analysis of large, variable landforms using the infinite slope model.

If we want to predict a possible value of the factor of safety, we take a possible value for each input variable and use the appropriate performance function (a stability equation) to calculate the corresponding value of the factor of safety. This is known as one Monte Carlo pass or iteration. In Monte Carlo simulation we generate a large number of factor of safety values (say 1,000) by repeated, random, independent samplings of a set of possible input values and calculate a corresponding factor of safety value for each pass. The set of possible input values for each input parameter is described by a probability distribution. The final simulation output is a set of 1,000 possible factor of safety values that can

be displayed as a histogram. The relative frequencies of these 1,000 values are assumed to be representative of the frequencies we would have obtained had we analyzed all possible combinations of the input variables. Thus, the relative frequency of the computed factors of safety less than or equal to 1 is an estimate of the probability of occurrence of factors of safety less than or equal to 1 in nature (as defined by the user). We obtain the probability of failure by dividing the total number of passes into the number of calculated factor of safety values less than or equal to 1.

#### **1.4 Meaning of the Probability of Failure Estimated by LISA**

The probability of failure, strictly speaking, is the total number of Monte Carlo iterations divided into the number of calculated factors of safety with a value less than or equal to one. In other words, it is the relative frequency with which possible values of the factor of safety in the simulation are less than or equal to one. The probability of failure estimated by LISA should be reported as a *conditional* probability given that the considered storm event with the resulting groundwater distribution used in the analysis occurs.

It is common to view the probability of an event as the likelihood of that event occurring. This meaning does not work well for the probability of failure in a large, variable landform, because the possibility of just one failure occurring in the landform gives a probability of landslide occurrence of one. It is more useful to think of the probability of failure of a large landform as the relative frequency of failure events. For example, if landform A has a probability of failure of 0.05 and landform B has one of 0.025, we would expect landslides to be twice as severe, in number or size, in landform A. The probability of failure can be viewed as the probability of landslide occurrence *if* the area analyzed is small enough (i.e., one slope or one drainage) so that only one failure could occur within the area.

With few data, the input distributions represent one's uncertainty about the variables as well as one's best guess about their spatial variability across the landform. Therefore, because of the two-dimensional nature of the infinite slope analysis, the estimated probability of failure can best be thought of as the likelihood that any possible randomly selected cross-section through the slope would be analyzed as unstable. As more data are available, the probability distribution of each input variable represents more the spatial variability of that variable and less the uncertainty. Here the probability of failure should be an estimate of the expected percentage area of the landform involved in failure *during the period appropriate to the analysis*, that is, during the period of minimum root strength following timber harvest, or during the rain or snowmelt event causing the groundwater levels used in the analysis.<sup>1</sup> Thinking of the probability of failure as the expected portion of the landform in, or potentially in, failure can indicate to management the magnitude of consequences to expect. However, this meaning for the probability of failure should be verified by comparison with field observations.

Landslide inventories provide the best means to verify whether the estimated probability of failure values are reasonable. Landslide inventories traditionally have been used to assess relative hazard by drawing the inductive conclusion that landslides will occur again in areas where they have occurred previously.

---

<sup>1</sup>A method for conditioning the LISA probability of failure estimates with the probability of certain rainfall or snowmelt events occurring during some specified length of time is discussed in appendix D.

Therefore, areas with many inventoried landslides should have a high probability of failure as predicted by LISA. When considering the percentage of land area involved in landslides, we must realize that these “high” probabilities of failure may actually occur on a small portion of the landscape. Published landslide inventories report values on the order of 0.5 to 15 percent of the area inventoried (Ice 1985). If the input distributions are based on subjective estimates rather than estimated from actual data, there may be only a relative comparison between probabilities of failure predicted by LISA and percentage of area in slope failure. But we still should see the relative relationship that areas with a higher probability of failure as predicted by LISA should have a higher frequency of occurrence of landslides than do areas with a lower probability of failure.

- As with any computer program, “garbage in = garbage out.” *If the input distributions do not describe realistically the values and distributions of the factors on the ground, then the simulated probability of failure will not provide a realistic measure of landslide hazard.* A method for quantifying the reliability in the LISA results is desirable based on whether the initial input distributions are formulated from field measurements or from subjective estimates. With such a method, as more field measurements are made and subsequent data are fed back into LISA from Level II and Level III field investigations, the increase in reliability of the LISA simulation can be documented. Methods to accomplish this currently are under study.

### 1.5 Use of the Probability of Failure

The probability of failure can be used qualitatively to make relative comparisons between landforms to identify areas that should be targeted for additional analysis. The probability of failure also can be used quantitatively in a risk analysis, such as an expected monetary value (EMV) decision analysis. Research efforts are continuing in this area.

- Often in land management planning, one has to make subjective judgments about what probability of failure is acceptable. *Interpretation of the probability of failure as the percentage area expected in failure can help geotechnical specialists recommend to land managers what probability of failure is excessive. However, the possible consequences of failure, such as an estimate of the quantity of material that may impact downslope lands or streams, also need to be addressed.*

- Reporting a single probability of failure value tends to imply precision in the results. Therefore, *we encourage users to report a range of probability of failure values obtained from several simulations using the same input distributions* but different random number seeds. Also, one may perform sensitivity analyses with LISA, changing the shape and values describing the input distributions over realistic ranges to see how the probability of failure is affected. Again, the range of values obtained should then be reported. Used as an iterative tool, LISA can help the user document personal judgments and observations about an area, communicate them to land managers and to other geotechnical specialists, and help identify factors critical to landslide hazard assessment in a given area.

## 1.6 Limitations of the LISA Analysis (What LISA Does Not Do)

LISA does not simulate the size or number of failures that might occur on a particular landform. Nor can LISA predict exact locations of any failures, or the type of failure (although it should give more accurate results for translational failure modes). Therefore, LISA cannot be used to directly estimate the consequences of failure, such as whether sediment will reach a stream, or the volume of sediment delivered.

## 1.7 How Factor of Safety Relates to Probability of Failure

One approach to estimating a “likelihood” of failure is to measure or estimate either average or conservative values for each variable, and calculate a factor of safety deterministically. If the resulting factor of safety is fairly high, say 1.2, one could conclude that the likelihood of failure would be low. But how low depends on whether average or conservative input values were used, and what the possible variation in factors of safety is. In this section, we will discuss three concepts concerning the relationship of factor of safety to probability of failure.

The first concept is that the mean factor of safety for a landform is not a good indication of the probability of failure. This is because the probability of failure depends not only on the mean, but also on the variance of the factors of safety, which is controlled by the variance in the input distributions. An example is given in figure 1.1 and table 1.1 in which LISA gave similar mean factors of safety (1.26 and 1.19) for two hypothetical landforms, but a much higher probability of failure for landform 1, which has larger standard deviations for the input distributions. Table 1.1 shows the input distributions used. One should be aware that larger standard deviations for the input distributions might lower the probability of failure when the mean factor of safety is less than one.

The second concept is that the deterministic factor of safety calculated from the mean values of each input distribution may not equal the mean of the distribution of the factor of safety values, even when all of the input distributions are symmetrical. Take, for example, landform 1 in table 1.1. The mean values of the input distributions yield a deterministic factor of safety of 1.18 while the mean of the distribution of factors of safety from Monte Carlo simulation is 1.26. This is due to the fact that the factor of safety distribution for landform 1 is skewed to the right, which shifts the mean factor of safety to a higher value than that for a symmetrical distribution. In general, the expectation (or mean) of a nonlinear function, in our case the infinite slope equation, is not equal to the value of the function obtained when the mean values of each input variable are used in the function. Therefore, the mean of the factor of safety distribution should not necessarily be used as a substitute for a deterministic value (or vice versa), particularly when the distribution is highly skewed. The mean is just one measure of central tendency of the distribution. Commonly, the median or the mode value is closer to the deterministic factor of safety value than is the mean value.

Note that the mean value of the distribution for landform 2 (1.19) is very close to the value obtained from the means of the input variables (1.18). This happens because the distribution of factors of safety for landform 2 is relatively symmetrical.

The third concept, often difficult for engineers to comprehend when first introduced to probabilistic concepts, is that a slope with a computed factor of safety of 1.0 is not necessarily on the verge of failure. The probability of failure is not 1.0. In fact, the probability of failure is on the order of about 0.4 to 0.6,

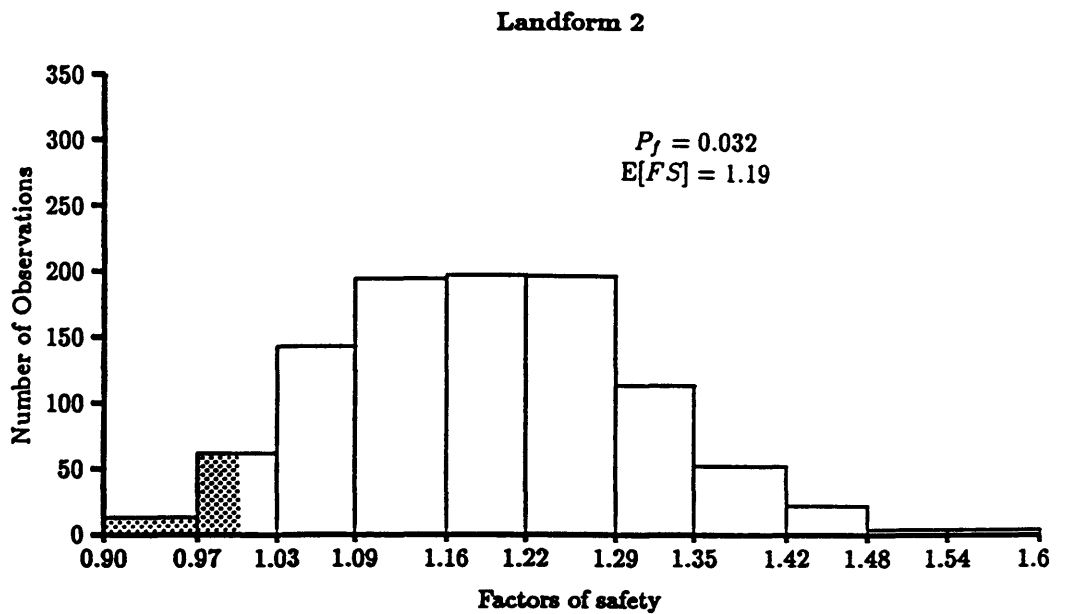
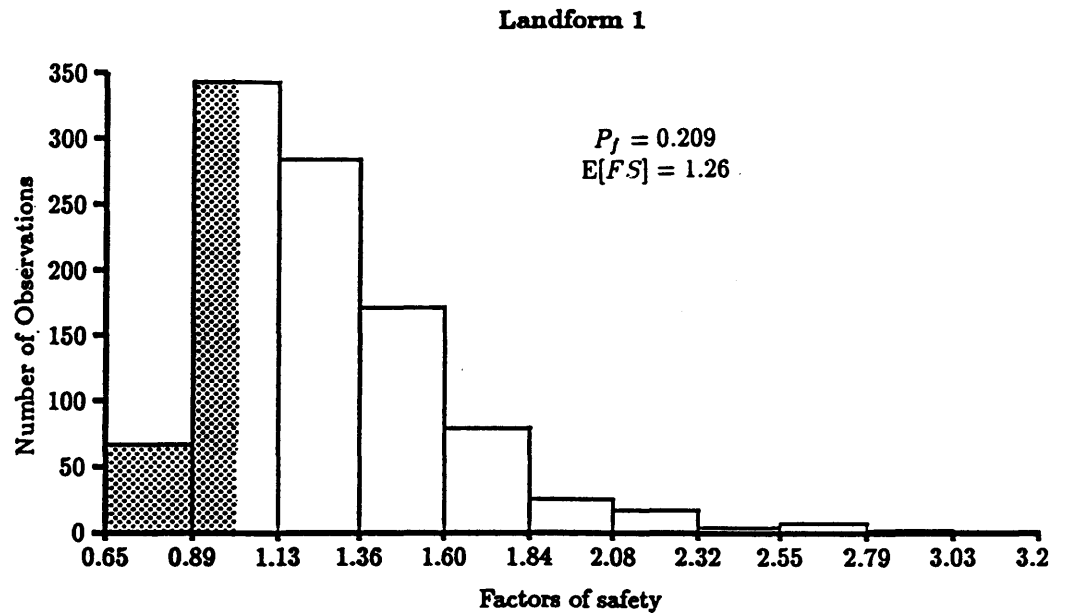


Figure 1.1—The distributions of factor of safety for two landforms. The landforms have nearly the same mean factor of safety but quite different probabilities of failure. The shaded area in each histogram represents values of factor of safety less than 1.

depending on the skewness of the factor of safety distribution. If the factor of safety distribution is symmetrical, the probability of failure is 0.5. This illustrates that the computed factor of safety may not be a good predictor of the behavior of the slope because of the natural variability of the physical factors and because of our inability to know without error the values of these factors.

Table 1.1—Distributions used for figure 1.1

	Landform 1			Landform 2		
	Distribution	$\bar{x}$	$s$	Distribution	$\bar{x}$	$s$
Soil depth	$T[1, 4, 7]$	4.0	1.2	$T[3, 4, 5]$	4.0	0.4
Slope	$U[60, 80]$	70.0	5.8	$T[65, 70, 75]$	70.0	2.0
Tree surcharge	$U[5, 15]$	10.0	2.9	$U[5, 15]$	10.0	2.9
Root cohesion	$U[20, 140]$	80.0	35.0	$T[50, 70, 120]$	80.0	14.6
Friction angle	$N[34, 1]$	34.0	1.0	$N[34, 0.5]$	34.0	0.5
Soil cohesion	$N[50, 15]$	50.0	14.6	$N[50, 10]$	50.0	10.0
Dry unit weight	$N[100, 1]$	100.0	1.0	$N[100, 1]$	100.0	1.0
Moisture content	$N[20, 0.5]$	20.0	0.5	$N[20, 0.5]$	20.0	0.5
Specific gravity	2.66			2.66		
$D_w/D$	$U[0.4, 1]$	0.7	5.8	$T[.5, .7, .9]$	0.7	0.08
Factor of safety	see fig. 1.1	1.26	0.3	see fig. 1.1	1.19	0.1
Deterministic factor of safety	1.18			1.18		

## CHAPTER 2—PROBABILITY THEORY REVIEW

The user should be familiar with the following concepts and terms when using LISA. We advise that you also read a good textbook if the material is new to you. Readable discussions are contained in Benjamin and Cornell (1970), Newendorp (1975), and Smith (1986).

### 2.1 Definitions and Relationships

#### EVENT

In probability theory, it is assumed that a random experiment, or sampling exercise, will have outcomes that depend on chance. A collection of one or more outcomes is known as an *event*. For example, consider a laboratory testing program wherein the dry unit weight is determined for each of 10 soil specimens randomly selected from a Shelby tube sample. An outcome is one test result (say, 103 pcf). An event is a collection of outcomes, such as all test results greater than 106 pcf, or all results between 100 and 110 pcf.

$P[B]$  is the probability that event  $B$  will occur.  $P[B]$  is a real number between 0 and 1 assigned to event  $B$ .

$P[\bar{B}]$  is the probability that event  $B$  will not occur and is known as the complement of  $P[B]$ .  $P[\bar{B}] = 1 - P[B]$ .

#### RANDOM VARIABLE

A *random variable* (*r.v.*) is a variable or attribute (such as a physical property or characteristic) that takes on different values according to the outcomes of repeated experiments or sampling events.

These values cannot be predicted with certainty; thus, each possible range of values has an associated probability (or likelihood) of occurrence. For this reason, *r.v.*'s often are called *stochastic* variables to indicate the stochastic, or probabilistic, nature of their values. The term *random* here does not imply that the variable itself is random or has randomly distributed values, but rather that the values occur in a probabilistic manner. In the previous example for *event*, the dry unit weight of the soil is an *r.v.* If the value of a variable is known with certainty or with negligible uncertainty (at the time of analysis or decision making), then the variable is called a *deterministic* variable.

#### PROBABILITY DISTRIBUTION

A *probability distribution* is a discrete or continuous function that defines the likelihood, or the probability, that a random variable will have some particular range of values. Probability distributions can be expressed in two forms: the cumulative distribution function (CDF) and the probability density function (PDF). These are shown in figure 2.1 and described below.

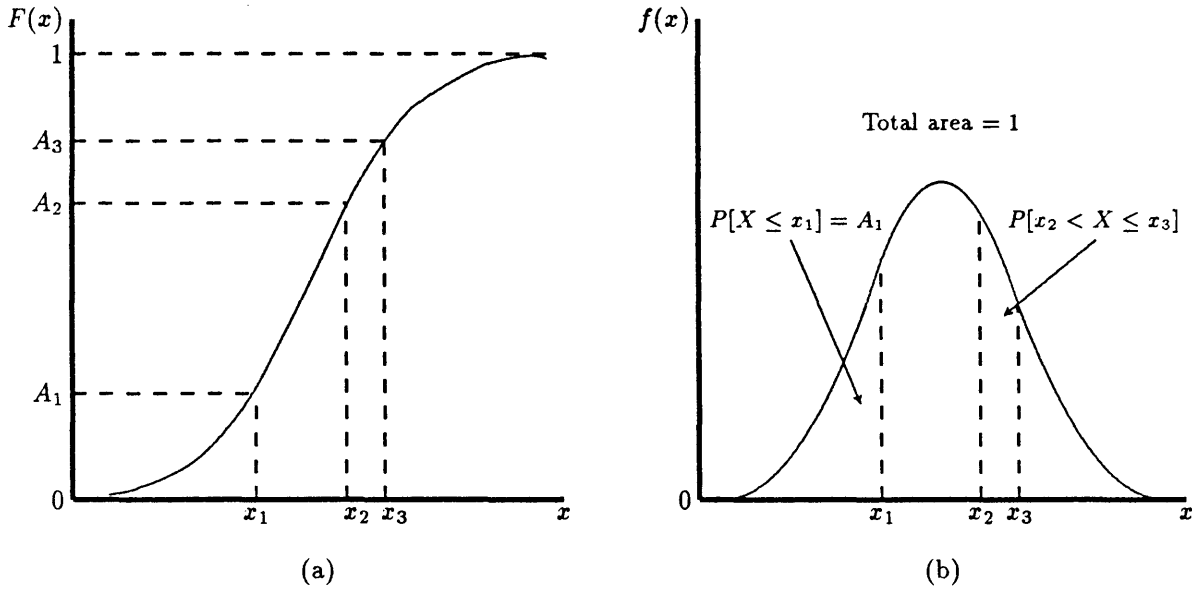


**Figure 2.1**—Example CDF (a) and PDF (b). In each, the probability that the random variable  $X$  takes on a value less than or equal to  $x_1$  is equal to  $A_1$ . This is expressed mathematically as  $P[X \leq x_1] = A_1$ . The probability that the random variable  $X$  takes on a value between  $x_2$  and  $x_3$  is equal to  $A_3 - A_2$  on the CDF, and to the area under the curve between  $x_2$  and  $x_3$  on the PDF.

**CUMULATIVE  
DISTRIBUTION  
FUNCTION (CDF)**

The CDF for the *r.v.*  $X$  is a function that describes the probability that the *r.v.*  $X$  takes on a value less than or equal to  $x$ :

$$F(x) = P[X \leq x]$$

The properties of a CDF are:

- It has values between 0 and 1 inclusive.
- It is a nonnegative, nondecreasing function of a real-valued variable. A CDF can be defined for discrete or continuous *r.v.*'s.

**PROBABILITY  
DENSITY  
FUNCTION (PDF)**

The PDF for a continuous *r.v.*  $X$  is defined as:

$$f(x) = \frac{d[F(x)]}{dx}$$

The properties of a PDF are:

- It is a nonnegative function where  $\int_{-\infty}^{+\infty} f(x)dx = 1$
- The probability that the *r.v.*  $X$  will take on a value between  $x_2$  and  $x_3$  is equal to the area under the PDF curve between  $x_2$  and  $x_3$ :

$$P[x_2 < X \leq x_3] = \int_{x_2}^{x_3} f(x)dx$$

This is illustrated in figure 2.1b. PDF's are used in LISA to describe input variability.

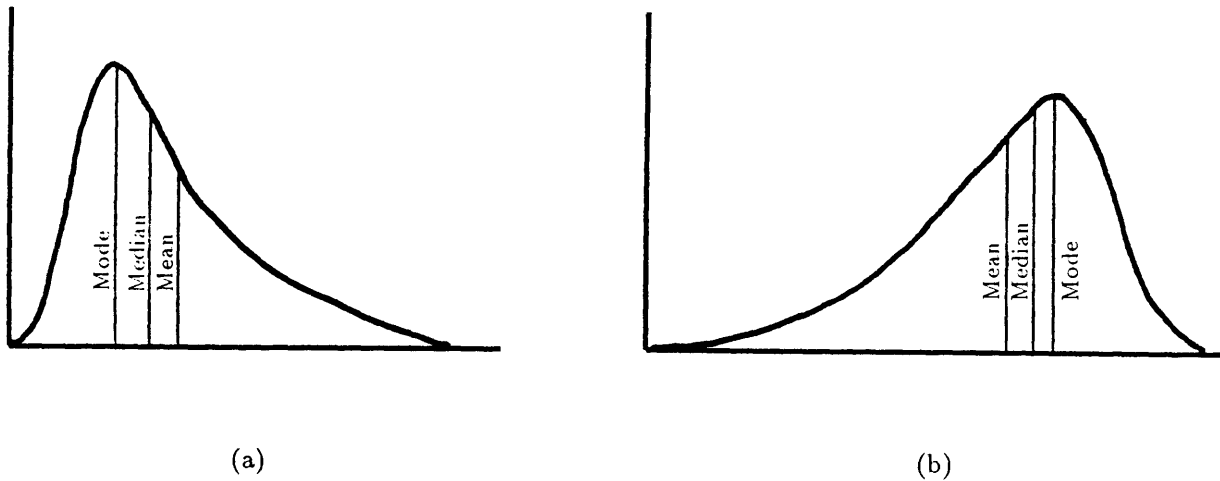


Figure 2.2—The relationship between mean, mode and median for a skewed right PDF (a) and a skewed left PDF (b).

**Measures of Central Tendency**— There are specific values that give important and useful information about a PDF. These values describe the central tendency of a PDF and the variability or range within which an *r.v.* is distributed. There are three measures of the central tendency of a PDF—the *mean*, the *median*, and the *mode*.

#### MEAN

The *mean* value of a PDF is the weighted average value of an *r.v.* where the weighting factors are the probabilities of occurrence. The mean value of a PDF is also called the expectation of the *r.v.* ( $E[X]$ ). If the *r.v.*  $X$  has a known PDF (described by  $f(x)$ ), then  $E[X]$  can be computed by:<sup>2</sup>

$$\mu_X = E[X] = \int_{\text{all } x} x f(x) dx.$$

$E[X]$  can be thought of and is mathematically equivalent to the centroidal axis of the PDF.

#### MODE

The *mode* of a distribution is the value that occurs with the greatest frequency, or the value that is most probable. Thus, it is the peak of the PDF curve. A distribution may have one mode, more than one mode, or no mode. A distribution having only one mode is called *unimodal*.

#### MEDIAN

The *median* of a distribution is the value of the *r.v.* corresponding to a vertical line that divides the PDF into two parts having equal areas. That is, there is a 0.50 probability that the *r.v.* will take on a value greater than (or less than) the median value.

<sup>2</sup>The general definition for expectation is:  $E[h(x)] = \int_{\text{all } x} h(x)f(x)dx$  where  $h(x)$  is a function of  $x$ . The mean is a special case in which  $h(x) = x$ .

The mean, mode, and median all coincide for symmetrical PDF's. However, for asymmetrical PDF's, this will not be the case. Figures 2.2a and b illustrate the relationship between the mean, mode, and median for a distribution skewed to the right and a distribution skewed to the left, respectively. You should note that for the skewed distribution, the mean value is not the most probable value—the mode is. Often in deterministic studies, we think of the single value estimate as being the mean or average value. However, the mean is just one measure of central tendency of the distribution and may not necessarily be the best single value to use to characterize the distribution; the median or mode may be better (see also section 1.7 for additional discussion).

**Measures of Variability**— There are also three measures of variability. They are the *range* (the difference between maximum and minimum value), the *variance*, and the *standard deviation*.

**VARIANCE** A common measure of the dispersion of the distribution of the *r.v.*  $X$  about its mean is given by the *variance* of  $X$ :

$$\text{Var}[X] = \int_{\text{all } x} (x - \mu_X)^2 f(x) dx$$

If the variance is low, the values will be concentrated near the mean. If the variance is high, the values will be scattered over a wide range.

**STANDARD DEVIATION** The *standard deviation* measures how far a typical or average value of the *r.v.*  $X$  deviates from the mean. It is computed as the positive square root of the variance of  $X$ :

$$\sigma_X = \sqrt{\text{Var}[X]}$$

The units on the standard deviation are the same as the units on the *r.v.*

**COVARIANCE** The *covariance* between two random variables  $X$  and  $Y$  is a measure of the stochastic dependence between  $X$  and  $Y$ . It is defined as:

$$\text{Cov}[X, Y] = E[(X - \mu_X)(Y - \mu_Y)]$$

**JOINT PROBABILITY DENSITY FUNCTION** When two random variables are being considered simultaneously, their joint behavior is described by a *joint probability density function*. Joint behavior need only be considered for LISA when the behavior of one random variable is dependent on another (for example,  $Cs'$  and  $\phi'$ , as discussed in section 4.2). A joint PDF is denoted by  $f_{X,Y}(x, y)$ .

**MARGINAL PDF** A *marginal* PDF describes the relative likelihood of values of one of the variables considered in a joint PDF, irrespective of the other. A marginal PDF is denoted by  $f_X(x)$ .

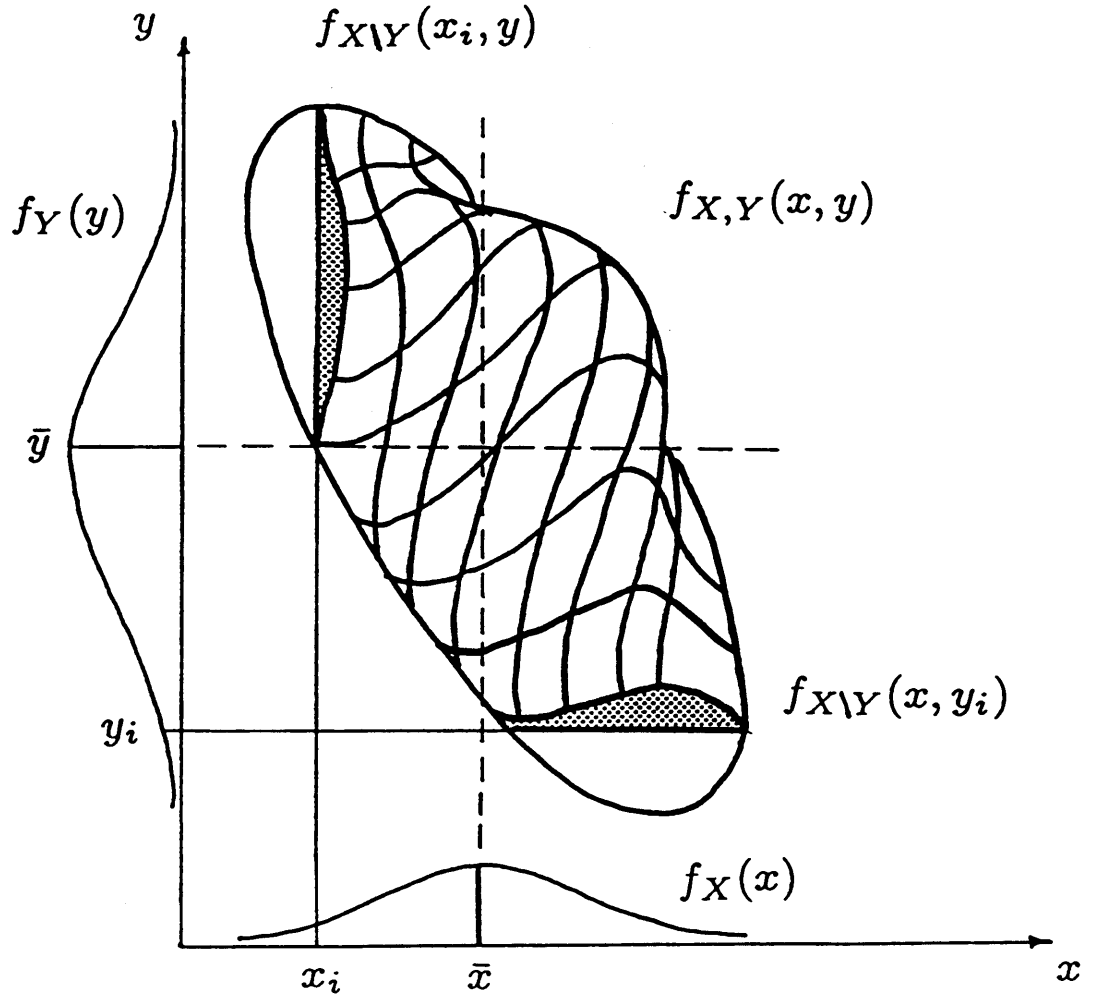


Figure 2.3—Joint PDF ( $f_{X,Y}(x,y)$ ) illustrating a negative correlation between two random variables. Also shown are the marginal PDF's ( $f_Y(y)$  and  $f_X(x)$ ) and the conditional PDF's at  $y_i$  ( $f_{X|Y}(x, y_i)$ ) and  $x_i$  ( $f_{Y|X}(x_i, y)$ ). Note that the shaded areas shown as conditional PDF's technically are not the true conditional PDF's because the area under each curve does not equal 1. To be true conditional PDF's, they need to be normalized by dividing by  $f_X(x)$  or  $f_Y(y)$ . However, the shaded areas graphically represent the conditional PDF's.

CONDITIONAL  
PDF

A *conditional* PDF describes the relative likelihood of values of one variable when one value of the other variable is given. A conditional PDF is denoted by  $f_{X|Y}(x, y_i)$ .

The joint, marginal, and conditional PDF's are illustrated in figure 2.3.

MEAN AND  
STANDARD  
DEVIATION OF  
A STATISTICAL  
SAMPLE

In civil engineering and geology, the term *sample* means a single item, such as a soil sample. In statistics, the term *sample* means a set of items, test results, or values. To distinguish between the two meanings, the term *specimen* is preferred for an engineering or geological sample. Thus, we can speak of a sample of 20 soil specimens, or a sample of 25 slope measurements.

Generally,  $n$  specimens or measurements will yield one statistical sample. The mean of the sample,  $\bar{x}$ , can be calculated by:

$$\bar{x} = \frac{x_1 + x_2 + x_3 + \dots + x_n}{n}$$

where  $n$  is the number of data values. The standard deviation of the sample can be calculated by:<sup>3</sup>

$$s = \sqrt{\frac{\sum(x - \bar{x})^2}{n - 1}}$$

In LISA, as in most situations, the sample mean and standard deviation are used to estimate the population (true) mean and standard deviation when there are at least 30 data values. Thus:

$$\bar{x} = \hat{\mu}_X, \text{ where } \mu_X = E[X]$$

$$s = \hat{\sigma}_X, \text{ where } \sigma_X = \sqrt{\text{Var}[X]}$$

The  $\hat{\phantom{x}}$  denotes an estimated value.

COEFFICIENT OF VARIATION

The sample *coefficient of variation* ( $c_v$ ) is a dimensionless measure of dispersion and is equal to the ratio of the sample standard deviation to the sample mean:  $c_v = s/\bar{x}$ .

CORRELATION COEFFICIENT

The *correlation coefficient* ( $r$ ) is a measure of the *linear* dependence between two random variables. The value of  $r$  varies between  $-1$  and  $+1$ . A negative sign ( $-$ ) means a negative linear correlation, and a positive sign ( $+$ ) means a positive linear correlation between the two *r.v.*'s. The correlation coefficient is defined as:

$$r = \frac{\text{cov}[x, y]}{s_X s_Y}$$

If the *r.v.*'s  $X$  and  $Y$  are statistically independent, then their covariance, and  $r$ , are zero. However,  $r$  can be small even if their covariance is not small, such as in the case where  $X$  and  $Y$  are *nonlinearly* related. In addition, a high value of  $r$  can result for independent variables if, in a scatter plot, all of the values except one are clustered together, and the one outlier value lies well outside all the others. This is known as a spurious correlation. Therefore, it is highly recommended that you view a scatter plot of the data to ensure correct interpretation of the  $r$  value.

---

<sup>3</sup>Division by  $n-1$  instead of by  $n$  is required here because  $s$  is obtained using one calculated term ( $\bar{x}$ ), as well as using all of the data values. Thus, one degree of freedom is lost from the data set. In other words, if you were provided with 19 data values and  $\bar{x}$  for a sample with 20 observations; you could calculate the 20th value (using  $\sum(x_i - \bar{x}) = 0$ ). Thus, only  $n - 1$  of the data values are freely determined, and the  $n$ th value depends on the others.

The correlation coefficient can be calculated by taking the square root of the coefficient of determination ( $r^2$ ). The value of  $r^2$  is a number between 0 and 1 (inclusive) that describes the fraction of the variation in  $Y$  that is explained by the variation in  $X$ , and can be obtained from a least-squares linear regression between  $r.v.$ 's  $X$  and  $Y$ . The sign of  $r$  is the same as the sign of the slope of the line obtained from the regression.

**Important Relationships**—For a constant  $c$  and a random variable  $X$ ,  $E[cX] = cE[X]$ ;  $\text{Var}[X + c] = \text{Var}[X]$ ; and  $\text{Var}[cX] = c^2\text{Var}[X]$ . For two random variables  $X$  and  $Y$ ,  $E[X + Y] = E[X] + E[Y]$ .

## 2.2 Probability Distributions

The probability density functions (PDF's) used in LISA are described in this section. Formulas for the function ( $f(x)$ ), the mean ( $\bar{x}$ ), and the standard deviation ( $s$ ) of each distribution are given in the figures. These formulas are for user reference only; the parameters that LISA requires for each PDF are shown as USER INPUT. A shorthand notation for each distribution that is used in this manual is also shown. Note that the  $y$ -axis of the PDF curve is labeled  $f(x)$ ; that is, for a given value of the random variable  $X$ , the  $y$ -ordinate of the PDF curve will be given by the function  $f(x)$ . This function gives values for the  $y$ -axis such that the area under the PDF curve is exactly 1. Remember, the probability of a random variable taking on a value between two values is given by the area under the PDF curve between those values.

### 2.2.1 Uniform Distribution

The uniform distribution describes a random variable for which any numerical value between the upper and lower limit is equally likely to occur. The PDF of a uniform distribution has the shape of a rectangle as shown in figure 2.4. This distribution is appropriate when limited information is available allowing an estimate of the minimum and maximum values, but not an estimate of the distribution shape. An example is a soils inventory that describes soil depth as between 3 and 10 feet. The uniform distribution would, of course, also be appropriate when the sample data suggest a uniformly distributed variable.

### 2.2.2 Triangular Distribution

The triangular distribution has the shape of a triangle that can be symmetrical or skewed in either direction (fig. 2.5). As with the uniform distribution, the triangular distribution would be used when relatively limited information is available; however, enough information should be available to estimate a most likely value as well as a minimum and maximum value. Note that the probability of a value occurring close to the minimum or maximum value of a triangular distribution is small, in contrast to a uniform distribution in which the probability of a value close to the minimum or maximum value occurring is the same as for any other value. Therefore, it is advisable when using a triangular distribution to extend the minimum and maximum values slightly beyond those you would specify for a uniform distribution.

### 2.2.3 Normal Distribution

The normal, or Gaussian, distribution has the familiar bell-shaped symmetry about the mean (fig. 2.6) and is defined by the mean and standard deviation. Of the total area under the normal curve, 68.26 percent occurs between the limits of the mean plus 1 standard deviation and the mean minus 1 standard deviation. This means that the probability of a normally distributed random variable having a value between the limits of the mean  $\pm 1$  standard deviation is 0.6826.

$$f(x) = \begin{cases} \frac{1}{b-a}, & \text{if } a \leq x \leq b; \\ 0, & \text{otherwise.} \end{cases}$$

$$E[X] = \frac{a+b}{2}$$

$$\text{Var}[X] = \left(\frac{b-a}{\sqrt{12}}\right)^2$$

USER INPUT:  $a$  and  $b$

NOTATION:  $U[a, b]$

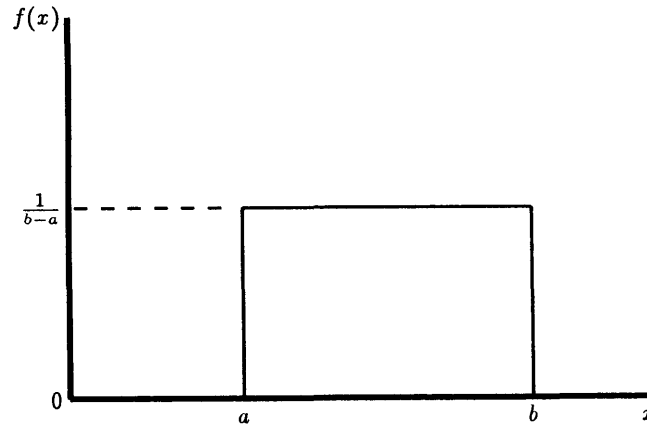


Figure 2.4—Uniform PDF.

$$f(x) = \begin{cases} \frac{2(x-a)}{(c-a)(b-a)}, & \text{if } a \leq x \leq b; \\ \frac{2(c-x)}{(c-a)(c-b)}, & \text{if } b \leq x \leq c; \\ 0, & \text{otherwise.} \end{cases}$$

$$E[X] = \frac{a+b+c}{3}$$

$$\text{Var}[X] = \frac{a(a-b) + b(b-c) + c(c-a)}{18}$$

USER INPUT:  $a$ ,  $b$ , and  $c$

NOTATION:  $T[a, b, c]$

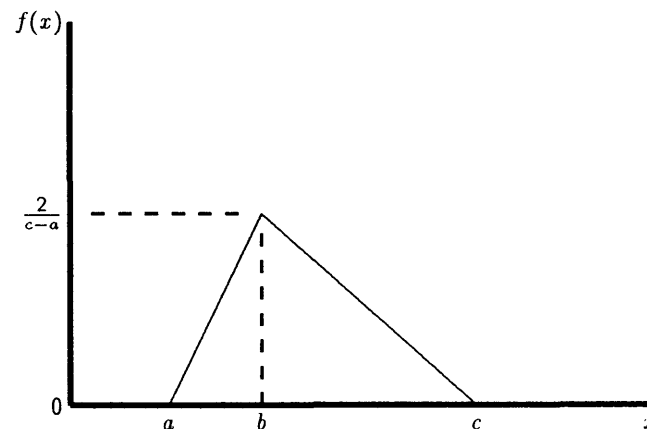


Figure 2.5—Triangular PDF.

Thus, when considering a sample data set, about 68 percent of the data points would be included in the interval defined by the mean  $\pm 1$  standard deviation if the random variable is normally distributed. Further, 95.84 percent of the total area under the curve is bound by the mean  $\pm 2$  standard deviations, and 99.72 percent by the mean  $\pm 3$  standard deviations.

Although the theoretical limits of the normal distribution are positive and negative infinity, LISA limits the distribution to  $\pm 3.09$  standard deviations (thereby sampling throughout 99.8 percent of the area under the normal PDF curve). These limiting values are indicated on the plot you obtain with the **Plot** option while viewing a data file (see part 2, section 3.10). Understanding these limits is helpful in estimating a realistic mean and standard deviation from limited information.

*A good rule of thumb for estimating the standard deviation of a normally distributed variable is to divide the range by 4.* For example, suppose that the forest soils inventory estimates that soil depths in a particular study area are in the range of 2 to 8 feet, and your past experience indicates that depths are likely normally distributed. A realistic mean and standard deviation would then be

$$f(x) = \frac{e^{-\frac{1}{2}\left(\frac{x-\mu}{\sigma}\right)^2}}{\sigma\sqrt{2\pi}}, \quad -\infty < x < \infty$$

$$E[X] = \mu$$

$$\text{Var}[X] = \sigma^2$$

USER INPUT:  $\hat{\mu}$  and  $\hat{\sigma}$   
 (approximately  $\bar{x}$  and  
 $s$  for large samples)

NOTATION:  $N[\bar{x}, s]$

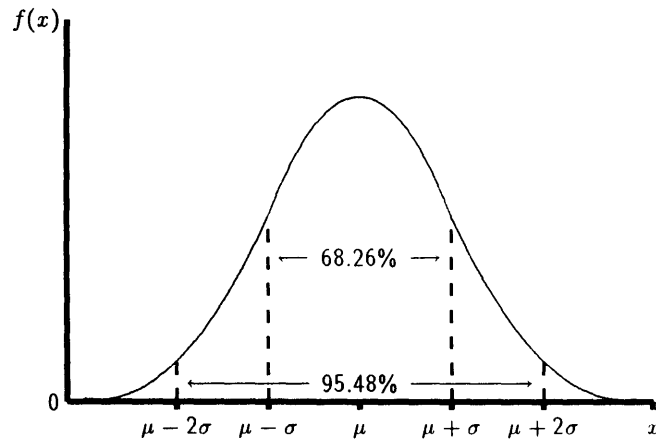


Figure 2.6—Normal PDF.

5 and 1.5 feet, respectively. LISA then will simulate values between 0.4 and 9.6 feet, with about 95 percent of the values between 2 and 8 feet.

If a standard deviation that is too large for a given mean is used, unrealistic endpoints for the normal distribution can result. For example, a normal distribution with a mean of 5 and a standard deviation of 3 will have limiting values of  $-4.3$  and  $14.3$  (at the mean  $\pm 3.09$  standard deviations). Obviously, negative values for the physical factors in the infinite slope equation make no sense. To prevent simulation of negative values, LISA will check the value at the mean  $-3.09$  standard deviations upon data entry, and if it is negative, LISA will display a warning message and wait for the user to enter values for the mean and standard deviation such that the value of the mean  $-3.09$  standard deviations becomes positive.

### 2.2.4 Lognormal Distribution

The lognormal distribution is skewed to the right, indicating there is a relatively small probability of large values for the random variable. Figure 2.7 illustrates the general shape of the lognormal distribution.

If a random variable,  $X$ , is lognormally distributed, the logarithms of the values of  $X$  are normally distributed. By taking the logarithms of the values and computing the mean and standard deviation of these transformed values, one can use a standard normal distribution table to compute probabilities. One also can compute the mean and standard deviation of the logarithms of the values of  $X$  directly using the following formulas:

$$\hat{\mu}_l = \ln \bar{x} - \frac{\sigma_l^2}{2}$$

$$\hat{\sigma}_l = \sqrt{\ln \left[ \frac{s^2}{\bar{x}^2} + 1 \right]}$$

where  $\bar{x}$  and  $s$  are the mean and standard deviation of the actual data values, and  $\hat{\mu}_l$  and  $\hat{\sigma}_l$  are the estimated mean and standard deviation of the log-transformed variable, respectively. To simplify input, LISA users enter only the mean and standard deviation of the actual data values,  $\bar{x}$  and  $s$ .

The shape of the lognormal distribution varies quite drastically with the coefficient of variation ( $c_v$ ). If the  $c_v$  is less than about 0.08, the lognormal distribution is nearly symmetrical and looks like a normal distribution. As the  $c_v$

$$f(x) = \begin{cases} \frac{e^{-0.5\left(\frac{\ln x - \mu_l}{\sigma_l}\right)^2}}{x \sigma_l \sqrt{2\pi}}, & \text{if } x > 0; \\ 0, & \text{otherwise.} \end{cases}$$

$$E[X] = e^{\mu_l + 0.5\sigma_l^2}$$

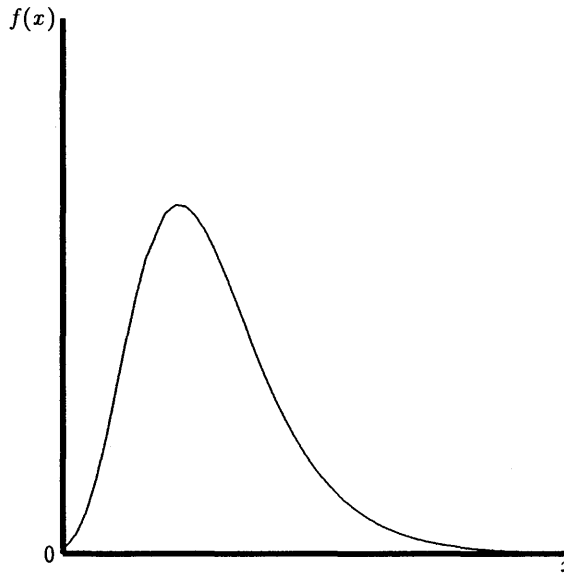
$$\text{Var}[X] = E[X]^2(e^{\sigma_l^2} - 1)$$

$$\mu_l = \ln(E[X]) - \frac{\sigma_l^2}{2}$$

$$\sigma_l^2 = \ln\left\{\frac{\text{Var}[X]}{E[X]^2} + 1\right\}$$

USER INPUT:  $\hat{\mu}$  and  $\hat{\sigma}$

NOTATION:  $L[\bar{x}, s]$



$\mu_l$  is the mean of the logarithms of the values of the random variable.  
 $\sigma_l^2$  is the variance of the logarithms of the values of the random variable.  
 $\hat{\mu}$  is approximately  $\bar{x}$  of the values of the random variable for large samples.  
 $\hat{\sigma}$  is approximately  $s$  of the values of the random variable for large samples.

Figure 2.7—Lognormal PDF.

increases, the lognormal distribution becomes skewed more strongly to the right. The lognormal distribution is defined from zero to positive infinity, but LISA limits the simulation to values of the transformed mean ( $\mu_l$ )  $\pm 3.09$  times the transformed standard deviation ( $\sigma_l$ ). These values are shown on the distribution plot using the **Plot** option in LISA. The plotting option is helpful in selecting a mean and standard deviation that will give the desired shape and minimum and maximum values (see sections 3.10 and 3.11 in part 2).

## 2.2.5 Beta Distribution

The beta distribution requires four parameters to describe it—a minimum value ( $a$ ), a maximum value ( $b$ ), and two shape parameters ( $P$  and  $Q$ ). The advantage of the beta distribution over some of the other distribution types is that the limits of the distribution are specified by the user, which eliminates the care required with the normal or lognormal distribution in the selection of a reasonable mean and standard deviation in order to obtain a realistic range of simulated values.

Also, the beta distribution can take on a wide variety of shapes; it can be skewed left, skewed right, or symmetrical, depending on the values of  $P$  and  $Q$ . In general, when  $P$  and  $Q$  are equal, the distribution is symmetrical; when  $P$  is greater than  $Q$ , the distribution is skewed left; and when  $P$  is less than  $Q$ , the distribution is skewed right. As the values of  $P$  or  $Q$  or both increase, the distribution becomes more peaked (greater kurtosis). Some of the possible shapes are shown in figure 2.8. Because the shape of the beta can be so variable, the **Plot** option in LISA is extremely useful in selecting appropriate  $P$  and  $Q$  values.

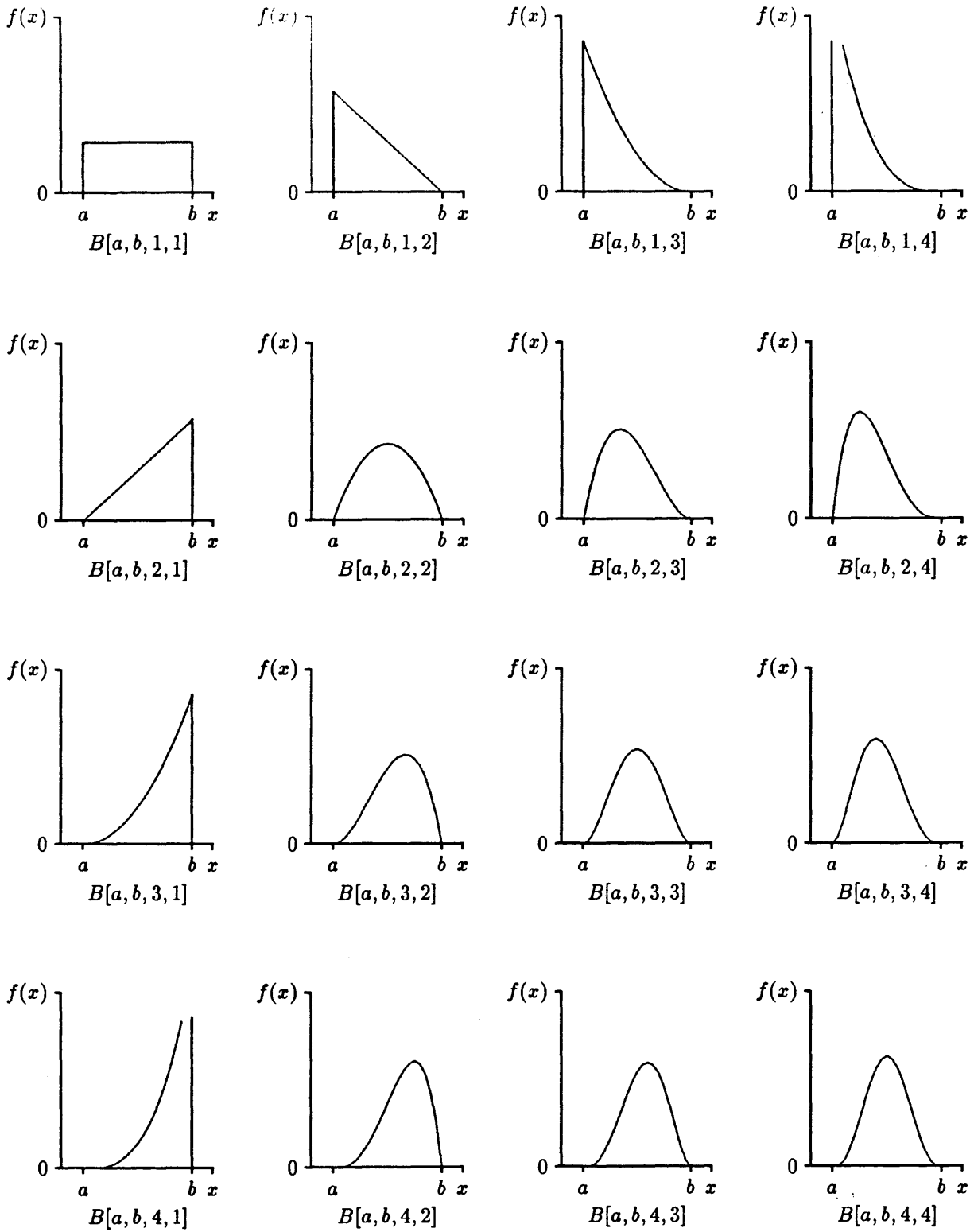


Figure 2.8—Beta PDF.

$$f(x) = \begin{cases} \frac{\Gamma(P+Q)}{\Gamma(P)\Gamma(Q)} \left[ \frac{(x-a)^{P-1}(b-x)^{Q-1}}{(b-a)^{P+Q-1}} \right], & \text{if } a \leq x \leq b; \\ 0, & \text{otherwise.} \end{cases}$$

$$E[X] = \frac{aQ + bP}{P + Q}$$

$$\text{Var}[X] = \frac{(b-a)^2 PQ}{(P+Q)^2(P+Q+1)}$$

$P$  and  $Q$  must be greater than 0.

$\Gamma$  is the complete gamma function:

$$\Gamma(a) = \int_0^{\infty} u^{a-1} e^{-u} du = (a-1)\Gamma(a-1).$$

When  $a$  is a positive integer, then  $\Gamma(a) = (a-1)!$ .

USER INPUT:  $a, b, P, Q$

NOTATION:  $B[a, b, P, Q]$

Figure 2.8—(Con.)

$P$  and  $Q$  also can be estimated from the sample mean ( $\bar{x}$ ) and standard deviation ( $s$ ) using the following equations:

$$\hat{P} = \frac{\frac{(b-a)^2}{s^2}c - (c+1)^2}{(c+1)^3}$$

$$\hat{Q} = \hat{P}c$$

where

$$c = \frac{b - \bar{x}}{\bar{x} - a},$$

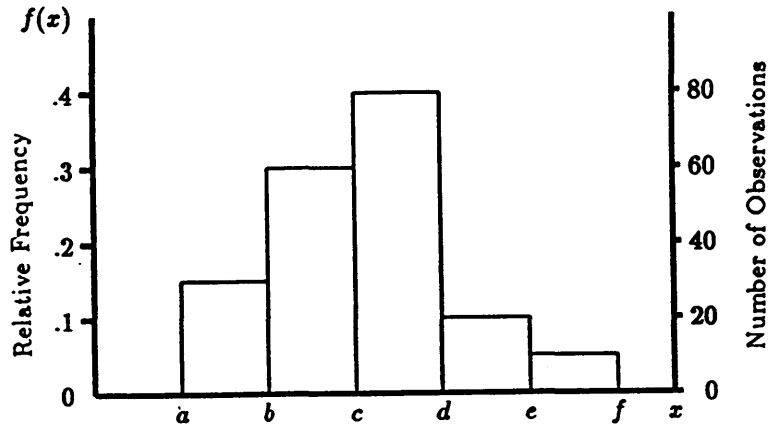
and  $a$  and  $b$  are the minimum and maximum values, respectively.

The disadvantage of using the beta distribution is that it requires approximately 20 to 30 times the computational time as do the other distributions. For example, it takes approximately 85 seconds to sample 1,000 values for the beta, while only 4 seconds for the other distributions on an 8.5 MHz machine with a math coprocessor; and 12 seconds for a beta while only 0.5 seconds for the others on a 20 MHz (80386) machine.

## 2.2.6 Relative-Frequency Histogram Distribution

A useful first step in selecting a PDF is to plot a histogram or relative-frequency histogram. This is done by grouping data into classes and then plotting a bar graph with the height of each bar equal either to the number of observations (to obtain a histogram), or to the relative frequency of observations (to obtain a relative-frequency histogram). The relative frequency is the number of observations in each class divided by the total number of observations. The histogram or relative-frequency histogram gives a good picture of the range and the distribution of data values. The relative-frequency histogram can be used directly in LISA, or the shape of the histogram or relative-frequency histogram might suggest another distribution that can be used to model the data.

Figure 2.9 shows an example histogram and relative-frequency histogram. Note that in LISA you enter the relative frequency expressed as a percentage.



$$f(x) = f_i = \frac{n_i}{n}$$

$$E[X] = \frac{1}{n} \sum_{i=1}^k f_i x_i$$

$$\text{Var}[X] = \frac{1}{n-1} \left[ \sum_{i=1}^k f_i x_i^2 - \frac{(\sum_{i=1}^k f_i x_i)^2}{n} \right]$$

where:

$k$  = number of classes

$n$  = total number of observations

$n_i$  = number of observations in the  $i^{\text{th}}$  class

$f_i$  = frequency of observations in the  $i^{\text{th}}$  class

$x_i$  = midpoint of the  $i^{\text{th}}$  class

Formulas apply only when classes are of equal widths

USER INPUT: Number of classes, values of class boundaries, percentage of observations in each class

NOTATION:  $H[k, f_1, f_2, \dots, f_k]$

Figure 2.9—A histogram PDF (right axis) and relative-frequency histogram PDF (left axis).

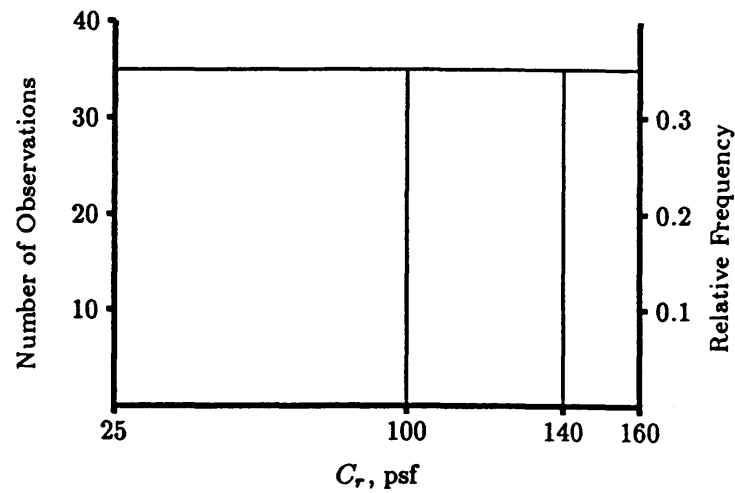
The relative frequency represents the probability of the random variable taking on a value in that class interval. Therefore, the percentages in all the classes must sum to 100 percent.

The appearance of the relative-frequency histogram can be affected significantly by the number and width of the class intervals used. Sturges (1926) suggests as a guide for selecting the number of classes of equal width

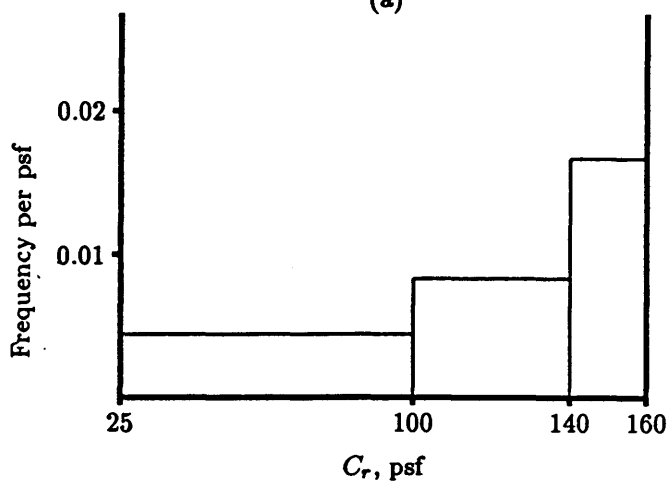
$$k = 1 + 3.3 \log_{10} n$$

where  $k$  is the number of classes and  $n$  is the number of data values. If too few classes are used, details of the shape of the data distribution will be lost. If too many are used, the histogram or relative-frequency histogram will appear erratic.

One comment on class width must be made. It can be convenient and is legitimate to use classes of unequal widths in the relative-frequency histogram. However, when unequal class widths are used, be aware that the relative-frequency histogram may give an incorrect picture of what the actual PDF looks like. This happens because the relative-frequency histogram is not a true PDF; that is, the *area* under the curve, computed as the sum of each class width times the frequency of observations in that class, does not, in general, equal 1. To obtain the true PDF, the frequency of observations in each class must be divided by the class width. This gives units on the  $y$ -axis of frequency per  $z$ , where  $z$  is in



(a)



(b)

Figure 2.10—A histogram and relative-frequency histogram with unequal class widths (a) and the corresponding frequency density distribution (b).

the units of the random variable, and gives the area under the curve equal to 1. This true PDF is called a frequency density distribution.

Let's take a simple example. Figure 2.10a shows a histogram and relative-frequency histogram for 99 measurements of root strength ( $C_r$ ) in which 33 measurements fall into each of three classes of unequal width. Notice that it looks like a uniform distribution. Figure 2.10b shows the frequency density distribution obtained by dividing 0.33, the relative frequency, by each class width. The shape of the distribution is drastically different, more like a triangular distribution. It is this true PDF that you see with the **Plot** option in LISA, and when you view the histogram of the simulated data after execution.

An example in which the use of unequal class widths is convenient is shown in figure 2.11. A soils inventory indicated that soil depths are predominantly between 24 and 48 inches with 15 percent of the landform having soils greater than 48 inches. Because the maximum soil depth is uncertain, several widths

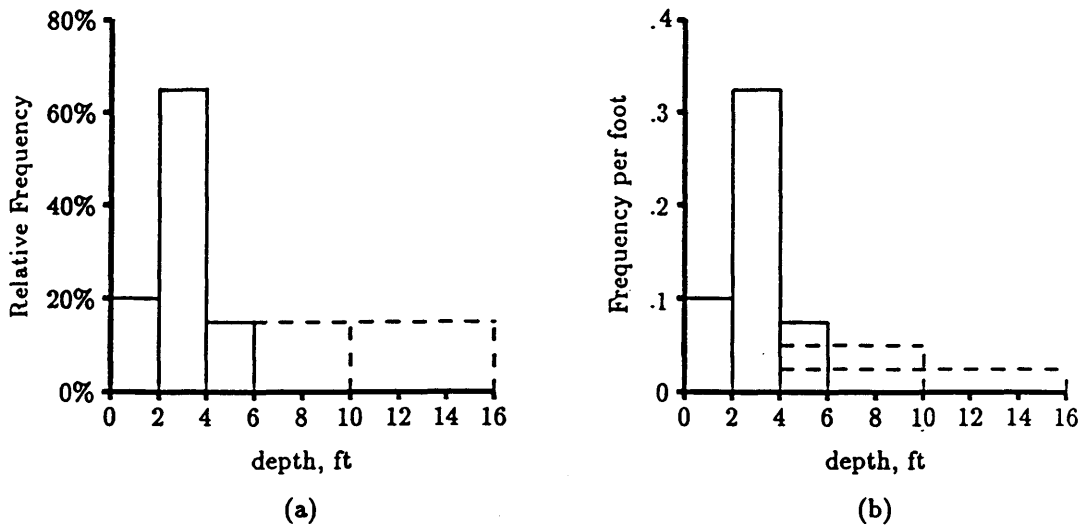


Figure 2.11—The relative-frequency histogram (a) and the frequency density distribution (b) for a histogram at three possible maximum values.

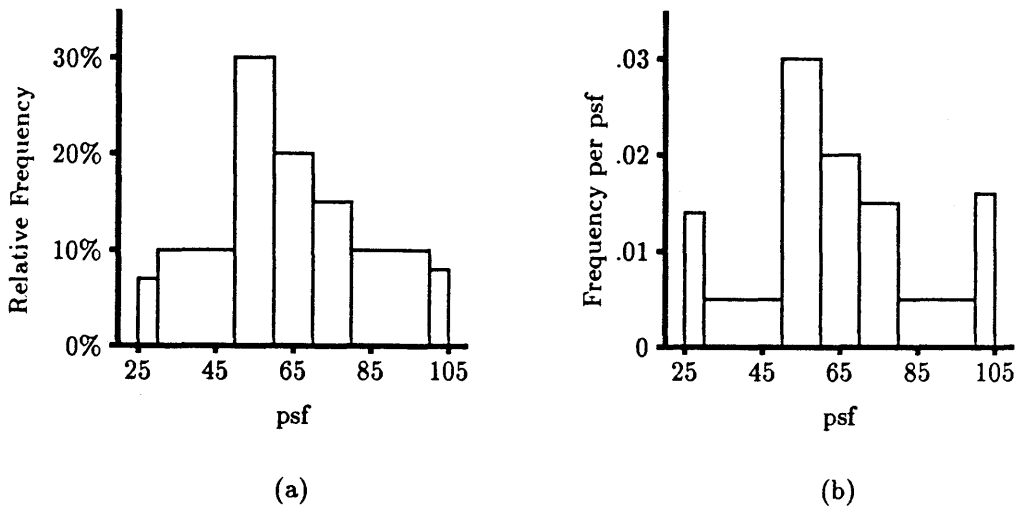


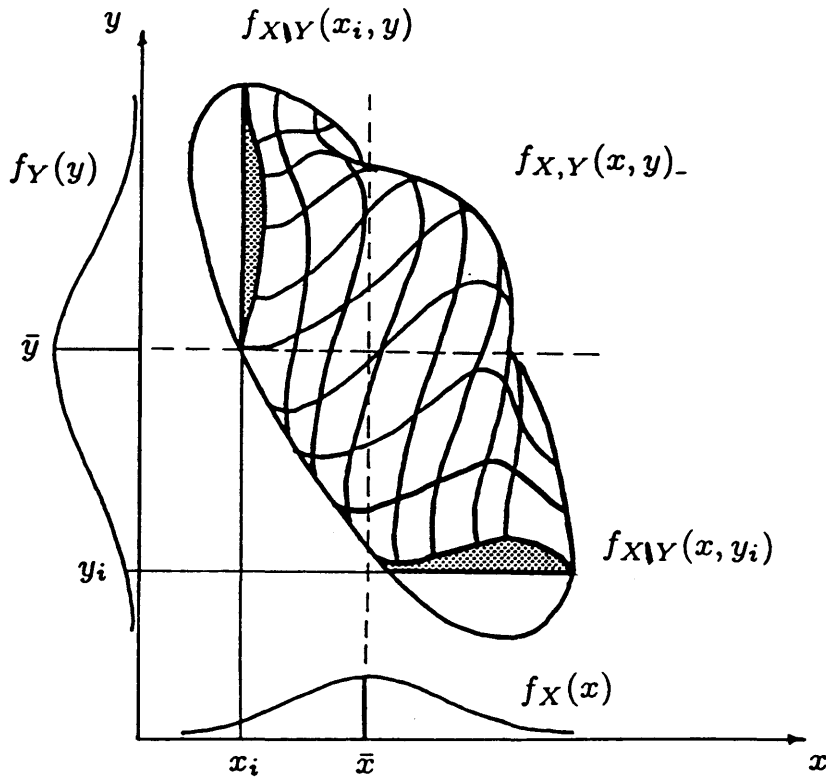
Figure 2.12—The relative-frequency histogram (a) and the frequency density distribution (b) for a histogram of unequal class widths.

for the last class might be used to evaluate the sensitivity of the probability of failure to the maximum value. Figure 2.11b shows the effect of class width on class height in the frequency density distribution.

Another situation in which the difference between the relative-frequency histogram and the frequency density distribution appears is the case of narrow classes on the end of the histogram, as illustrated in figure 2.12. Tacking on narrow classes with small frequencies is an easy fix to make percentages sum to 100 percent. Just be aware that this can cause LISA to sample more values in those classes than may have been intended.

### 2.2.7 Bivariate Normal Distribution

The bivariate normal distribution is a joint PDF that can be used to model the linear correlation between  $C'_s$  and  $\phi'$  (see section 4.2) and is available only for these two parameters. Figure 2.13 illustrates a bivariate normal PDF. The bivariate normal PDF is defined by specifying the normal marginal distributions



$$x = \phi' \quad y = C'_s$$

$$f_{X,Y}(x,y) = \frac{1}{2\pi\sigma_X\sigma_Y\sqrt{1-r^2}} \exp\left\{-\frac{1}{2(1-r^2)}\left[\left(\frac{x-\mu_X}{\sigma_X}\right)^2 - 2r\frac{(x-\mu_X)(y-\mu_Y)}{\sigma_X\sigma_Y} + \left(\frac{y-\mu_Y}{\sigma_Y}\right)^2\right]\right\}$$

$-\infty \leq x \leq \infty, -\infty \leq y \leq \infty$

$$E[X] = \mu_X \quad \text{Var}[X] = \sigma_X^2 \quad f_X(x) = \frac{1}{\sqrt{2\pi}\sigma_X} \exp\left[-\frac{1}{2}\left(\frac{x-\mu_X}{\sigma_X}\right)^2\right], \quad -\infty \leq x \leq \infty$$

$$E[Y] = \mu_Y \quad \text{Var}[Y] = \sigma_Y^2 \quad f_Y(y) = \frac{1}{\sqrt{2\pi}\sigma_Y} \exp\left[-\frac{1}{2}\left(\frac{y-\mu_Y}{\sigma_Y}\right)^2\right], \quad -\infty \leq y \leq \infty$$

USER INPUT:  $\bar{x}, s_X, \bar{y}, s_Y, r_{X,Y}$

NOTATION:  $BN[\bar{x}, s_X, \bar{y}, s_Y, r]$

Figure 2.13—A bivariate normal distribution.

for  $C'_s$  and  $\phi'$  (that is, the means and standard deviations) and the correlation coefficient ( $r$ ) between  $C'_s$  and  $\phi'$ .

## CHAPTER 3—THE INFINITE SLOPE MODEL

### 3.1 Description

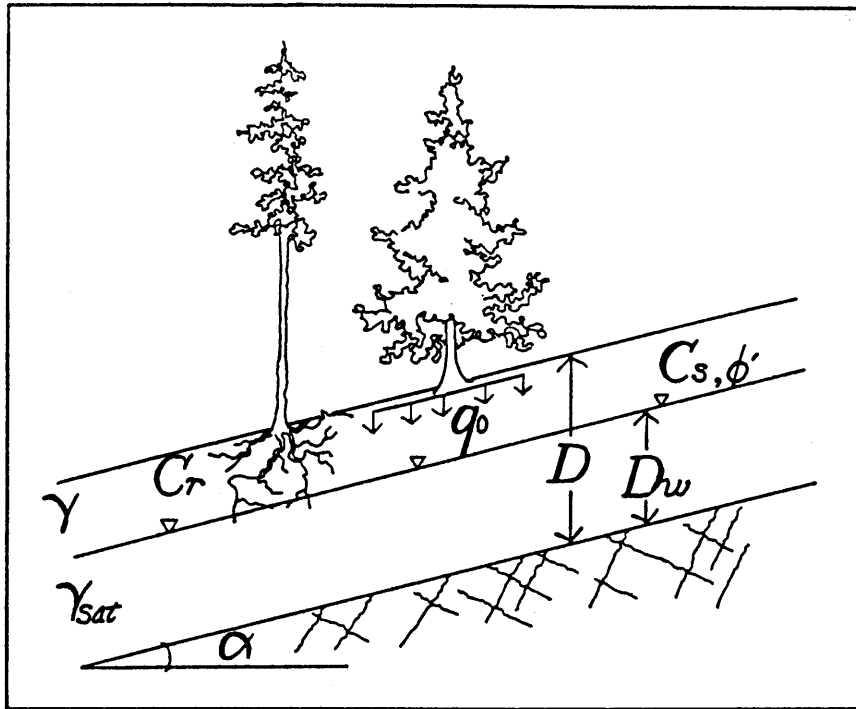
LISA uses the infinite slope stability model to calculate the factor of safety. The infinite slope model geometry and equation are shown in figure 3.1. Appendix A gives the derivation of the infinite slope equation. We selected the infinite slope model primarily because the model's simplicity allows for easy use in Monte Carlo simulation, not because of its accuracy. However, experience has shown that if used carefully, it does adequately analyze for planning purposes the most common failure types found in the mountainous West—debris flows and debris avalanches characterized by the failure of a soil mantle that overlies a sloping drainage barrier (Gray and Megahan 1981; Prellwitz and others 1983; Sidle and others 1985; Wu and others 1979). The drainage barrier may be bedrock or a denser soil mass. The factor of safety calculated by the infinite slope equation corresponds closely with that calculated for translational failures using a more rigorous method of slices, such as Janbu's Simplified Method. In general, the infinite slope equation, and therefore LISA, does not adequately analyze deep-seated rotational failure modes. However, the probability of rotational slope failures may be reasonably estimated using LISA if conditions that exist at the center of gravity of a failure mass are used in the analysis. The procedure for estimating the conditions at the center of gravity is described in detail by Prellwitz (1988), and an example application is given by Ristau (1988).

### 3.2 Assumptions

The infinite slope model relies on several simplifying assumptions. First, the failure plane and the groundwater (phreatic) surface are assumed to be parallel to the ground surface. The drainage barrier and ground surface often are found to be nearly parallel on colluvial slopes. Also, a large hydraulic conductivity contrast between the soil and drainage barrier can cause groundwater flow to be nearly parallel to the drainage barrier. Therefore, the conditions of parallelism often are approximately met. However, the user should be aware that parallel seepage may not be the case, and if not, the factor of safety may be significantly overestimated or underestimated, depending on the actual seepage direction (Iverson and Major 1987, 1986).

Second, the failure plane is assumed to be of infinite extent. Of course, in nature the failure plane does extend to the ground surface. Therefore, values for root strength and soil shear strength that reflect conditions along the true failure plane, not just along the drainage barrier, should be used. For example, when the infinite slope failure plane is beneath the root zone, implying no root strength, some root strength still should be used in the analysis to account for the true failure plane passing through the root zone to the ground surface along the lateral and head scarps. The values of root strength used should, however, be less than if the failure plane passed entirely through the root zone. Suggested root strength values for these different conditions are given in section 5.3.4.

Third, only a single soil layer is considered. In the case of multiple layers, the soil shear strength values occurring at the base should be given the most weight, but as with root strength, values should be adjusted (weighted) to account for the shear strength along the entire failure plane as it extends to the ground surface. For example, suppose 80 percent of the failure plane passed through soil



$$FS = \frac{C_r + C_s' + \cos^2 \alpha [q_0 + \gamma(D - D_w) + (\gamma_{sat} - \gamma_w)D_w] \tan \phi'}{\sin \alpha \cos \alpha [q_0 + \gamma(D - D_w) + \gamma_{sat} D_w]}$$

where FS = factor of safety

$\alpha$  = slope of the ground surface, degrees

$D$  = total soil thickness, ft

$D_w$  = saturated soil thickness, ft

$C_r$  = tree root strength expressed as cohesion, psf

$q_0$  = tree surcharge, psf

$C_s'$  = soil cohesion, psf

$\phi'$  = effective internal angle of friction, degrees

$\gamma_d$  = dry soil unit weight, pcf

$\gamma$  = moist soil unit weight, pcf

$\gamma_{sat}$  = saturated soil unit weight, pcf

$\gamma_w$  = water unit weight, pcf

Figure 3.1—The infinite slope equation and variables used in LISA.

with  $C_s' = 20$  psf and  $\phi' = 36^\circ$ , and 20 percent through soil with  $C_s' = 120$  psf and  $\phi' = 22^\circ$ . The weighted values then would be:

$$C_s' = 0.8(20 \text{ psf}) + 0.2(120 \text{ psf}) = 40 \text{ psf}$$

$$\phi' = 0.8(36^\circ) + 0.2(20^\circ) = 33.2^\circ$$

And last, the infinite slope equation is a two-dimensional analysis. Thus, the user must assume that a two-dimensional analysis is appropriate. Comparison of the infinite slope with a three-dimensional block model (Burroughs 1984) shows that the infinite slope model gives the same answer for blocks with widths greater than about 25 to 30 feet. Therefore, a two-dimensional analysis is most appropriate for wide blocks where resistance along failure sides is not significant relative to resistance along the base. If failures are narrower, the infinite slope model is conservative (it calculates lower factors of safety than does a three-dimensional analysis). A Monte Carlo simulation program using the three-dimensional model (called 3DLISA) is currently under development and evaluation at the Intermountain Research Station in cooperation with the University of Idaho and the Bureau of Land Management.

### 3.3 Sensitivity to Input Values

A sensitivity analysis of the infinite slope model is helpful to identify the most important variables and thus guide the user in expending time and money collecting information. One method for evaluating the sensitivity of the factor of safety ( $FS$ ) to each variable has been outlined by Simons and others (1978):

1. Select a realistic range of values for each input variable.
2. Calculate a base  $FS$  value using some central value for each variable, such as the mean, median, or mode value.
3. Vary the value for one input variable at a time over the range of realistic values and compute the  $FS$  values.
4. Plot the percentage of change in  $FS$  ( $\% \Delta FS$ ) relative to the base value against the percentage of change in each input variable relative to the central value ( $\% \Delta X$ ), where the percentage of change is calculated as:

$$\% \Delta FS = \frac{FS \text{ using } x_i - FS \text{ using central } x}{FS \text{ using central } x} \times 100\%$$

$$\% \Delta X = \frac{x_i - \text{central } x}{\text{central } x} \times 100\%$$

Figure 3.2 is a sensitivity plot for a selected set of central values. It is obvious from this figure that increasing soil and root strength will increase the  $FS$ , and increasing slope and groundwater-soil depth ratio (or groundwater height) will decrease the  $FS$ . Generally, the  $FS$  is most sensitive to slope and insensitive to soil unit weight, soil moisture content, and tree surcharge. ( $FS$  is so insensitive to the last three factors that they are not even shown on fig. 3.2.) Therefore, it is important to have good field estimates of slope, while unit weight, moisture content, and tree surcharge values can be estimated from the literature.

The relative sensitivity of the  $FS$  to the other variables will change depending on the central values selected. This is illustrated by figure 3.3, in which only the central value for soil depth has been changed from 10 feet in figure 3.2 to 2 feet in figure 3.3. The  $FS$  becomes more sensitive to soil and root cohesions and less sensitive to groundwater-soil depth ratio and  $\phi'$  when the central value for soil depth is decreased. The sensitivity of  $FS$  to soil depth is discussed in greater detail below.

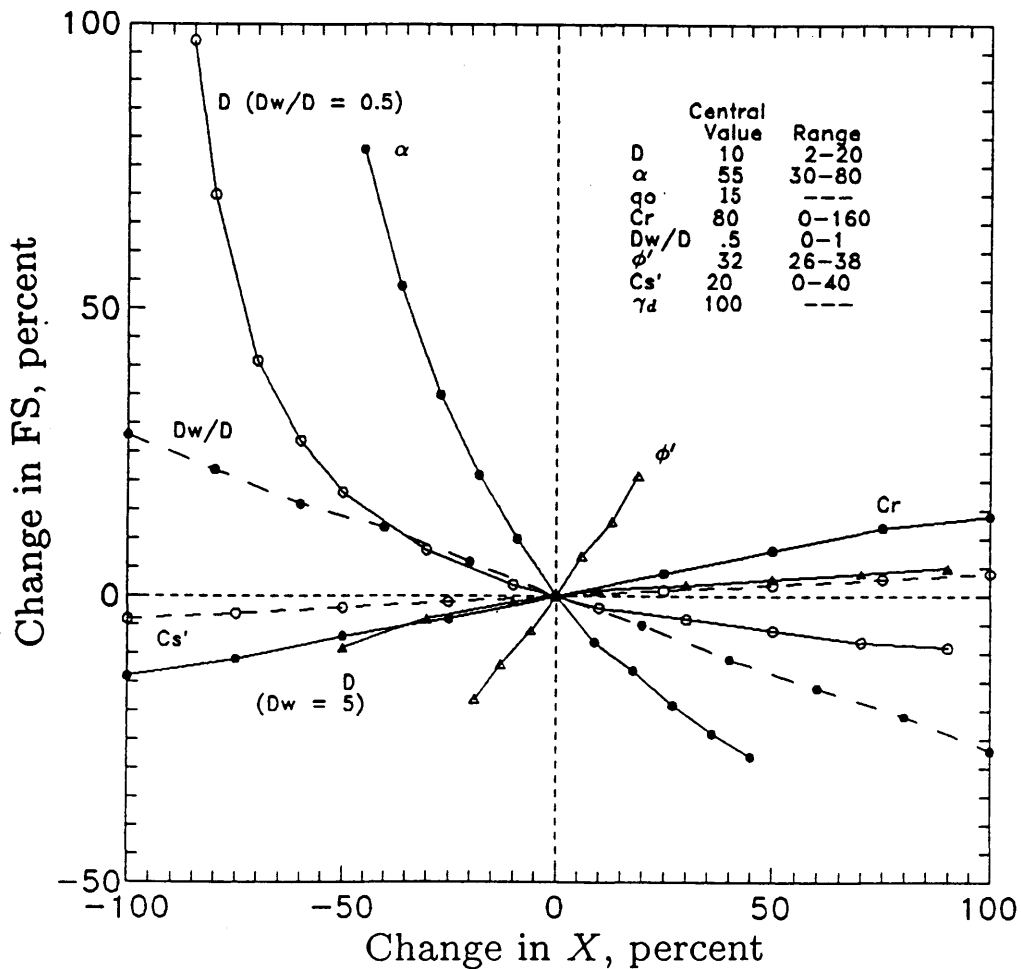


Figure 3.2—Example sensitivity plot for the infinite slope equation with central soil depth equal to 10 feet.

Other important sensitivity trends and interdependencies between variables should be noted.<sup>4</sup> Figure 3.4 shows that soil and root cohesions ( $C_r + C_s$ ) affect the factor of safety more on thin soils than on thick soils.<sup>5</sup> Another study (Sidle 1984a) shows that the sensitivity of  $FS$  to  $C_r + C_s$  is even more pronounced on steep slopes, particularly when the soils are saturated. Thus, altering  $C_r$  through timber harvest would affect the stability of thin, steep sites more than thick, gentle sites. Conversely,  $\phi'$  affects the  $FS$  more on thick soils (particularly with gentle slopes) than on thin soils (fig. 3.5). These trends should be expected, because frictional strength is more important in conditions of high

<sup>4</sup>Unless otherwise stated, the central values for figures 3.4 to 3.7 are the same as those used in figure 3.2. These figures show the percentage of change in  $FS$  relative to the lowest value of  $X$  used, rather than to the central value. Plotting in this fashion makes the trends easier to see.

<sup>5</sup>The resisting force in the infinite slope equation is expressed as:  $S = C_r + C'_s + \sigma'_n \tan \phi'$ . Because soil and root cohesions are added, the sensitivity of  $FS$  to each is the same. Thus, the sensitivity to cohesion, irrespective of whether it is from the soil or roots, can be examined by looking at the sum.

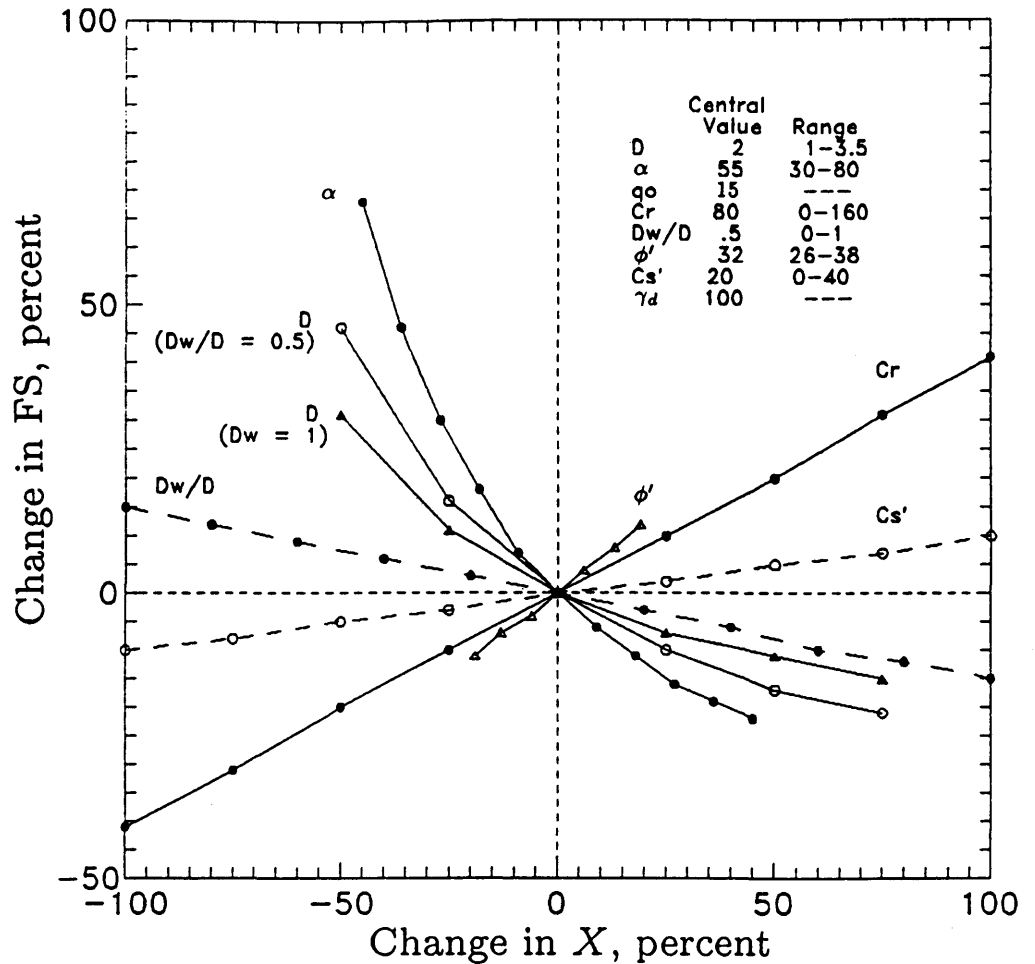


Figure 3.3—Example sensitivity plot for the infinite slope equation with central soil depth equal to 2 feet.

normal stress, and cohesive strength is more important in conditions of low normal stress.

The effect of soil depth ( $D$ ) on the  $FS$  depends on (1) whether or not there is soil or root cohesion and (2) how groundwater is handled in the analysis; that is, the effect of  $D$  on  $FS$  is different when  $D_w/D$  is held constant as  $D$  is varied than when  $D_w$  is held constant, because when  $D_w/D$  is held constant,  $D_w$  also varies. Although LISA uses  $D_w/D$ , it is informative to note the effects on  $FS$  caused by changing  $D$  with  $D_w$  held constant. The relative magnitude of these effects depends on slope, but the same trends occur on slopes between 20 and 150 percent, the range investigated by the authors.

Figure 3.6 shows the effects of changing  $D$  when there is *no* cohesion ( $C_r + C'_s = 0$ ). Three observations can be made:

- When there is *no* groundwater ( $D_w/D = 0$ ), there is *no change* in the  $FS$  as  $D$  varies. The change in driving force directly balances the change in resisting force. (The infinite slope equation for this case simplifies to  $FS = \tan \phi' / \tan \alpha$ , showing directly that  $FS$  is independent of  $D$ .)

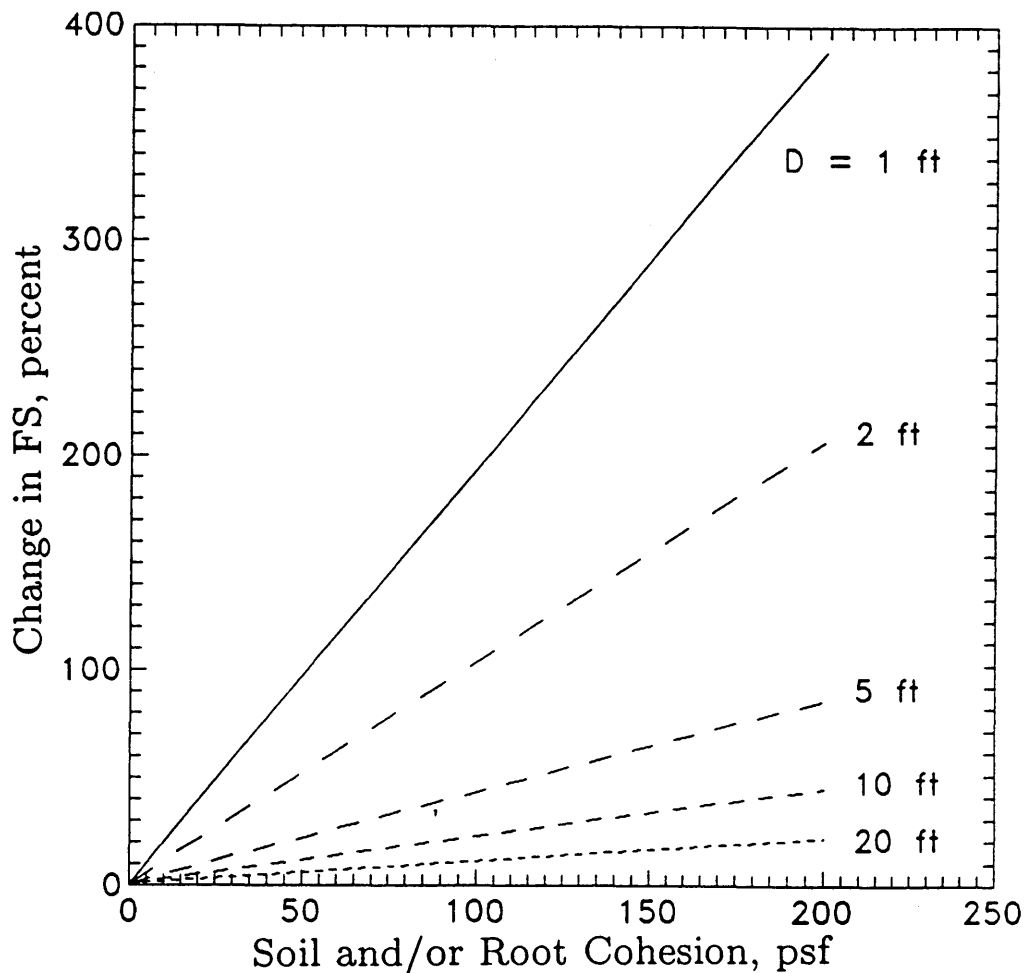


Figure 3.4—Sensitivity of  $FS$  to soil and root cohesion at various soil depths.

- When  $D_w/D$  is held constant at any value greater than zero,  $FS$  decreases slightly with increasing  $D$ .
- When  $D_w$  is held constant at any value greater than zero,  $FS$  increases with increasing  $D$ .

Figure 3.7 shows the effects of changing  $D$  when there *is* cohesion ( $C'_s + C_r > 0$ ). The variation in  $FS$  with changing  $D$  is quite different than when  $C'_s + C_r = 0$ .

- When there is *no* groundwater ( $D_w/D = 0$  or  $D_w = 0$ ), there is a fairly large decrease in  $FS$  with increasing  $D$ .
- When  $D_w/D$  is held constant at any value greater than zero, there is even greater decrease in  $FS$  with increasing  $D$ .
- When  $D_w$  is held constant, different effects on the  $FS$  with changing  $D$  are observed. For every set of central values, there will be one value for  $D_w$  for which there will be *no* change in  $FS$  as  $D$  varies (3.4 ft in fig. 3.7). For  $D_w$  values greater than this equilibrium value of  $D_w$ , the  $FS$  will *in-*

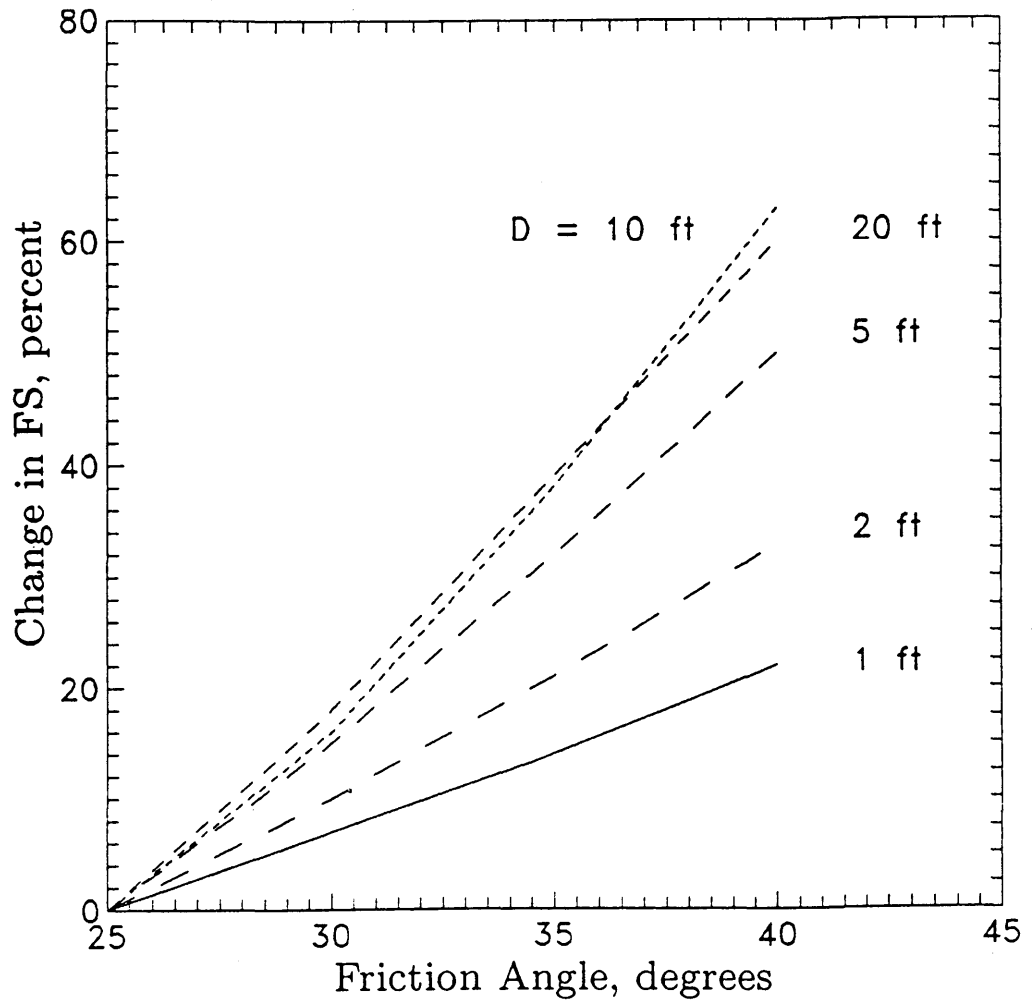


Figure 3.5—Sensitivity of  $FS$  to friction angle at various soil depths.

*crease* as  $D$  increases. For  $D_w$  values less than this equilibrium value, the  $FS$  will *decrease* as  $D$  increases.

Thus, the user should appreciate that whether the  $FS$  increases or decreases with changing soil depth, as well as the sensitivity of the  $FS$  to soil depth, depends on the groundwater and cohesion ( $C'_s + C_r$ ) values used. However, in general, it is wise to consider the  $FS$  sensitive to  $D$  and plan on spending some effort in obtaining reliable field estimates for  $D$  values.

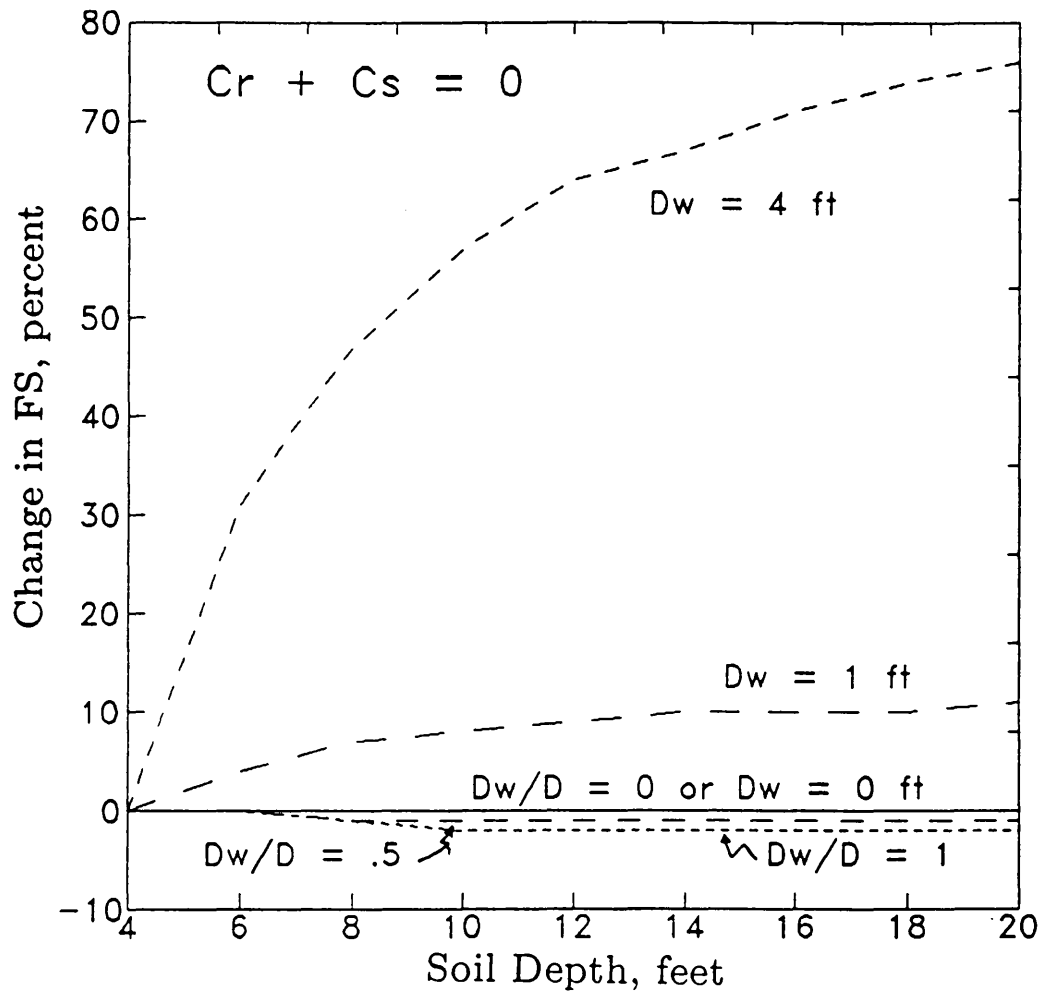


Figure 3.6—Sensitivity of  $FS$  to soil depth when there is no soil or root cohesion. Sensitivity varies depending on how groundwater is handled.

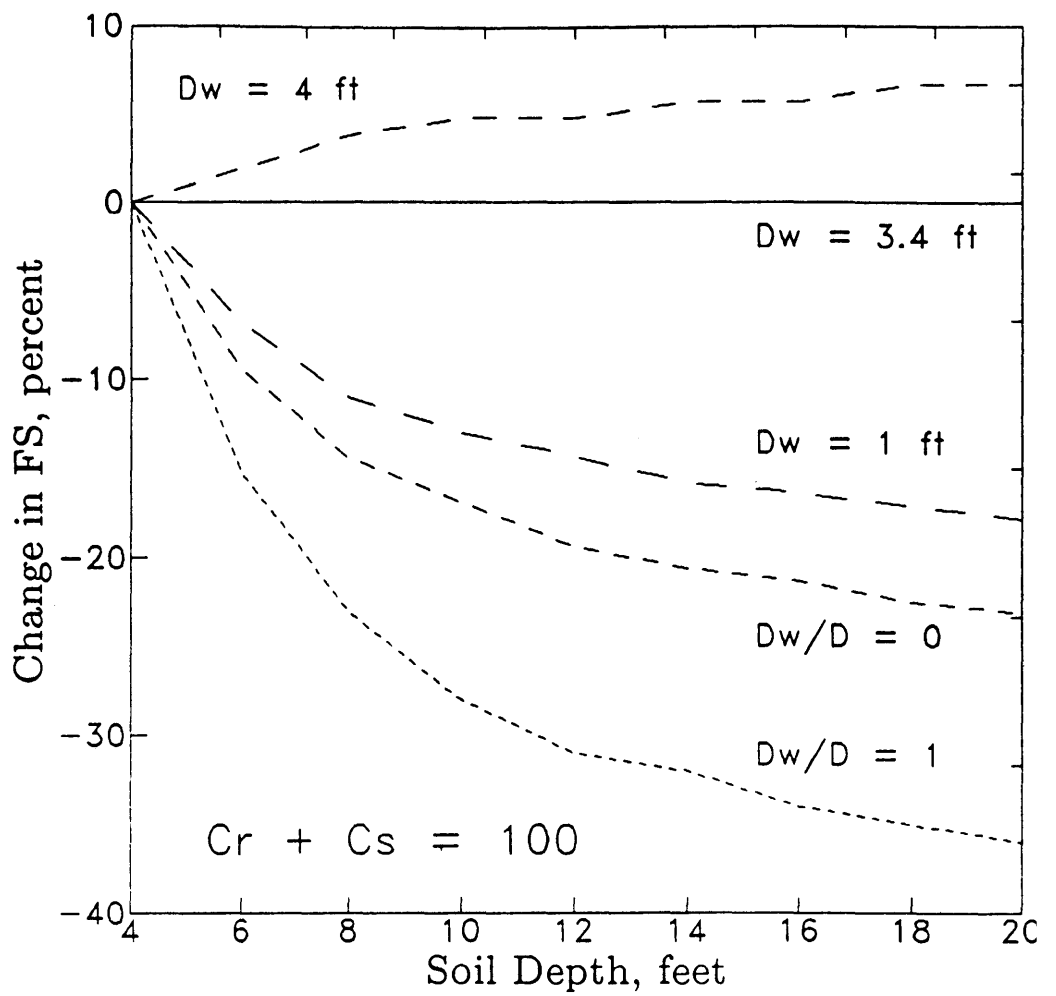


Figure 3.7—Sensitivity of  $FS$  to soil depth when there is soil or root cohesion or both. Again, sensitivity varies depending on how groundwater is handled.

# CHAPTER 4—HOW THE LISA PROGRAM WORKS (THE INSIDE NUTS AND BOLTS)

## 4.1 Overview

In general, the operation of LISA is as follows:

1. The user selects a distribution type for each input parameter in the infinite slope equation and then enters the values to describe that distribution. The user may choose a constant value or a uniform, normal, lognormal, triangular, beta, or relative-frequency histogram distribution. A bivariate-normal distribution also may be selected for  $C'_s$  and  $\phi'$ .
2. LISA generates a column of up to 1,000 values for each parameter. The number of values is specified by the user. The various procedures for simulating values from the distributions are beyond the scope of this paper, but procedures can be found in Abramowitz and Stegun (1965), Hall and Kendall (1992), Iman and Shortencarier (1984), Newendorp (1975), and Rubinstein (1981). A frequency histogram of the 1,000 values for each parameter will closely match the shape of the distribution specified by the user, but the 1,000 values are generated in a random order (unless they are correlated to another input parameter as discussed in section 4.2). LISA displays the minimum, maximum, mean, and standard deviation for each variable as the values are generated.
3. LISA then calculates the factor of safety for each set of generated values. The result is 1,000 possible realizations of the factor of safety, with relative frequencies being a result of the distributions used for each input variable. The minimum, maximum, mean, and standard deviation for the factor of safety and probability of failure are displayed.
4. The user then may view the frequency histogram of the factor of safety values and of the values simulated for each variable, and may view scatter plots of any pair of variables, or of a variable and the factors of safety.

Detailed descriptions of LISA operations are found in Part 2—Program Operation.

## 4.2 Correlation Between Variables

Some of the stochastic variables in the infinite slope equation are not independent. The relationship between these variables must be accounted for to achieve a realistic simulation of  $FS$  values. The variables treated as dependent by LISA are  $C'_s$  and  $\phi'$ , and  $\gamma_d$  and  $\phi'$ .

Although there exists some contradiction in the literature,  $C'_s$  and  $\phi'$  generally are considered to be inversely related, as illustrated in figure 4.1. Correlation coefficient ( $r$ ) values of  $-0.2$  to  $-0.85$  have been reported (Cherubini and others 1983). Figure 4.2 illustrates how treating  $C'_s$  and  $\phi'$  as independent variables could result in simulating unrealistic values of soil shear strength. Illustrated are three sets of shear strength tests on a particular soil, resulting in three Mohr-Coulomb failure envelopes that clearly show an inverse relationship between  $C'_s$  and  $\phi'$ . If LISA selected values of  $C'_s$  and  $\phi'$  independently, the highest value for each could be selected from the test data ( $C'_{s3}$  with  $\phi'_1$ ), and the upper dashed failure envelope shown in figure 4.2 could result. Obviously this failure envelope is outside the possibilities given by the test data and would result in shear strength values that are too high. Similarly, shear strength values that are too low also could be simulated using  $C'_{s1}$  with  $\phi'_3$  as illustrated by the lower dashed envelope in figure 4.2.

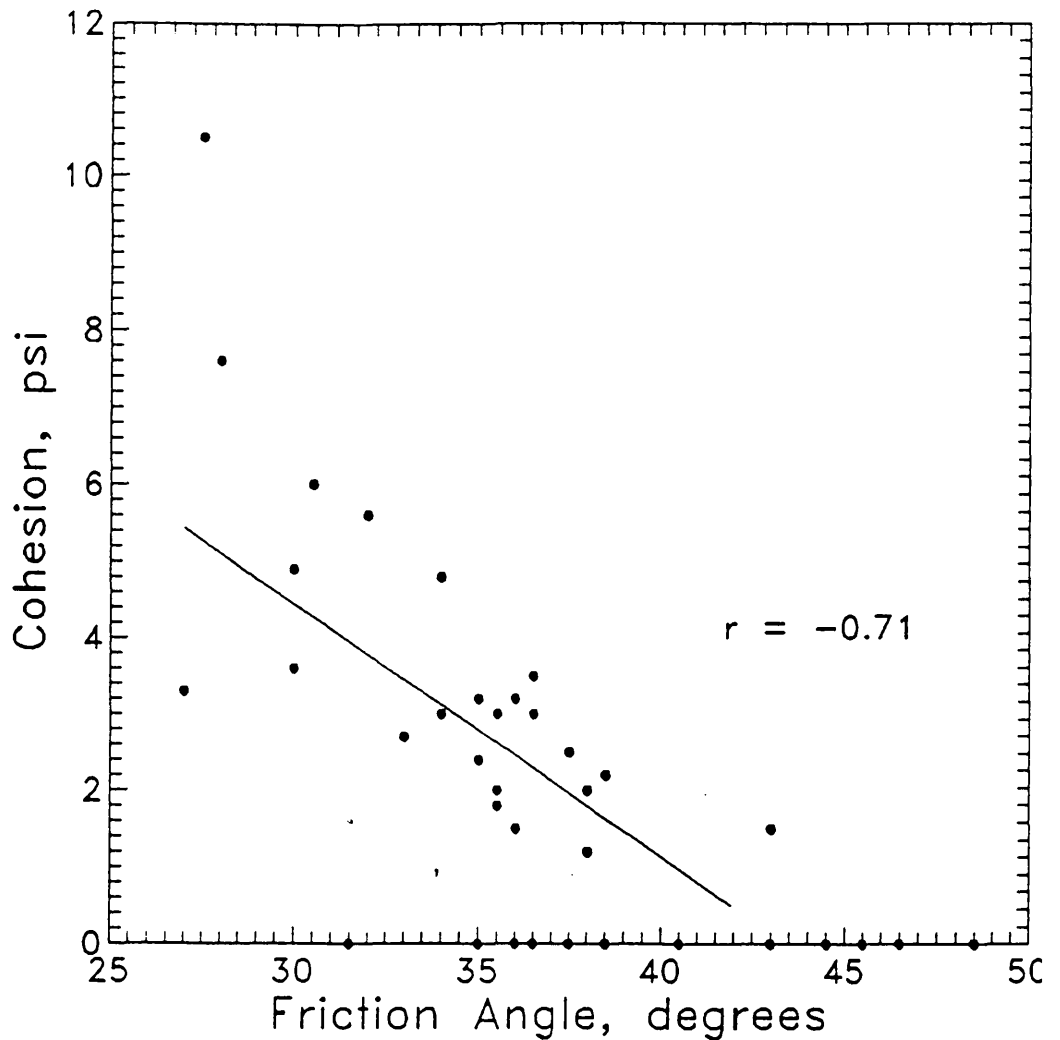


Figure 4.1—Illustration of the inverse relationship between  $C'_s$  and  $\phi'$  (data from Hampton and others 1974).

Figure 4.3a and 4.3b contrasts how larger negative values of  $r$  act to reduce the variance of simulated shear strength. Values for  $r$  may be obtained from laboratory data or estimated from the literature. Section 5.3.5.6 describes how to obtain values for  $r$ .

The second relationship considered by LISA is the positive correlation that exists between  $\gamma_d$  and  $\phi'$ . Figure 4.4 shows this correlation for a decomposed granitic soil. The correlation coefficient for this data set is +0.79. LISA handles this relationship simplistically by using the same random number to sample from the univariate distributions for  $\gamma_d$  and  $\phi'$ . Therefore, when a high value is sampled for  $\gamma_d$ , a high value is sampled for  $\phi'$  to model the desired proportional relationship. This method produces correlation coefficient between  $\gamma_d$  and  $\phi'$  of 0.95 to 1.0 (with 1.0 occurring when the same distribution type is used for both variables). This degree of correlation is much greater than is found in nature. However, because the infinite slope equation is insensitive to  $\gamma_d$ , the probability of failure values are affected only slightly (usually reduced slightly).

The same random number is *not* used to sample values for  $\gamma_d$  and  $\phi'$  when using the bivariate normal PDF for  $C'_s$  and  $\phi'$ . The reason for this is that the bivariate normal would most likely be used to model the shear strength of over-

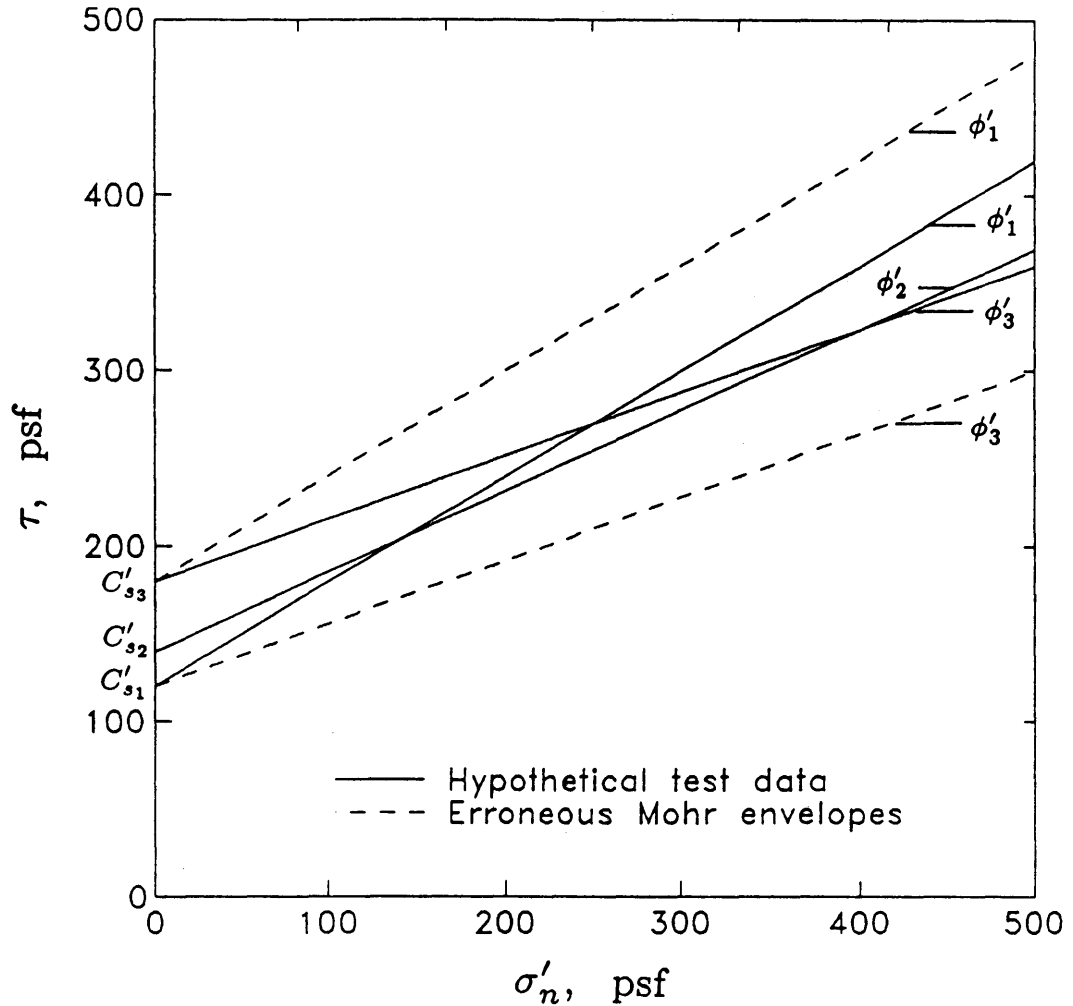


Figure 4.2—Independent sampling of  $C'_s$  and  $\phi'$  could result in unrealistic values of shear strength as illustrated by the dashed lines.

consolidated clay which typically shows a  $C'_s$ - $\phi'$  correlation due to curvature of the Mohr-Coulomb failure envelope (see section 5.3.5.3.2). Because of this curvature, it is unclear whether overconsolidated clay will exhibit a correlation between  $\gamma_d$  and  $\phi'$ .

Your field experience may lead you to believe that other variables in the infinite slope equation are correlated. For example, an inverse relationship between soil depth and ground slope is commonly observed. However, it is difficult to obtain a functional relationship that can be used to simulate this correlation without significant amounts of data. A correlation between variables can be accounted for somewhat by more detailed mapping of sites and use of distributions for each site which reflect the observed correlation. Figure 4.5 illustrates distributions for two hypothetical sites in a particular study area which reflect an inverse relationship between soil depth and slope. For individual Monte Carlo passes,  $D$  and  $\alpha$  values will be simulated independently, so that large  $D$  and  $\alpha$  values (for site 1, for example) certainly can be simulated on any given pass. However, for the entire simulation, many small  $D$  values will be simulated with large  $\alpha$  values, so that the inverse relationship will loosely hold for the site.

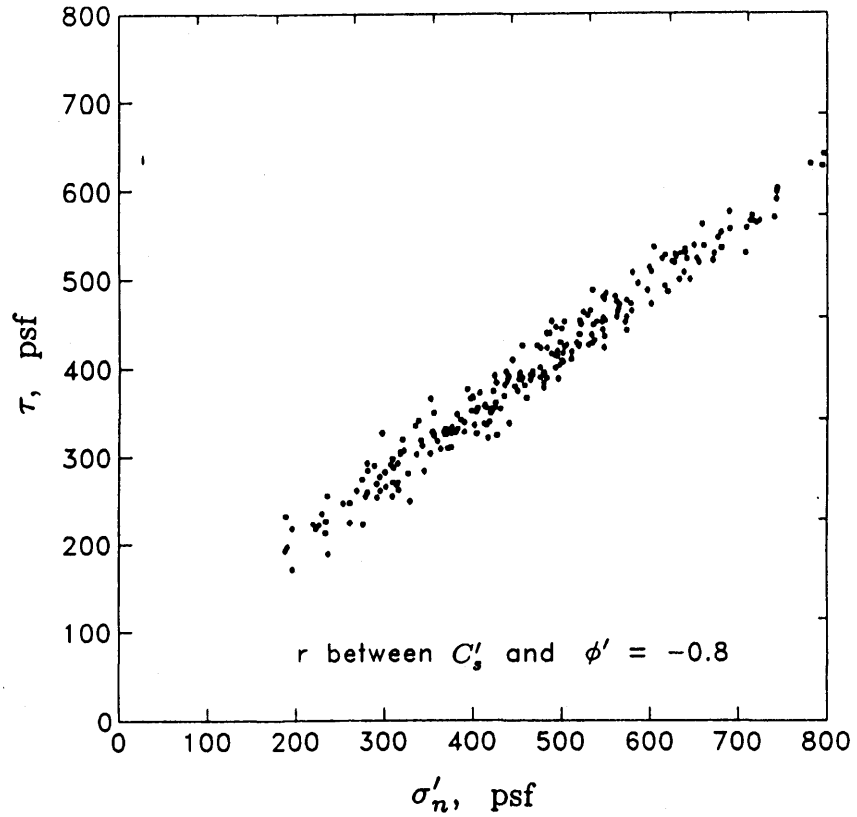
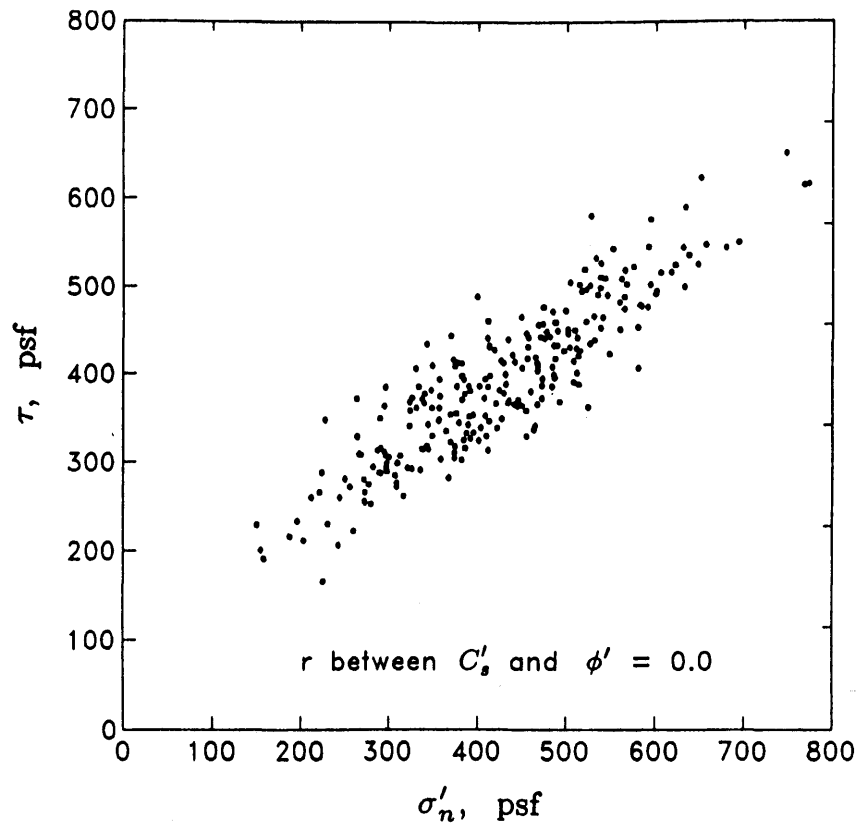


Figure 4.3—An inverse correlation between  $C'_s$  and  $\phi'$  reduces the variance of soil shear strength.

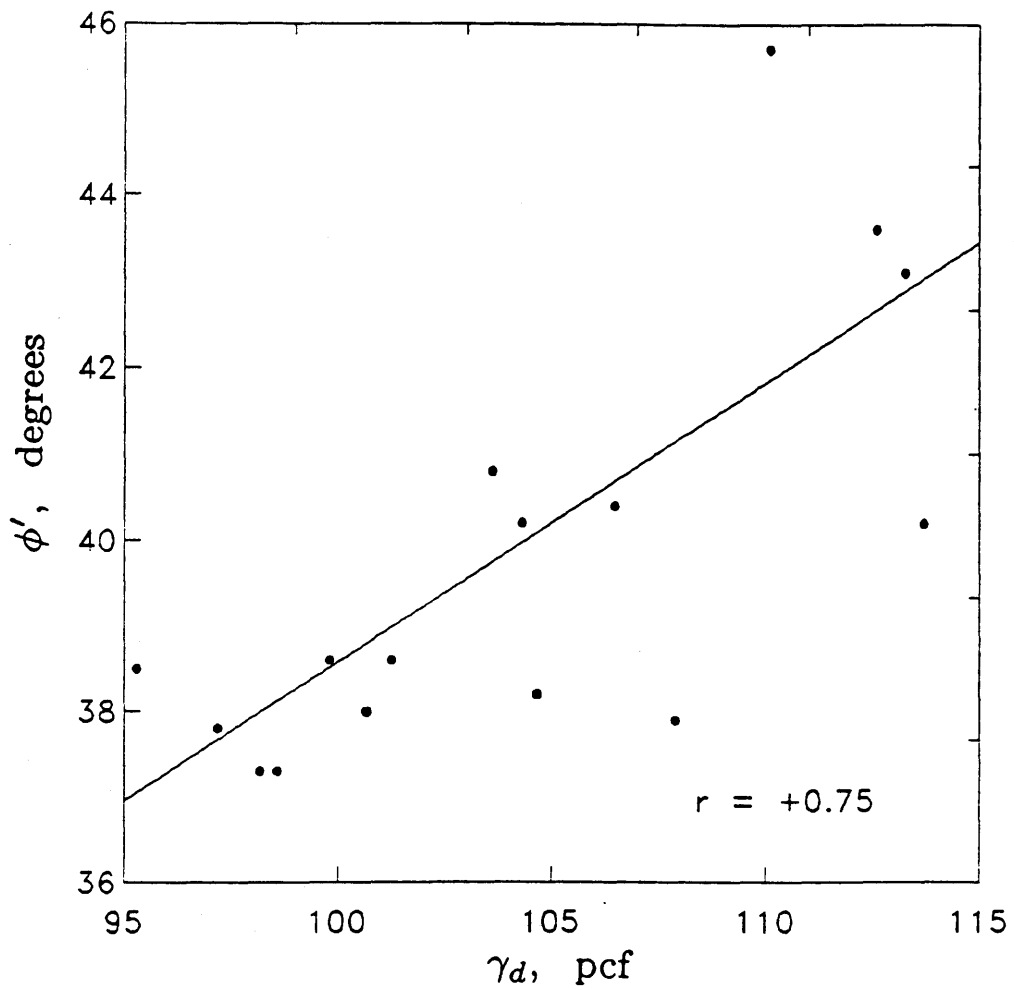


Figure 4.4—Example laboratory data illustrating a linear correlation between  $\gamma_d$  and  $\phi'$  (data from Hammond and Hardcastle 1991).

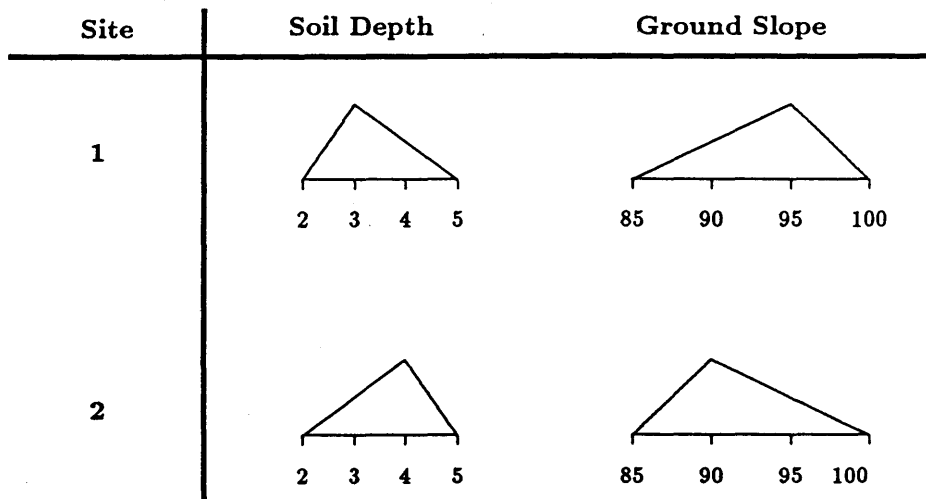


Figure 4.5—Distributions for two sites showing an inverse relationship between soil depth and ground slope.

Another method to account for a correlation between two variables on a given site is to analyze narrow enough classes for one variable so that within each class, the second variable can be considered to be independent of the first. The result is a conditional probability of failure for each class. For example, if slopes were analyzed in narrow classes, the results would be interpreted thus—“for areas of the site where the slope is between 45 and 55 percent, the probability of failure is 0.014, and for areas where the slope is between 55 and 65 percent, the probability of failure is 0.036.” The specific locations of each class on the site would not have to be known to use this procedure.

The conditional probability of failure for each class of the first variable can be multiplied by the probability of the variable being in that class to give a weighted probability of failure. The weighted probabilities of failure for all classes then can be summed to give the average, or expected, probability of failure for the entire site. (Note that the probabilities of the variable being in each class must sum to 1.)

A future version of LISA may allow the user to enter a functional relationship between selected variables, thereby accounting for correlation in a more rigorous manner.

### 4.3 Simulating Groundwater Values

To prevent simulating a groundwater height ( $D_w$ ) inconsistent with the simulated soil depth ( $D$ ) on any given pass, LISA simulates a value of groundwater-soil depth ratio ( $D_w/D$ ) from a distribution defined by the user. LISA then multiplies the simulated value of  $D_w/D$  by the simulated value of  $D$  to obtain a value of  $D_w$  to use in the infinite slope equation. Because the infinite slope model assumes a phreatic groundwater surface (see appendix A), LISA does not correctly calculate the  $FS$  if  $D_w/D$  values are negative or greater than 1, so effective stresses due to either capillary suction or artesian pressures cannot be analyzed. To prevent errors, LISA does not accept a distribution with  $D_w/D$  values that are negative or greater than 1.

### 4.4 Reproducibility of the Probability of Failure

If the user repeats a simulation with the same input PDF's but specifies a different seed number for the random number generator, LISA will simulate a different sequence of values for each random variable. This results in a different histogram of factors of safety and a slightly different value for the probability of failure. The more iterations (passes) used, the less the difference between simulation runs will be. The number of iterations required to provide consistent, stable results is a function of the shapes and ranges of the probability distributions used for each input variable.

Figure 4.6 illustrates how the variation between simulations decreases as the number of iterations in each simulation increases. In this example, 30 simulations were run with 100 iterations, then 30 simulations with 200 iterations, and so on up to 1,000 iterations, and the standard deviations of each set of the resulting 30 probabilities of failure computed. Clearly 100 iterations produce a large variation between simulation results, and the variation drops off rapidly with more than 200 iterations. ***In order to produce stable results, we recommend that 1,000 iterations, the maximum allowed by LISA, be used for all production work. Even with 1,000 iterations, there will be some variation between simulations. Therefore, we also recommend that several simulation runs be performed using the same input distributions and different random seeds (those***

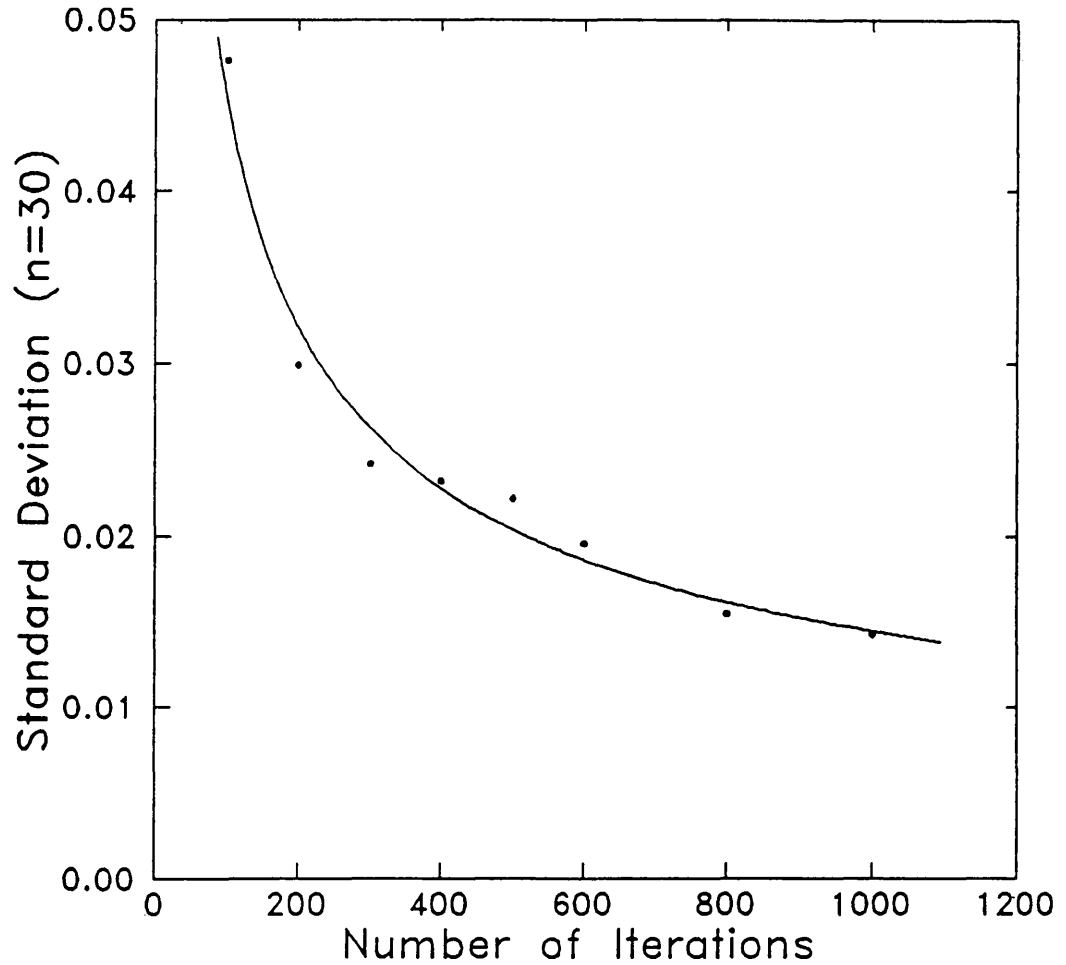


Figure 4.6—The standard deviations of 30 probability of failure values plotted against the number of iterations in each of the 30 simulations.

*generated by LISA), and that the range of probability of failure values obtained be reported.* This helps to reinforce the concept that LISA is a simulation that does not produce a unique “right” answer. Figure 4.7 illustrates typical amounts of variation in the probabilities of failure to expect from repeated simulations of 1,000 iterations. The amount of variation is proportionately larger for probabilities of failure that are smaller in magnitude, as demonstrated by the coefficients of variations.

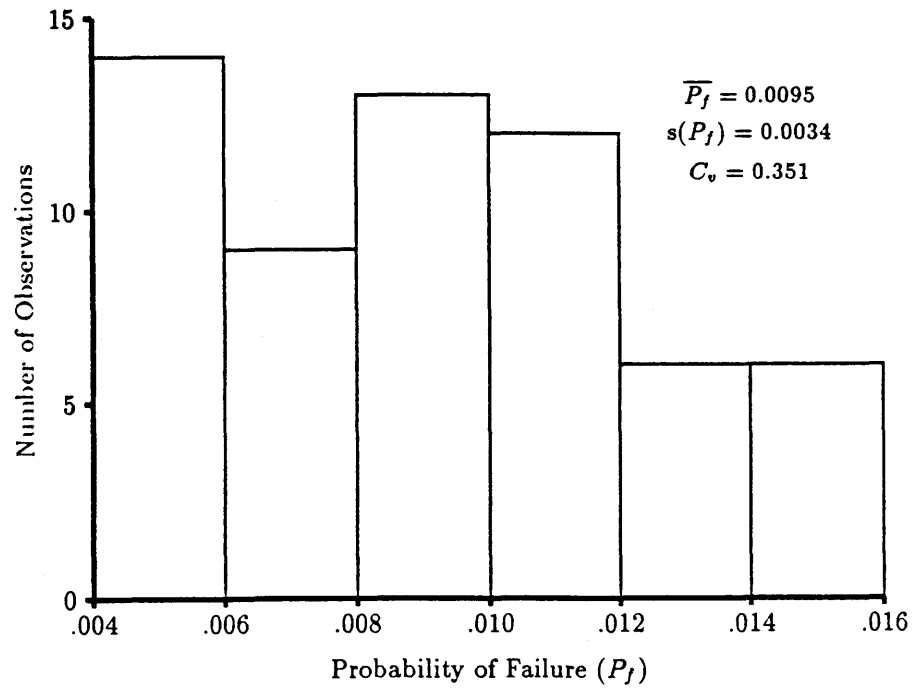
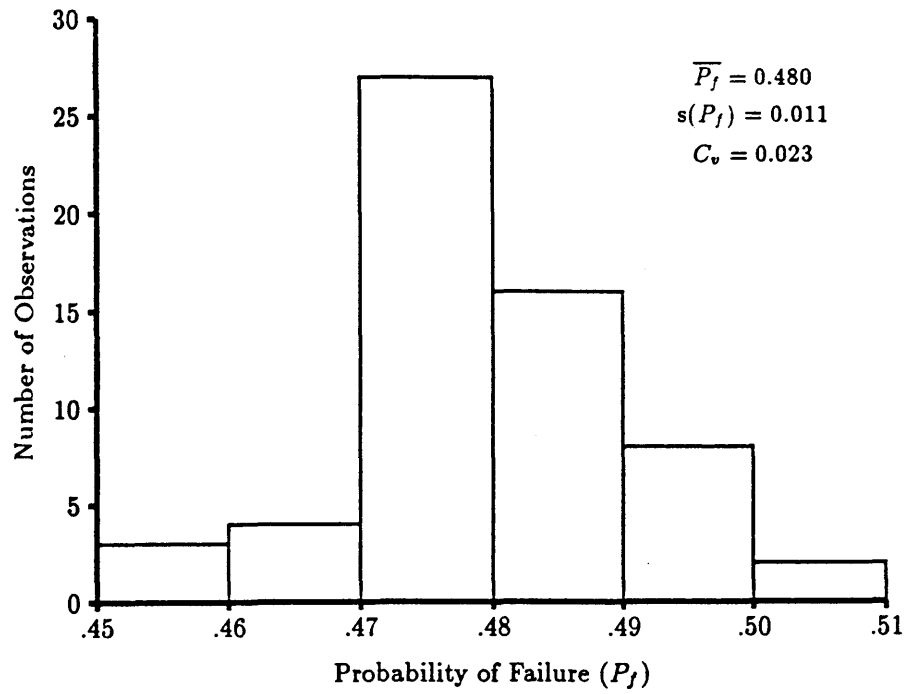


Figure 4.7—Illustrations of typical amounts of variation in probability of failure to expect with repeated simulations for two different sets of input distributions ( $n = 60$ ).

## CHAPTER 5—APPLYING LISA

### 5.1 Getting Started

#### 5.1.1 General

By definition, a Level I stability analysis is a broad, multiproject analysis intended to support planning-level decision making (Prellwitz 1985a). A Level I analysis will generally be performed for relatively large landforms using information gathered primarily from soils, geology, and other resource inventories, air photo interpretations, the scientific literature, and the user's knowledge of a particular area. Some field verification of input values and distributions used, and of the LISA results by comparison to the locations, numbers, and sizes of actual failures on this or similar landforms, should be made. The reliability of the analysis should be qualitatively assessed by reporting the source of the input data and the amount of field verification that was done.

When first using LISA, it is instructive to use the program on areas for which field information is available and the failure potential is fairly well known and understood. This should include both stable and unstable areas. This will give the first-time user practice in developing input distributions for a well-known area, a feeling for the range of probability of failure values to expect from LISA, and help in developing confidence in the analysis method and results.

Before running LISA for a particular study area, we recommend that the user perform sensitivity analyses using the DLISA program, which is described in part 2, chapter 4. Sensitivity analyses will aid the user in selecting ranges of input values that give the desired ranges in factors of safety and in identifying which variables are most important for that area. When possible, DLISA should be used to perform back-analyses on existing failures to estimate values for unknown variables—usually groundwater height, soil strength, and root strength.

#### 5.1.2 Delineating Polygons

A polygon, as used in this manual, is a piece of ground for which PDF's for each input variable need to be estimated for a LISA analysis, and can vary in size depending on the scope of the analysis. We suggest that for preliminary analyses, the user start with available polygons for which there is existing information. Examples include the land type map units delineated in Land System Inventories (LSI) used in the Northern Region of the Forest Service, U. S. Department of Agriculture; soil units delineated in the Soil Resource Inventories (SRI's) used in the Pacific Northwest Region; and geologic units delineated in the Geologic Resources and Conditions (GRC) maps, also used in the Pacific Northwest Region.

If these polygons are deemed inadequate or inappropriate, polygons should be delineated based on bedrock and surficial geology, and geomorphic landform. Further refinement could be made based on slope, vegetative cover, and groundwater characteristics. A polygon might also be some area of interest, such as a harvest unit.

#### 5.1.3 Using LISA for Level II Analyses

The infinite slope equation—thus, the LISA program itself—also may be applied to stability analyses for single projects; that is, an analysis of natural slopes or specific harvest units within timber sales that are anticipated (through a Level I analysis) to have stability problems. A stability analysis for project planning is, by definition, a Level II stability analysis (Prellwitz 1985a). The main difference between a Level I and Level II analysis of natural slopes is that typically a Level II analysis will have a greater quantity of field measurements and observations, and therefore a greater reliability in the results. The techniques discussed in section 5.3 also can be used to obtain the information for a Level II analysis.

One also could use the SARA (Stability Analysis for Road Access) program (Prellwitz and Hall 1992) to perform Level II natural slope analyses because it too performs a Monte Carlo simulation of the infinite slope equation. The intent of including the infinite slope equation in SARA is to allow users to analyze the stability of natural slopes along road locations prior to analyzing the stability of the road prism itself, because one would not want to locate a road on a slope that was inherently unstable. An advantage of using the SARA program for analysis of natural slopes away from road locations is that data files that are derived primarily from field observations and measurements (SARA data files) can be kept separate from data files derived primarily from inventory information (LISA files).

#### 5.1.4 Data Files and Map Unit Subdirectories

There are three types of LISA data files—site, material, and groundwater. Site files contain the PDF's for ground slope, soil depth, root strength, and tree surcharge. Material files contain the PDF's for soil unit weight, friction angle, cohesion, and moisture content above the phreatic surface. The groundwater file contains only the PDF for groundwater-soil depth ratio. The data are broken into these three categories to facilitate the analysis of various site conditions with a single material type.

The data files are stored on computer disk in a subdirectory with an .MPU extension. We call this subdirectory a "map unit." A map unit is nothing more than a mechanism for grouping data files and can represent whatever is convenient for the user. For example, a map unit might represent a landtype map unit (from a Northern Region Land System Inventory), a planning analysis area, or a timber sale.

### 5.2 Selecting Input Distributions—General Comments and Helpful Hints

For analysis of large landforms, statistical distributions that represent the spatial distribution of the values for each parameter are required. For example, in a particular landform, we estimate that 40 percent of the land area has soil depths between 2 and 4 feet, and 60 percent of the land area has soils depths between 4 and 8 feet. This spatial distribution could be represented by a frequency histogram with two classes. In a Level I analysis, the goal is not to determine where those soils depths are located on a particular piece of ground; this more site-specific information is obtained during a Level II or III investigation.

If measurements are available for any variable, the distribution selected can be whatever shape best represents the data. An initial step in this modeling process consists of plotting a relative-frequency histogram of the data using *equal* class widths. As stated earlier, this relative-frequency histogram may be used directly in LISA, or another distribution that generally fits the shape of the frequency histogram may be used. One may feel more comfortable using actual data in the form of a histogram. However, another sample set likely would have different frequencies. Also, unless the sample is large (more than 30 data values), it may not characterize actual field spatial variability, and use of a general statistical model may be more appropriate. Selection of a model can be done by visual comparison of the histogram of the data to a distribution shape plotted with the **Plot** option in LISA. With more than 30 data values, statistical tests for goodness-of-fit (such as the Chi-squared, K-S, or maximum likelihood) to the selected distribution can be performed. Benjamin and Cornell (1970) describe these techniques in section 4 of their chapter 4.

As mentioned in sections 2.2.1 and 2.2.2, when you have few or no data, then information from resource inventories (LSI, SRI, or GRC), slope maps, and air photos can be used to estimate a realistic range of values (a uniform distribution) or a range and most likely value (a triangular distribution) for some variables. We also discussed in section 2.2.3 a method for estimating the values for the mean and standard deviation for a normal distribution given a range of values.

Keep in mind that resource inventories usually are based heavily on air photo interpretation with limited field checking. The level of mapping is such that inclusions of other contrasting mapping units may exist in any mapping unit. The Clearwater National Forest LSI states that these inclusions may make up 15 percent of the land area in any given mapping unit (Wilson and others 1983). Therefore, when using soil depths or slope ranges, or estimating values for shear strength parameters based on the soil type given for a mapping unit, it may be advisable to extend the range of values beyond what is given. For example, one might use a histogram with three classes: one class with 85 percent of the values in the range given for the mapping unit, and two classes, each containing 7.5 percent of the values, with ranges greater than and less than the given range. Also, keep in mind that ranges given for SRI and LSI map units generally apply to the whole Forest. These ranges could be modified by air photo interpretation or by limited field sampling within the area being analyzed.

There is a natural but incorrect tendency to select a single value for a variable in the absence of field data. Single values imply certainty and no variability, which is unlikely. When you have no field data, your uncertainty is greatest, and the uniform distribution, which generally has the highest variance for a given range of numbers, is probably most appropriate.

A few general comments should be made regarding the normal and triangular distributions. The normal (or Gaussian) distribution is probably the most widely used distribution in probability and statistics. It typically is used to describe a process in which values are scattered about one "true" value such as would be observed in repeated laboratory experiments on a single specimen. It is quite natural to think of variability of a natural factor as being symmetrical about the mean value, and therefore the tendency might be to select a normal, or a symmetrical triangular or beta distribution. But keep in mind that when describing the spatial distribution of a variable such as soil depth or slope, there is no reason that it has to be symmetrical about a central value, and asymmetrical distributions should be given serious consideration.

There are a few other things to keep in mind when using the triangular distribution. As mentioned in section 2.2.2, the probability of a value occurring close to the minimum or maximum value is small. Therefore, you should use a slightly wider range of values than you would for a uniform or a histogram distribution, as illustrated in figure 5.1.

Also, the triangular distribution may poorly represent highly skewed or gapped data, in that more values will be simulated in the intermediate range than occur in the data, as illustrated by figure 5.2. There are two schools of thought here. You might assume that, if you had more data, the triangle would "fill in," and the triangular distribution is appropriate. Or you might decide to model your data as closely as possible by using a relative-frequency histogram or a lognormal with a fairly large coefficient of variation.

In summary, the particular distribution you select to model the estimated values of data is largely a matter of personal preference and judgment based on

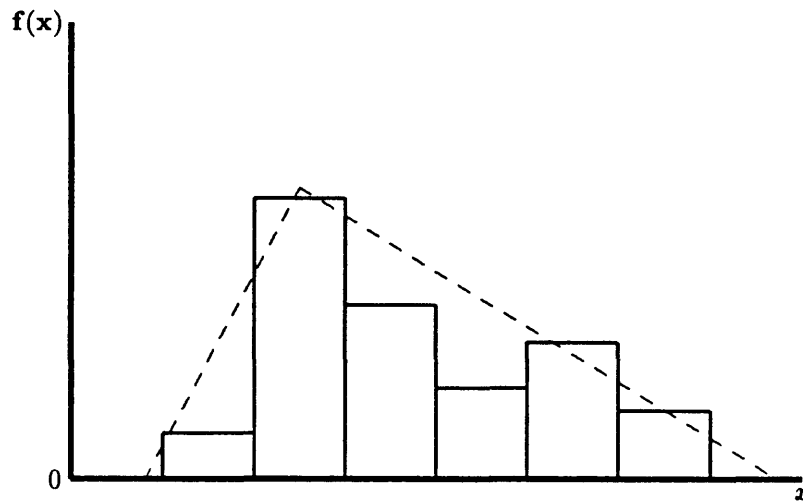


Figure 5.1—Extend the range of a triangular distribution compared to a uniform or histogram distribution.

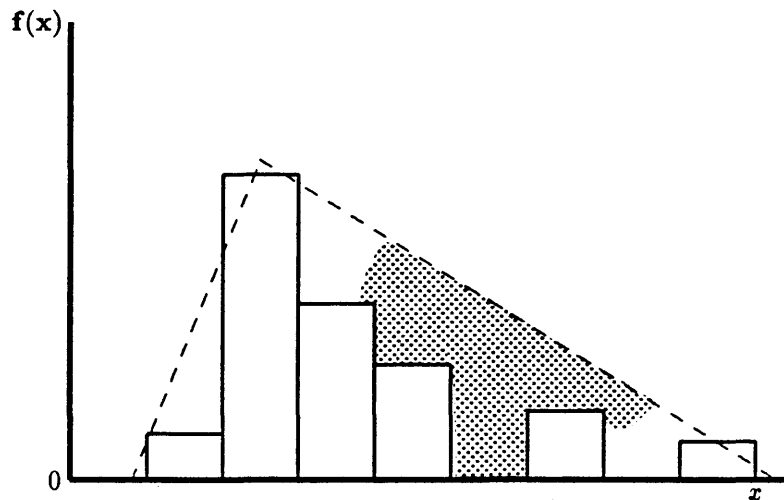


Figure 5.2—Triangular distribution may not represent highly skewed data well by oversampling values in the intermediate (stippled) range.

- your information and experience. *We strongly suggest that when more than one distribution is reasonable, or suggested by your information, you perform several simulations with each distribution and report the range of probabilities of failure obtained.*

### 5.3 Estimating Input Values and Selecting Distributions for Each Variable

Although the primary sources of information for developing distributions for a Level I stability analysis are resource inventories, geologic/soils maps, air photo interpretations, the scientific literature, and the user's experience and knowledge of a particular area, some data collection for verification of distributions

is recommended to lend credence to LISA results. *If field observations are to be made, at least 30 observations are needed to reasonably estimate the probability distribution of a given variable, although 10 to 12 observations could suffice if the user has field experience or knowledge of the variable.* This section is intended to provide guidance on data collection for slope, soil depth, and tree surcharge. In addition, possible values and distributions are discussed for tree surcharge, soil shear strength, tree root strength, and groundwater height, based on literature reviews.

### 5.3.1 Ground Slope

Within each polygon, slope measurements can be obtained from topographic maps. To avoid bias and to obtain a representative sample, it is recommended that a stratified random sampling scheme be used whereby a regular grid of cells is laid out over the polygon and a random location is selected within each grid cell. The ideal number of cells would be about 30 to 60, but 10 to 15 may suffice. At each location, the slope is calculated by using the map scale and contour interval. The slope values then are displayed in a histogram plot to assist the user in selecting an appropriate probability distribution to model the slope. Figure 5.3 illustrates a possible sampling grid. For smaller polygons, 30 to 60—even 10—cells may be impractical, requiring a different approach. In this case, measure a minimum, maximum, and most frequently occurring slope within the polygon to define a triangular distribution.

Through the use of digital elevation models (DEM's) or GIS (such as TIN in the ARC/INFO system), slope maps soon (or already) may be available. From these maps a histogram can be developed by measuring the percentage of the land area in the polygon that falls into various slope ranges (or classes).<sup>6</sup>

Because the factor of safety calculated with the infinite slope equation is quite sensitive to slope, some followup field measurements should be made. These measurements can be made using a hand-held inclinometer or Brunton compass and likely would be taken along roads or trails when the user is in the field gathering information on soil depth and vegetation cover.

Always keep in mind when making slope measurements that the surface slope is assumed to be parallel to the failure plane (commonly the soil-bedrock interface) in the infinite slope model. This assumption often is valid for some lateral extent, particularly in colluvial slopes. However, there may be field conditions where the ground surface is not parallel to the failure plane, such as with benched surface topography caused by glacial-fluvial or alluvial deposits over a planar bedrock surface. In this case, using the ground slope variations in LISA may be inappropriate; rather, estimates of the slope of the potential failure plane should be used. This slope might be observed in stream channels or by using an impact penetrometer (section 5.3.2). If rotational failures develop in the benches, using LISA with the conditions that exist at the center of gravity of the failure mass might be more appropriate (Prellwitz 1988).

### 5.3.2 Soil Depth

Soil depth does not necessarily mean the total thickness of unconsolidated material. It is common to apply the infinite slope model to conditions of a thin soil mantle overlying competent bedrock. In this case, soil depth is obviously the depth to bedrock. However, a translational failure plane may develop at any hydraulic conductivity contrast where positive pore water pressures can develop. Therefore, the depth to the failure plane may be much less than the depth to

---

<sup>6</sup>Information on existing digital elevation models can be obtained from: Western Mapping Center, National Cartographic Information Center, U.S. Geological Survey, 345 Middlefield Road, Menlo Park, CA 94025; phone (415) 329-4309, or FTS 459-4353.

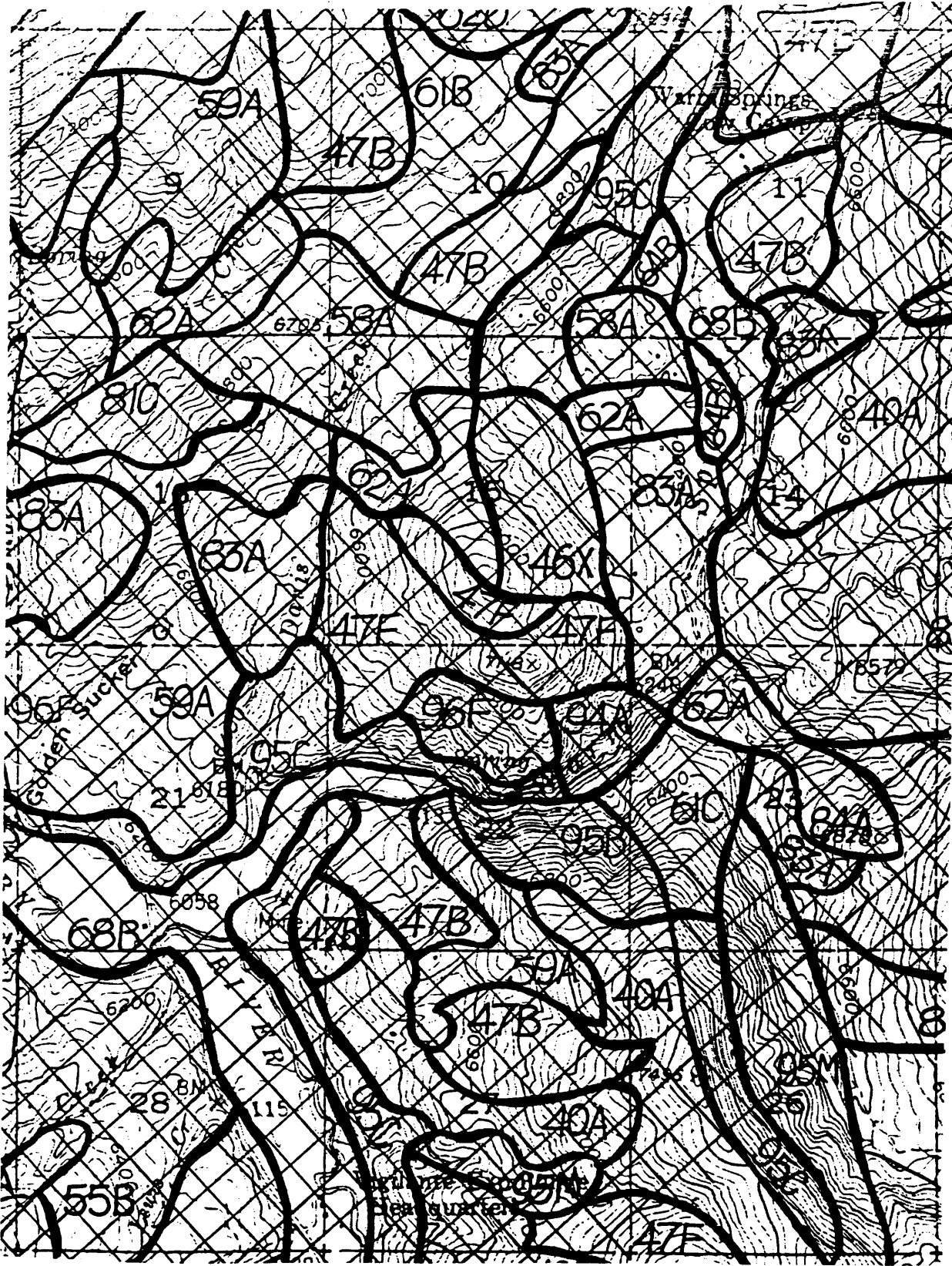


Figure 5.3—Stratified-random sampling grid for sampling ground slope.

competent bedrock. Examples of such conditions include loose near-surface soil in thick glacial or slope failure deposits, loose volcanics overlying denser soil layers, and loose colluvial soil overlying decomposed residual soil common in granitic terrane. *It is the depth to potential failure planes that should be described by the soil depth distribution.*

Initial estimates of the ranges in soil depth values usually can be obtained or inferred from resource inventories compiled by the forest soil scientist and geologist. The ranges then can be modeled with a uniform probability distribution. In most cases, some field measurements will be necessary to increase the reliability of the available soil depth information. Readily available locations for observing soil profiles include road cuts, ephemeral stream beds on valley side slopes, and root-throw pits formed at the base of blown-down trees. The latter two sources often will be accessible only on foot. If limited field reconnaissance is justified, then a hand-held, impact-driven soil penetrometer should be taken along to make as many soil depth soundings as time permits, ideally using a stratified random sampling scheme. When a stratified random sampling scheme is not feasible, then sampling can be done parallel to a road or along a given elevation contour or contours. In this situation, soil depth readings can be taken at regular intervals deemed appropriate by the investigator or at random locations within regular cells along the sampling trace.

Remember that the apparent soil depth measured as the slope distance along a cut face must be converted to vertical soil depth, as shown in figure 5.4. Seismic refraction is also a viable method for measuring soil depth. Also shown in figure 5.4 is the conversion for seismic refraction, which measures soil depth perpendicular to the refracting interface.

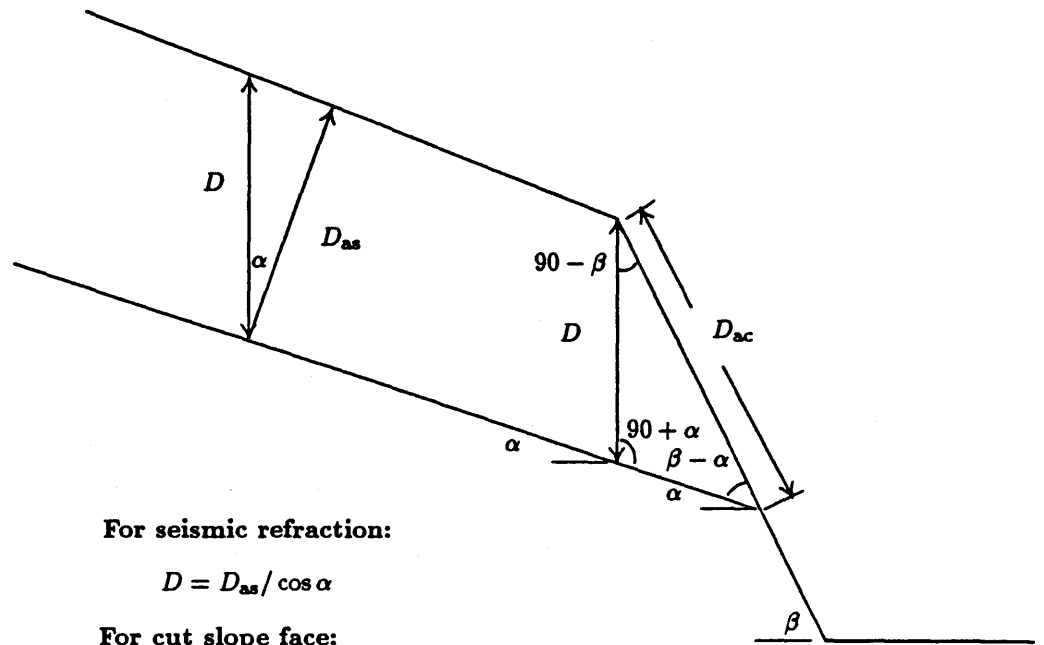
If bedrock cannot be observed or probed at a given sampling site, one can say that the soil is thicker than the observed soil depth. Likewise, if there are natural bedrock outcrops in the area, then the minimum soil depth should be considered negligible or nil. These observations, known as “soft data” or “inequality data,” can help bracket the range of soil depths in a polygon.

### 5.3.3 Tree Surcharge

As stated in section 3.3, the factor of safety calculated by the infinite slope equation is fairly insensitive to the value of tree surcharge ( $q_0$ ), particularly when soil depths are greater than 5 feet. Consequently, tree surcharge often is omitted from the infinite slope equation. When soil depths are less than 5 feet and especially when less than about 2 feet, the factor of safety may vary slightly with tree surcharge. Simons and others (1978) have shown that when  $C_s + C_r < 62.4D_w \tan \phi' \cos^2 \alpha$ , tree surcharge will have a positive effect on stability. Otherwise, tree surcharge will have a negative effect. Therefore, LISA includes tree surcharge so that its actual effect can be evaluated for any given set of field conditions.

Tree surcharge depends on the species, size, and density of the timber stand. Considering the weight to be uniformly distributed across the entire slope area is a common assumption for stability analysis (Greenway 1987; Sidle 1984a; Wu and others 1979). Estimates of equivalent uniform tree surcharge can be obtained from timber inventories of the volume of timber per acre and the weight per board foot of that timber. If the values given are for merchantable timber, they should be increased somewhat to account for the nonmerchantable volumes. The estimated range of tree surcharge values then can be modeled with a uniform distribution. An example calculation is shown below:

$$(3 \text{ to } 5 \text{ lb/bf}) \times (100,000 \text{ bf/acre}) \times (1 \text{ acre}/43,560 \text{ ft}^2) = 7 \text{ to } 12 \text{ psf}$$



For seismic refraction:

$$D = D_{as} / \cos \alpha$$

For cut slope face:

$$\text{from law of sines, } \frac{D}{\sin(\beta - \alpha)} = \frac{D_{ac}}{\sin(90 + \alpha)}:$$

$$D = \frac{D_{ac} \sin(\beta - \alpha)}{\sin(90 + \alpha)}$$

Figure 5.4—Conversion of apparent soil depth measured along a cut slope face ( $D_{ac}$ ) and apparent soil depth measured by seismic refraction ( $D_{as}$ ) to vertical soil depth ( $D$ ).

Gray and Leiser (1982) discussed a slightly different method for calculating tree surcharge. They considered a Douglas-fir stand in the Cascade Range of central Oregon that contained 50,000 to 65,000 board feet of merchantable timber per acre. At 10 lb/bf, the uniform surcharge would be 12 to 15 psf. If the weight of the trees is divided by the actual basal area of the trees (300 to 500 ft<sup>2</sup>/acre), the stress directly under a tree would be about 1,400 psf. They then assumed that the weight of the trees was distributed over 75-ft<sup>2</sup> circles spaced 30 feet apart in a cubic array. In this case, the 1,400 psf surface stress would produce a stress increase of 20 to 75 psf midway between trees at depths of 5 and 20 feet, respectively. They concluded that even with this more exact analysis method, tree surcharge plays an insignificant role in slope stability.

Without tree species and density data, estimates of tree surcharge can be taken from the literature. When doing so, care must be exercised to ascertain whether an equivalent uniform surcharge or a surcharge directly under the tree is being reported. An equivalent uniform surcharge is recommended because the stresses at depth and between trees will not be as high as the surcharge directly under the tree. Some equivalent uniform surcharge values from the literature are listed in table 5.1.

### 5.3.4 Root Strength

It is well documented that tree roots provide some shear strength to a soil mass (Gray and Leiser 1982; Greenway 1987). In a general sense, tree roots are thought to stabilize slopes in three ways:

Table 5.1—Tree surcharge values reported in the literature

	Species	$q_0$ , psf
Greenway 1987	Unspecified, 30–80 m high	10–40
Sidle 1984a	Sitka spruce, Alaska	$N[52.5, 10.4]$
Wu and others 1979	Sitka spruce, 100 to 200 feet high	50

- By providing a laterally reinforcing surface layer that acts as a membrane to “hold the underlying soil in place” (O’Loughlin and Ziemer 1982).
- By anchoring an unstable soil mantle to stable subsoils or rock where the roots penetrate a potential failure surface.
- By acting as buttress piles or arch abutments or both to support the soil uphill from the trees (Gray and Megahan 1981).

Gray and Leiser (1982) suggested that roots reinforce soil by providing tensile resistance in a manner similar to the reinforcement provided by steel straps in mechanically stabilized earth-retaining structures, except that metal bars are much stiffer than roots. Gray and Ohashi (1983) found that soil reinforced with natural and artificial fibers exhibited larger peak shear strength in loose and dense sands and less postpeak reduction in shear strength in dense sand at high strains. They also found that fibers slipped and pulled out, which limited the strength increase to values much less than would be predicted by the tensile strength of the fibers alone. Gray and Ohashi (1983) and O’Loughlin and Ziemer (1982) found that fibers and roots did not affect the angle of internal friction of sand. Therefore, root strength can be thought of as supplemental cohesion that is added to the soil shear strength in the numerator of the infinite slope equation.

Some attempts have been made to quantify the magnitude of root reinforcement by measuring the tensile strength of individual roots, by direct shear tests on soil-root masses, by pull tests on large root systems or whole trees, and by back-analysis of existing failures. These methods are described in detail in appendix B. Measurements using each of these methods clearly show that root reinforcement increases with greater root density (area of roots per area of soil).

Several researchers have used the tensile strength of individual roots ( $T_r$ ) in mathematical models to estimate the root resistance per unit soil area ( $t_R$ ) (Gray and Leiser 1982; Gray and Ohashi 1983; Waldron 1977; Waldron and Dakessian 1981; Wu and others 1979). These models are all similar in that they resolve the tensile force that develops in the roots during shear ( $T_r$ ) into a tangential component ( $T_s$ ) that directly resists shear, and a normal component ( $T_n$ ) that increases the confining stress on the shear plane, thereby increasing the frictional component of soil shear strength. Figure 5.5 illustrates the general model.

The models generally have two flaws:

- They do not consider that during a slope failure, not all roots will mobilize their maximum tensile resistance at the same time.
- Except for Gray and Ohashi (1983), they do not consider that roots may not mobilize their maximum tensile resistance because they may slip or pull out before they break in tension.

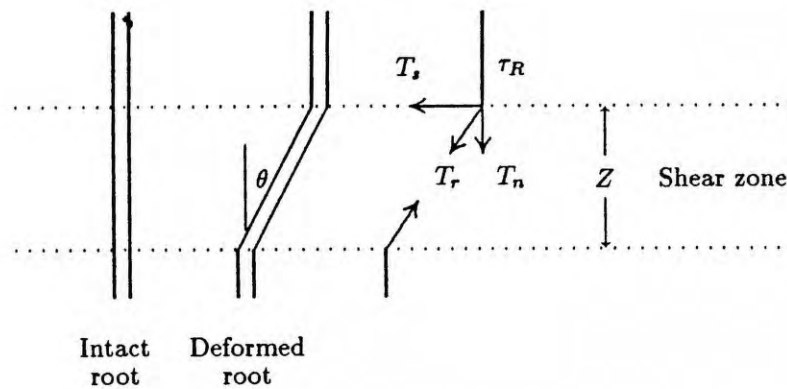


Figure 5.5—Fiber reinforcement model (after Gray and Ohashi 1983).

Additional research is necessary to increase our understanding of soil-root interaction during slope failure and to estimate defensible values for root strength to use in stability analysis. In the meantime, we suggest using root strength values reported in the literature, considering also root density and root distribution along the failure plane, as discussed in the next three sections.

#### 5.3.4.1 Values of Root Strength Measured

Table 5.2 summarizes measurements of root strength per unit area of soil ( $t_R$ ) made by several studies. Figure 5.6 shows a histogram created by stacking the ranges of values reported in each study. This histogram helps to visualize the most common measurements obtained by the studies. These values cover several species and a wide range of root densities.

#### 5.3.4.2 Effect of Root Morphology and Suggested Probability Distributions

As discussed above, root strength depends not only on the tensile strength of the individual roots, but also on the pull-out resistance (or skin friction), and probably most importantly, on the morphology of the root system; that is, how many roots there are and whether they cross the failure plane. For example, western larch and black spruce have shallow root systems that spread laterally with small vertical sinker roots that penetrate deeper into the soil, while Douglas-fir has more ball-shaped root systems with a tap root that can penetrate deeply into the soil. Therefore, one might expect a greater potential root strength from Douglas-fir, particularly in deeper soils. Root tensile strength and morphology do not depend solely on the species of the tree. Within species, differences due to climate and site factors have been measured. Burroughs and Thomas (1977), for example, found that the roots of coastal Oregon Douglas-fir were twice as strong as the roots of central Idaho Douglas-fir. It is also known that the root systems of the same species can take on different shapes and strengths because of different slope, soil, and groundwater conditions. For example, uphill roots have been shown to be stronger than downhill roots, perhaps due to root tissue differences (Greenway 1987).

Use of the root strength values listed in table 5.2 requires some knowledge of root density and morphology at the site. Following the approach of Wooten (1988), we have adopted a soil-root classification scheme presented by Tsukamoto and Kusakabe (1984). This classification scheme attempts to account for the

Table 5.2—Root strength values reported in the literature

Investigator	Soil/vegetation type	Root strength, $t_R$	
		kPa	psf <sup>1</sup>
Endo and Tsuruta (1969a) <sup>2</sup>	cultivated nursery soil/1–2 m alder saplings <sup>3</sup>	1.6–11.5	33–240
Endo and Tsuruta (1969b) <sup>4,5</sup>	<i>Poa annua</i> , Ezo mugwort Ochada 0–5 cm depth	10.7–12.1	224–253
	(Bamboo) 5–20 cm depth	1.5– 4.9	31–102
Burroughs and Thomas (1977) <sup>4</sup>	Tyee S.S. (SM)/coastal Oregon Douglas-fir	11.5–22.7	240–474
	Idaho Batholith (SM)/ Douglas-fir	4.2–14.0	88–293
Wu and others (1979) <sup>4</sup>	SM ( $\phi' = 35 - 37^\circ$ )/mixed Sitka spruce & hemlock	4.2– 5.5	88–115
Waldron and Dakessian (1981) <sup>2,4</sup>	clay loam/ponderosa pine seedlings	5.0	104
Ziemer (1981a) <sup>2</sup>	coastal sands/lodgepole <sup>3</sup>	0.2–17.3	4–362
O'Loughlin and others (1982) <sup>2,6</sup>	stony loam/beach	3.3	69
Waldron and others (1983) <sup>2</sup>	clay loam/5-year pine seedlings	3.7– 6.4	77–134
Riestenberg and Sovonick-Dunford (1983) <sup>4</sup>	silty clay ( $\phi' = 12^\circ$ ) / sugar maples – head scarp	6.2– 7.0	130–146
	– slip surface	3.8– 4.6	79– 96
	– average, entire slide	5.8	121
Wu (1984) <sup>4</sup>	SM ( $\phi' = 30^\circ$ )/hemlock	5.6–12.6	117–263
	Sitka spruce	3.7– 7.0	77–146
	yellow cedar	5.4	113
Tsakamoto and Minematsu (1987) <sup>7</sup>	nursery loam/Sugi	1.8– 5.7	38–119

<sup>1</sup> 1 kPa = 20.9 psf

<sup>2</sup> Direct shear tests

<sup>3</sup> Measured over a wide range of root densities

<sup>4</sup> Tensile strength tests on individual roots

<sup>5</sup> Pull tests on roots

<sup>6</sup> Referred to by Sidle and others (1985) but not reviewed by these authors

<sup>7</sup> Isolated small trees and pulled—measuring basal shear resistance

differences in root morphology and density in relation to the location of the failure plane in estimating appropriate values for root strength. Figure 5.7 describes the four soil-root morphology types.

Figure 5.8 shows *suggested* PDF's for each soil-root morphology type for both densely forested and clearcut conditions. These PDF's were selected based on the following observations and assumptions:

- The measured values of root strength reported in the literature and summarized in table 5.2 and figure 5.6 were assumed to apply to densely forested types B and C, where roots intersect the entire failure plane. The mean and range of values are larger for type C to account for greater tree buttressing and root penetration along the base of the failure plane.
- The mean and range of values were reduced for types B and D based on three-dimensional modeling of failures as described in appendix C.
- All distributions have large standard deviations to account for the great variability and uncertainty in reported values.
- Lognormal probability distributions were selected to reflect the tendency for right skew in the data (fig. 5.6), thereby giving a low, but possible, probability of simulating relatively high values.

Appendix C discusses in greater detail the rationale for selecting the suggested PDF's for dense timber stands.

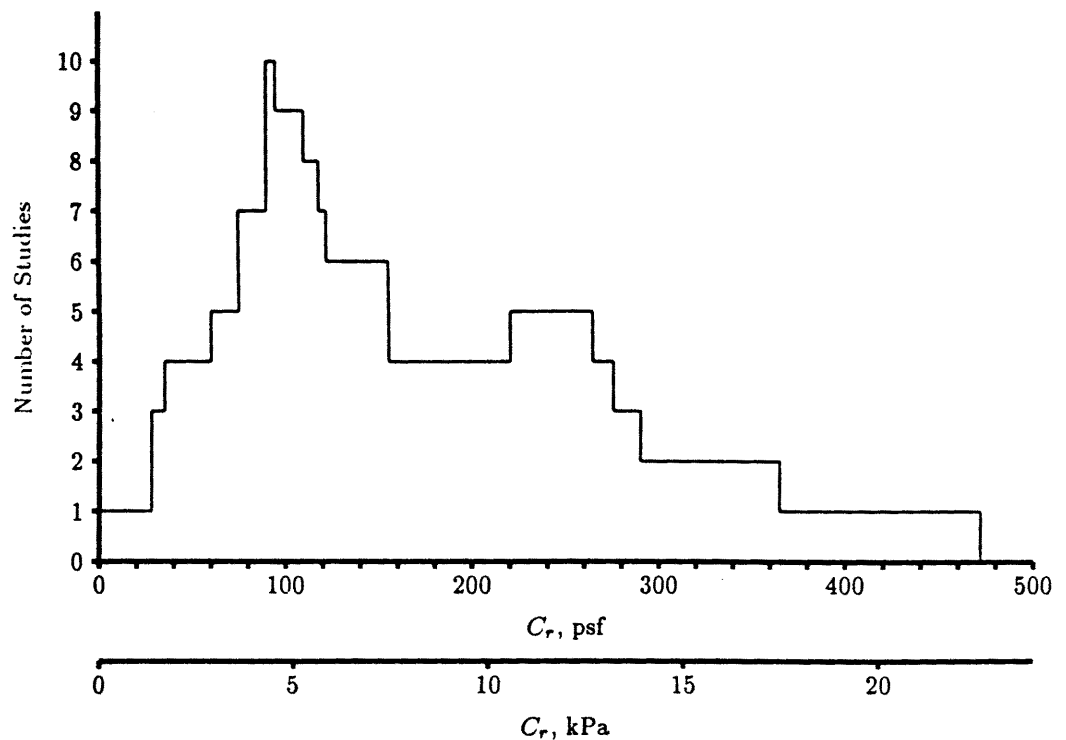


Figure 5.6—Root strength values given in 11 studies.

The user should adjust the suggested distributions to account for other factors such as roots in saturated clay (Waldron and Dakessian 1981), less dense timber stands, or the user’s personal judgment and experience. We also suggest that the user talk to local soil scientists or silviculturists for their viewpoints as to which soil–root morphology type may apply in each polygon.

#### 5.3.4.3 Effect of Timber Harvest on Root Strength

Much empirical evidence indicates that clearcutting increases the frequency of landslides, particularly debris avalanches on steep slopes with shallow soils. Gray and Leiser (1982), for example, cite 16 references that document this relationship. The primary reasons that tree removal causes instability are the resulting increase in groundwater height and the reduction of root strength. The increase in groundwater due to timber harvest is discussed in section 5.3.7.1.

After timber harvest, root decay causes both the numbers of roots and the tensile strength of the remaining individual roots to decrease with time (Burrroughs and Thomas 1977). Ziemer (1981a, b) and O’Loughlin (1974) also measured a decrease in biomass and, consequently, root strength, with time after harvest using direct shear tests. These studies indicate that the period of minimum root strength is from about 3 to 5 years until about 10 to 20 years after harvest, depending on climate, which affects root decay and vegetation regrowth. In areas severely burned following harvest, minimum root strength may occur even sooner (0–3 years) (Prellwitz 1989). After about 10 to 20 years postharvest, root reinforcement will increase to its uncut level if significant regrowth has occurred.

Ziemer (1981a, b) estimated that, at its minimum, root reinforcement conceptually could be 20 to 40 percent of its undisturbed value (fig. 5.9). Therefore, we suggest using the distributions shown in figure 5.8 to represent the time of *minimum* root reinforcement after clearcut timber harvest for each soil-root morphology type. These distributions were obtained by finding a mean and standard deviation for a lognormal distribution which gives a mode value equal to about 30 percent of the mode for the uncut distribution.

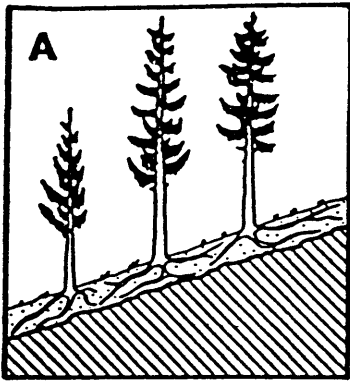
If harvesting methods other than clearcutting are used, root strength may decrease less, and the distributions in figure 5.8 should be modified. Ziemer (1981b) discusses conceptual models for the change in relative root reinforcement following shelterwood and selection harvesting systems (fig. 5.9). A shelterwood system is described as having 70 percent of the original stand being harvested, followed by removal of the remaining trees 10 years later. For this system, Ziemer hypothesized the root reinforcement drops to about 70 percent of its uncut value at about 2 to 3 years postharvest, then rises to about 10 percent above the uncut value about 7 years after harvest as the residual trees quickly expand. About 5 years after the residual trees are harvested, root reinforcement again will drop to about 50 percent of the uncut value. The selection harvesting system is described as having 20 percent of the trees cut every 10 years. Ziemer anticipates that the root strength could decrease by about 3 percent 2 years after harvest, then increase to about 7 percent above the uncut strength due to the rapid expansion of the roots of the remaining trees.

### 5.3.5 Soil Shear Strength and Unit Weight

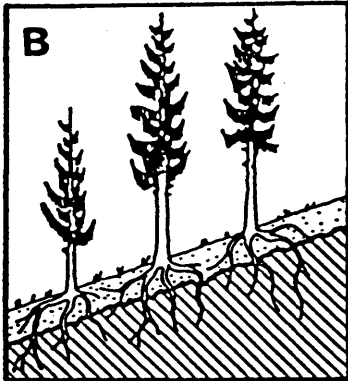
Little or no shear strength testing will be performed for a Level I investigation. When there are few shear strength data available for a soil from past Level II or Level III investigations, shear strength values likely will be estimated from values reported in the geotechnical literature, or be inferred indirectly from other soil properties that are available, such as soil gradation and relative density, or plasticity. Either method will require that the soil be classified according to the Unified Soil Classification (USC) system (ASTM D-2487-85 and D-2488-84). Field verification of soil classifications can be obtained by visual inspections of the *in situ* soils when the investigator is in the field measuring soil depth or ground slope. In addition, estimates of soil cohesion ( $C'_s$ ) and friction angle ( $\phi'$ ) values are possible by conducting back-analyses of slope failures observed in the study area, if there are any. Using all the above methods, the range and shape of the probability distributions for  $C'_s$  and  $\phi'$  can be estimated.

When estimating values and PDF's for soil shear strength, keep in mind that the soil at the failure plane may not have the same properties as the bulk of the overlying material. Examples of this situation include thin clay seams at the failure plane, or a frictional resistance between soil and schist or phyllite bedrock that is less than within the soil mass itself (Alexander 1989). Therefore, sampling or testing the upper soil material may give inappropriate values. If multiple soil layers exist, weighted average values for soil shear strength parameters may be used to account for the portion of the failure plane passing through each soil type (see section 3.2). However, this refinement may not be justified for a Level I analysis.

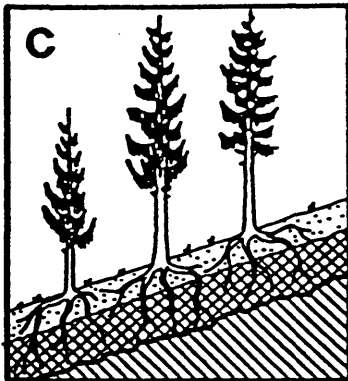
If the unit weight of the material overlying the failure plane is different from the unit weight of the material through which the failure plane passes, the unit weight of the overlying material should be used, as that will give a more accurate computed value for effective stress. Again, with multiple soil layers, a weighted average value could be used, although again it might not be justified for a Level I analysis, particularly since the infinite slope equation is insensitive to unit weight.



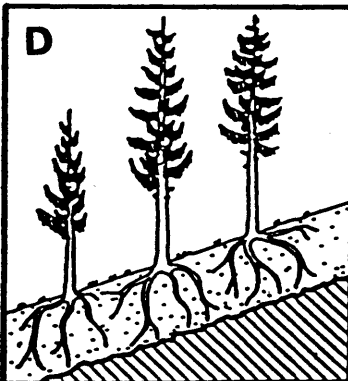
**Type A**—consists of shallow soils overlying fairly competent rock that roots cannot penetrate easily. The failure plane is mostly below the root zone, except where it intersects the ground surface. Because these roots are constrained by the bedrock, root densities may be greater than those for type D allowing for greater root reinforcement.



**Type B**—consists of shallow soils overlying fractured or weathered rock or compact glacial till that allows some root penetration. The amount of penetration depends on the number and nature of the discontinuities in the substratum; but in general the roots are restricted somewhat by the substratum. Root reinforcement is fairly significant because roots tend to intersect the failure plane along its full length.



**Type C**—consists of a transition zone; that is, a nondistinct zone in which the soil shear strength and unit weight increase gradually with depth. It is assumed that the transition zone acts as a drainage barrier allowing the concentration of groundwater and the development of high pore-water pressure. As a result, the failure plane passes somewhere through the transition zone. It is assumed also that this zone is penetrated more easily by roots than is a less fractured substrate of type B. Therefore, the maximum root reinforcement is expected in type C. Examples of type C include decomposed granite over granite bedrock, and a loose ash or glacial till overlying a medium-dense compacted till over bedrock.



**Type D**—consists of soils and a potential failure plane both deeper than the root zone of the trees. The actual depth of the soil needed for a type D classification depends on the root morphology of the particular tree species. For example, less soil depth would be required for Sitka spruce, which has a shallow lateral root system, than for Douglas-fir, which has a deep root system. Because the bedrock does not constrain the root system, the root densities, and therefore the root strength, are assumed to be less than for those associated with type A.

Figure 5.7—Soil-root morphology types (after Tsukamoto and Kusakabe 1984).

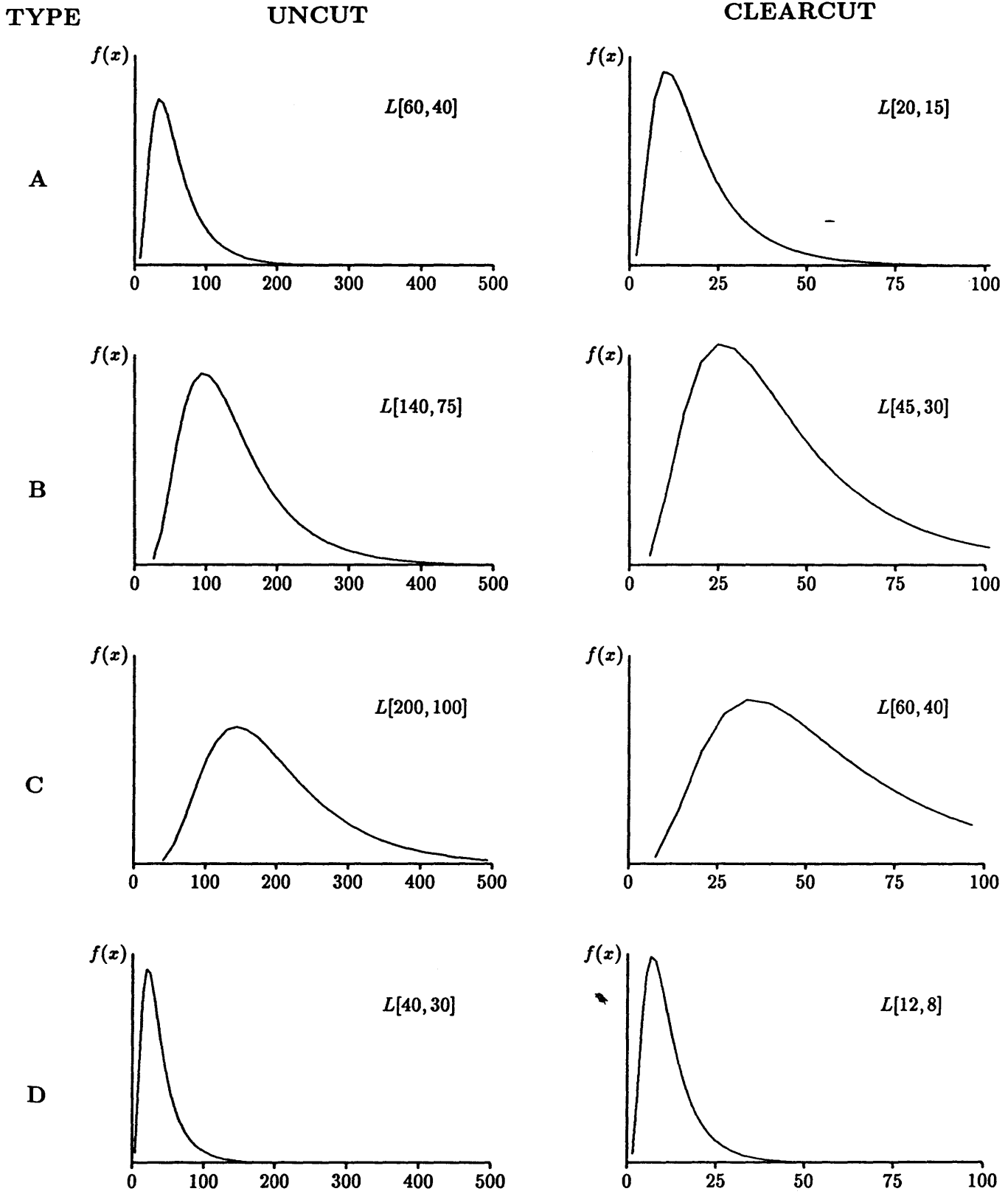


Figure 5.8—Suggested lognormal distributions describing possible ranges of  $C_r$  values for each soil-root morphology type in densely forested conditions, and during the 3- to 10-year period of minimum root strength after clearcut timber harvest.

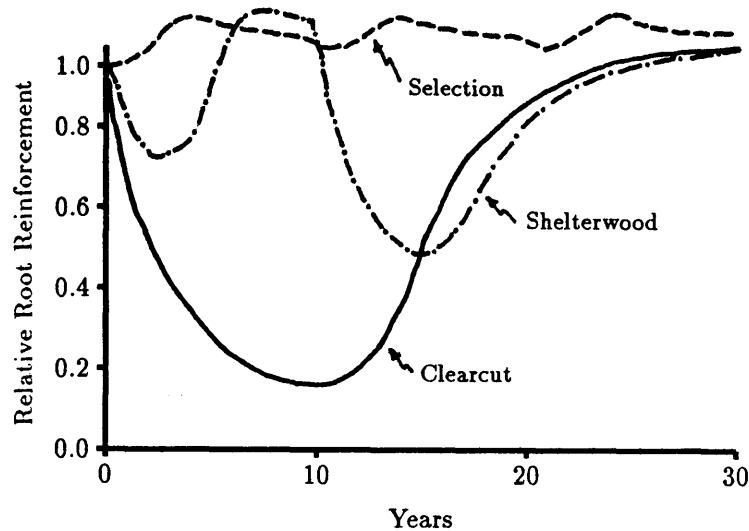


Figure 5.9—Changes in relative root reinforcement that occur after clearcut, selection, and shelterwood harvesting methods (after Ziemer 1981b).

The following subsections review shear behavior of sands, gravels, and clays, and discuss values and distributional shapes for  $C'_s$ ,  $\phi'$ , and unit weight ( $\gamma_d$ ) reported in the literature.

### 5.3.5.1 Distributions Reported in the Literature

Even nominally homogeneous soil is characterized by some spatial variation that must be described with a statistical model in a Level I analysis (Lumb 1975). However, the task of selecting appropriate PDF's for  $C'_s$ ,  $\phi'$ , and  $\gamma_d$  is made difficult by other errors and uncertainties, namely:

- Uncertainty in the state of nature; that is, a lack of knowledge concerning the soil type that is actually within the polygon. This uncertainty can be reduced with extensive sampling.
- Random measurement errors, both in laboratory and in *in situ* tests.
- Systematic uncertainty in  $C'_s$  and  $\phi'$  due to interpretations of laboratory test results. Some examples of interpretation differences are:
  - If one engineer arbitrarily defines failure in triaxial shear tests at 10 percent axial strain for a strain hardening soil, he or she would obtain lower values for friction angle than another engineer who defines failure at 15 percent axial strain.
  - If a linear regression is performed on four tests for cohesionless soils, a higher  $C'_s$  and lower  $\phi'$  will commonly result than if  $C'_s$  was assumed to equal zero and the four resulting  $\phi'$  averaged. This is true when the failure envelope is nonlinear.
  - With undrained triaxial shear tests, different  $C'_s$  and  $\phi'$  values will be obtained depending on whether the maximum deviator stress or the maximum stress ratio is used as the failure criterion.
- Systematic conversion errors when predicting  $C'_s$  or  $\phi'$  from *in situ* tests. For example, even if SPT blow counts are measured without error, there is still scatter in the relationships between blow count, relative density, and  $\phi'$ , which results in uncertainty in the estimates of  $\phi'$ .

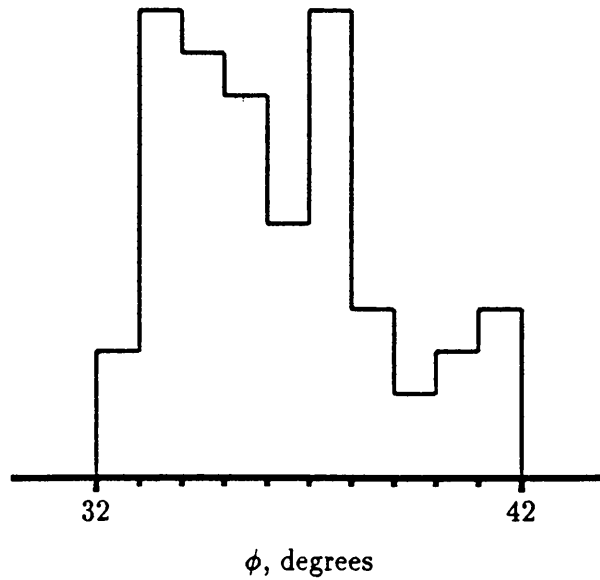


Figure 5.10—Histogram of  $\phi'$  values reported by Schultz (1971) illustrating the limits and skewness of his data.

Variability and uncertainty in soil shear strength parameters have received a great deal of attention over the past 20 years as probabilistic methods in slope stability analysis have been studied. Early workers such as Lumb (1966, 1970) and Schultz (1971) recognized that the beta distribution best described the distribution of  $C'_s$  and  $\phi'$  because observed values were limited in range and their distributions were asymmetrical (skewed). For example, figure 5.10 shows a histogram of  $\phi'$  values reported by Schultz (1971). Although the distributions were asymmetrical, these early workers advocated using normal distributions because the mathematical rigor for calculating the probability of failure was greatly simplified. More recently authors have used (or recommended using) the beta distribution (Athanasίου-Grivas and Harrop-Williams 1979; Harr 1977; Oboni and Bourdeau 1983; Rétháti 1983) because with computers and simulation techniques the mathematical rigor is essentially avoided. Krahn and Fredlund (1983) used triangular distributions computing the limits from their sample data using:

$$\begin{aligned} \text{Minimum} &= \bar{x} - 1.96s \\ \text{Maximum} &= \bar{x} + 1.96s \\ \text{Apex} &= \bar{x} - 3(\bar{x} - \text{median}) \end{aligned}$$

Other authors have reported coefficients of variation ( $c_v$ ). A mean value for  $C'_s$  and  $\phi'$  then can be multiplied by the  $c_v$  to obtain a reasonable estimate for the standard deviation. However, the shape of the distribution still must be selected.  $c_v$  and typical means and standard deviations for  $\phi'$  as summarized by Harr (1977) are:

Soil	$c_v$	$\bar{x}$	$s$
GP	6.0%	36°	2.2°
GM, GW	5.3	37	2.0
SP, SW	5-15	35.6-40.5	2.8-5.3
SM	15.8	34.7	5.5

These large values of  $c_v$  apparently cover all relative densities and result in a wide range of  $\phi'$  values. For example, if  $\phi'$  of an SM soil was assumed to be normally distributed with a mean of  $34.7^\circ$  and a standard deviation of  $5.5^\circ$ , 95 percent of the values would lie between  $23.7^\circ$  and  $45.7^\circ$ , a range that effectively covers the observed range of sands. Therefore, these values have little practical usefulness. Lumb (1970) also provided some  $c_v$  values for comparison:

Soil	$c_v$ for $C'_s$	$c_v$ for $\phi'$
Clay shale	95%	46%
Cohesive till	100	18
Residual sands and silts	17	6

These reported values of  $c_v$  do show that more variation in  $C'_s$  and  $\phi'$  values typically can be expected for sands than for gravels, and much more variation can be expected in cohesive soils. Again, using these large values for  $c_v$  is probably not the best means to obtain PDF's for use in LISA. Rather, *we suggest that the user understand the shear behavior of sands and clays as discussed in the following sections, and then rely on the tables and figures presented there, along with knowledge of soil gradation, relative density, particle angularity, mineralogy, and PI to estimate shear strength values. These values then can be used to establish a probability distribution. We suggest using a uniform, triangular or relative-frequency histogram probability distribution when shear strength values are based on the tables and figures.* Although a beta distribution is more consistent with distributional shapes reported in the literature, the extra effort required to select  $P$  and  $Q$  values is probably not justified unless the user has some test data. Table 5.3 summarizes the information provided in sections 5.3.5.2 through 5.3.5.5 for estimating shear strength values.

### 5.3.5.2 Shear Strength of Sands and Gravels

The shear strength of sands and gravels results primarily from the frictional resistance of particle-to-particle contacts similar to those of a solid block sliding on a plane. Therefore, shear strength is directly related to the effective normal stress by the coefficient of friction,  $\mu$ :

$$\tau = \sigma'_n \mu = \sigma'_n \tan \phi' \quad (5.1)$$

where  $\tau$  is the shear strength,  $\sigma'_n$  is the effective normal stress, and  $\phi'$  is the effective angle of internal friction (or friction angle). If soil cohesion exists, the equation for shear strength becomes:

$$\tau = C'_s + \sigma'_n \tan \phi' \quad (5.2)$$

where  $C'_s$  is the effective soil cohesion, which is the shear strength at zero normal force. Values for  $C'_s$  and  $\phi'$  are measured in the laboratory using direct shear, triaxial compression, or (less commonly) ring shear testing devices (Bishop 1966; Bjerrum and Bjerrum 1960; Negussey and others 1988).

The angle of internal friction attributed to frictional resistance alone is called  $\phi_\mu$ . For quartz and feldspar,  $\phi_\mu = 26^\circ$  to  $28^\circ$  and for mica,  $\phi_\mu = 7^\circ$  to  $23^\circ$  (Horn and Deere 1962; Lee and Seed 1967). Sand, however, is not a solid block but an aggregate of interlocking particles. Additional energy is required to dilate, rearrange, or crush particles in order to shear the soil, which increases strength resulting in friction angles greater than  $\phi_\mu$  (Lee and Seed 1967; Rowe 1962, 1963).

Table 5.3—Summary of suggested values for  $C'_s$  and  $\phi'$

		Peak strength		Residual strength		Apparent cohesion
		$C'_s$	$\phi'_p$	$C'_s$	$\phi'_r$	
<b>Silts, sands &amp; gravels</b>		0	From table 5.5, eq. 5.3, or fig. 5.11	0	Use table 5.5, eq. 5.3 or fig. 5.11 at $D_r = 0\%$	Depends on capillary suction and $\phi^b$ . Back-analysis commonly shows 20–60 psf for silty sands.
<b>Clays</b>	NC	0	From fig. 5.13	< 25% clay	0	Same as for sands and gravels.
				> 25%–< 50% clay <sup>1</sup>	0	Use fig. 5.16 or 5.17 $\pm 3 - 5^\circ$
	OC	Depends on stress history. Typically 100–500 psf.	Depends on stress history. Heavily OC 25–40°. Lightly OC 20–30°, or use NC $\phi'_p$ .	> 50% clay	0	10° – 24° for hydrous mica, 14° – 15° for kaolinites 9° – 15° for illite 4° – 10° for montmorillonites

<sup>1</sup> Note, these may not classify as clays according to the USCS, but clay significantly affects the  $\phi'_r$  value.

As the void ratio of sand decreases (unit weight increases) so does particle interlocking and, hence, friction angle.

Void ratio is most important in controlling the friction angle of sands. However, soil gradation, grain shape and roughness, grain size, and mineralogy also have some effect, with grain shape being most significant. The friction angles of angular soils tend to be greater than those of rounded soils, and those of well graded soils greater than those of poorly graded soils, because there is more particle interlocking. Mineralogy generally is considered to have little effect on the shear strength of sands and gravels. For instance, the  $\phi_\mu$  of mica is much less than the  $\phi_\mu$  of quartz, but highly micaceous sands have friction angles that are at most 1 or 2 degrees less than similar nonmicaceous soils when compared at the same unit weight or relative density (Hammond and Hardcastle 1987). However, mica can reduce the unit weight of soils, which indirectly causes lower friction angles.

It generally is assumed that, because of greater interlocking, coarse-grained soils have higher friction angles than do fine-grained soils when compared at a given relative density. This relationship can be seen in figure 5.11 and table 5.4, which give typical values of  $\phi'$  for nonplastic silts, sands, and gravels. However, gradation and particle angularity generally play a more important role. For instance, one would expect poorly graded GM soils containing rounded gravels (such as soils originating from alluvial or glacial deposits) to have friction angles *less than* those of well graded SM soils containing angular fragments (such

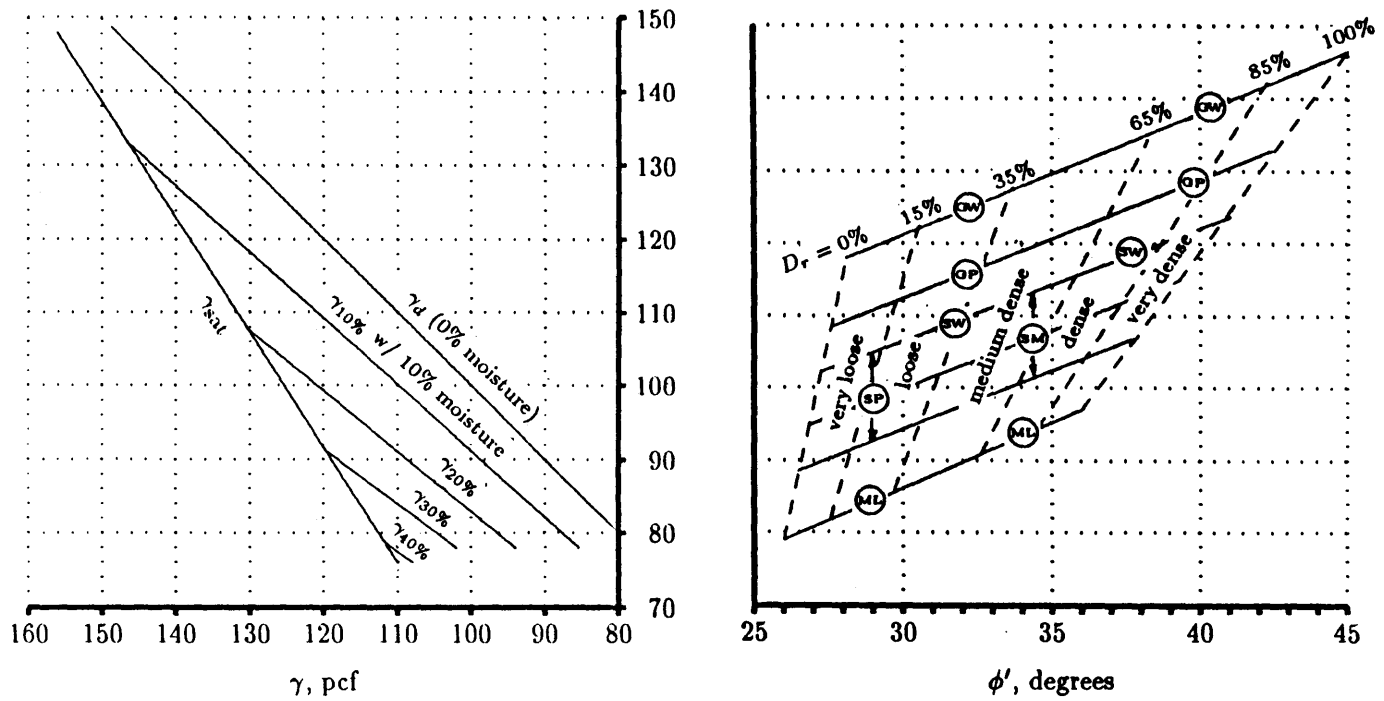


Figure 5.11—Relationship between  $D_r$ , and  $\gamma$  and  $\phi'$  for nonplastic silts, sands, and gravels using  $G_s = 2.68$  (after Prellwitz 1981 and U.S. Department of Navy 1974).

**Table 5.4— $\phi'$  vs.  $D_r$  from Prellwitz (1981)**

Soil type	$\phi'$		$k_{\phi 1}$	$k_{\phi 2}$
	$D_r = 0\%$	$D_r = 100\%$		
GW	35°	45°	1.43	0.0043
GP, GM, or Coarse SW	33°	43°	1.54	0.0047
Med. SW, Coarse SP or SM	31°	41°	1.66	0.0051
Fine SW, Med. SP or SM	29°	39°	1.80	0.0057
Fine SP or SM	27°	37°	1.96	0.0064
ML	26°	36°	2.05	0.0067

as colluvial or residual soils) at the same relative density, which is contrary to the trend shown in figure 5.11 and table 5.4.

It also generally is assumed that gravelly sands would have higher friction angles than do sands containing no gravel. However, the effect of gravel on the shear strength of soils has not yet been explained fully in the literature. It is a difficult task to assess the effect of gravel on shear strength because it is difficult to sample and test specimens containing large particles. Conflicting test results are produced because the changes in gradation, void ratio, and limiting unit weights that occur when coarse fragments are added or removed make comparison of the shear strengths of fine and coarse soils uncertain. Several studies have shown an increase in friction angle as coarse sand and gravel are added to a soil when compared at the same relative density ( $D_r$ ) (Holtz and Gibbs 1956; Wu and Baladi 1986). However, Holtz and Ellis (1961) and Siddiqi (1984) showed that adding gravel to fine soils had no effect on friction angles until the soils contained more than about 50 to 65 percent gravel. Siddiqi explains that with less than about 50 to 65 percent gravel (depending on the specific gravity of the soil particles), the gravels merely are floating in a matrix of finer soil, and shear strength is controlled by the fine soil alone. The gravel fragments do not contribute to strength until there is a high enough percentage that the fragments are in contact with each other.

Lambe and Whitman (1969) also note that large particles may lead to lower friction angles because large particles are able to roll more easily due to their centers of gravity being farther away from the plane of shear.

Also note that many studies cited in the literature have compared friction angles of fine and gravelly soils at the same void ratio rather than at the same  $D_r$ . Comparisons made on the basis of void ratio always show that the friction angles of sands are greater than those of gravels (Leslie 1963; Marachi and others 1969; Wu and Baladi 1986). This is because the addition of coarse fragments decreases void ratio but also increases the limiting unit weights. Therefore, at a given void ratio, a gravel soil will behave during shear as a looser soil (lower  $D_r$ ) than a sand soil will, resulting in lower friction angles for the gravel.

**5.3.5.2.1 Typical Strength Values and PDF's for  $C'_s$  and  $\phi'$** —Typical values of  $\phi'$  for nonplastic silts, sands, and gravels can be found in many textbooks (for example, Hough 1957; Lambe and Whitman 1969). Figure 5.11 and tables 5.4 and 5.5 can be used to obtain estimates of values for  $\phi'$  and dry unit weight ( $\gamma_d$ ) when no other information is available. Prellwitz (1981) comments that  $\phi'$  values given by figure 5.11 appear conservative compared to data from

other literature. He developed a correlation equation for  $\phi'$  to relative density ( $D_r$ ) from these other sources:

$$\cot \phi' = k_{\phi 1} - k_{\phi 2} D_r \quad (5.3)$$

where  $k_{\phi 1}$  and  $k_{\phi 2}$  are coefficients given in table 5.4.

Estimates of  $D_r$  can be obtained using various penetration methods described by Prellwitz (1981) or by the portable density probe developed by Williamson on the Willamette National Forest (Williamson 1989).

Table 5.5 summarizes shear strength and  $\gamma_d$  values for cohesionless soils reported by several authors. This listing of  $C'_s$ ,  $\phi'$ , and  $\gamma_d$  values is by no means exhaustive. The intent is to show the most likely values and the wide variety of values that can be obtained for any given soil classification. Table 5.5 is divided into three relative density classes—very loose to loose ( $D_r < 35$  percent), medium dense (35 percent  $< D_r < 65$  percent), and dense to very dense ( $D_r > 65$  percent). In general, loose relative densities apply to volcanic ash, loess, and highly micaceous soils, and to the residual friction angle ( $\phi'_r$ ) for any soil (see section 5.3.5.4). Medium-dense relative densities apply to most residual and colluvial soils, and dense to very dense relative densities to compacted glacial tills and compacted fills. References 7 and 15 in table 5.5 correspond to equation 5.3 and figure 5.11, respectively.  $\phi'$  values are peak values ( $\phi'_p$ ) unless otherwise noted.

Equation 5.3 and figure 5.11 (references 7 and 15 in table 5.5) represent data compiled from several sources, whereas the other references in table 5.5 are single studies. Equation 5.3 and figure 5.11 therefore cover a wider range of soil characteristics in terms of particle angularity, surface roughness, and mineralogy. Therefore, if you do not know much about a soil other than its USC classification, you might want to weigh equation 5.3 and figure 5.11 more heavily. If you do know more about the soil's characteristics, you might temper your estimate of  $\phi'$  with values from other references. For instance, suppose you wish to estimate  $\phi'$  values for a loose, medium- to coarse-grained SM with subrounded particles. Reference 7 indicates  $\phi'$  in the range of 29° to 34°, and reference 15 indicates a range of 27° to 32.5°. Reference 17, however, shows  $\phi'$  values of 27° to 28° for subrounded particles. This might suggest a triangular distribution with minimum, most likely, and maximum values of 26.5°, 27.5°, and 32.5°.

Nonplastic silts, sands, and gravels have no true cohesion ( $C'_s = 0$ ). However, back-analyses of existing failures often yield  $C'_s$  values of 20 to 60 psf (<100 psf), particularly for silty cohesionless soils (Prellwitz 1989). Values of this magnitude in a uniform PDF would be appropriate for use in LISA in lieu of other information. This apparent cohesion may result from capillary suction (see section 5.3.5), or simply from differences between the actual failure mechanism and the assumptions of the infinite slope model.

Table 5.5 shows that several authors report large values for cohesion, up to 1,000 psf, in cohesionless sands and gravels (Holtz and Gibbs 1956; Schroeder and Alto 1983; Schroeder and Swanston 1987). This, of course, is not true cohesion but may result from the way in which laboratory test results are interpreted. Figure 5.12 illustrates that a cohesion intercept can result when a straight line Mohr's failure envelope is fit either to test data that are curved due to diminishing dilation with increasing effective stress, or to scattered test data that are due to test specimen variability or testing errors or both. The latter can result in either positive or negative intercepts. In either case, the positive  $C'_s$  and  $\phi'$  values reported may be inappropriate for use in stability analysis at small effective stresses (shallow soil depths or steep slopes) because shear strength will

be overestimated. On the other hand, ignoring the cohesion intercept and using only the reported  $\phi'$  value to compute shear strength could underestimate the actual shear strength at all confining stresses. This problem can be alleviated by performing shear tests only at effective stresses consistent with the *in situ* conditions or by modeling the Mohr's failure envelope as a curve with a power function (Miller and Borgman 1984). The power function option may be incorporated in future versions of LISA.

**5.3.5.2.2 Typical Values for Unit Weight**—Figure 5.11, tempered by values listed in table 5.5, can be used to estimate a uniform distribution for unit weight ( $\gamma_d$ ). Figure 5.11 shows that  $\gamma_d$  for gravels is greater than  $\gamma_d$  for sands, which is greater than  $\gamma_d$  for silt. Also, angular soils tend to have lower  $\gamma_d$  than do rounded soils because angular particles tend to bridge and pack less efficiently (Wu and Baladi 1986).

In humid regions, soils may contain large amounts of organic matter that would give them unit weights much lower than those shown in figure 5.11. Alexander (1989) found that for inorganic soil horizons with more than 0.2 percent organic matter,

$$D_b = Ae^{-0.12OC^{1/2}} \quad (5.4)$$

where  $D_b$  is the bulk density of the  $-2\text{mm}$  fraction in  $\text{Mgm}^{-3}$ ;  $A$  is 2.24 for loamy sands, 1.86 for sandy loams, and 1.73 for silts; and  $OC$  is organic carbon in  $\text{gkg}^{-1}$ . This equation had an  $r^2$  of 0.850 and may not be applicable outside of southeastern Alaska where it was developed.

The dry unit weight in pcf can be estimated from  $D_b$  and the specific gravity of the soil particles ( $G_s$ ) by

$$\gamma_d = \frac{D_b}{\left(\frac{D_b}{G_s \gamma_w} - 1\right)k + 1} \times 62.5 \frac{\text{pcf}}{\text{Mgm}^3} \quad (5.5)$$

where  $\gamma_w$  is the unit weight of water =  $1 \text{ Mgm}^{-3}$ , and  $k$  is the soil fraction greater than 2 mm by weight (Hammond and Hardcastle 1991).

### 5.3.5.3 Shear Strength and Unit Weight of Clays

In the stability analysis of natural slopes it generally will be correct to consider clays as  $C'_s - \phi'$  soils and to perform an effective stress analysis. A total strength analysis (assuming  $\phi' = 0$ ) is appropriate only for stability assessment of a saturated soil that is stressed quickly compared to the consolidation time of the soil, for example, when a clay slope is loaded or excavated quickly (Lambe and Whitman 1969).

**5.3.5.3.1 Normally Consolidated Clays**—The shear behavior of normally consolidated clays is similar to that of loose sands. Effective cohesion for normally consolidated clay is generally considered to be negligible (0–100 psf). Peak  $\phi'$  ( $\phi'_p$ ) for normally consolidated clays has been found to decrease with increasing plasticity index, although there is much scatter in published data. Figure 5.13 shows a plot from Kenney (1959) illustrating this relationship. Bjerrum and Simons (1960) show a similar relationship. An equation for the line in figure 5.13 is:

$$\sin \phi'_p = 0.808 - 0.229 \log_{10} \text{PI} \quad (5.6)$$

where  $\phi'_p$  is the peak  $\phi'$  for normally consolidated clay, and PI is the plasticity index in percentage. We suggest that the value from equation 5.6  $\pm 5^\circ$  or  $6^\circ$  be

Table 5.5—Reported values of  $\gamma_d$ ,  $C'_s$  and  $\phi'$  for silts, sands, and gravels

USC	% $D_r$	$\gamma_d$ , pcf	$C'_s$ , psf	$\phi'$ , deg.	Source <sup>1</sup>	Material <sup>2</sup>
GW loose						
	0-35	* <sup>3</sup>	0	35-38	7	
	"	118-128	0	28-33.5	15	
	0	98-111	0	36.3-39.3	1	A, crushed
GW medium-dense						
	35-65	*	0	38-41	7	
	"	128-135	0	33.5-38.5	15	
	58	127	0	38.4-39	11	50% R-SR gravel
GW dense to very dense						
	65-100	*	0	41-45	7	
	"	135-145	0	38.5-45	15	
	"	125-135	0	> 38	16	
	*	119.5-137	0	39-46	6	SA-SR [alluvium]
	70	123-125.4	790-1140	38.0-41.4	3	50-65% SA-SR gravel
GP loose						
	0-35	*	0	33-36	7	
	"	108-118	0	27.5-32.5	15	
GP medium-dense						
	35-65	*	0	36-39	7	
	"	118-124	0	32.5-37	15	
	50	117-122	288-432	38.7-40.4	3	65-82% A gravel
GP dense to very dense						
	65-100	*	0	39-43	7	
	"	124-134	0	37-42.5	15	
	"	115-125	0	> 37	16	
	*	111-124	0	38-42	6	52-100% SA-SR gravel [alluvium]
	70	126.5	432	40.4	3	65% A gravel
	90	129.1	432	44.4	3	82% A gravel
GM loose						
	0-35	*	0	33-36	7	
	0	114	*	*	11	50% R-SR gravel
	*	51.5-91	104-200	33.6-43	9	Colluvium [graywacke]
GM medium-dense						
	65-100	*	0	36-39	7	
	*	119	430	39.5	13	
GM dense to very dense						
	65-100	*	0	39-43	7	
	"	120-135	0	> 37	16	
GC dense to very dense						
	65-100	115-130	0	> 31	16	
	90% of T99 $\gamma_{max}$	123-125	650-720	32.2-34.2	4	50-65% SA-SR gravel
	*	106-118	0-360	33.6-44.7	9	Glacial till [graywacke]

(con.)

Table 5.5—(Con.)

USC	% $D_r$	$\gamma_d$ , pcf	$C'_s$ , psf	$\phi'$ , deg.	Source <sup>1</sup>	Material <sup>2</sup>
SW loose						
	0-35	* <sup>3</sup>	0	29-32	7	Fine grained
	"	*	0	31-34	7	Medium grained
	"	*	0	33-36	7	Coarse grained
	"	103-110	0	27-32.5	15	
	*	93.3	320	36.2	13	
	*	95-103	0	33-37	2	Coarse to fine
	0	91.8-103.5	0	32.0-36.2	1	A [crushed] ] [ Coarse sand with
	0	109	0	27.0-31.0	1	50% A, 50% SR ]   20% gravel
	0	112	0	27.1-30.4	1	SR [alluvium] ]   4-10% silt
SW medium-dense						
	35-65	*	0	32-35	7	Fine grained
	"	*	0	34-37	7	Medium grained
	"	*	0	36-39	7	Coarse grained
	"	110-116	0	32.5-36	15	
	"	104-108	0	38-41	2	Coarse to fine, peak
	"	"	0	36.5-38	2	Coarse to fine, residual
	50	105-112	130-600	33.0-35.8	3	0-20% SA-SR gravel
	47-63	115-119	0	35.7-38.7	1	SW-SM w/19% A gravel, 12%ML
SW dense to very dense						
	65-100	*	0	35-39	7	Fine grained
	"	*	0	37-41	7	Medium grained
	"	*	0	39-43	7	Coarse grained
	"	116-124	0	36-41	15	
	"	110-130	0	38	16	
	*	110-118	0	39-42	2	Coarse to fine, residual
	*	110-118	0	43-47	2	Coarse to fine, peak
	70	109-119	400-950	35.8-41.4	3	0-49% SA-SR gravel
	79-98	124-130	0	47.5-55.9	1	SW-SM w/19% A gravel, 12% ML
SP loose						
	0-35	*	0	27-30	7	Fine grained
	"	*	0	29-32	7	Medium grained
	"	*	0	31-34	7	Coarse grained
	"	88-110	0	27-32.5	15	
	"	92-98	0	33-35	2	Coarse to medium, residual
	"	92-98	0	33-37	2	Coarse to medium, peak
SP medium-dense						
	35-65	*	0	30-33	7	Fine grained
	"	*	0	32-35	7	Medium grained
	"	*	0	34-37	7	Coarse grained
	"	95-116	0	31-36	15	
	"	100-104	0	36-37.4	2	Coarse to medium, residual
	"	100-104	0	37.8-40.3	2	Coarse to medium, peak
	60	107-111	30	37.4	14	SA gravelly SP-SM, 11% ML

(con.)

Table 5.5—(Con.)

USC	% $D_r$	$\gamma_d$ , pcf	$C'_s$ , psf	$\phi'$ , deg.	Source <sup>1</sup>	Material <sup>2</sup>
SP dense to very dense						
	65-100	* <sup>3</sup>	0	33-37	7	Fine grained
	"	*	0	35-39	7	Medium grained
	"	*	0	37-41	7	Coarse grained
	"	100-121	0	34-41	15	
	"	100-121	0	37	16	
	"	99-103	0	37.1-39.0	2	Coarse to medium, residual
	"	99-103	0	40.2-43.5	2	Coarse to medium, peak
	*	107-122	0	39-42	6	SA-SR, 0-40% gravel
	*	112-115	0	37.5-39.5	6	R, 0% gravel
SM loose						
	0-35	*	0	27-30	7	Fine grained
	"	*	0	29-32	7	Medium grained
	"	*	0	31-34	7	Coarse grained
	"	88-110	0	27-32.5	15	
	"	88-93	0	32-34.3	2	Medium to fine, residual
	"	88-93	0	32-35.5	2	Medium to fine, peak
	0	79.1-83.9	0	24-26.8	1	A, fine grained
	0	88.5-94.0	0	27.8-29.6	1	A, medium grained
	0	99.5	0	31.6	1	A, coarse grained
	0	92.2	0	28	1	50% A, 50% SR, medium grained
	0	94.6-94.7	0	27	1	SR, medium grained
	0	102.8	0	27.9	1	SR, coarse grained
SM medium-dense						
	35-65	*	0	30-33	7	Fine grained
	"	*	0	32-35	7	Medium grained
	"	*	0	34-37	7	Coarse grained
	"	95-116	0	31-36	15	
	*	93.5-103.5	-130-680	29.9-38.1	13	*
	35-65	94-110	-346-125	27-50	14	Most $\phi'$ 's=35-45° SA-SR fine to coarse
	44-57	115-119	0	36.0-40.6	11	R-SR
	35-65	95-98	0	34.9-36.3	2	Medium to fine, residual
	"	95-98	0	36.7-39.0	2	Medium to fine, peak
	*	70-107	0-840	30.6-41.4	8	Undisturbed sandstone colluvium & glacial till
	90% of T99 $\gamma_{max}$	63.7-103.6	0-390	34.5-48.9	8	Sandstone colluvium & glacial till
	62-63	99.9-100.3	0	33.6	1	A, fine grained
	54-65	104.3-112.8	0	33.4-34.4	1	A, medium grained
	51-63	112.9-116.7	0	35.4	1	A, coarse grained

(con.)

Table 5.5—(Con.)

USC	% $D_r$	$\gamma_d$ , pcf	$C'_s$ , psf	$\phi'$ , deg.	Source <sup>1</sup>	Material <sup>2</sup>
SM dense to very dense						
	65-100	* <sup>3</sup>	0	33-37	7	Fine grained
	"	*	0	35-39	7	Medium grained
	"	*	0	37-41	7	Coarse grained
	"	100-121	0	34-41	15	
	"	110-125	0	34	16	
	"	98-118	0	32-46	5	
	65-100	99-103	0	37.1-39.0	2	Medium to fine, residual
	"	99-103	0	40.2-43.5	2	Medium to fine, peak
	100% of T99 $\gamma_{max}$	70.5-114.8	0-655	30.6-40.5	8	Sandstone colluvium & glacial till
	65-100	90-120	-100-131	30-48	14	55% of $\phi'$ 's 38-42°, SA-SR, fine to coarse
	81-98	108-117	0	35.1-49.9	1	A, fine grained
	72-100	115-123	0	37.1-52.4	1	A, medium grained
	67-96	118-128	0	38.1-50.7	1	A, coarse grained
SM						
	*	*	0	34-42	10	Fine to coarse sand
	*	34-106	0-740	24.9-44.4	9	Ash, till, decomposed limestone or colluvial graywacke
SC dense to very dense						
	*	105-125	230	31	16	
	*	103.6	144	32.1	8	Undisturbed glacial till
	90% of T99 $\gamma_{max}$	95-97	40-160	23.6-29.2	8	Glacial till
	100% of T99 $\gamma_{max}$	107-109	0-185	33.7-39.6	8	Glacial till
	*	68-113	80-360	33.1-40.7	9	Glacial till or decomposed graywacke
ML loose						
	0-35	*	0	26-29	7	
	"	80-86	0	26-30	15	
	*	62.4-68.1	0	31.5-33.7	14	Mt. Mazama ash from Idaho
	0	68.3	0	22.2-25.2	1	Crushed
ML medium-dense						
	35-65	*	0	29-32	7	
	"	86-92	0	30-32.5	15	
ML dense to very dense						
	65-100	*	0	32-36	7	
	"	92-98	0	32.5-36	15	
	"	95-120	190	32	16	

(con.)

Table 5.5—(Con.)

USC	% $D_r$	$\gamma_d$ , pcf	$C'_s$ , psf	$\phi'$ , deg.	Source <sup>1</sup>	Material <sup>2</sup>
ML	Unknown	55.1–106.4	250–380	30.0–41.1	13	
	"	77–80	55–640	23–43	12	Cohesive clayey silt
	"	59.5–96.9	160–280	32.1–34.4	9	Glacial till–phyllite/schist
	"	86–120	0	33–45	5	
MH–all	*	70–90	420	25	16	
	*	68.6	145	34.5	8	Undisturbed glacial till
	90% of T99 $\gamma_{max}$	70.5	0	39.6	8	Glacial till
	100% of T99 $\gamma_{max}$	77.5	144	36.1	8	Glacial till
	*	48.4–107.3	80–300	34.4–39.2	9	Alluvium
	*	82–115	0	27–47	5	
	82–100	94.5–102.6	0	34.7–43.7	1	A, crushed material

<sup>1</sup> Sources for table 5.5

1 Wu and Baladi 1986; Note:  $\phi$  = angle of repose obtained by measuring the angle of a loosely poured cone of soil; it represents a residual  $\phi$ .

2 Burmister 1962

3 Holtz and Gibbs 1956

4 Holtz and Ellis 1961

5 Holtz and Krizek 1972

6 Leslie 1963

7 equation 5.3 (Prellwitz 1981)

8 Schroeder and Alto 1983

9 Schroeder and Swanston 1987

10 Schultz 1971

11 Siddiqi 1984

12 Singh and Lee 1970

13 USDA FS R1 unpublished data

14 Hammond 1986

15 figure 5.11 (U.S. Department of Navy 1974 and Prellwitz 1981)

16 table 1 (U.S. Department of Navy 1974)

<sup>2</sup>A = angular, SA = subangular, SR = subrounded, R = rounded.

<sup>3</sup>\* = values not reported.

used as a first estimate of minimum and maximum values for a uniform PDF when selecting a PDF for  $\phi'_p$  for normally consolidated clays.

**5.3.5.3.2 Overconsolidated Clays**—The strength of clay, like sand, depends ultimately on the void ratio. But unlike sands, clay readily compresses when the effective confining stress ( $\sigma'$ ) increases. If  $\sigma'$  subsequently decreases, the clay rebounds, but not back to the original void ratio. Therefore, at a given  $\sigma'$ , the overconsolidated clay has a lower void ratio than does the same clay in the normally consolidated state, which results in a greater strength for the over-

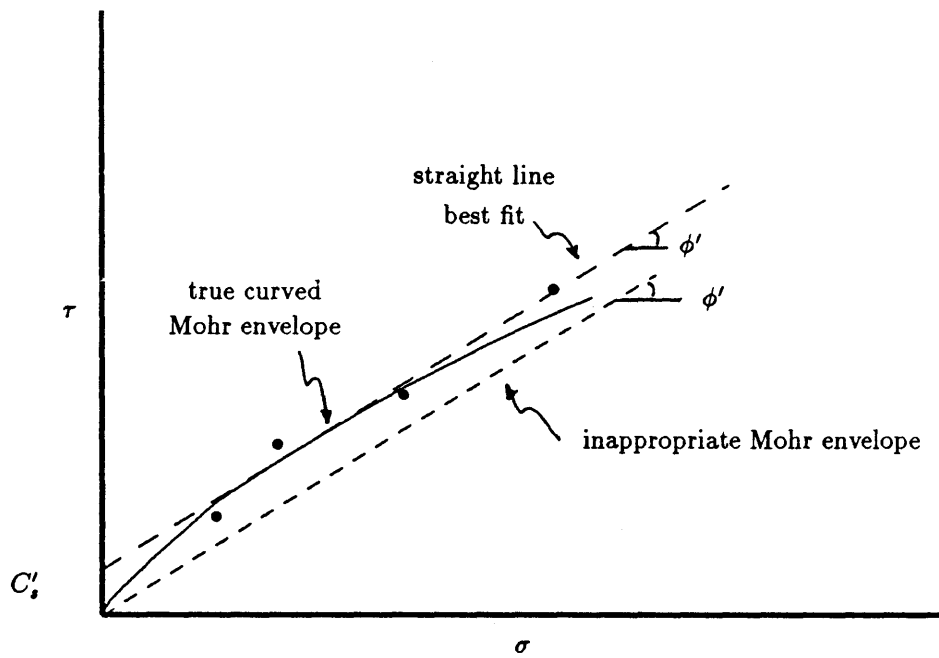


Figure 5.12—Sources of cohesion intercept from laboratory tests on cohesionless soils.

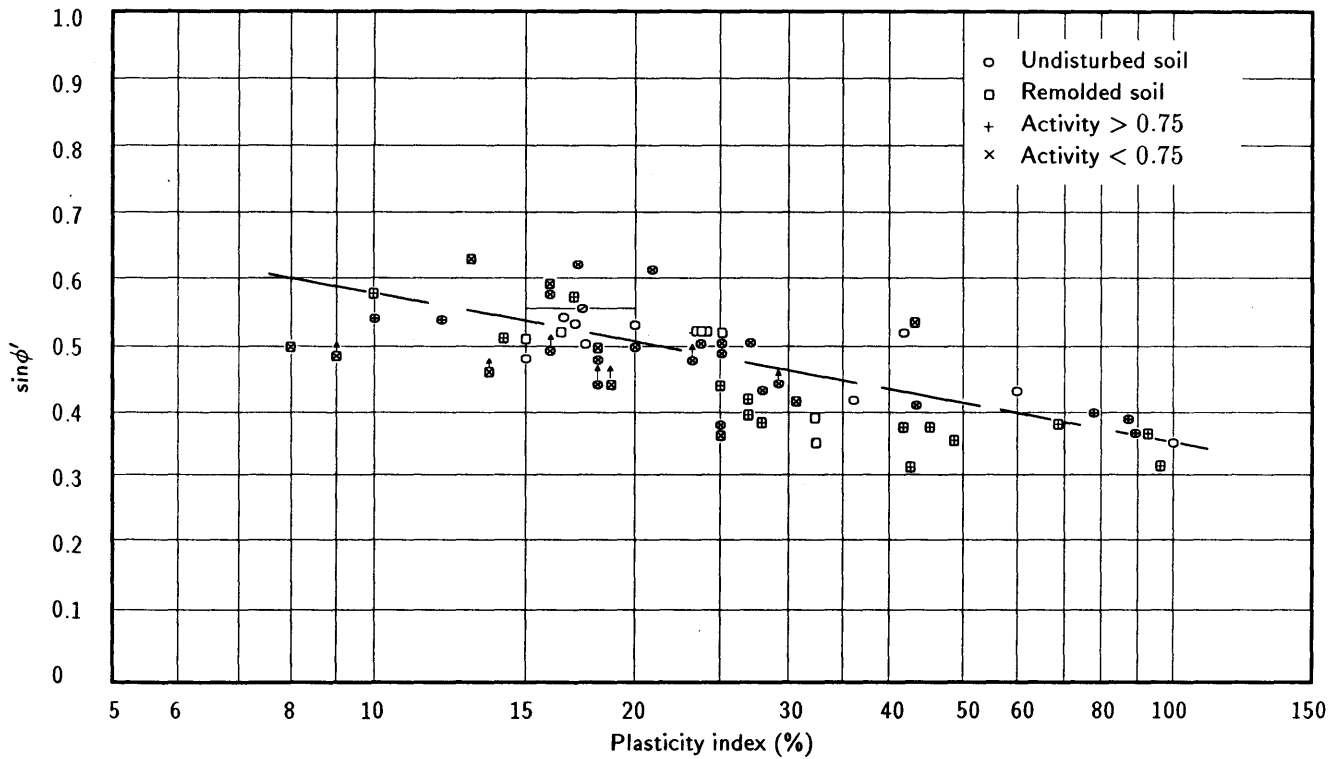


Figure 5.13—Relationship between  $\sin \phi'$  and plasticity index for normally consolidated soils (from Kenny 1959).

consolidated clay. This is analogous to a dense sand that has a higher strength than does loose sand at a given  $\sigma'$ .

Geologic conditions that result in overconsolidation include removal of overburden pressure by erosion of overlying material or by melting of a glacier. Other causes include construction loads and fluctuations in the pore-water pressure, which change the effective stress.

Overconsolidation produces *true* cohesion because the clay platelets are pushed together so tightly that molecular forces prevent them from moving apart when the load is removed (Lambe and Whitman 1969; Taylor and Cripps 1987). The magnitude of true cohesion, as well as  $\phi'$ , depends on the magnitude of the preconsolidation stress. Reasonable values of true  $C'_s$  range from 100 to 500 psf (Lambe and Whitman 1969), although values in the thousands of psf have been reported (Lumb 1966; Taylor and Cripps 1987). These large  $C'_s$  values should be used with extreme caution because they frequently result from performing consolidated drained tests so rapidly that pore pressures develop, or as discussed below, are the results of tests at large confining stresses that may not match current *in situ* stress conditions. Reasonable values for  $\phi'_p$  range from 20° to 30° for lightly overconsolidated clay, to 25° to 40° for heavily overconsolidated clay (Taylor and Cripps 1987).

Figure 5.14 compares the Mohr's failure envelope of a normally consolidated clay with that of an overconsolidated clay. The Mohr failure envelope for overconsolidated clay is curved. Typically, the  $C'_s$  and  $\phi'$  used are defined by a straight line tangent to the Mohr envelope at the value of stress corresponding to the stress conditions in the field. These  $C'_s$  and  $\phi'$  are often called apparent values and typically exhibit a high inverse correlation (Taylor and Cripps 1987) that can be modeled in LISA using the bivariate normal PDF. The apparent  $C'_s$  ( $C'_a$ ) value can be quite large (2,000 to 5,000 psf) when the current stress is close to the preconsolidation stress (low overconsolidation ratio, OCR). In this case, the apparent  $\phi'$  ( $\phi'_a$ ) is close to the value for the normally consolidated clay. When the current stress is much less than the preconsolidation stress (high OCR), the  $C'_a$  value will be close to the true  $C'_s$ , and the  $\phi'_a$  value can be quite large (greater than 40°). In any case, the current stress and the preconsolidation stress, which is determined from a one-dimensional compression test on an undisturbed specimen, must be known to obtain appropriate values of  $C'_s$  and  $\phi'$ .

The strength of overconsolidated clays also is affected by weathering and fissuring, typically causing a large reduction in true  $C'_s$  and a smaller reduction in  $\phi'_p$ . The weathering process eventually returns the clay to the normally consolidated state with its associated normally consolidated shear strength parameters. Weathering explains the common observation that overconsolidated clays are weaker near the ground surface than at depth.

Because  $C'_s$  and  $\phi'_p$  for overconsolidated clays depend on stress history, the current effective stress, and the degree of weathering, it is difficult to obtain typical values from the literature and be assured that they are appropriate for the current *in situ* conditions being analyzed using LISA. Fortunately, there is a simplifying factor. Back-analyses on existing *first-time* failures in overconsolidated clays show that the *average* shear stress along the entire failure plane is much less than the peak strength of the clay as measured in the laboratory; in fact, the strength parameters corresponding to the average stress often are very close to  $C'_s$  and  $\phi'_p$  of the normally consolidated clay (Taylor and Cripps 1987). Therefore, from a practical standpoint, it is probably not necessary to discern whether a clay is overconsolidated and its preconsolidation stress for a Level I

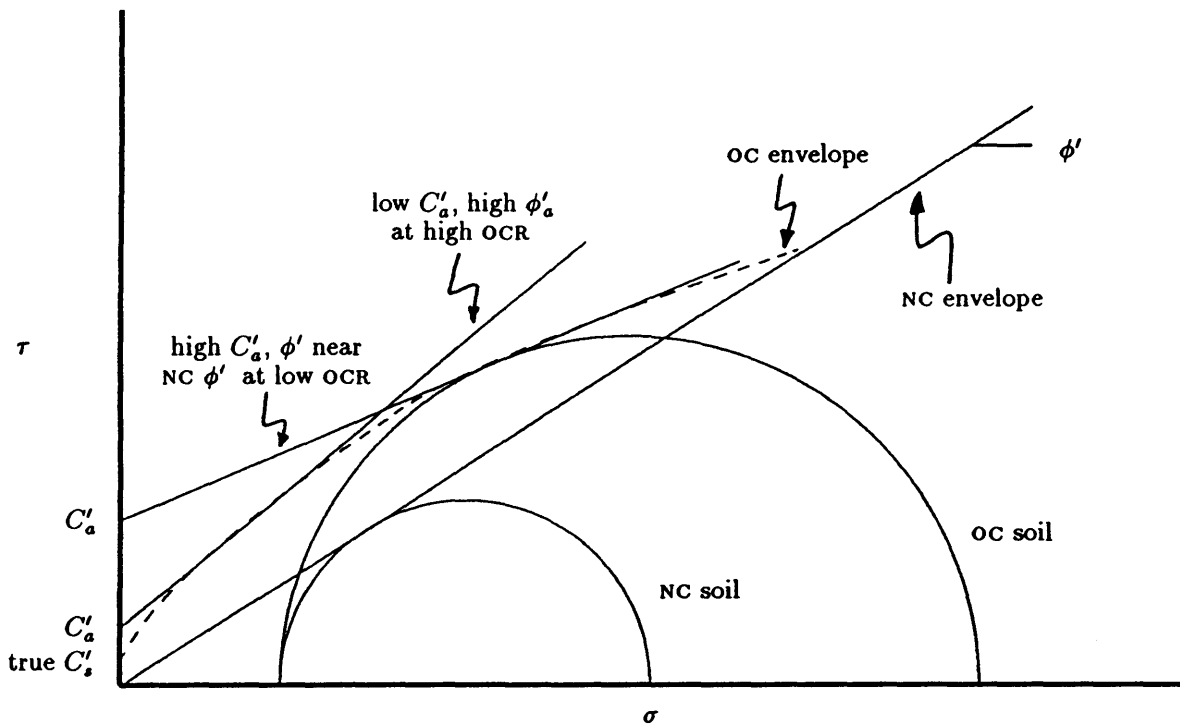


Figure 5.14—Mohr failure envelopes for a clay soil in the normal (NC) and overconsolidated (OC) states.

analysis; rather  $\phi'_p$  can be estimated as for normally consolidated clays using figure 5.13.  $C'_s$  may remain between 100 and 500 psf but may be less;  $C'_s$  and  $\phi'_p$  should still be considered to be inversely correlated, which can be modeled by using the bivariate normal PDF.

**5.3.5.3.3 Unit Weight**—The dry unit weights ( $\gamma_d$ ) of clay soils typically are reported relative to consistency. Values given in the literature range from 60 to 95 pcf for very soft to soft clay, 30 to 50 pcf for soft organic clay, 75 to 110 pcf for medium clay, and 90 to 130 pcf for stiff to very stiff clay, with values up to 135 pcf for clays containing sand and gravel (Bowles 1968; Dunn and others 1980; Hough 1957; Taylor and Cripps 1987). We suggest using uniform PDF's within these ranges.

#### 5.3.5.4 Residual Shear Strength of Sands and Clays

**5.3.5.4.1 Background**—The residual friction angle ( $\phi'_r$ ; also called ultimate friction angle,  $\phi'_{ult}$ ) is the friction angle of soil at very large strain and is applicable to sites that have failed previously and those that undergo long-term progressive (occasional or continuous) failure. Figure 5.15 shows idealized stress-strain curves for sand and clay illustrating the change in strength with strain for loose and dense sands (a) and normally and overconsolidated clays (b). The value of  $\phi'_r$  is considered to be a fundamental property of a particular soil in that it is independent of the initial void ratio or confining pressure (Lambe and Whitman 1969; Negussey and others 1988). For clay,  $\phi'_r$  is also independent of the stress history of the clay because, as the clay is sheared, the plate-shaped particles become aligned and the adhesive bonds between clay particles are broken. This results also in  $C'_s$  becoming negligible as it is with normally consol-

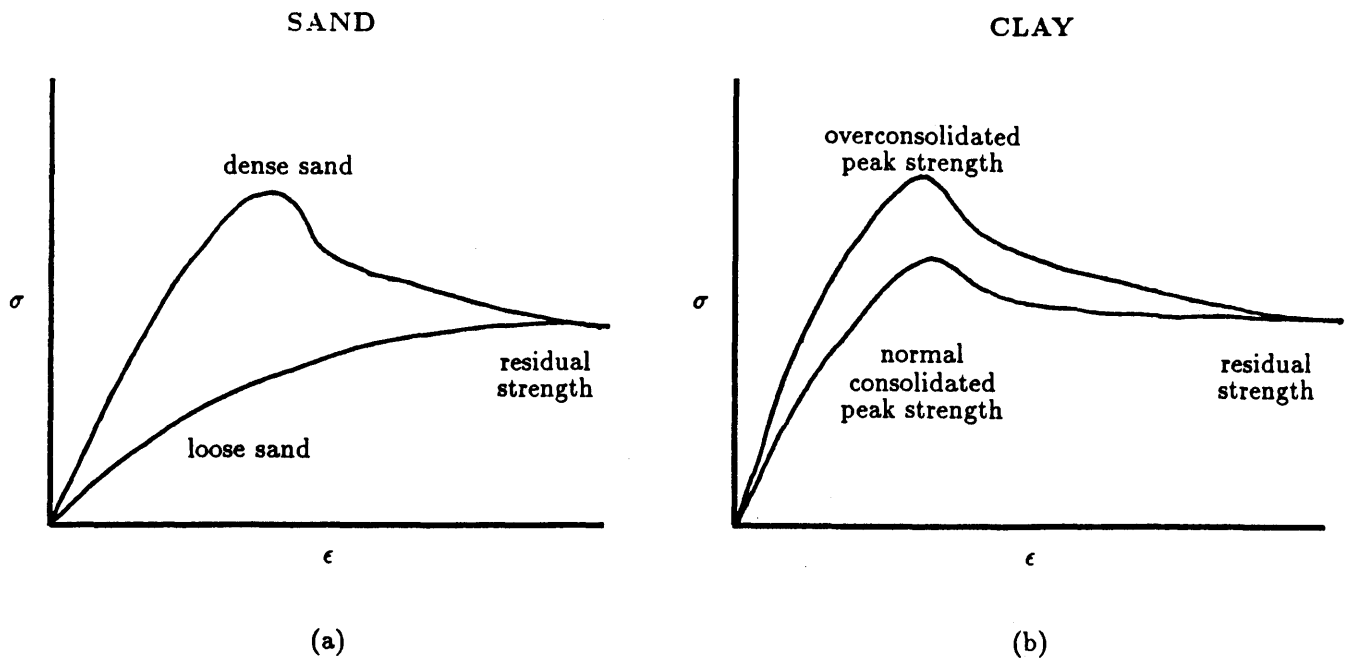


Figure 5.15—Idealized stress-strain curves for sand (a) and clay (b) soils.

idated clays.  $\phi'_r$  is less than  $\phi'_p$  for the same clay whether overconsolidated or normally consolidated. The most reliable laboratory values for  $\phi'_r$  are obtained with a ring shear device, although comparable results have been achieved using triaxial compression tests on initially loose sand specimens (Negussey and others 1988) and by multidirection direct shear tests on clays (Skempton 1985).

**5.3.5.4.2 Suggested Values and PDF's**—For sands and gravels, values for  $\phi'_r$  can be estimated from equation 5.3, figure 5.11, or table 5.5 at a  $D_r$  of 0 percent, and PDF's selected as for  $\phi'_p$ . For soils containing clay,  $\phi'_r$  depends primarily on the clay content and clay mineralogy. Skempton (1985) says that if the clay content is less than about 20 to 25 percent, the clayey soil will behave much like a sand or silt. Therefore, we suggest estimating ranges of values and PDF's for  $\phi'_r$  as one would for silts and sands. When the clay content is greater than 50 percent,  $\phi'_r$  is controlled by the sliding friction of clay minerals and will not change with further increase in clay content. Skempton (1985) and Taylor and Cripps (1987) suggest using 10 to 24° for hydrous mica clays, 14 to 22° with a most likely value of 15° for kaolinites, 9 to 15° with a most likely value of 10° for illite, and 4° (Na) to 10° (Ca) with a most likely value of 5° for montmorillonites (smectites). These ranges can be used to define a uniform or triangular PDF.

When the clay content lies between 25 and 50 percent,  $\phi'_r$  decreases with increasing clay content. Figure 5.16 plots  $\phi'_r$  against clay content from data presented by Skempton (1964, 1985). Collota and others (1989) show a similar relationship between  $\phi'_r$  and clay content but also include liquid limit and plasticity index (fig. 5.17). Either figure could be used to estimate a range of values to define a uniform PDF for  $\phi'_r$  when the clay content is between 25 and 50 percent.

### 5.3.5.5 Apparent Cohesion

Negative pore-water pressure develops in unsaturated soils due to capillary action (Lambe and Whitman 1969). Negative pore-water pressure (also called

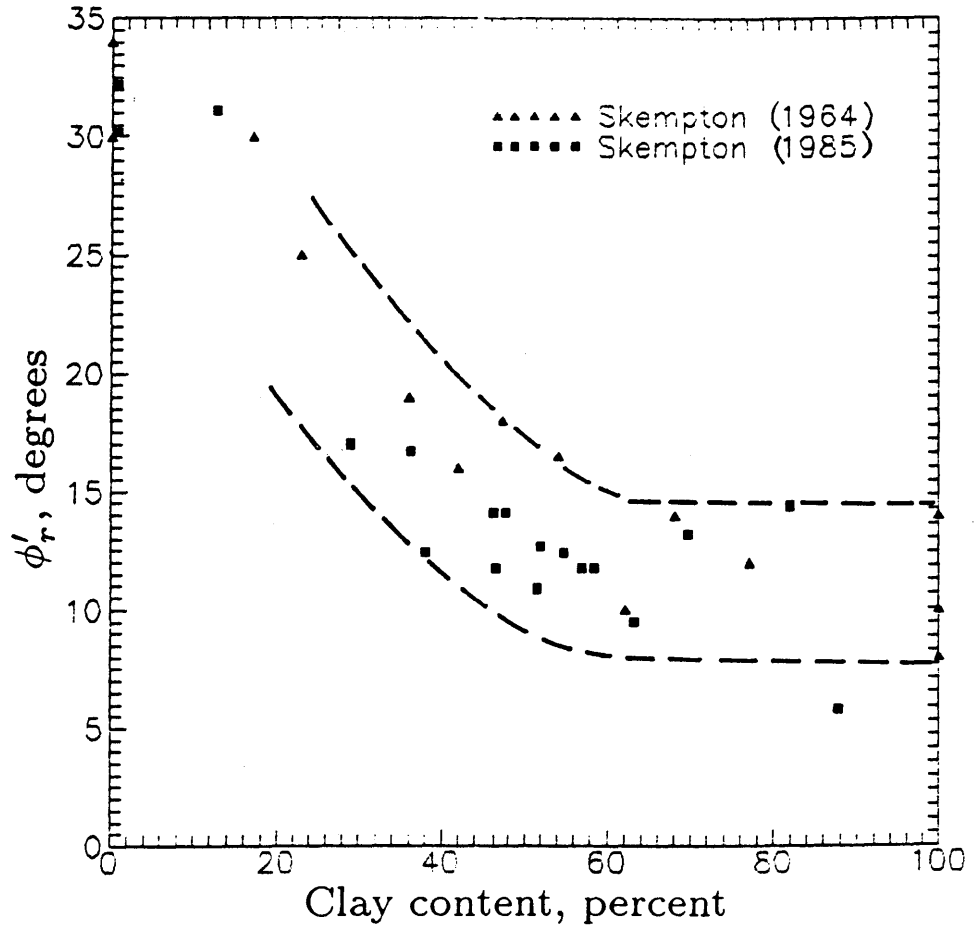


Figure 5.16—Relationship between  $\phi'_r$  and percentage clay (from Skempton 1964, 1985).

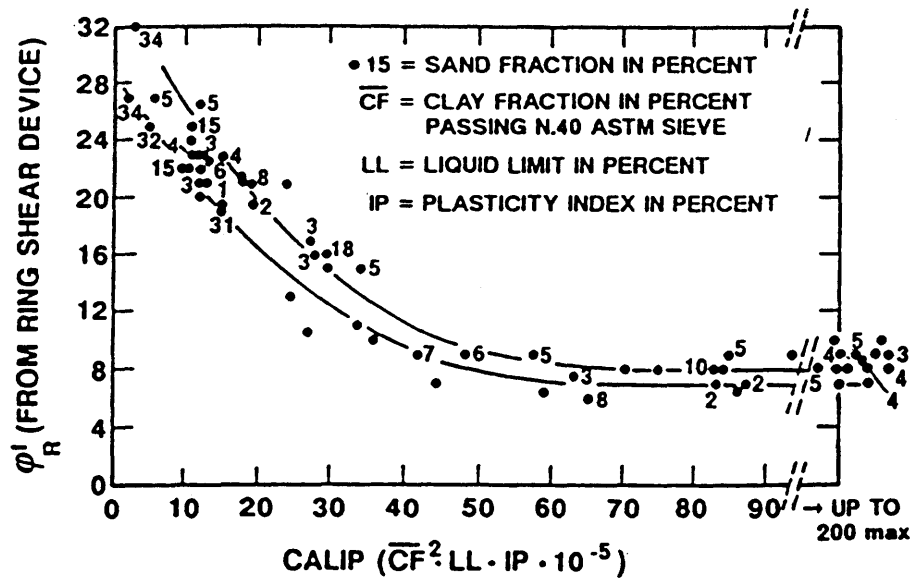


Figure 5.17—Relationship between  $\phi'_r$ , gradation, and index properties of cohesive soils (from Collatta and others 1989).

capillary suction, capillary pressure, or matric suction) produces shear resistance that is called apparent cohesion ( $C_{app}$ ).

Slope failures have been documented to occur as a result of a decrease in capillary suction, and hence apparent cohesion, without the development of positive pore-water pressure (Matsuo and Ueno 1979). However, this is not the usual case. Slope failures usually occur below the phreatic surface where pore-water pressure is positive and apparent cohesion is zero. Even for the latter case, some  $C_{app}$  may be appropriate in the analysis to account for the strength along the portion of the failure surface that passes through the unsaturated zone to the ground surface.

Triaxial compression tests on unsaturated specimens have shown that there is a linear relationship between apparent cohesion and capillary suction (fig. 5.18) (Fredlund 1987). Fredlund terms the slope of this line  $\phi^b$ . Typical values for  $\phi^b$  range from 13 to 23°, with 15° being common. This range of values appears to apply to both sands and clays. By knowing the value of  $\phi^b$  for a given soil and the capillary suction profile in the field, apparent cohesion can be calculated using equation 5.7 or figure 5.19. Values for  $C_{app}$  would be added to any true cohesion.

$$C_{app} = (u_a - u_w) \tan \phi^b \quad (5.7)$$

where  $C_{app}$  is apparent cohesion due to capillary suction,  $u_a$  is pore-air pressure,  $u_w$  is pore-water pressure, and  $(u_a - u_w)$  is capillary suction. For most practical problems,  $u_a$  can be assumed to equal atmospheric pressure (or zero gauge pressure).

The magnitude of hydrostatic capillary suction is equal to the product of the height above the phreatic surface and the unit weight of water, as long as water films on the soil particles are continuous. Thus, the capillary suction at a given point in the soil profile will change as the phreatic surface fluctuates. Also, the capillary suction near the ground surface is usually greater (pore-water pressure more negative) than hydrostatic suction during dry seasons due to desiccation, and less (pore-water pressure more positive) than hydrostatic suction during wet seasons due to water infiltration.

Measuring and predicting the soil suction profiles with the seasons and assessing the appropriate profile to use for a particular problem is difficult. Therefore, reasonable values for  $C_{app}$  to use in LISA will likely come from back-analysis on existing failures. Cohesion determined by back-analysis would include both true and apparent cohesions.

### 5.3.5.6 Obtaining Values for Correlation Coefficient ( $r$ )

As discussed in section 4.2, values of  $-0.2$  to  $-0.85$  have been reported for the  $r$  between  $C'_s$  and  $\phi'$  (Cherubini and others 1983). If the user wishes to model the correlation, but no laboratory data exist, we suggest that values in this range be used with the bivariate normal PDF to perform a sensitivity analysis to evaluate the effect of the correlation on the probability of failure. We advise using the same random seed number for each run to eliminate the variation in probability of failure that usually occurs with repeated simulations.

If laboratory data exist, it is simple to obtain values for the correlation coefficient between  $C'_s$  and  $\phi'$ . First, plot  $C'_s$  against  $\phi'$  to observe whether a linear correlation exists and the degree of scatter in the correlation. Then perform a linear regression on the  $C'_s - \phi'$  data. Graphics programs and spreadsheets such as Golden Software's GRAPHER and LOTUS 1-2-3, respectively, perform regressions and report the coefficient of determination ( $r^2$ ). Programmable calculators, such as the HP41 with STAT PAC, also can be used. The correlation

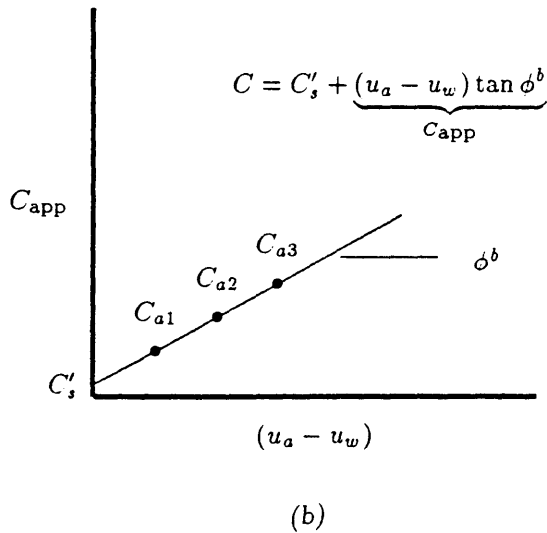
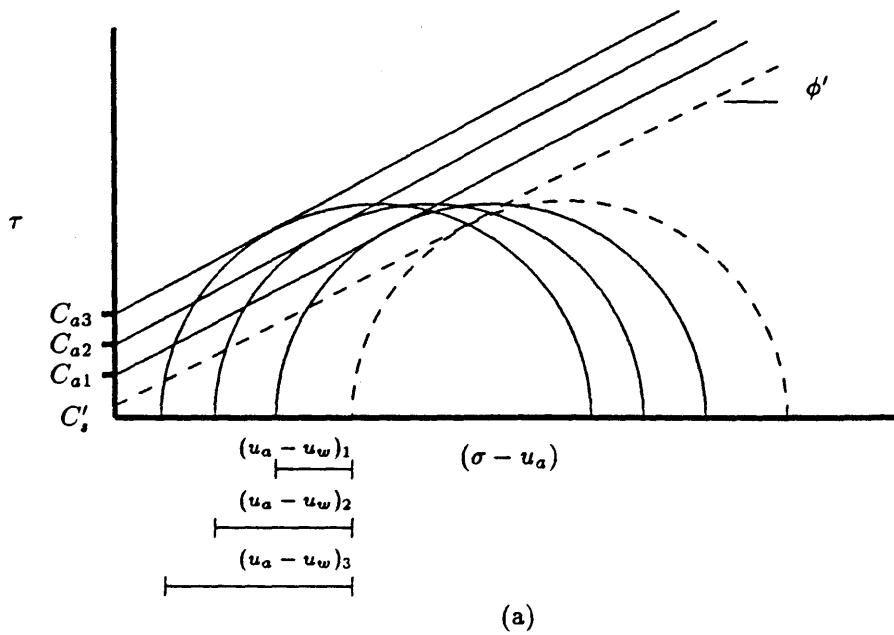


Figure 5.18—Mohr's failure circles on unsaturated soils showing apparent cohesion (a). Determination of  $\phi^b$  (b).

coefficient,  $r$ , is simply the square root of  $r^2$  and has the sign of the slope of the regression equation.

Apparent soil cohesion due to capillary suction is not inversely correlated to  $\phi'$ , so  $r$  may be taken as zero and univariate distributions used for  $C'_s$  and  $\phi'$  in LISA simulations.

### 5.3.6 Moisture Content

Moisture content is used to compute the moist soil unit weight ( $\gamma$  or  $\gamma_m$ ) of the soil above the phreatic surface. The moisture content is not uniform throughout the soil but varies with depth depending on the soil gradation and climate and groundwater conditions. For instance, fine-textured soils can maintain a significant thickness of saturated soil above the phreatic surface, the "capil-

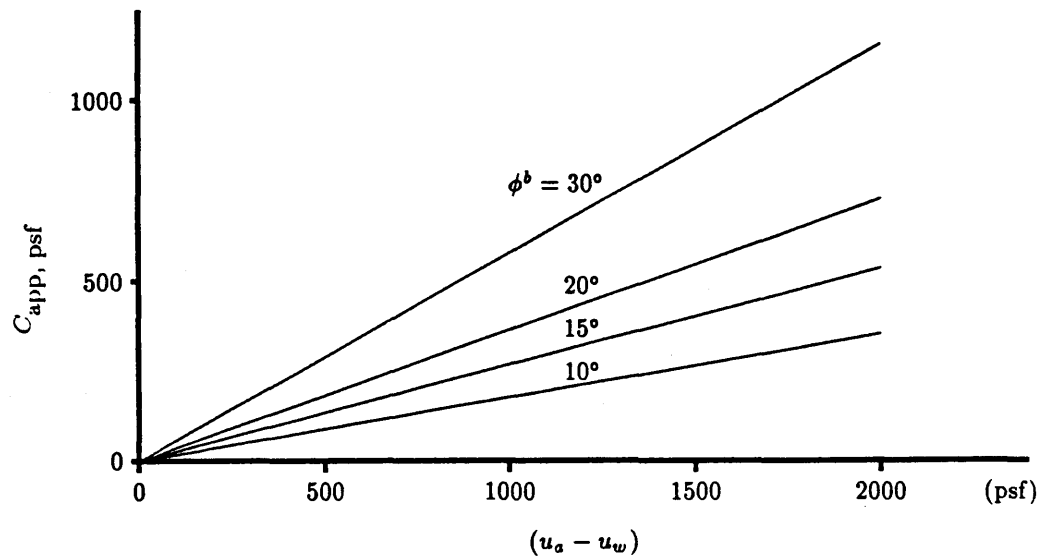


Figure 5.19—Relationship between capillary suction and apparent cohesion for various values of  $\phi^b$ .

lary fringe,” which is due to capillary suction; whereas coarse-textured soils can maintain little or no capillary fringe. However, since the infinite slope equation is relatively insensitive to the value of moist unit weight used in the analysis, the assumption of a uniform moisture content within the soil profile should cause no significant inaccuracies.

Reasonable values for moisture content can be obtained by calculating the saturated moisture content of the soil over the range of unit weights to be used; the DLISA program does this for you automatically. Then select a range of values some percentage less than the saturated moisture content values. For instance, if you are assuming a major rainfall or snowmelt event for the analysis, it would be reasonable to select moisture contents just a few percent less than the saturated moisture content.

Because dry unit weight and moisture content are simulated independently, it is possible to simulate on any given pass a value for moisture content that is greater than the saturated moisture content. If this happens, LISA will use the saturated moisture content to compute the moist unit weight of the soil. It should be obvious that this has happened if, when you view the histogram or scatter plot of the moist and saturated unit weights, some (or many) of the values for moist unit weight are the same as for the saturated unit weight.

### 5.3.7 Groundwater

Positive pore-water pressure due to increasing groundwater levels is widely recognized as the triggering mechanism for most slope failures based both on direct measurements of initiation or acceleration of slope movement coincident with increasing pore-water pressure (Iverson and Major 1987; Reid and others 1988), and on the observation that slope failure occurrences increase during periods of intense rainfall or major rain-on-snow events (Brand and others 1984; Campbell 1975; DeGraff and others 1984; Ellen and Wiczorek 1988; Keefer and others 1987; Pierson 1980; Sidle 1984a, 1986; Ziemer 1984).

The groundwater environment modeled with LISA is assumed to result from rain or snowmelt infiltration rather than a permanent groundwater system. The

subsurface flow (often called "through flow") is ephemeral, resulting from water infiltrating the surface soil, perching on a water-impeding layer, and flowing laterally toward streams or depressions.

*The groundwater distribution used in LISA represents the spatial variation of the peak groundwater-soil depth ratios ( $D_w/D$ ) expected across the landform during some infiltration event, either by rainfall or snowmelt.* To illustrate this statement, consider a landform in which 80 percent of the slopes are straight or convex and do not concentrate groundwater, while in 20 percent of the landform groundwater flowlines converge in a draw, resulting in high groundwater levels. During a major infiltration event, the soils in these concentration areas are expected to become saturated to or near the ground surface. This landform might be represented by a frequency histogram with two classes: one class with  $D_w/D$  ratios between, say 0.1 and 0.3, with an 80 percent frequency; the second class with  $D_w/D$  ratios between 0.7 and 1.0 with a 20 percent frequency. Conceptually, the groundwater distributions would be different for different landforms depending on whether the flowlines tend to converge or diverge. The groundwater distribution also would vary depending on whether an average or major infiltration event was considered.<sup>7</sup>

Obtaining the input data needed to estimate the probability distribution for  $D_w/D$  can be time-consuming and difficult. Drill holes equipped with standpipe piezometers or slotted pipe observation wells provide a fairly reliable means for obtaining field data on water levels. However, these data are seldom available at the reconnaissance mode of Level I. The user will have to depend heavily on experience and limited qualitative information that can be obtained by ground inspections of the polygon. The presence of springs, seeps, boggy areas, and thriving vegetation indicate groundwater levels at the ground surface. Seasonal fluctuations in this seepage activity may provide some clues to the groundwater system. Soil pits also can provide clues about the maximum level to which groundwater usually rises at a site. A gray soil color, typical of a reducing environment, can indicate nearly continuous saturation. Orange and yellow mottles typical of an oxidizing environment can indicate seasonal or periodic saturation of the soil, although soils can experience periodic saturation without mottles developing.

Trial computations with LISA can be directed toward a sensitivity study of the water level's effect on slope stability in the polygon. These results, combined with field information and the user's experience and judgment, should yield a reasonable range of water level values and perhaps a most likely value, leading to a triangular probability distribution.

Back-analysis of groundwater heights at existing failures can indicate a range of groundwater heights to expect in the regions of a landform where groundwater concentrates. Failed sites are useful because at the time of failure, the factor of safety must have equaled 1.0. The soil and site conditions at the time of failure need to be estimated and used in the back-analysis. Using DLISA, the ranges of  $D_w$  or  $D_w/D$  needed to give a factor of safety of 1 can be determined quickly for a variety of combinations of other input variables. The portion of the landform over which this range of  $D_w/D$  might be found can be estimated from the topography, seeps, vegetation, and other conditions described earlier.

Although field observations of groundwater conditions are preferable, the user may begin a LISA assessment using a catalog of groundwater distributions for

---

<sup>7</sup>A method for conditioning the LISA probability of failure estimates with the probability of certain infiltration events occurring during some specified length of time is discussed in appendix D.

the landforms on their forests. The user may develop such a catalog by relating a distribution to a particular landform shape, considering also aspect, elevation, position on the slope, vegetation, and other influencing factors. For example, a concave slope with numerous draws that converge groundwater flow lines (causing areas of high groundwater levels) should have a distribution that gives a higher probability of high groundwater than would a straight slope or a convex slope where groundwater flow lines diverge. Wooten (1988) took this approach on the Gifford Pinchot National Forest and found it useful for preliminary assessment. Figure 5.20 illustrates hypothetical groundwater-soil depth distributions for two landforms. The groundwater distributions shown are *not* based on any groundwater monitoring or modeling.

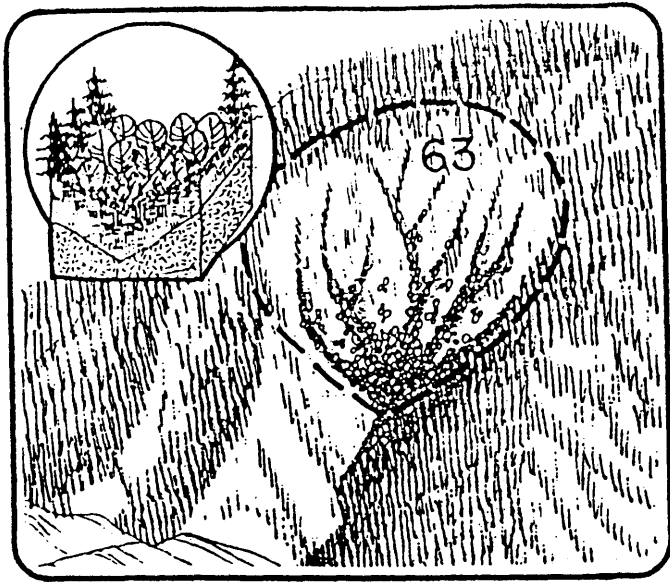
When attempting to formulate probability distributions for  $D_w/D$ , the user should remember that this ratio is somewhat controlled by soil thickness. In particular, all other factors being equal, landforms with thin soils should have higher  $D_w/D$  ratios than do those with deep soils. Also, care should be taken not to overestimate the portion of land area with high  $D_w/D$ . A recent study by Petch (1988) concerning the spatial distribution of soil saturation suggests that for small, steep ( $30^\circ$  slope) first-order basins, the portion of the land area in which the soils are saturated to or near the surface ( $D_w/D > 0.8$  or  $0.9$ ) with a large storm or snowmelt event may be on the order of 5 percent. The portion of the land area with little or no saturated soil ( $D_w/D < 0.1$  or  $0.2$ ) may be on the order of 40 percent. Gentle basins ( $< 10^\circ$ ) or basins containing areas of poorly drained soils may have larger portions (25 to 75 percent) of nearly saturated conditions (Dunne, in Kirkby 1978; Hookey 1987; Peck and Williamson 1987).

Studies also have shown that in some cases, soil saturation patterns are less dependent on topographic convergence than on the spatial variation of soil hydraulic conductivity or soil water storage (Petch 1988; Reid and others 1988). Therefore, individual sites may not follow gross generalizations made between landform and spatial distribution of  $D_w/D$ . Large-scale groundwater flow systems, such as groundwater base flow from bedrock fractures (Hodge and Freeze 1977; Okunushi and Okimura 1987) and flow in soil pipes (Jones 1988; Pierson 1983), also may be important at some sites.

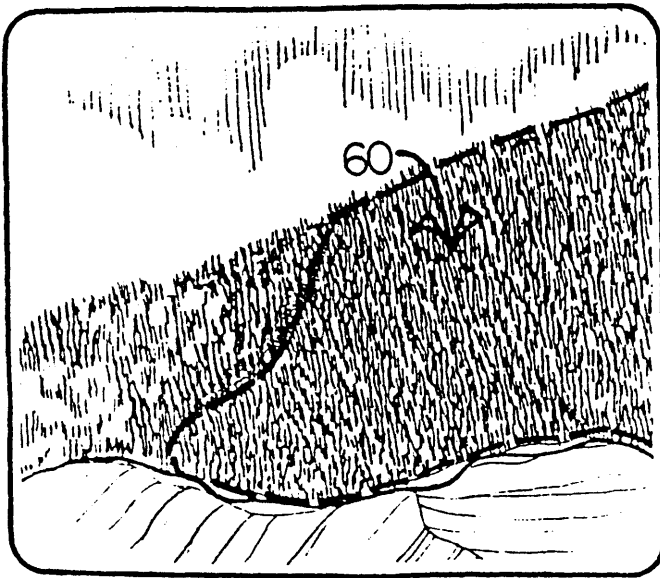
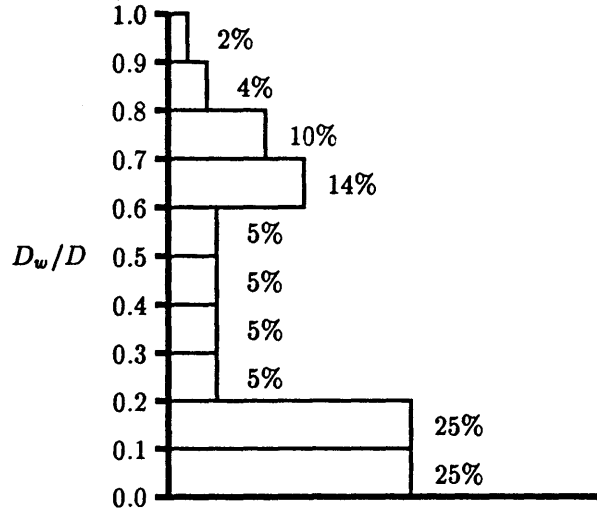
#### **5.3.7.1 Effects of Timber Harvest on Groundwater Levels**

Clearcutting has the potential for increasing the areal extent and the thickness of the saturated zone by increasing the amount of water available for infiltration. The increase in available water results from a decrease in rain or snow interception and evaporation, increases in snow accumulation and the rate of snowmelt, and to a lesser extent, a decrease in transpiration (Megahan 1983). The increase in available water and the resulting increase in streamflow due to clearcutting have been well documented. (Some recent references include Berris and Harr 1987; Harr 1986; Toews and Gluns 1986; Troendle 1987; Troendle and King 1987.)

Several studies have shown increases in groundwater rise and the extent of saturated soil conditions due to clearcutting. Some of the studies looked at gentle watersheds with thick soils and found increases in the minimum water table measured during the summer months (Borg and others 1988; Holstener-Jorgensen 1967; Peck and Williamson 1987). Borg and his coworkers measured an increase in minimum groundwater levels for 2 to 4 years and then declining levels as the forest regenerated. They estimated that groundwater levels will



**LANDFORM 63 STREAM HEADLANDS**



**LANDFORM 60 NONDISSECTED STREAM BREAKLANDS**

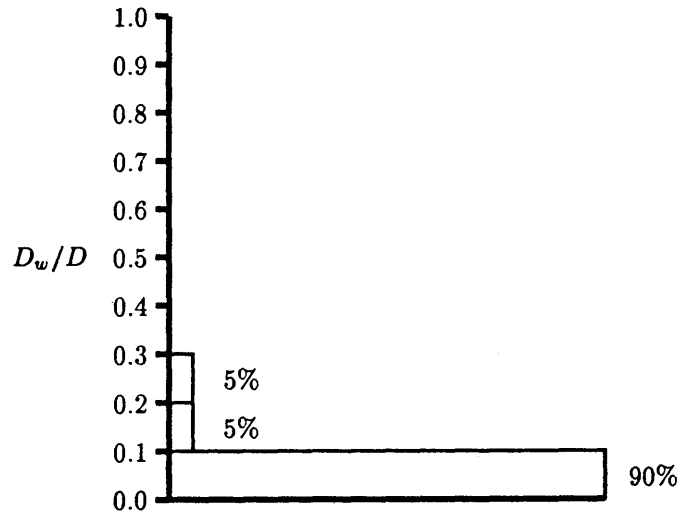


Figure 5.20—Illustrations of landforms and corresponding hypothetical groundwater distributions. The landforms are from the Clearwater National Forest in the Northern Region of the Forest Service (Wilson and others 1983).

reach the levels they would have been without logging within 15 years after the beginning of regeneration.

Peck and Williamson (1987) measured increases in both the annual minimum and annual peak water tables in a basin converted from forest to agriculture. The water levels increased steadily over the 10 years following timber harvest, suggesting that water accumulates until a new input-output equilibrium is achieved.

Other studies have monitored the effect of clearcutting on shallow, perched subsurface runoff that typically results in short-term saturated conditions. These studies also seem to show an increase in the peak groundwater levels recorded during rainfall or snowmelt events (Gray and Megahan 1981; Megahan 1984; Wu 1984). Troendle (1987) reported increases in intercepted subsurface lateral flow due to clearcutting. Groundwater levels were measured but not reported; however, it is logical to assume that if groundwater flow volume increased, groundwater levels would also. Petch (1988) compared the groundwater response to rainfall of a forested basin and a grass basin and found the weekly peak water table levels were usually lower in the forested basin. He attributed the difference primarily to the high interception loss of 49 percent in the forest. Mathematical models also demonstrate the link between timber harvest and increases in soil moisture and groundwater level (Hillman and Verschuren 1988).

The magnitude of the groundwater rise resulting from clearcutting is difficult to predict because, first, it is site specific, depending on the soils, geology, and topography of the site. Second, groundwater levels will vary with annual variations in rain or snowfall, snowmelt, and evapotranspiration. Therefore, it becomes difficult with a limited amount of preharvest and postharvest monitoring data to separate the effects of clearcutting from climatic variations. However, Megahan (1984) did estimate an average increase of 68 percent in the annual peak piezometric levels resulting from clearcutting for 3 postharvest years.

With so little monitoring data available, it is difficult to recommend how much to increase a groundwater distribution to assess with LISA the effects of clearcutting. That is, it appears that groundwater levels at specific points in the basin increase on the order of 50 percent, but the portion of the basin showing higher groundwater levels is a function of site characteristics. Narrow draws with steep side-slopes might show an increase in groundwater level but little increase in the area with high groundwater. Broad, gentle basins might show less increase, but the increase may affect a greater portion of the basin (Dunne in Kirkby 1978; Peck and Williamson 1987).

It is only through additional groundwater monitoring supplemented by modeling that we may begin to gain knowledge on the spatial variation of groundwater levels. Additional research is needed to improve tools to quantify spatial variability and the likelihood of occurrence of peak groundwater levels expected during a specified period, with and without timber harvest.

# CHAPTER 6 — EXAMPLE APPLICATION: DARK 3 PLANNING AREA, GIFFORD PINCHOT NATIONAL FOREST

## 6.1 Introduction

The Dark 3 planning area is on the Randle Ranger District, Gifford Pinchot National Forest, in Washington (Pacific Northwest Region). Jones (1990) performed a Level I stability analysis over the entire area and evaluated three timber sale alternatives. Figure 6.1 shows the topographic map of the Dark 3 planning area and the Level I polygons. (Unlabeled polygons are primarily flood plain deposits and were not analyzed.) The District then requested additional analysis (Level II) on one harvest unit for which field observations supported by the initial LISA analysis indicated a high probability of failure after timber harvest. The District desired to harvest the potentially unstable unit for silvicultural reasons. Both analyses will be described in this chapter. (Using LISA to perform a Level II analysis is discussed in section 5.1.3.)

## 6.2 Geology, Soils, and Topography

The bedrock geology and soil conditions of the Dark 3 planning area are shown in the Geologic Resources and Conditions (GRC) map (fig. 6.2). The bedrock geology of the western half of the area consists of extrusive igneous and minor pyroclastic rocks dipping to the west at 5 to 15 degrees. This bedrock forms a tablelike topographic surface with surface slopes ranging primarily from 20 to 50 percent. The overlying soils consist of 2 to 5 (locally 10+) feet of colluvium and residuum (GW-SM) with minor amounts of glacial till (SM-GM and GMu). It was anticipated that this region would have few stability problems because of the gentle slopes and therefore was analyzed with only two LISA polygons (designated as 3M and 4W in fig. 6.1).

A crescent-shaped area of steep ground with slopes generally greater than 70 percent extends from the northwestern to the southeastern boundary of the planning area. The soils of this steep crescent, which is the edge of the table of volcanic rocks, generally consist of 1 to 2 feet of coarse tephra overlying 2 to 3 feet of colluvium and minor residuum developed from the underlying volcanics (SM-GW). While most of the area appears dry and well drained, areas of springs and seeps are observed. The elevated groundwater and steep slopes apparently have caused rockfalls and debris avalanches, several of which are mapped on the GRC map. Because of the steep slopes and past failure activity, there was concern that timber harvest or road construction in the area would increase the mass failure potential with the possible impacts of loss of the soil resource and damage to the water quality and fisheries of Summit Prairie Creek. Therefore, the crescent was divided into several small polygons of four types (1D, 1M, 2D, 2M), differentiated by slope and groundwater conditions.

In the northeastern third of the area, the bedrock consists of pyroclastic rocks with minor intrusive and extrusive igneous rocks. The bedrock is overlain by glacial till, colluvium, and residuum with minor alluvium, averaging 5 to 10 (locally 30+) feet in thickness. The topography consists of moderate slopes (40 to 90 percent). The area is generally considered to be dry with low failure potential and therefore was analyzed with one LISA polygon (5D).

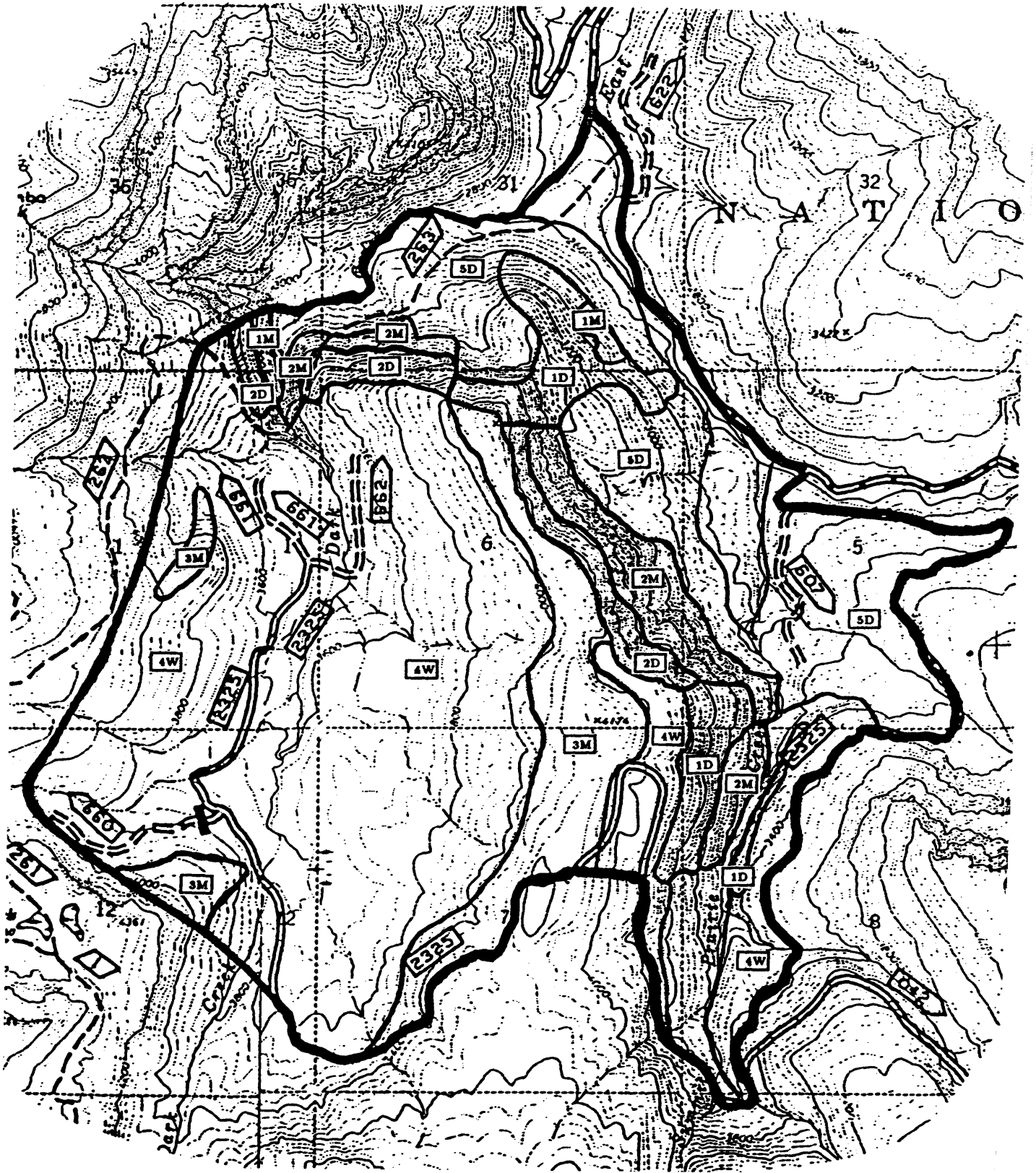


Figure 6.1—Dark 3 planning area and Level I polygons.

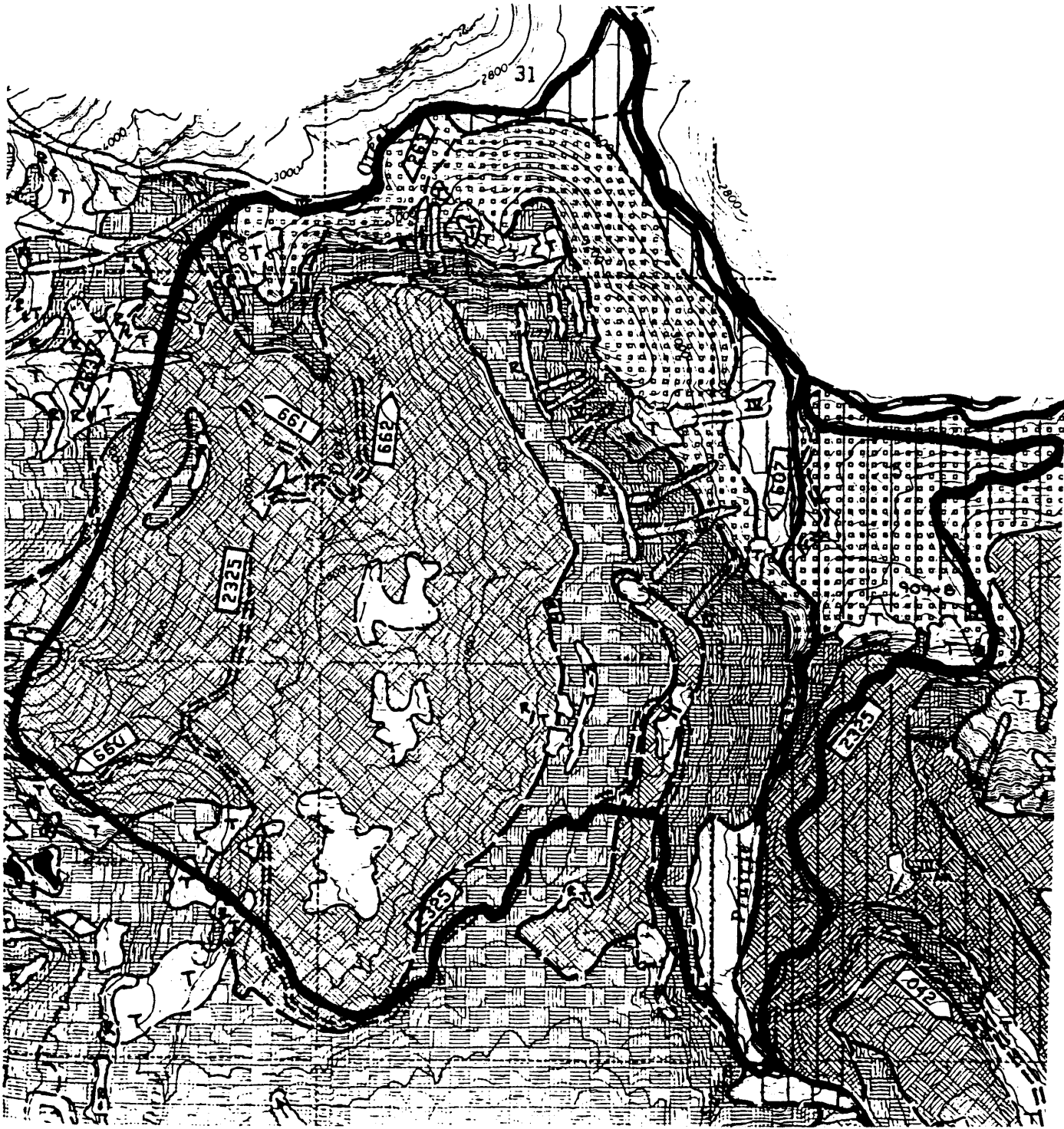


Figure 6.2—Geologic Resources and Conditions (GRC) map for the Dark 3 planning area.

**Mapping Boundary**

- Ground Verified
- - - - - Inferred

**Geologic Resources**

**Mineral Materials**

- — Developed Source
- — Undeveloped Source
- ⊗ — Depleted Source
- ⊞ — Closed Source
- △ — Terminated Source
- ⊕ — Geologic Point of Interest

⊕ — **Underground Space**

⊕ — **Groundwater Extraction**

**Geologic Conditions**

- (R) — Exposed Rock
- (T) — Exposed Talus
- ✕ — Wet Area
- ↗ — Spring

**Slope Stability**

- I — Slide
- II — Flow
- III — Rockfall
- IV — Avalanche
- V — Sidecast Failure > 55% Slope
- VI — Fill Failure < 55% Slope
- VII — Cutslope Failure



- A = Active Slide
- PA = Past Active Slide
- N = Naturally Occurring
- M = Man Related



**NAME/ORIGIN:** Colluvium and residuum overlying extrusive igneous and minor pyroclastic rock.

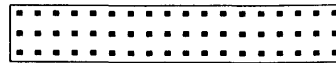
**SOIL:** Nonplastic loose silty sand to well graded gravel (USC:SM-GW). Avg depth < 5'.

**ROCK:** Basalt (URC:BBEA); andesite (URC:BBEA-DDEC); basalt breccia, tuff, tuff breccia (URC:BCEB-CCEB), BRU 2021.

**SIGNIFICANT CONDITIONS:** Unit is characterized by sparsely vegetated steep slopes with thin rocky soil, numerous avalanche chutes, rock outcrop and talus slopes. Wet talus slopes are common. Unit is similar to map unit [diagonal lines] except that this unit has steeper slopes and thinner soil. Minimum surfacing will probably be required for subgrade strength. There is a good potential for quality material sources, but development may be difficult due to steep slopes.

**Special Considerations**

- The compartment is overlain with 2–4' of past and recent Mount St. Helens pumice and ash consisting of poorly graded sand to silty sand (USC:SP-SM). Tephra is free-draining, easily eroded, and may be washed and accumulated into thicknesses up to 12'+.
- Several sidecast failures occur along the 29 Rd. adjacent to McCoy Creek.

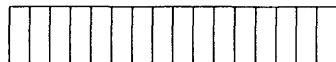


**NAME/ORIGIN:** Colluvium, residuum, and local deposits of glacial till overlying pyroclastic and minor intrusive and extrusive igneous rock.

**SOIL:** Colluvium and residuum—nonplastic to slightly plastic silty sand to silty gravel (USC:SM/SM<sub>U</sub>-GM/GM<sub>U</sub>). Avg depth: 3–9', locally 12'+. Glacial till—nonplastic silty sand to silty gravel (USC:SM-GM), and slightly plastic silty gravel (USC:GM<sub>U</sub>), local nonplastic silt (USC:ML). Avg depth: 3–8', locally up to 30'.

**ROCK:** Tuff, tuff breccia, subordinate felsic tuff (URC:BCEA-DDED); basalt, andesite (URC:BBEA), BRU 4005D.

**SIGNIFICANT CONDITIONS:** Plastic soil is not free-draining, susceptible to slope failure when disturbed on steep slopes, and generally a weak subgrade material. There is a low potential for material sources in this unit. Refer to map unit [diagonal lines] for significant conditions for glacial till.



**NAME/ORIGIN:** Glacial till, colluvium, residuum, and minor alluvium overlying pyroclastic and minor intrusive and extrusive igneous rock.

**SOIL:** Glacial till—nonplastic silty sand to silty gravel (USC:SM-GM), and slightly plastic silty gravel (USC:GM<sub>U</sub>), local nonplastic silt (USC:ML). Avg depth: 5–10', locally 30'+. Colluvium and residuum—nonplastic to slightly plastic silty sand to silty gravel (USC:SM/SM<sub>U</sub>-GM/GM<sub>U</sub>). Avg depth: 4–8'. Alluvium—poorly graded sand to poorly graded gravel (USC:SP-GP). Avg depth: < 5'.

**ROCK:** Tuff, tuff breccia, local felsic tuff (URC:BCEA-DDED); basalt, andesite (URC:BBEA), BRU 4005D.

**SIGNIFICANT CONDITIONS:** Till is locally plastic and/or compact and not free-draining resulting in elevated water tables. Loose till is subject to raveling resulting in increased road maintenance. Plastic soil is susceptible to slope failure when disturbed on steep slopes, and is generally a weak subgrade material.



**NAME/ORIGIN:** Colluvium, residuum, and local deposits of glacial till overlying extrusive igneous and minor pyroclastic rock.

**SOIL:** Colluvium—silty sand to silty gravel (USC:SM-GM). Avg depth: 3–5', locally up to 15'. Residuum—nonplastic to slightly plastic silty sand (USC:SM/SM<sub>U</sub>). Avg depth: 2–4', locally up to 12'+. Glacial till—nonplastic silty sand to silty gravel (USC:SM-GM), and slightly plastic silty gravel (USC:GM<sub>U</sub>). Avg depth: 2–5', locally up to 10'+.

**ROCK:** Basalt (URC:BBEA); andesite (URC:BBEA-DDEC); basalt breccia, tuff, tuff breccia (URC:BCEA-DDED), BRU 2021.

**SIGNIFICANT CONDITIONS:** Unit is characterized by gentle to moderate slopes with poor surficial drainage indicated by the presence of wet areas. Plastic residuum is not free-draining and is generally a weak subgrade material. Glacial till—refer to significant conditions of map unit [diagonal lines]. Till occurs mainly in the Dark Creek drainages.

Figure 6.2—(Con.)

### 6.3 Polygon Delineation and Distribution Selection—Level I

Jones (1990) delineated polygons for the initial Level I analysis using 1:7,200 topographic maps and the soil/geology type as mapped in the GRC. In areas with slopes greater than 65 percent, additional polygons were delineated using low-altitude aerial photographs to better describe slope and groundwater characteristics. Initial soil type and soil depth estimates were obtained from the GRC map and the Soil Resource Inventory (SRI). Shear strength and unit weight values and distributions then were estimated from the USC classification and previous experience and by using table 5.4 and figure 5.11 of this manual. Groundwater distributions used were developed from the groundwater characteristics mapped on the GRC, field observations, and by using a catalog of distributions tied to various landforms developed by Wooten (1988). Root strength distributions used were those suggested by Wooten (1988) for a type B soil-root morphology class. Figure 6.3 contains Wooten's suggested distributions. Limited field checking was performed to verify office findings. Table 6.1 gives the distributions used in the analysis.

### 6.4 Level I Results

Table 6.2 lists the ranges of the probabilities of failure for each polygon as estimated using the LISA program for both the natural and clearcut states. The range of probability of failure values was obtained from five simulations, each using a different seed number for the random number generator. The probabilities of failure for clearcut harvest are conditional on a "major" rainfall or rain-on-snow event occurring during the period of minimum root strength. Also given are relative probabilities of landslide hazard based on the experience and interpretation of the Gifford Pinchot National Forest geotechnical group. This scale can aid individuals not familiar with the LISA program and those uncomfortable with probability numbers in interpreting LISA results. It is not an absolute scale that would necessarily be applicable elsewhere; it is only a *relative* scale based on the experience of the geotechnical group on the Gifford Pinchot.

The proposed cutting units for three timber sale alternatives were overlain on the LISA polygons, and the land area in low, moderate, and high failure-potential polygons was measured. These results are summarized in table 6.3. For each proposed cutting unit, the potential impacts should a failure occur were evaluated as either localized or as having the potential to deliver sediment to Summit Prairie Creek. One of the harvest units (unit 7) of timber sale alternative 1 was located partially in the high failure-potential polygon 2M, with the potential impact of delivering sediment to the creek. Because of this LISA result, along with observations of instability along road 2325 above unit 7, further analysis of the unit was deemed necessary. This analysis is discussed in the next two sections.

### 6.5 Polygon Delineation and Distribution Selection—Level II

Jones (1990) spent approximately 3.5 days in the field gathering slope, soil type, soil depth, and groundwater information to further evaluate the portion of the Dark 3 planning unit surrounding harvest unit 7. Based on the field evaluation, Jones modified the polygons in that portion as shown in figure 6.4. Slopes were measured with a clinometer and soil depth with a hand auger at random

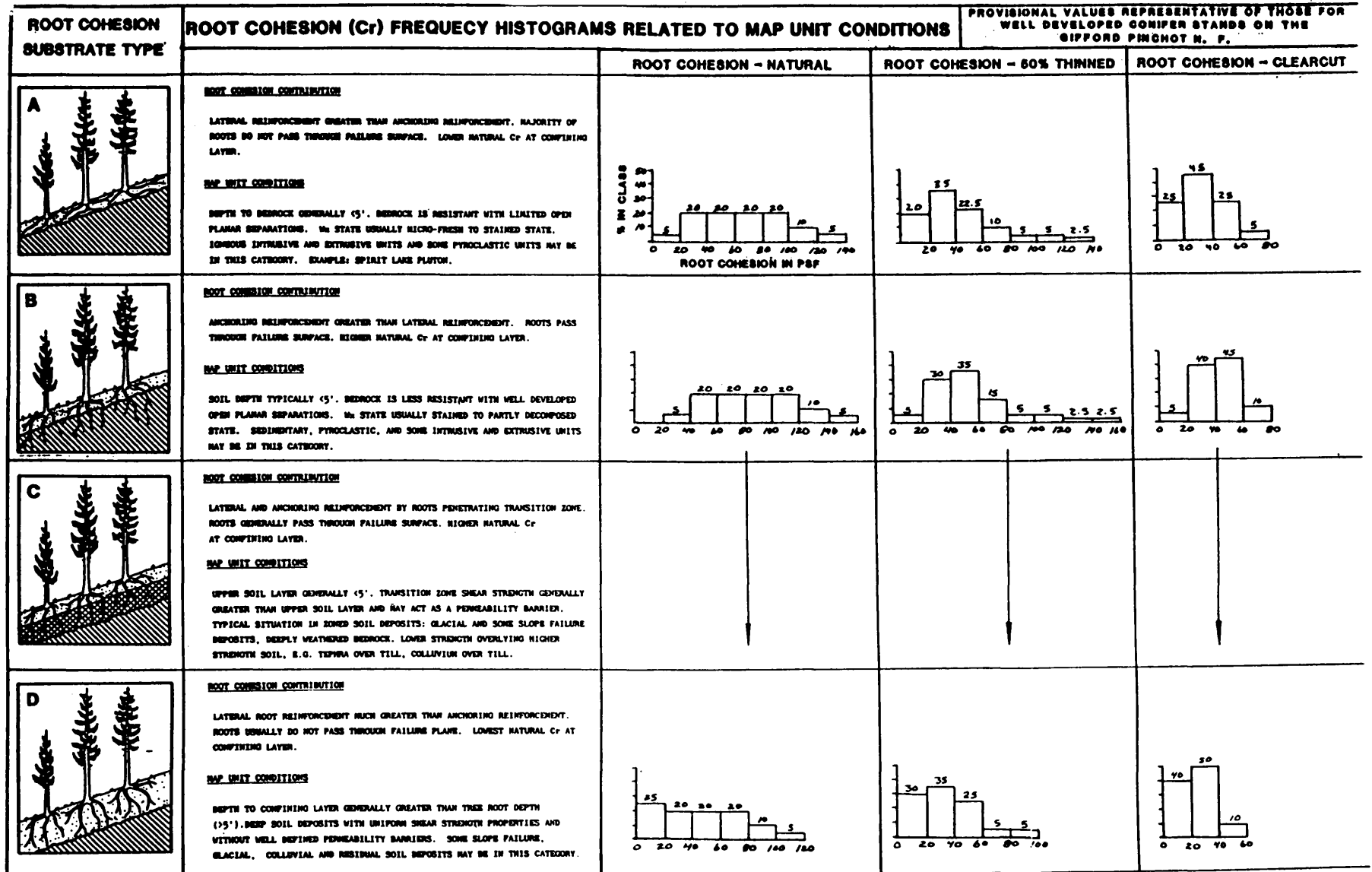


Figure 6.3—Root cohesion distributions suggested by Wooten (1988) for use on the Gifford Pinchot National Forest.

**Table 6.1—Distributions used in the Dark 3 Level I analysis**

Polygon	<i>D</i>	$\alpha$	<i>C'<sub>s</sub></i>	$\phi'$	<i>D<sub>w</sub>/D</i>	
					Natural	Clearcut
1D	<i>T</i> [1, 3, 5]	<i>T</i> [65, 75, 95]	<i>U</i> [10, 75]	<i>U</i> [31, 38]	<i>T</i> [0, .2, .4]	<i>T</i> [0, .25, .5]
1M	<i>T</i> [1, 3, 5]	<i>T</i> [65, 75, 95]	<i>U</i> [10, 75]	<i>U</i> [31, 38]	<i>T</i> [0, .2, .5]	<i>T</i> [0, .3, .6]
2D	<i>T</i> [1, 3, 5]	<i>T</i> [70, 85, 110]	<i>U</i> [10, 75]	<i>U</i> [31, 38]	<i>T</i> [0, .2, .4]	<i>T</i> [0, .25, .5]
2M	<i>T</i> [1, 3, 5]	<i>T</i> [70, 85, 110]	<i>U</i> [10, 75]	<i>U</i> [31, 38]	<i>T</i> [0, .2, .5]	<i>T</i> [0, .3, .6]
3M	<i>T</i> [2, 4, 10]	<i>T</i> [20, 30, 70]	<i>U</i> [10, 50]	<i>U</i> [34, 42]	<i>T</i> [0, .2, .5]	<i>T</i> [0, .3, .6]
4W	<i>T</i> [3, 5, 10]	<i>U</i> [20, 50]	<i>U</i> [20, 100]	<i>U</i> [28, 38]	<i>T</i> [0, .3, .5]	<i>T</i> [0, .4, .7]
5D	<i>T</i> [3, 9, 30]	<i>T</i> [40, 50, 90]	<i>U</i> [40, 100]	<i>U</i> [32, 38]	<i>T</i> [0, .2, .4]	<i>T</i> [0, .3, .5]

For all polygons, *g*<sub>0</sub>: *U*[6, 12]  
*C<sub>r</sub>* (Natural): *H*[4, 5, 80, 10, 5] (or *H*[7, 5, 20, 20, 20, 20, 10, 5]; see fig. 6.3)  
*C<sub>r</sub>* (Clearcut): *H*[4, 5, 40, 45, 10] (see fig. 6.3)  
 $\gamma_a$ : *N*[95, 5]  
*w*: *U*[10, 25]  
*G<sub>s</sub>*: 2.4

**Table 6.2—Dark 3 Level I results**

Polygon	Natural state		Clearcut state	
	<i>P<sub>f</sub></i>	Hazard <sup>1</sup>	<i>P<sub>f</sub></i>	Hazard <sup>1</sup>
1D	0.005–0.010	VL	0.073–0.085	L to M
1M	.008– .013	VL	.091– .119	M
2D	.025– .040	VL to L	.161– .174	H
2M	.029– .043	VL to L	.201– .223	H
3M	.000– .000	VL	.000– .002	VL
4W	.000– .000	VL	.000– .002	VL
5D	.014– .024	VL	.176– .215	H

<sup>1</sup>Relative hazard based on experience of Gifford Pinchot National Forest geotechnical group:

- 0–0.029 = Very low (VL)
- 0.030–0.079 = Low (L)
- 0.080–0.159 = Moderate (M)
- 0.160–0.249 = High (H)
- 0.250+ = Very high (VH)

**Table 6.3—Summary of potentially unstable slopes affected by timber harvest**

	Acres affected		
	Alt. 1	Alt. 2	Alt. 3
Low hazard	16.3	13.7	11.0
Moderate hazard	0.0	0.0	0.0
High hazard	4.5	0.0	0.0

locations when a change in conditions was perceived. Jones recognized that depth measured to “refusal” using a hand auger may not necessarily be the depth to bedrock, as cobbles and boulders also can cause refusal. Therefore, the maximum depth used in the input distributions was somewhat greater than actually measured in the field. The soil type was finer textured (SP–SM) than was predicted by the GRC maps, with slightly plastic fines, and was easily excavated by hand ( $D_r$  of 25 to 45 percent). Shear strength and unit weight values for this different soil type were again estimated from table 5.4 and figure 5.11 of this manual. Several springs were observed in areas that were assumed to be dry in the Level I analysis, although the slopes were relatively dry overall. Therefore, distributions were developed to describe the observed conditions, rather than using the catalog of distributions developed by Wooten (1988). The distributions used for each polygon are given in table 6.4.

## 6.6 Level II Results

Table 6.5 gives the probabilities of failure and relative landslide hazard for each polygon. The more detailed Level II analysis using the LISA program indicates that a large portion of harvest unit 7 has a very low to low probability of failure even after timber harvest, primarily because of the gentle slopes. However, approximately 4.7 acres lie in moderate landslide hazard ground with localized failure impact, and 3.9 acres lie in high landslide hazard ground with a high likelihood of sediment entering Summit Prairie Creek should a failure occur.

Based on the Level II analysis, the District modified the unit boundary to omit the 3.9 acres having high landslide hazard. In addition, because of the observed indications of instability on the fill slope of road 2325 through the unit, Jones (1990) recommended that if timber sale alternative 1 was selected as the preferred alternative, further Level II analysis using the SARA program should be performed on the existing road and on any proposed new construction in harvest unit 7 to determine the need for further subsurface investigation, and stability analysis and design (Level III).

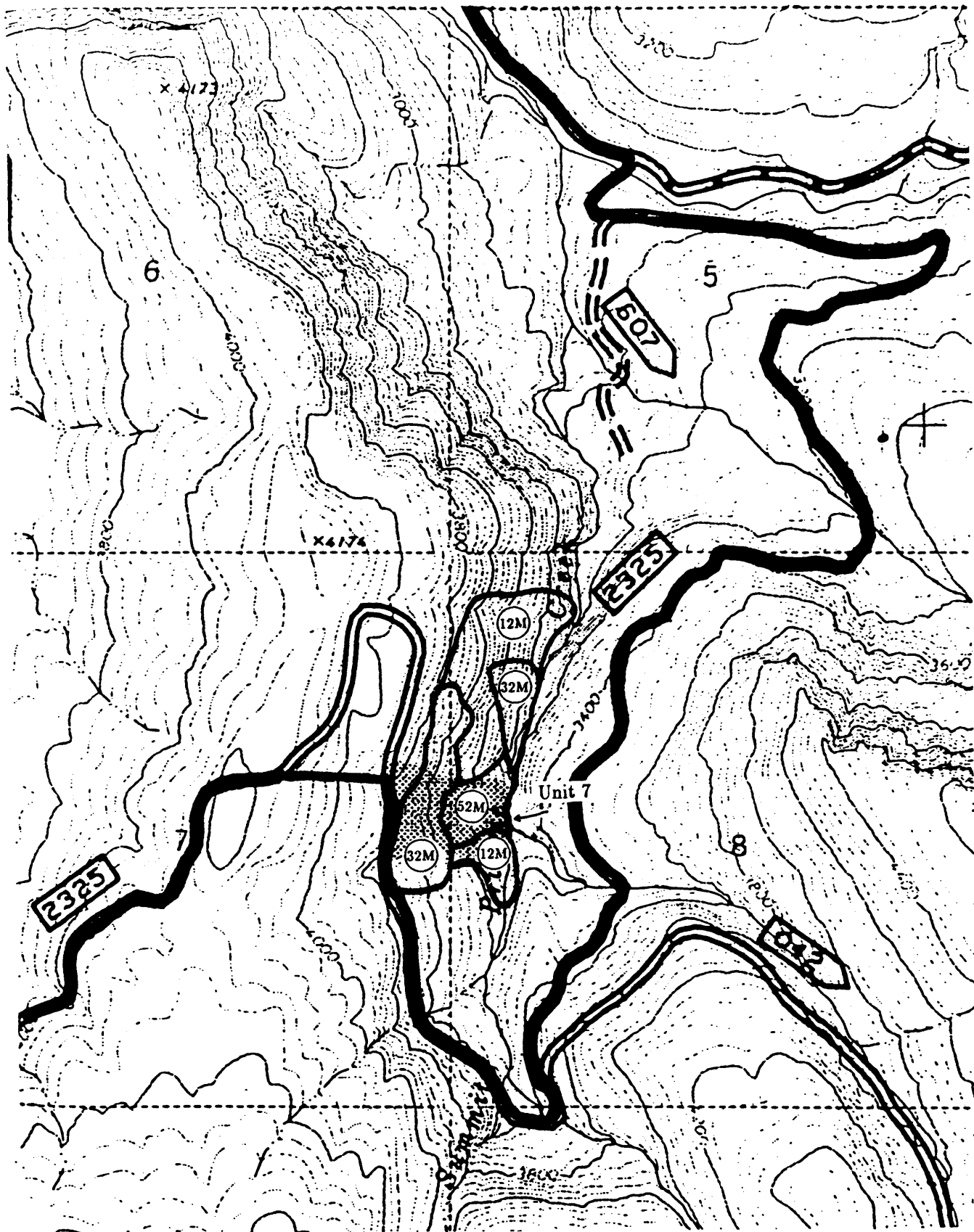


Figure 6.4—Level II analysis polygons.

**Table 6.4—Distributions used in the Dark 3 Level II analysis**

Polygon	$D$	$\alpha$			
12M	$T[2, 3.5, 5]$	$T[60, 70, 85]$			
32M	$T[2, 3.5, 5]$	$T[65, 75, 95]$			
52M	$T[2, 4, 6]$	$T[35, 55, 65]$			
For all polygons, $q_0$ : $U[6, 12]$					
$C_r$ (Natural): $H[4, 5, 80, 10, 5]$ (see fig. 6.3)					
$C_r$ (Clearcut): $H[4, 5, 40, 45, 10]$					
$\gamma_a$ : $N[95, 5]$					
$w$ : $U[10, 25]$					
$G_s$ : 2.4					
$C'_s$ : $U[20, 75]$					
$\phi'$ : $B[28, 36, 2, 2]$					
$D_w/D$ (Natural): Histogram					
Min 0.0 Max 0.1 % 15					
.1 .2 40					
.2 .3 20					
.3 .4 15					
.4 .5 5					
.5 .6 1					
.6 .7 1					
.7 .8 1					
.8 .9 1					
.9 1.0 1					
$D_w/D$ (Clearcut): Histogram					
Min 0.0 Max 0.1 % 5					
.1 .2 10					
.2 .3 20					
.3 .4 40					
.4 .5 15					
.5 .6 6					
.6 .7 1					
.7 .8 1					
.8 .9 1					
.9 1.0 1					

**Table 6.5—Dark 3 Level II results**

Polygon	Natural state		Clearcut state	
	$P_f$	Hazard <sup>1</sup>	$P_f$	Hazard <sup>1</sup>
12M	0.019–0.025	VL	0.117–0.125	M
32M	.026–.039	VL to L	.210–.244	H
52M	.001–.004	VL	.009–.014	VL

<sup>1</sup>Relative hazard based on experience of Gifford Pinchot National Forest geotechnical group:

- 0–0.029 = Very low (VL)
- 0.030–0.079 = Low (L)
- 0.080–0.159 = Moderate (M)
- 0.160–0.249 = High (H)
- 0.250+ = Very high (VH)

## REFERENCES BY AUTHOR

- Abe, K.; Iwamoto, M. 1985. Effect of tree roots on soil shearing strength. In: Proceedings, international symposium on erosion, debris flow and disaster prevention: 1985 September 3–5; Tsukuba, Japan. Tsukuba, Japan: Erosion Control Engineering Society. 341–346.
- Abramowitz, M.; Stegun, I. A., eds. 1965. Handbook of mathematical functions with formulas, graphs, and mathematical tables. New York, NY: Dover Publ. 1046 p.
- Alexander, E. B. 1989a. Bulk density equations for southern Alaska soils. Canadian Journal of Soil Science. 69: 177–180.
- Alexander, E. B. 1989b. Personal communication.
- Athanasίου-Grivas, D.; Harrop-Williams, K. 1979. Joint distribution of the components of soil strength. In: Proceedings of ICASP 3, the third international conference on applications of statistics and probability in soil and structural engineering; 1979 January 29–February 2; Sydney, Australia. Kensington, NSW, Australia: Unisearch Ltd. 1: 189–197.
- Benjamin, J. R.; Cornell, C. A. 1970. Probability, statistics, and decision for civil engineers. New York: McGraw Hill. 684 p.
- Berris, S. N.; Harr, R. D. 1987. Comparative snow accumulation and melt during rainfall in forested and clear-cut plots in the western Cascades of Oregon. Water Resources Research. 23(1): 135–142.
- Bishop, A. W. 1966. The strength of soils as engineering materials. 6th Rankine lecture. Géotechnique. 16(2): 91–128.
- Bjerrum, A. W.; Bjerrum, L. 1960. The relevance of the triaxial test to the solution of stability problems. In: Research conference on shear strength of cohesive soils; 1960 June 13–17; Boulder, CO. New York: American Society of Civil Engineers. 437–501.
- Bjerrum, L.; Simons, N. E. 1960. Comparison of shear strength characteristics of normally consolidated clays. In: Research conference on shear strength of cohesive soils; 1960 June 13–17; Boulder, CO. New York: American Society of Civil Engineers. 711–726.
- Borg, H.; Stoneman, G. L.; Ward, C. G. 1988. The effect of logging and regeneration on groundwater, streamflow and stream salinity in the southern forests of western Australia. Journal of Hydrology. 99: 253–270.
- Bowles, J. E. 1968. Foundation analysis and design. New York: McGraw-Hill. 659 p.
- Brand, E. W.; Premchitt, J.; Phillipson, H. B. 1984. Relationship between rainfall and landslides in Hong Kong. In: IV international symposium on landslides. 1984 September 16–21; Toronto, ON, Canada. Downsview, ON, Canada: University of Toronto, Canadian Geotechnical Society. 1: 377–384.
- Burmister, D. M. 1962. Physical, stress-strain and strength responses of granular soils. In: Field testing of soils, Special technical publication 322. New York: American Society for Testing and Materials. 67–97.

- Burroughs, E. R., Jr. 1984. A landslide hazard rating for portions of the Oregon Coast range. In: O'Loughlin, C. L.; Pearce, A. J., eds. Symposium on effects of forest land use on erosion and slope stability; 1984 May 7-11; Honolulu, HI. Honolulu, HI: University of Hawaii, East-West Center, Environment and Policy Institute. 265-274.
- Burroughs, E. R., Jr.; Thomas, B. R. 1977. Declining root strength in Douglas-fir after felling as a factor in slope stability. Res. Pap. INT-190. Ogden, UT: U.S. Department of Agriculture, Forest Service, Intermountain Forest and Range Experiment Station. 27 p.
- Campbell, R. H. 1975. Soil slips, debris flows, and rainstorms in the Santa Monica Mountains and vicinity, Southern California. U.S. Geol. Surv. Prof. Pap. 851. Reston, VA: U.S. Geological Survey. 51 p.
- Cherubini, C.; Cotechia, V.; Renna, G.; Schiraldi, B. 1983. The use of bivariate probability density functions in Monte Carlo simulation of slope stability in soils. In: Proceedings of ICASP 4, the fourth international conference on applications of statistics and probability in soil and structural engineering; 1983 June 13-17; Firenze, Italy. Bologna, Italy: Pitagora Editrice. 1401-1411.
- Chowdhury, R. N.; Tang, W. H. 1987. Comparison of risk models for slopes. In: Lind, N.C., ed. Reliability and risk analysis in civil engineering: proceedings of ICASP 5, the fifth international conference on applications of statistics and probability in soil and structural engineering; 1987 May 25-29; Vancouver, BC. Waterloo, ONT: Institute for Risk Research, University of Waterloo. 2: 863-869.
- Collotta, T.; Cantoni, R.; Moretti, P. C. 1989. Italian motorway system: experiences with *in situ* tests and inclinometer surveys for urgent remedial works. Transportation Res. Rec. 1235. Washington, DC: Transportation Research Board. 55-59.
- DeGraff, J. V.; McKean, J.; Watanabe, P. E.; McCaffrey, W. F. 1984. Landslide activity and groundwater conditions: insights from a road in the central Sierra Nevada, California. Transportation Res. Rec. 965. Washington, DC: Transportation Research Board. 32-37.
- Dunn, I. S.; Anderson, L. R.; Kiefer, F. W. 1980. Fundamentals of geotechnical analysis. New York: John Wiley and Sons. 414 p.
- Ellen, S. D.; Wieczorek, G. F., eds. 1988. Landslides, floods, and marine effects of the storm of January 3-5, 1982, in the San Francisco Bay region, California. U.S. Geol. Surv. Prof. Pap. 1434. Washington, DC: U.S. Geological Survey. 14 p.
- Endo, T.; Tsuruta, T. 1969a. The effect of the tree's roots upon the shear strength of soil. In: 1968 annual report of the Hokkaido branch, Forest Experiment Station, Sapporo, Japan. 167-182. Translated from Japanese by J. M. Arata and R. R. Ziemer, U.S. Department of Agriculture, Forest Service, Pacific Southwest Station.
- Endo, T.; Tsuruta, T. 1969b. A report in regards to the reinforcement action of the vegetational roots upon the tensile strength of the natural soil. In: 1968 annual report of the Hokkaido Branch, Forest Experiment Station, Sapporo, Japan. 183-189. Translated from Japanese by J. M. Arata and R. R. Ziemer, U.S. Department of Agriculture, Forest Service, Pacific Southwest Station.

- Fredlund, D. G. 1987. Slope stability analysis incorporating the effect of soil suction. In: Anderson, M. G.; Richards, K. S., eds. Slope stability. New York: John Wiley and Sons. 113–144.
- Gray, D. H.; Leiser, A. T. 1982. Biotechnical slope protection and erosion control. New York: Van Nostrand Reinhold. 279 p.
- Gray, D. H.; Megahan, W. F. 1981. Forest vegetation removal and slope stability in the Idaho Batholith. Res. Pap. INT-271. Ogden, UT: U.S. Department of Agriculture, Forest Service, Intermountain Forest and Range Experiment Station. 23 p.
- Gray, D. H.; Ohashi, H. 1983. Mechanics of fiber reinforcement in sand. American Society of Civil Engineers, Journal of the Geotechnical Engineering Div. 109(3). 335–353.
- Greenway, D. R. 1987. Vegetation and slope stability. In: Anderson, M. G.; Richards, K. S., eds. Slope stability. New York: John Wiley and Sons. 187–230.
- Hall, D. E.; Kendall, K. S. 1992. Technical documentation for the LISA program. U.S. Department of Agriculture, Forest Service, Intermountain Research Station, Forestry Sciences Laboratory, RWU 4702, Moscow, ID. In process.
- Hammond, C. J. 1986. Shear strength of the ash cap on the Clearwater National Forest, R1. U.S. Department of Agriculture, Forest Service. Unpublished report on file at Intermountain Res. Sta., Moscow, ID. U.S. Department of Agriculture, Forest Service, Intermountain Research Station, Forestry Sciences Laboratory, RWU 4702, Moscow, ID. Unpaginated.
- Hammond, C. J.; Hardcastle, J. H. 1987. Shear strengths and densities of micaceous sands. In: Proceedings, 8th Panamerican conference of soil mechanics and foundation engineering; 1987 August 16–21; Cartagena, Colombia. Bogotá, Colombia: National University of Colombia. 1: 45–56.
- Hammond, C. J.; Hardcastle, J. H. 1992. Determination of values for shear strength parameters using improved methodology. Final report for cooperative agreement No. 22-C-4-INT-166, U.S. Department of Agriculture, Forest Service. Unpublished report on file at Intermountain Res. Sta., Moscow, ID. U.S. Department of Agriculture, Forest Service, Intermountain Research Station, Forestry Sciences Laboratory, RWU 4702, Moscow, ID. In process.
- Hammond, C. J.; Miller, S. M.; Prellwitz, R. W. 1988. Estimating the probability of landslide failure using Monte Carlo simulation. In: Proceedings, 24th engineering geology and soils engineering symposium; 1988 February 29–March 2; Coeur d'Alene, ID. Moscow, ID: University of Idaho. 319–331.
- Hammond, C. J.; Prellwitz, R. W.; Miller, S. M. 1992. Landslide hazard assessment using Monte Carlo simulation. In: Bell, D., ed. Landslides: proceedings of the 6th international symposium. 1992, February 10–14; Christchurch, New Zealand. Rotterdam, Netherlands: A. A. Balkema Publishers. 959–964.
- Hampton, D.; Megahan, W. F.; Clayton, J. L. 1974. Soil and rock properties research in the Idaho Batholith. Report on a cooperative research effort between Howard University, Washington, DC, and U.S. Department of Agriculture, Forest Service, Forestry Sciences Laboratory, Boise, ID. 126 p.
- Harr, M. E. 1977. Mechanics of particulate media — a probabilistic approach. New York: McGraw-Hill. 543 p.

- Harr, R. D. 1986. Effects of clearcutting in rain-on-snow runoff in western Oregon: a new look at old studies. *Water Resources Research*. 22(7): 1095–1100.
- Hillman, G. R.; Verschuren, J. P. 1988. Simulation of the effects of forest cover, and its removal, on subsurface water. *Water Resources Research*. 24(2): 305–314.
- Hodge, R. A. L.; Freeze, R. A. 1977. Groundwater flow systems and slope stability. *Canadian Geotechnical Journal*. 14(4): 466–476.
- Holstener-Jorgensen, H. 1967. Influences of forest management and drainage on ground-water fluctuations. In: Sopper W. E.; Lull, H. W., eds. *International symposium on forest hydrology; 1965 August 29–September 10; University Park, PA. New York, NY: Pergamon Press. 325–333.*
- Holtz, W. G.; Ellis, W. 1961. Triaxial shear characteristics of clayey gravel soils. In: *Proceedings, 5th international conference on soil mechanics and foundation engineering; 1961 July 17–22; Paris, France. Paris, France: Dunod. 1: 143–149.*
- Holtz, W. G.; Gibbs, H. J. 1956. Triaxial shear tests of pervious gravelly soils. *American Society of Civil Engineers, Journal of Soil Mechanics and Foundations Division*. 82(SM1): Paper 867. 22 p.
- Holtz, W. G.; Krizek, R. J. 1972. Statistical evaluation of soils test data. In: Lumb, P., ed. *Proceedings of ICASP 1, the first international conference on applications of statistics and probability to soil and structural engineering; 1971 September 13–16; Hong Kong. Hong Kong: Hong Kong University Press. 230–266.*
- Hookey, G. R. 1987. Prediction of delays in groundwater response to catchment clearing. *Journal of Hydrology*. 94: 181–198.
- Horn, H. M.; Deere, D. U. 1962. Frictional characteristics of minerals. *Géotechnique*. 12(4): 319–335.
- Hough, B. K. 1957. *Basic soils engineering*. New York: Ronald Press. 513 p.
- Ice, G. G. 1985. *Catalog of landslide inventories for the Northwest*. NCASI Tech. Bulletin 456. New York, NY: National Council of the Paper Industry for Air and Stream Improvement. 160 p.
- Iman, R. L.; Shortencarier, M. J. 1984. *A FORTRAN 77 program and user's guide for the generation of Latin hypercube and random samples for use with computer models*. Sandia National Laboratories. 67 p.
- Iverson, R. M.; Major, J. J. 1986. Groundwater seepage vectors and the potential for hillslope failure and debris flow mobilization. *Water Resources Research*. 22(11): 1543–1548.
- Iverson, R. M.; Major, J. J. 1987. Rainfall, ground-water flow, and seasonal movement at Minor Creek landslide, northwestern California: physical interpretation of empirical relations. *Geological Society of America Bulletin*. 99: 579–594.
- Jones, J. A. A. 1988. Modelling pipeflow contributions to stream runoff. *Hydrological Processes*. 2: 1–17.

- Jones, S. 1990. Dark 3 timber sale slope stability assessment. Packwood, WA: U.S. Department of Agriculture, Forest Service, Gifford Pinchot National Forest. Unpublished report.
- Keefer, D. K.; Wilson, R. C.; Mark, R. K.; [and others]. 1987. Realtime landslide warning during heavy rainfall. *Science*. 238(4829). 921-925.
- Kenney, T. C. 1959. Discussion of geotechnical properties of glacial lake clays. American Society of Civil Engineers, *Journal of the Soil Mechanics and Foundations Division*. 85(SM3): 67-79.
- Kirkby, M. J., ed. 1978. Hillslope hydrology. New York: John Wiley and Sons. 389 p.
- Krahn, J.; Fredlund, D. G. 1983. Variability in the engineering properties of natural deposits. In: Proceedings of ICASP 4, the fourth international conference on applications of statistics and probability in soil and structural engineering; 1983 June 13-17; Firenze, Italy. Bologna, Italy: Pitagora Editrice. 1017-1029.
- Lambe, T. W.; Whitman, R. V. 1969. Soil mechanics. New York: John Wiley and Sons. 553 p.
- Lee, K. L.; Seed, H. B. 1967. Drained strength characteristics of sands. American Society of Civil Engineers, *Journal of the Soil Mechanics and Foundations Division*. 93(SM6): 117-141.
- Leslie, D. D. 1963. Large-scale triaxial tests on gravelly soils. In: Proceedings, 2nd Panamerican conference on soil mechanics and foundation engineering; 1963 July 14-24; São Paulo, SP, Brasil: Associação Brasileira de Mecânica dos Solos. 1: 181-202.
- Lumb, P. 1966. The variability of natural soils. *Canadian Geotechnical Journal*. 3(2): 74-97.
- Lumb, P. 1970. Safety factors and the probability distribution of soil strength. *Canadian Geotechnical Journal*. 7(3): 225-242.
- Lumb, P. 1975. Spatial variability of soil properties. In: Proceedings of ICASP 2, the second international conference on applications of statistics and probability to soil and structural engineering; 1975 September 15-18; Aachen, Germany. Essen, Germany: Deutsche Gesellschaft fuer Erd-und Grundbau. 2: 397-421.
- Marachi, N. D.; Chan, C. K.; Seed, H. B.; Duncan, J. M. 1969. Strength and deformation characteristics of rockfill materials. Report TE 69-5, Berkeley, CA: University of California, Berkeley. Pages unknown.
- Matsuo, M.; Ueno, M. 1979. Prediction of slope slide by probability of failure. In: Proceedings of ICASP 3, the third international conference in the applications of statistics and probability in soil and structural engineering; 1979 January 29-February 2; Sydney, Australia. Kensington, NSW, Australia: Unisearch Ltd. 2: 449-458.
- Megahan, W. F. 1983. Hydrologic effects of clearcutting and wildfire on steep granitic slopes in Idaho. *Water Resources Research*. 19(3): 811-819.
- Megahan, W. F. 1984. Snow melt and logging influence on piezometric levels in steep forested watersheds in Idaho. *Transportation Res. Rec.* 965. Washington, DC: Transportation Research Board. 1-8.

- Miller, S. M. 1988. A temporal model for landslide risk based on historical precipitation. *Journal of Mathematical Geology*. 20(5): 529-542.
- Miller, S. M.; Borgman, L. E. 1984. Probabilistic characterization of shear strength using results of direct shear tests. *Géotechnique*. 34: 273-276.
- Negussey, D.; Wijewickreme, W. D.; Vaid, Y. P. 1988. Constant-volume friction angle of granular materials. *Canadian Geotechnical Journal*. 25: 50-55.
- Newendorp, P. D. 1975. *Decision analysis for petroleum exploration*. Tulsa, OK: PennWell Publishing Co. 668 p.
- Oboni, F.; Bourdeau, P. L. 1983. Determination of the critical slip surface in stability problems. In: *Proceedings of ICASP 4, the fourth international conference on applications of statistics and probability in soil and structural engineering*. 1983 June 13-17; Firenze, Italy. Bologna, Italy: Pitagora Editrice. 1413-1424.
- Okunishi, K.; Okimura, T. 1987. Groundwater models for mountain slopes. In: Anderson, M. G.; Richards, K. S., eds. *Slope stability*. New York: John Wiley and Sons. 265-286.
- O'Loughlin, C. L. 1974. A study of tree root strength deterioration following clearfelling. *Canadian Journal of Forest Research*. 4(1): 107-113.
- O'Loughlin, C. L.; Rowe, L. K.; Pearce, A. J. 1982. Exceptional storm influences on slope erosion and sediment yields in small forest catchments, North Westland, New Zealand. *National Conference Publication 82/6*. Barton, ACT, Australia: Institute of Engineering. 84-91.
- O'Loughlin, C. L.; Ziemer, R. R. 1982. The importance of root strength and deterioration rates upon edaphic stability in steepland forests. In: *Carbon uptake and allocation in subalpine ecosystems as a key to management: Proceedings of an IUFRO workshop*. 1982 August; Corvallis, OR. Corvallis, OR: Oregon State University Forest Research Laboratory. 70-78.
- Peck, A. J.; Williamson, D. R. 1987. Effects of forest clearing on groundwater. *Journal of Hydrology*. 94: 47-65.
- Petch, R. A. 1988. Soil saturation patterns in steep, convergent hill slopes under forest and pasture vegetation. *Hydrologic Processes*. 2: 93-103.
- Pierson, T. C. 1980. Piezometric response to rainstorms in forested hillslope drainage depressions. *Journal of Hydrology (New Zealand)*. 19(1): 1-10.
- Pierson, T. C. 1983. Soil pipes and slope stability. *Quarterly Journal of Engineering Geology, London*. 16: 1-11.
- Prellwitz, R. W. 1981. *Forest Service Handbook 7709.11, Transportation Engineering Handbook, Region 1, Supplement 11, Chapter 60, Foundation Engineering*. U.S. Department of Agriculture, Forest Service.
- Prellwitz, R. W. 1985. A complete three-level approach for analyzing landslides on forest lands. In: *Proceedings: a workshop on slope stability: problems and solutions in forest management*. Gen. Tech. Rep. PNW-180. 1984 February 6-8; Seattle, WA. Portland, OR: U.S. Department of Agriculture, Forest Service, Pacific Northwest Forest and Range Experiment Station. 94-98.

- Prellwitz, R. W. 1988. "SSIS" and "SSCHFS"—preliminary slope stability analysis with the HP41 programmable calculator. EM 7170-9. Washington, DC: U.S. Department of Agriculture, Forest Service. 174 p.
- Prellwitz, R. W. 1989. Personal communication.
- Prellwitz, R. W.; Hall, D. E. 1992. SARA—Stability Analysis for Road Access (Level II) user documentation. Unpublished peer review draft. Intermountain Res. Sta., Moscow, ID. U.S. Department of Agriculture, Forest Service, Intermountain Research Station, Forestry Sciences Laboratory, RWU 4702, Moscow, ID. In process.
- Prellwitz, R. W.; Howard, T. R.; Wilson, W. D. 1983. Landslide analysis concepts for management of forest lands on residual and colluvial soils. Transportation Res. Rec. 919. Washington, DC: Transportation Research Board. 27-36.
- Reid, M. E.; Nielsen, H. P.; Dreiss, S. J. 1988. Hydrologic factors triggering a shallow hillslope failure. Bulletin of the Association of Engineering Geologists. 25(3): 349-361.
- Rétháti, L. 1983. Distribution functions of the soil physical characteristics. In: Proceedings, 8th European conference on soil mechanics and foundation engineering; 1983 May 23-26; Helsinki, Finland. Rotterdam, Netherlands: A. A. Balkema. 1: 405-410.
- Riestenberg, M.; Sovonick-Dunford, S. 1983. The role of woody vegetation in stabilizing slopes in the Cincinnati area, Ohio. Geological Society of America Bulletin. 94: 506-518.
- Ristau, J. M. 1988. Verification of soil slope instability using level one stability analysis. In: Proceedings, 24th engineering geology and soils engineering symposium. 1988 February 29-March 2; Coeur d'Alene, ID. Moscow, ID: University of Idaho. 333-344.
- Rowe, P. W. 1962. The stress-dilatancy relation for static equilibrium of an assembly of particles in contact. Proceedings of the Royal Society of London. 296(A): 500-527.
- Rowe, P. W. 1963. Stress-dilatancy, earth pressures and slopes. American Society of Civil Engineers, Journal of the Soil Mechanics and Foundations Div. 89(SM3): 37-61.
- Rubenstein, R. Y. 1981. Simulation and the Monte Carlo method. New York: John Wiley and Sons. 278 p.
- Schroeder, W. L.; Alto, J. V. 1983. Soil properties for slope stability analysis; Oregon and Washington coastal mountains. Forest Science. 29(4): 823-833.
- Schroeder, W. L.; Swanston, D. N. 1987. Application of geotechnical data to resource planning in Southeast Alaska. Gen. Tech. Rep. PNW-198. Corvallis, OR: U.S. Department of Agriculture, Forest Service, Pacific Northwest Forest and Range Experiment Station. 22 p.
- Schultze, E. 1971. Frequency distributions and correlations of soil properties. In: Lumb, P., ed. Proceedings of ICASP 1, the first international conference on applications of statistics and probability to soil and structural engineering; 1971 September 13-16; Hong Kong. Hong Kong: Hong Kong University Press. 371-387.

- Siddiqi, F. H. 1984. Strength evaluation of cohesionless soils with oversize particles. Davis, CA: University of California. 170 p. Dissertation.
- Sidle, R. C. 1984a. Relative importance of factors influencing landsliding in Coastal Alaska. In: Proceedings, 21st annual engineering geology and soils engineering symposium; 1984 April 5-6; Moscow, ID. Moscow, ID: Idaho Transportation Department and University of Idaho. 311-324.
- Sidle, R. C. 1984b. Shallow groundwater fluctuations in unstable hillslopes of Coastal Alaska. *Zeitschrift fur Gletscherkunde und Glazialgeologie*. 20(2): 79-95.
- Sidle, R. C. 1986. Groundwater accretion in unstable hillslopes of coastal Alaska. In: Conjunctive water use: Proceedings of the symposium; 1986 July; Budapest, Hungary. IAHS Publ. 156. Washington, DC: International Association of Hydrological Sciences Press. 335-343.
- Sidle, R. C.; Pearce, A. J.; O'Loughlin, C. L. 1985. Hillslope stability and land use. *Water Resources Monogr. Ser. 11*. Washington, DC: American Geophysical Union. 140 p.
- Simons, D. B.; Li, R. M.; Ward, T. J. 1978. Mapping of potential landslide areas in terms of slope stability. Contract No. 16-712.01-CA, Colorado State University, Fort Collins, CO. Flagstaff, AZ: U.S. Department of Agriculture, Forest Service, Rocky Mountain Forest and Range Experiment Station. 73 p. Draft final report.
- Singh, A.; Lee, K. L. 1970. Variability in soil parameters. In: Proceedings, 8th annual engineering geology and soils engineering symposium; 1970 April; Boise, ID. Boise, ID: Boise State University. 159-185.
- Skempton, A. W. 1964. Long-term stability of clay slopes. *Géotechnique*. 14(2): 77-101.
- Skempton, A. W. 1985. Residual strength of clays in landslides, folded strata and in the laboratory. *Géotechnique*. 35(1): 3-18.
- Smith, G. N. 1986. Probability and statistics in civil engineering. New York: Nichols Publishing Co. 244 p.
- Sturges, H. A. 1926. The choice of a class interval. *Journal of the American Statistical Association*. 21: 65-66.
- Taylor, R. K.; Cripps, J. C. 1987. Weathering effects: slopes in mudrocks and overconsolidated clays. In: Anderson, M. G.; Richards, K. S., eds. *Slope stability*. New York: John Wiley and Sons. 405-445.
- Toews, D. A. A.; Gluns, D. R. 1986. Snow accumulation and ablation on adjacent forested and clearcut sites in Southeastern British Columbia. In: Proceedings, 54th annual meeting, western snow conference; 1986 April 15-17; Phoenix, AZ. Fort Collins, CO: Colorado State University. 101-111.
- Troendle, C. A. 1987. Effect of clearcutting on streamflow generating processes from a subalpine forest slope. In: *Forest hydrology and watershed management: Proceedings of the symposium*; 1987 August; Vancouver, BC. IAHS Publ. 167. Washington, DC: International Association of Hydrological Sciences Press. 545-552.
- Troendle, C. A.; King, R. M. 1987. The effect of partial and clearcutting on streamflow at Deadhorse Creek, Colorado. *Journal of Hydrology*. 90: 145-157.

- Tsukamoto, Y.; Kusakabe, O. 1984. Vegetation influences on debris slide occurrences on steep slopes in Japan. In: O'Loughlin, C. L.; Pearce, A. J., eds. Symposium on effects of forest land use on erosion and slope stability; 1984 May 7-11; Honolulu, HI. Honolulu, HI: University of Hawaii, East-West Center, Environment and Policy Institute. 63-72.
- Tsukamoto, Y.; Minematsu, H. 1987. Evaluation of the effect of deforestation on slope stability and its application to watershed management. In: Forest hydrology and watershed management: Proceedings of a symposium; 1987 August 9-22; Vancouver, BC. IAHS Publ. 167. Washington, DC: International Association of Hydrological Sciences. 181-189.
- U.S. Department of Navy. 1974. Soil mechanics, foundation and earth structures. NAVFAC DM-7.
- Waldron, L. J. 1977. Shear resistance of root permeated homogeneous and stratified soil. *Journal of the Soil Science Society of America*. 41: 843-849.
- Waldron, L. J.; Dakessian, S. 1981. Soil reinforcement by roots: Calculation of increased soil shear resistance from root properties. *Soil Science*. 132(6): 427-435.
- Waldron, L. J.; Dakessian, S.; Nemson, J. A. 1983. Shear resistance enhancement of 1.22-meter diameter soil cross sections by pine and alfalfa roots. *Journal of the Soil Science Society of America*. 47: 9-14.
- Williamson, D. 1989. Personal communication.
- Wilson, D.; Coyner, J.; Dechert, T. 1983. Land system inventory of the Clearwater National Forest, Region 1 — First Review Draft. Orofino, ID: U.S. Department of Agriculture, Forest Service. 400 p.
- Wooten, R. M. 1988. Level I stability analysis validation report. Cook, WA: U.S. Department of Agriculture, Forest Service, Gifford Pinchot National Forest, Zone II Engineering. Unpublished in-service report.
- Wu, T. H. 1984. Effect of vegetation on slope stability. *Transportation Res. Rec.* 965. Washington, DC: Transportation Research Board. 37-46.
- Wu, T. H.; Beal, P. E.; Lan, C. 1988a. *In situ* shear test of soil-root systems. *American Society of Civil Engineers, Journal of the Geotechnical Engineering Div.* 114(12): 1376-1394
- Wu, T. H.; McKinnell, W. P., III; Swanston, D. N. 1979. Strength of tree roots and landslides of Prince of Wales Island, Alaska. *Canadian Geotechnical Journal*. 16(1): 19-33.
- Wu, T. H.; McOmber, R. M.; Erb, R. T.; Beal, P. E. 1988c. Study of soil-root interaction. *American Society of Civil Engineers, Journal of the Geotechnical Engineering Div.* 114(12): 1351-1375.
- Wu, T. T. H.; Baladi, G. Y. 1986. The effects of grain characteristics on the limiting densities and angle of repose of cohesionless soils. Preprint, Transportation Research Board annual meeting; 1986 January; Washington, DC.
- Ziemer, R. R. 1981a. Roots and the stability of forested slopes. In: Davies, T. R. H. and Pearce, A. J., eds. International symposium on erosion and sediment transport in Pacific rim steeplands; 1981 January 25-31; Christchurch, New Zealand. IAHS Publ. 132. Washington, DC: International Association of Hydrological Sciences Press. 341-361.

- Ziemer, R. R. 1981b. The role of vegetation in the stability of forested slopes. In: Proceedings, International Union of Forestry Research Organizations XVII World Conference; 1981 September 6–17; Kyoto, Japan. Ibaraki, Japan: Japanese IUFRO Congress Council. 1: 297–308
- Ziemer, R. R. 1984. Response of progressive hillslope deformation to precipitation. In: O'Loughlin, C. L.; Pearce, A. J., eds. Symposium on effects of forest land use on erosion and slope stability; 1984 May 7–11; Honolulu, HI. Honolulu, HI: University of Hawaii, East-West Center, Environment and Policy Institute. 91–98.

## REFERENCES BY SUBJECT

### General Slope Stability

- Dunn, I. S.; Anderson, L. R.; Kiefer, F. W. 1980. Fundamentals of geotechnical analysis. New York: John Wiley and Sons. 414 p.
- Hammond, C. J.; Miller, S. M.; Prellwitz, R. W. 1988. Estimating the probability of landslide failure using Monte Carlo simulation. In: Proceedings, 24th engineering geology and soils engineering symposium; 1988 February 29–March 2; Coeur d'Alene, ID. Moscow, ID: University of Idaho. 319–331.
- Hammond, C. J.; Prellwitz, R. W.; Miller, S. M. 1992. Landslide hazard assessment using Monte Carlo simulation. In: Bell, D., ed. Landslides: proceedings of the 6th international symposium. 1992, February 10–14; Christchurch, New Zealand. Rotterdam, Netherlands: A. A. Balkema Publishers. 959–964.
- Ice, G. G. 1985. Catalog of landslide inventories for the Northwest. NCASI Tech. Bulletin 456. New York, NY: National Council of the Paper Industry for Air and Stream Improvement. 160 p.
- Jones, S. 1990. Dark 3 timber sale slope stability assessment. Packwood, WA: U.S. Department of Agriculture, Forest Service, Gifford Pinchot National Forest. Unpublished report.
- Lambe, T. W.; Whitman, R. V. 1969. Soil mechanics. New York: John Wiley and Sons. 553 p.
- Prellwitz, R. W. 1985. A complete three-level approach for analyzing landslides on forest lands. In: Proceedings: a workshop on slope stability: problems and solutions in forest management. Gen. Tech. Rep. PNW-180. 1984 February 6–8; Seattle, WA. Portland, OR: U.S. Department of Agriculture, Forest Service, Pacific Northwest Forest and Range Experiment Station. 94–98.
- Prellwitz, R. W. 1988. "SSIS" and "SSCHFS"—preliminary slope stability analysis with the HP41 programmable calculator. EM 7170-9. Washington, DC: U.S. Department of Agriculture, Forest Service. 174 p.
- Prellwitz, R. W.; Hall, D. E. 1992. SARA—Stability Analysis for Road Access (Level II) user documentation. Unpublished peer review draft. Intermountain Res. Sta., Moscow, ID. U.S. Department of Agriculture, Forest Service, Intermountain Research Station, Forestry Sciences Laboratory, RWU 4702, Moscow, ID. In process.

- Prellwitz, R. W.; Howard, T. R.; Wilson, W. D. 1983. Landslide analysis concepts for management of forest lands on residual and colluvial soils. *Transportation Res. Rec.* 919. Washington, DC: Transportation Research Board. 27-36.
- Ristau, J. M. 1988. Verification of soil slope instability using level one stability analysis. In: *Proceedings, 24th engineering geology and soils engineering symposium*. 1988 February 29-March 2; Coeur d'Alene, ID. Moscow, ID: University of Idaho. 333-344.
- Side, R. C. 1984a. Relative importance of factors influencing landsliding in Coastal Alaska. In: *Proceedings, 21st annual engineering geology and soils engineering symposium*; 1984 April 5-6; Moscow, ID. Moscow, ID: Idaho Transportation Department and University of Idaho. 311-324.
- Side, R. C.; Pearce, A. J.; O'Loughlin, C. L. 1985. Hillslope stability and land use. *Water Resources Monogr. Ser. 11*. Washington, DC: American Geophysical Union. 140 p.
- Wilson, D.; Coyner, J.; Dechert, T. 1983. Land system inventory of the Clearwater National Forest, Region 1 — First Review Draft. Orofino, ID: U.S. Department of Agriculture, Forest Service. 400 p.
- Wooten, R. M. 1988. Level I stability analysis validation report. Cook, WA: U.S. Department of Agriculture, Forest Service, Gifford Pinchot National Forest, Zone II Engineering. Unpublished in-service report.

### **Probability and Monte Carlo Sampling**

- Abramowitz, M.; Stegun, I. A., eds. 1965. *Handbook of mathematical functions with formulas, graphs, and mathematical tables*. New York, NY: Dover Publ. 1046 p.
- Benjamin, J. R.; Cornell, C. A. 1970. *Probability, statistics, and decision for civil engineers*. New York: McGraw Hill. 684 p.
- Cherubini, C.; Cotechia, V.; Renna, G.; Schiraldi, B. 1983. The use of bivariate probability density functions in Monte Carlo simulation of slope stability in soils. In: *Proceedings of ICASP 4, the fourth international conference on applications of statistics and probability in soil and structural engineering*; 1983 June 13-17; Firenze, Italy. Bologna, Italy: Pitagora Editrice. 1401-1411.
- Chowdhury, R. N.; Tang, W. H. 1987. Comparison of risk models for slopes. In: Lind, N.C., ed. *Reliability and risk analysis in civil engineering: proceedings of ICASP 5, the fifth international conference on applications of statistics and probability in soil and structural engineering*; 1987 May 25-29; Vancouver, BC. Waterloo, ONT: Institute for Risk Research, University of Waterloo. 2: 863-869.
- Hall, D. E.; Kendall, K. S. 1992. Technical documentation for the LISA program. U.S. Department of Agriculture, Forest Service, Intermountain Research Station, Forestry Sciences Laboratory, RWU 4702, Moscow, ID. In process.

- Iman, R. L.; Shortencarier, M. J. 1984. A FORTRAN 77 program and user's guide for the generation of Latin hypercube and random samples for use with computer models. Sandia National Laboratories. 67 p.
- Miller, S. M. 1988. A temporal model for landslide risk based on historical precipitation. *Journal of Mathematical Geology*. 20(5): 529-542.
- Newendorp, P. D. 1975. Decision analysis for petroleum exploration. Tulsa, OK: PennWell Publishing Co. 668 p.
- Rubenstein, R. Y. 1981. Simulation and the Monte Carlo method. New York: John Wiley and Sons. 278 p.
- Smith, G. N. 1986. Probability and statistics in civil engineering. New York: Nichols Publishing Co. 244 p.
- Sturges, H. A. 1926. The choice of a class interval. *Journal of the American Statistical Association*. 21: 65-66.

### **Root Strength**

- Burroughs, E. R., Jr. 1984. A landslide hazard rating for portions of the Oregon Coast range. In: O'Loughlin, C. L.; Pearce, A. J., eds. Symposium on effects of forest land use on erosion and slope stability; 1984 May 7-11; Honolulu, HI. Honolulu, HI: University of Hawaii, East-West Center, Environment and Policy Institute. 265-274.
- Burroughs, E. R., Jr.; Thomas, B. R. 1977. Declining root strength in Douglas-fir after felling as a factor in slope stability. Res. Pap. INT-190. Ogden, UT: U.S. Department of Agriculture, Forest Service, Intermountain Forest and Range Experiment Station. 27 p.
- Endo, T.; Tsuruta, T. 1969a. The effect of the tree's roots upon the shear strength of soil. In: 1968 annual report of the Hokkaido branch, Forest Experiment Station, Sapporo, Japan. 167-182. Translated from Japanese by J. M. Arata and R. R. Ziemer, U.S. Department of Agriculture, Forest Service, Pacific Southwest Station.
- Endo, T.; Tsuruta, T. 1969b. A report in regards to the reinforcement action of the vegetational roots upon the tensile strength of the natural soil. In: 1968 annual report of the Hokkaido Branch, Forest Experiment Station, Sapporo, Japan. 183-189. Translated from Japanese by J. M. Arata and R. R. Ziemer, U.S. Department of Agriculture, Forest Service, Pacific Southwest Station.
- Gray, D. H.; Leiser, A. T. 1982. Biotechnical slope protection and erosion control. New York: Van Nostrand Reinhold. 279 p.
- Gray, D. H.; Megahan, W. F. 1981. Forest vegetation removal and slope stability in the Idaho Batholith. Res. Pap. INT-271. Ogden, UT: U.S. Department of Agriculture, Forest Service, Intermountain Forest and Range Experiment Station. 23 p.
- Gray, D. H.; Ohashi, H. 1983. Mechanics of fiber reinforcement in sand. *American Society of Civil Engineers, Journal of the Geotechnical Engineering Div.* 109(3). 335-353.

- Greenway, D. R. 1987. Vegetation and slope stability. In: Anderson, M. G.; Richards, K. S., eds. Slope stability. New York: John Wiley and Sons: 187-230.
- O'Loughlin, C. L. 1974. A study of tree root strength deterioration following clearfelling. Canadian Journal of Forest Research. 4(1): 107-113.
- O'Loughlin, C. L.; Rowe, L. K.; Pearce, A. J. 1982. Exceptional storm influences on slope erosion and sediment yields in small forest catchments, North Westland, New Zealand. National Conference Publication 82/6. Barton, ACT, Australia: Institute of Engineering. 84-91.
- O'Loughlin, C. L.; Ziemer, R. R. 1982. The importance of root strength and deterioration rates upon edaphic stability in steepland forests. In: Carbon uptake and allocation in subalpine ecosystems as a key to management: Proceedings of an IUFRO workshop. 1982 August; Corvallis, OR. Corvallis, OR: Oregon State University Forest Research Laboratory. 70-78.
- Riestenberg, M.; Sovonick-Dunford, S. 1983. The role of woody vegetation in stabilizing slopes in the Cincinnati area, Ohio. Geological Society of America Bulletin. 94: 506-518.
- Simons, D. B.; Li, R. M.; Ward, T. J. 1978. Mapping of potential landslide areas in terms of slope stability. Contract No. 16-712.01-CA, Colorado State University, Fort Collins, CO. Flagstaff, AZ: U.S. Department of Agriculture, Forest Service, Rocky Mountain Forest and Range Experiment Station. 73 p. Draft final report.
- Tsukamoto, Y.; Kusakabe, O. 1984. Vegetation influences on debris slide occurrences on steep slopes in Japan. In: O'Loughlin, C. L.; Pearce, A. J., eds. Symposium on effects of forest land use on erosion and slope stability; 1984 May 7-11; Honolulu, HI. Honolulu, HI: University of Hawaii, East-West Center, Environment and Policy Institute. 63-72.
- Tsukamoto, Y.; Minematsu, H. 1987. Evaluation of the effect of deforestation on slope stability and its application to watershed management. In: Forest hydrology and watershed management: Proceedings of a symposium; 1987 August 9-22; Vancouver, BC. IAHS Publ. 167. Washington, DC: International Association of Hydrological Sciences. 181-189.
- Waldron, L. J. 1977. Shear resistance of root permeated homogeneous and stratified soil. Journal of the Soil Science Society of America. 41: 843-849.
- Waldron, L. J.; Dakessian, S. 1981. Soil reinforcement by roots: Calculation of increased soil shear resistance from root properties. Soil Science. 132(6): 427-435.
- Waldron, L. J.; Dakessian, S.; Nemson, J. A. 1983. Shear resistance enhancement of 1.22-meter diameter soil cross sections by pine and alfalfa roots. Journal of the Soil Science Society of America. 47: 9-14.
- Wu, T. H. 1984. Effect of vegetation on slope stability. Transportation Res. Rec. 965. Washington, DC: Transportation Research Board. 37-46.
- Wu, T. H.; Beal, P. E.; Lan, C. 1988a. *In situ* shear test of soil-root systems. American Society of Civil Engineers, Journal of the Geotechnical Engineering Div. 114(12): 1376-1394

- Wu, T. H.; McKinnell, W. P., III; Swanston, D. N. 1979. Strength of tree roots and landslides of Prince of Wales Island, Alaska. *Canadian Geotechnical Journal*. 16(1): 19-33.
- Wu, T. H.; McOmber, R. M.; Erb, R. T.; Beal, P. E. 1988c. Study of soil-root interaction. *American Society of Civil Engineers, Journal of the Geotechnical Engineering Div.* 114(12): 1351-1375.
- Ziemer, R. R. 1981a. Roots and the stability of forested slopes. In: Davies, T. R. H. and Pearce, A. J., eds. *International symposium on erosion and sediment transport in Pacific rim steeplands*; 1981 January 25-31; Christchurch, New Zealand. IAHS Publ. 132. Washington, DC: International Association of Hydrological Sciences Press. 341-361.
- Ziemer, R. R. 1981b. The role of vegetation in the stability of forested slopes. In: *Proceedings, International Union of Forestry Research Organizations XVII World Conference*; 1981 September 6-17; Kyoto, Japan. Ibaraki, Japan: Japanese IUFRO Congress Council. 1: 297-308

### Soil Shear Strength

- Alexander, E. B. 1989a. Bulk density equations for southern Alaska soils. *Canadian Journal of Soil Science*. 69: 177-180.
- Athanasiou-Grivas, D.; Harrop-Williams, K. 1979. Joint distribution of the components of soil strength. In: *Proceedings of ICASP 3, the third international conference on applications of statistics and probability in soil and structural engineering*; 1979 January 29-February 2; Sydney, Australia. Kensington, NSW, Australia: Unisearch Ltd. 1: 189-197.
- Bishop, A. W. 1966. The strength of soils as engineering materials. 6th Rankine lecture. *Géotechnique*. 16(2): 91-128.
- Bjerrum, A. W.; Bjerrum, L. 1960. The relevance of the triaxial test to the solution of stability problems. In: *Research conference on shear strength of cohesive soils*; 1960 June 13-17; Boulder, CO. New York: American Society of Civil Engineers. 437-501.
- Bjerrum, L.; Simons, N. E. 1960. Comparison of shear strength characteristics of normally consolidated clays. In: *Research conference on shear strength of cohesive soils*; 1960 June 13-17; Boulder, CO. New York: American Society of Civil Engineers. 711-726.
- Bowles, J. E. 1968. *Foundation analysis and design*. New York: McGraw-Hill. 659 p.
- Burmister, D. M. 1962. Physical, stress-strain and strength responses of granular soils. In: *Field testing of soils, Special technical publication 322*. New York: American Society for Testing and Materials. 67-97.
- Collotta, T.; Cantoni, R.; Moretti, P. C. 1989. Italian motorway system: experiences with *in situ* tests and inclinometer surveys for urgent remedial works. *Transportation Res. Rec.* 1235. Washington, DC: Transportation Research Board. 55-59.

- Fredlund, D. G. 1987. Slope stability analysis incorporating the effect of soil suction. In: Anderson, M. G.; Richards, K. S., eds. Slope stability. New York: John Wiley and Sons. 113–144.
- Hammond, C. J. 1986. Shear strength of the ash cap on the Clearwater National Forest, R1. U.S. Department of Agriculture, Forest Service. Unpublished report on file at Intermountain Res. Sta., Moscow, ID. U.S. Department of Agriculture, Forest Service, Intermountain Research Station, Forestry Sciences Laboratory, RWU 4702, Moscow, ID. Unpaginated.
- Hammond, C. J.; Hardcastle, J. H. 1987. Shear strengths and densities of micaeous sands. In: Proceedings, 8th Panamerican conference of soil mechanics and foundation engineering; 1987 August 16–21; Cartagena, Colombia. Bogotá, Colombia: National University of Colombia. 1: 45–56.
- Hammond, C. J.; Hardcastle, J. H. 1992. Determination of values for shear strength parameters using improved methodology. Final report for cooperative agreement No. 22-C-4-INT-166, U.S. Department of Agriculture, Forest Service. Unpublished report on file at Intermountain Res. Sta., Moscow, ID. U.S. Department of Agriculture, Forest Service, Intermountain Research Station, Forestry Sciences Laboratory, RWU 4702, Moscow, ID. In process.
- Hampton, D.; Megahan, W. F.; Clayton, J. L. 1974. Soil and rock properties research in the Idaho Batholith. Report on a cooperative research effort between Howard University, Washington, DC, and U.S. Department of Agriculture, Forest Service, Forestry Sciences Laboratory, Boise, ID. 126 p.
- Harr, M. E. 1977. Mechanics of particulate media — a probabilistic approach. New York: McGraw-Hill. 543 p.
- Holtz, W. G.; Ellis, W. 1961. Triaxial shear characteristics of clayey gravel soils. In: Proceedings, 5th international conference on soil mechanics and foundation engineering; 1961 July 17–22; Paris, France. Paris, France: Dunod. 1: 143–149.
- Holtz, W. G.; Gibbs, H. J. 1956. Triaxial shear tests of pervious gravelly soils. American Society of Civil Engineers, Journal of Soil Mechanics and Foundations Division. 82(SM1): Paper 867. 22 p.
- Holtz, W. G.; Krizek, R. J. 1972. Statistical evaluation of soils test data. In: Lumb, P., ed. Proceedings of ICASP 1, the first international conference on applications of statistics and probability to soil and structural engineering; 1971 September 13–16; Hong Kong. Hong Kong: Hong Kong University Press. 230–266.
- Horn, H. M.; Deere, D. U. 1962. Frictional characteristics of minerals. Géotechnique. 12(4): 319–335.
- Hough, B. K. 1957. Basic soils engineering. New York: Ronald Press. 513 p.
- Kenney, T. C. 1959. Discussion of geotechnical properties of glacial lake clays. American Society of Civil Engineers, Journal of the Soil Mechanics and Foundations Division. 85(SM3): 67–79.
- Krahn, J.; Fredlund, D. G. 1983. Variability in the engineering properties of natural deposits. In: Proceedings of ICASP 4, the fourth international conference on applications of statistics and probability in soil and structural engineering; 1983 June 13–17; Firenze, Italy. Bologna, Italy: Pitagora Editrice. 1017–1029.

- Lee, K. L.; Seed, H. B. 1967. Drained strength characteristics of sands. American Society of Civil Engineers, Journal of the Soil Mechanics and Foundations Division. 93(SM6): 117-141.
- Leslie, D. D. 1963. Large-scale triaxial tests on gravelly soils. In: Proceedings, 2nd Panamerican conference on soil mechanics and foundation engineering; 1963 July 14-24; São Paulo, SP, Brasil: Associação Brasileira de Mecânica dos Solos. 1: 181-202.
- Lumb, P. 1966. The variability of natural soils. Canadian Geotechnical Journal. 3(2): 74-97.
- Lumb, P. 1970. Safety factors and the probability distribution of soil strength. Canadian Geotechnical Journal. 7(3): 225-242.
- Lumb, P. 1975. Spatial variability of soil properties. In: Proceedings of ICASP 2, the second international conference on applications of statistics and probability to soil and structural engineering; 1975 September 15-18; Aachen, Germany. Essen, Germany: Deutsche Gesellschaft fuer Erd-und Grundbau. 2: 397-421.
- Marachi, N. D.; Chan, C. K.; Seed, H. B.; Duncan, J. M. 1969. Strength and deformation characteristics of rockfill materials. Report TE 69-5, Berkeley, CA: University of California, Berkeley. Pages unknown.
- Matsuo, M.; Ueno, M. 1979. Prediction of slope slide by probability of failure. In: Proceedings of ICASP 3, the third international conference in the applications of statistics and probability in soil and structural engineering; 1979 January 29-February 2; Sydney, Australia. Kensington, NSW, Australia: Unisearch Ltd. 2: 449-458.
- Miller, S. M.; Borgman, L. E. 1984. Probabilistic characterization of shear strength using results of direct shear tests. Géotechnique. 34: 273-276.
- Negussey, D.; Wijewickreme, W. D.; Vaid, Y. P. 1988. Constant-volume friction angle of granular materials. Canadian Geotechnical Journal. 25: 50-55.
- Oboni, F.; Bourdeau, P. L. 1983. Determination of the critical slip surface in stability problems. In: Proceedings of ICASP 4, the fourth international conference on applications of statistics and probability in soil and structural engineering. 1983 June 13-17; Firenze, Italy. Bologna, Italy: Pitagora Editrice. 1413-1424.
- Prellwitz, R. W. 1981. Forest Service Handbook 7709.11, Transportation Engineering Handbook, Region 1, Supplement 11, Chapter 60, Foundation Engineering. U.S. Department of Agriculture, Forest Service.
- Rétháti, L. 1983. Distribution functions of the soil physical characteristics. In: Proceedings, 8th European conference on soil mechanics and foundation engineering; 1983 May 23-26; Helsinki, Finland. Rotterdam, Netherlands: A. A. Balkema. 1: 405-410.
- Rowe, P. W. 1962. The stress-dilatancy relation for static equilibrium of an assembly of particles in contact. Proceedings of the Royal Society of London. 296(A): 500-527.
- Rowe, P. W. 1963. Stress-dilatancy, earth pressures and slopes. American Society of Civil Engineers, Journal of the Soil Mechanics and Foundations Div. 89(SM3): 37-61.

- Schroeder, W. L.; Alto, J. V. 1983. Soil properties for slope stability analysis; Oregon and Washington coastal mountains. *Forest Science*. 29(4): 823-833.
- Schroeder, W. L.; Swanston, D. N. 1987. Application of geotechnical data to resource planning in Southeast Alaska. Gen. Tech. Rep. PNW-198. Corvallis, OR: U.S. Department of Agriculture, Forest Service, Pacific Northwest Forest and Range Experiment Station. 22 p.
- Schultze, E. 1971. Frequency distributions and correlations of soil properties. In: Lumb, P., ed. *Proceedings of ICASP 1, the first international conference on applications of statistics and probability to soil and structural engineering*; 1971 September 13-16; Hong Kong. Hong Kong: Hong Kong University Press. 371-387.
- Siddiqi, F. H. 1984. Strength evaluation of cohesionless soils with oversize particles. Davis, CA: University of California. 170 p. Dissertation.
- Singh, A.; Lee, K. L. 1970. Variability in soil parameters. In: *Proceedings, 8th annual engineering geology and soils engineering symposium*; 1970 April; Boise, ID. Boise, ID: Boise State University. 159-185.
- Skempton, A. W. 1964. Long-term stability of clay slopes. *Géotechnique*. 14(2): 77-101.
- Skempton, A. W. 1985. Residual strength of clays in landslides, folded strata and in the laboratory. *Géotechnique*. 35(1): 3-18.
- Taylor, R. K.; Cripps, J. C. 1987. Weathering effects: slopes in mudrocks and overconsolidated clays. In: Anderson, M. G.; Richards, K. S., eds. *Slope stability*. New York: John Wiley and Sons. 405-445.
- U.S. Department of Navy. 1974. Soil mechanics, foundation and earth structures. NAVFAC DM-7.
- Wu, T. T. H.; Baladi, G. Y. 1986. The effects of grain characteristics on the limiting densities and angle of repose of cohesionless soils. Preprint, Transportation Research Board annual meeting; 1986 January; Washington, DC. Unpaginated.

## **Groundwater**

- Brand, E. W.; Premchitt, J.; Phillipson, H. B. 1984. Relationship between rainfall and landslides in Hong Kong. In: *IV international symposium on landslides*. 1984 September 16-21; Toronto, ON, Canada. Downsview, ON, Canada: University of Toronto, Canadian Geotechnical Society. 1: 377-384.
- Campbell, R. H. 1975. Soil slips, debris flows, and rainstorms in the Santa Monica Mountains and vicinity, Southern California. U.S. Geol. Surv. Prof. Pap. 851 Reston, VA: U.S. Geological Survey. 51 p.
- DeGraff, J. V.; McKean, J.; Watanabe, P. E.; McCaffrey, W. F. 1984. Landslide activity and groundwater conditions: insights from a road in the central Sierra Nevada, California. *Transportation Res. Rec.* 965. Washington, DC: Transportation Research Board. 32-37.

- Ellen, S. D.; Wieczorek, G. F., eds. 1988. Landslides, floods, and marine effects of the storm of January 3–5, 1982, in the San Francisco Bay region, California. U.S. Geol. Surv. Prof. Pap. 1434. Washington, DC: U.S. Geological Survey. 14 p.
- Hodge, R. A. L.; Freeze, R. A. 1977. Groundwater flow systems and slope stability. *Canadian Geotechnical Journal*. 14(4): 466–476.
- Iverson, R. M.; Major, J. J. 1986. Groundwater seepage vectors and the potential for hillslope failure and debris flow mobilization. *Water Resources Research*. 22(11): 1543–1548.
- Iverson, R. M.; Major, J. J. 1987. Rainfall, groundwater flow, and seasonal movement at Minor Creek landslide, northwestern California: physical interpretation of empirical relations. *Geological Society of America Bulletin*. 99: 579–594.
- Jones, J. A. A. 1988. Modelling pipeflow contributions to stream runoff. *Hydrological Processes*. 2: 1–17.
- Keefer, D. K.; Wilson, R. C.; Mark, R. K.; [and others]. 1987. Realtime landslide warning during heavy rainfall. *Science*. 238(4829): 921–925.
- Kirkby, M. J., ed. 1978. *Hillslope hydrology*. New York: John Wiley and Sons. 389 p.
- Okunishi, K.; Okimura, T. 1987. Groundwater models for mountain slopes. In: Anderson, M. G.; Richards, K. S., eds. *Slope stability*. New York: John Wiley and Sons. 265–286.
- Pierson, T. C. 1983. Soil pipes and slope stability. *Quarterly Journal of Engineering Geology, London*. 16: 1–11.
- Reid, M. E.; Nielsen, H. P.; Dreiss, S. J. 1988. Hydrologic factors triggering a shallow hillslope failure. *Bulletin of the Association of Engineering Geologists*. 25(3): 349–361.
- Side, R. C. 1984b. Shallow groundwater fluctuations in unstable hillslopes of Coastal Alaska. *Zeitschrift für Gletscherkunde und Glazialgeologie*. 20(2): 79–95.
- Side, R. C. 1986. Groundwater accretion in unstable hillslopes of coastal Alaska. In: *Conjunctive water use: Proceedings of the symposium; 1986 July; Budapest, Hungary*. IAHS Publ. 156. Washington, DC: International Association of Hydrological Sciences Press. 335–343.
- Ziemer, R. R. 1984. Response of progressive hillslope deformation to precipitation. In: O'Loughlin, C. L.; Pearce, A. J., eds. *Symposium on effects of forest land use on erosion and slope stability; 1984 May 7–11; Honolulu, HI*. Honolulu, HI: University of Hawaii, East-West Center, Environment and Policy Institute. 91–98.

## Timber Harvest Effects on Groundwater Levels

- Berris, S. N.; Harr, R. D. 1987. Comparative snow accumulation and melt during rainfall in forested and clear-cut plots in the western Cascades of Oregon. *Water Resources Research*. 23(1): 135-142.
- Borg, H.; Stoneman, G. L.; Ward, C. G. 1988. The effect of logging and regeneration on groundwater, streamflow and stream salinity in the southern forests of western Australia. *Journal of Hydrology*. 99: 253-270.
- Gray, D. H.; Megahan, W. F. 1981. Forest vegetation removal and slope stability in the Idaho Batholith. Res. Pap. INT-271. Ogden, UT: U.S. Department of Agriculture, Forest Service, Intermountain Forest and Range Experiment Station. 23 p.
- Harr, R. D. 1986. Effects of clearcutting in rain-on-snow runoff in western Oregon: a new look at old studies. *Water Resources Research*. 22(7): 1095-1100.
- Hillman, G. R.; Verschuren, J. P. 1988. Simulation of the effects of forest cover, and its removal, on subsurface water. *Water Resources Research*. 24(2): 305-314.
- Holstener-Jorgensen, H. 1967. Influences of forest management and drainage on ground-water fluctuations. In: Sopper W. E.; Lull, H. W., eds. International symposium on forest hydrology; 1965 August 29-September 10; University Park, PA. New York, NY: Pergamon Press. 325-333.
- Hookey, G. R. 1987. Prediction of delays in groundwater response to catchment clearing. *Journal of Hydrology*. 94: 181-198.
- Megahan, W. F. 1983. Hydrologic effects of clearcutting and wildfire on steep granitic slopes in Idaho. *Water Resources Research*. 19(3): 811-819.
- Megahan, W. F. 1984. Snow melt and logging influence on piezometric levels in steep forested watersheds in Idaho. *Transportation Res. Rec.* 965. Washington, DC: Transportation Research Board. 1-8.
- Peck, A. J.; Williamson, D. R. 1987. Effects of forest clearing on groundwater. *Journal of Hydrology*. 94: 47-65.
- Petch, R. A. 1988. Soil saturation patterns in steep, convergent hill slopes under forest and pasture vegetation. *Hydrologic Processes*. 2: 93-103.
- Pierson, T. C. 1980. Piezometric response to rainstorms in forested hillslope drainage depressions. *Journal of Hydrology (New Zealand)*. 19(1): 1-10.
- Toews, D. A. A.; Gluns, D. R. 1986. Snow accumulation and ablation on adjacent forested and clearcut sites in Southeastern British Columbia. In: Proceedings, 54th annual meeting, western snow conference; 1986 April 15-17; Phoenix, AZ. Fort Collins, CO: Colorado State University. 101-111.
- Troendle, C. A. 1987. Effect of clearcutting on streamflow generating processes from a subalpine forest slope. In: Forest hydrology and watershed management: Proceedings of the symposium; 1987 August; Vancouver, BC. IAHS Publ. 167. Washington, DC: International Association of Hydrological Sciences Press. 545-552.
- Troendle, C. A.; King, R. M. 1987. The effect of partial and clearcutting on streamflow at Deadhorse Creek, Colorado. *Journal of Hydrology*. 90: 145-157.

# APPENDIX A—DERIVATION OF THE INFINITE SLOPE EQUATION WITH SEEPAGE PARALLEL TO THE SLOPE

## Uplift Force on Base

**Pore-Water pressure**

$$u = \gamma_w h_p = \gamma_w D_w \cos^2 \alpha$$

**Uplift Force**

$$U = \frac{ub}{\cos \alpha} = \gamma_w D_w b \cos \alpha$$

## Other Forces

**Total Weight**

$$W_T = b(q_0 + \gamma_m D_m + \gamma_{\text{sat}} D_w)$$

**Normal Force**

$$N = W_T \cos \alpha = b \cos \alpha (q_0 + \gamma_m D_m + \gamma_{\text{sat}} D_w)$$

**Effective Normal Force**

$$\begin{aligned} N' &= N - U \\ &= b \cos \alpha (q_0 + \gamma_m D_m + \gamma_{\text{sat}} D_w) - \gamma_w D_w b \cos \alpha \\ &= b \cos \alpha [q_0 + \gamma_m D_m + (\gamma_{\text{sat}} - \gamma_w) D_w] \end{aligned}$$

**Shear Force**

$$T = W_T \sin \alpha = b \sin \alpha (q_0 + \gamma_m D_m + \gamma_{\text{sat}} D_w)$$

(Side forces are assumed to be equal and opposite, and therefore cancel out.)

## Stresses

**Effective Normal Stress**

$$\sigma' = \frac{N'}{b / \cos \alpha} = \cos^2 \alpha [q_0 + \gamma_m D_m + (\gamma_{\text{sat}} - \gamma_w) D_w]$$

**Shear Stress**

$$\tau = \frac{T}{b / \cos \alpha} = \cos \alpha \sin \alpha (q_0 + \gamma_m D_m + \gamma_{\text{sat}} D_w)$$

## Shear Strength

$$\begin{aligned} S &= C_r + C'_s + \sigma' \tan \phi' \\ &= C_r + C'_s + \cos^2 \alpha [q_0 + \gamma_m D_m + (\gamma_{\text{sat}} - \gamma_w) D_w] \tan \phi' \end{aligned}$$

## Factor of Safety

$$FS = \frac{S}{\tau} = \frac{C_r + C'_s + \cos^2 \alpha [q_0 + \gamma_m D_m + (\gamma_{\text{sat}} - \gamma_w) D_w] \tan \phi'}{\cos \alpha \sin \alpha (q_0 + \gamma_m D_m + \gamma_{\text{sat}} D_w)}$$

Substituting  $D - D_w$  for  $D_m$  and rearranging gives:

$$FS = \frac{C_r + C'_s + [q_0 + \gamma_m D + (\gamma_{\text{sat}} - \gamma_w - \gamma_m) D_w] \cos^2 \alpha \tan \phi'}{[q_0 + \gamma_m D + (\gamma_{\text{sat}} - \gamma_m) D_w] \cos \alpha \sin \alpha}$$

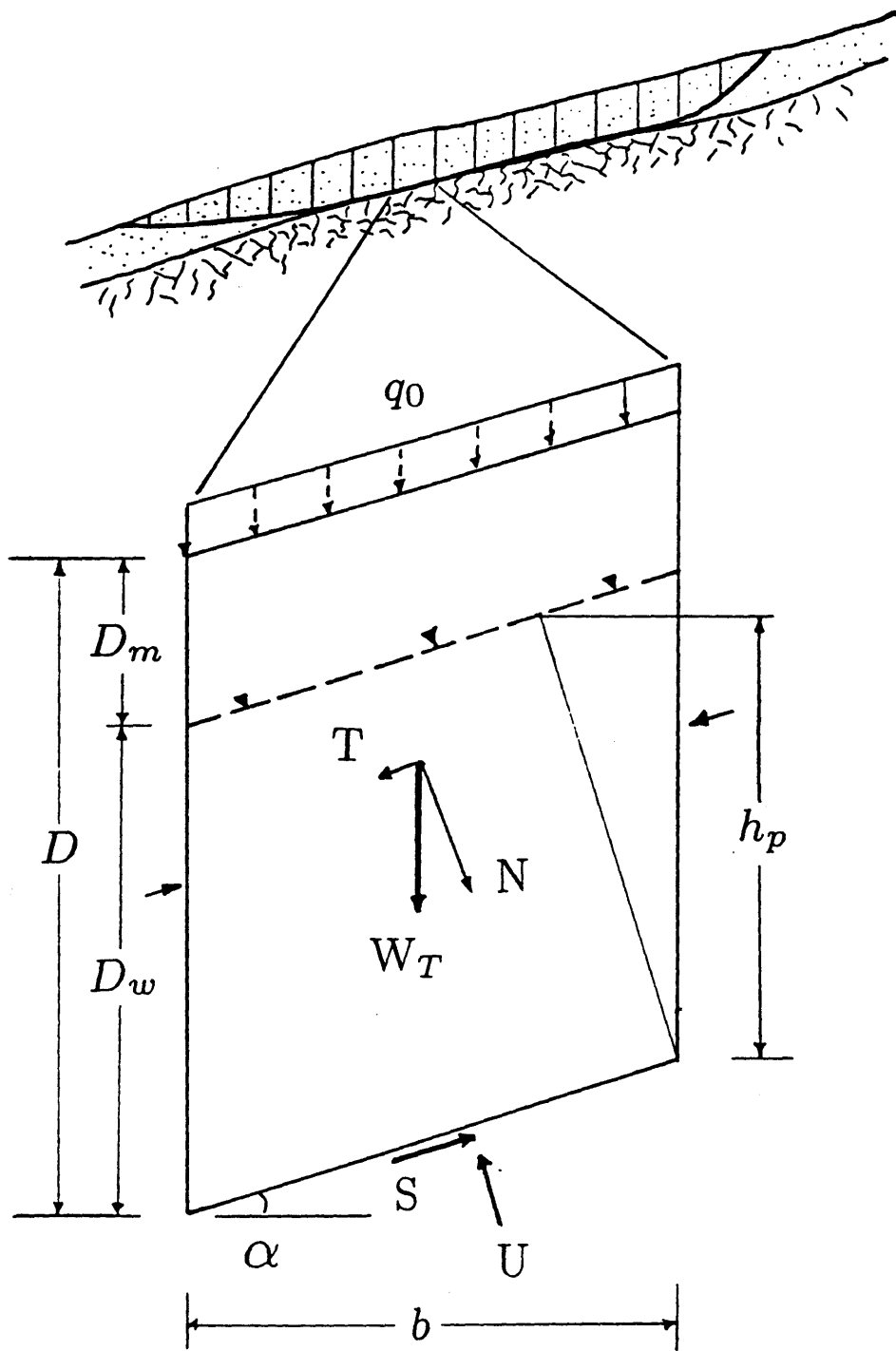


Figure A.1—Infinite slope model force diagram.

## APPENDIX B—ROOT STRENGTH: A DETAILED LITERATURE REVIEW

Root strength has been measured or estimated in four ways: tensile strength measurements of individual roots, direct shear tests on soil-root masses, pull tests on large root systems or whole trees, and by back-analysis of existing failures. Each of these methods is described in more detail below.

### Tensile Strength of Individual Roots and Their Use in Root Strength Models

Tensile strength of individual roots is measured by holding roots of various sizes in some type of clamp device and pulling until failure. Such measurements have found that the resisting tensile force increases with the diameter of the root, but the tensile strength per unit area of root decreases as the diameter of the root increases. These tensile strength values are used either directly or in a theoretical model.

When used directly, the root strength per unit area of soil, which is needed for stability analysis, is estimated from the tensile strength of individual roots and the numbers of roots. This typically is done by two mathematically similar methods. In the first method, the number of roots in various size classes within a soil sample are counted. The total root strength per unit soil area,  $t_R$ , is then computed by dividing the soil sample area into the sum of the products of the average resisting force of the roots and the number of roots for each size class. This can be expressed mathematically as:

$$t_R = \frac{\sum_{i=1}^N F_i n_i}{A} \quad (\text{B.1})$$

where  $t_R$  is the average tensile strength of roots per unit area of soil (psf),  $F_i$  is the average resisting tensile force of roots in the  $i$ th size class (lb),  $n_i$  is the number of roots in the  $i$ th size class, and  $A$  is the area of soil in the sample count ( $\text{ft}^2$ ).

Root strength measurements of this type have been made for Oregon coastal Douglas-fir by Burroughs and Thomas (1977), for hemlock and Sitka spruce by Wu and others (1979), for sugar maple by Reistenberg and Sovonick-Dunford (1983), and for 5-year-old yellow pine seedlings by Waldron and Dakessian (1981).

Greenway (1987) discusses a second (but mathematically equivalent) method for computing  $t_R$  based on work by Waldron (1977), Wu and others (1979), and Gray and Leiser (1982). In this method,  $t_R$  is estimated by multiplying the weighted average tensile strength per average area of root for roots of all size classes ( $T_R$ ) by the root area ratio ( $A_R/A$ ), which is the fraction of the soil area occupied by roots. Mathematically, this is expressed as:

$$t_R = T_R \left( \frac{A_R}{A} \right) \quad (\text{B.2})$$

where  $T_R$  is the weighted average tensile strength per average root cross-sectional area,  $A_R$  is the total cross-sectional area of all of the roots counted, and  $A$  is the area of soil in the sample count.

$T_R$  is computed by:

$$T_R = \frac{\sum T_i n_i a_i}{\sum n_i a_i} \quad (\text{B.3})$$

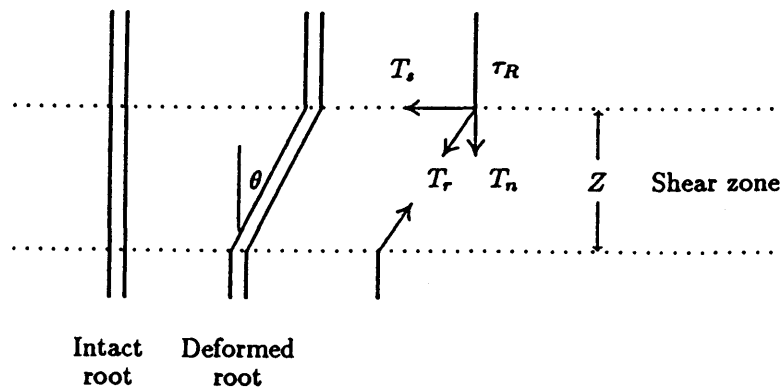


Figure B.1—Fiber reinforcement model (after Gray and Ohashi 1983).

where  $T_i$  is the average tensile strength per root cross-sectional area for the  $i$ th size class,  $a_i$  is the root cross-sectional area for the  $i$ th size class, and  $n_i$  is the number of roots in the  $i$ th size class.

Greenway (1987) has compiled  $T_R$  values for various species, which must then be multiplied by the  $A_R/A$  ratio at a given site to obtain  $t_R$  values for use in LISA.  $A_R/A$  values ranging from 0.0004 (Burroughs and Thomas 1977) to 0.0093 (Gray and Megahan 1981) to 0.017 (Gray and Ohashi 1983) have been reported.  $A_R/A$  values are so variable because they depend upon species, climate, and, most important, the depth at which the measurements are made. Therefore, it is difficult to estimate realistic  $A_R/A$  values from the literature; LISA users would need to make field measurements of  $A_R/A$ , which is impractical for a Level I or Level II analysis.

Waldron and Dakessian (1981) found with simulation studies using their model (described below) that even when roots were tightly held with no slippage, roots failed progressively during shear displacement. In other words, not all roots mobilize their maximum tensile resistance at the same time during slope failure. This limited the amount of root strength developed to about 56 percent of that calculated by assuming that all roots would mobilize maximum shear strength at the same time. Burroughs (1984) comments that  $t_R$  calculated by either equation B.1 or B.2 should be reduced by perhaps 25 percent for the same reason.

Waldron (1977), Wu and others (1979), Waldron and Dakessian (1981), and Gray and Leiser (1982) modify the tensile strengths of roots ( $t_R$ ) using mathematical models, to estimate the root resistance for use in stability analysis ( $C_r$ ). These models are all similar in that they resolve the tensile force that develops in the roots during shear ( $T_r$ ) into a tangential component ( $T_s$ ) that directly resists shear and a normal component ( $T_n$ ) that increases the confining stress on the shear plane, thereby increasing the frictional component of soil shear strength. Figure B.1 illustrates the basic model. The simplest of these mathematical models is:

$$C_r = t_R[\sin \theta + \cos \theta \tan \phi] \quad (\text{B.4})$$

where  $C_r$  is the shear strength increase from root reinforcement,  $t_R$  is the tensile strength of roots as computed by equation B.1 or B.2,  $\phi$  is the angle of internal friction of the soil, and  $\theta$  is the angle of shear distortion.

This model assumes that roots are initially oriented perpendicular to the failure plane. It is recognized that in nature, roots are likely oriented randomly

with respect to the failure plane, leading Gray and Leiser (1982) to propose a model in which the initial orientation angle is also a variable. However, Gray and Ohashi (1983) found with direct shear tests on fiber reinforced soils, that fibers oriented at  $90^\circ$  to the shear plane provided about the same increase in shear strength as randomly oriented fibers. They concluded that the assumption of perpendicular orientation satisfactorily approximates the shear strength increase along a surface crossed by randomly oriented roots.

Equation B.4 results in  $C_r$  being 0 to 30 percent greater than  $t_R$ , depending on the friction angle and angle of shear distortion. Because the angle of shear distortion usually is not known, Wu and others (1979) recommended that for soils with a friction angle between  $30$  and  $40^\circ$ , a value for  $C_r$  20 percent greater than  $t_R$  would be reasonable. Gray and Megahan (1981) recommend that  $C_r$  be 12 percent greater than  $t_R$ ; Gray and Leiser (1982) recommended that  $C_r$  be 15 percent greater. However, Reistenberg and Sovonick-Dunford (1983) and Waldron and Dakessian (1981) observed that the angle of shear distortion of roots was nearly  $90^\circ$  in slope failures, and therefore no increase in  $C_r$  above  $t_R$  would be predicted by the model.

Wu and others (1979) and Gray and Leiser (1982) used  $t_R$  computed as in equation B.1 or B.2, thereby assuming full mobilization of the tensile strength of roots. Other authors, particularly Waldron and Dakessian (1981) and Gray and Ohashi (1983) recognized that roots may slip or pull out before they break in tension. The pull-out resistance of roots is dependent on the soil type. It may be quite high for gravelly soils, where roots take tortuous paths around coarse fragments, but quite low for saturated clay soils. Waldron and Dakessian (1981) estimated root strength might be reduced by as much as 75 percent in saturated clay loam due to root pull out. This was estimated from a root strength of 5 kPa measured in direct shear compared to 18.5 kPa estimated using equation B.4 in which pull-out resistance is not considered. Gray and Ohashi (1983) therefore modified the model to account for pull-out resistance. Now:

$$t_R = \left( \frac{A_R}{A} \right) \sigma_R \quad (\text{B.5})$$

where  $t_R$  is the *mobilized* tensile strength of roots per unit area of soil, and  $\sigma_R$  is the tensile stress developed in the root at the shear plane.  $\sigma_R$  can be estimated from the following expression (which assumes a linear tensile stress distribution along the root length):

$$\sigma_R = \left( \frac{4E_R\tau_R}{D_R} \right)^{\frac{1}{2}} [z(\sec\theta - 1)]^{\frac{1}{2}} \quad (\text{B.6})$$

in which  $E_R$  is the longitudinal stiffness modulus of the root,  $\tau_R$  is the skin friction stress (or pull-out resistance) along the root,  $D_R$  is the diameter of the root, and  $z$  is the thickness of the shear zone. Note that  $t_R$  in this model is no longer the tensile strength of the roots as measured in equations B.1 or B.2, but depends upon the stiffness modulus of the root and the root pull-out resistance, as well as upon  $D_R$  and  $z$ .

Gray and Ohashi (1983) found that pull-out resistance depends not only upon soil type, but upon overburden pressure and fiber length. In their direct shear tests on fiber-reinforced sands, there was a threshold confining stress below which fibers slipped or were pulled out, resulting in little shear strength increase by the fibers. However, it should be noted that the fibers used did not have the interlocking behavior roots might possess in granular soils, so it is not known whether a threshold stress might control root strength in nature.

## Direct Shear Tests on Soil-Root Masses

Direct shear tests on soil-root masses have been performed in several ways. Waldron and Dakessian (1981) and Waldron and others (1983) performed laboratory direct shear tests on large columns of soil containing yellow pine roots. Endo and Tsuruta (1969a) carved out pedestals of soils beneath alder seedlings and sheared them along their base. Ziemer (1981a, 1981b) and Wu and others (1979, 1988a, 1988c) performed *in situ* direct shear tests on soil blocks isolated on the front, back, and bottom, and sheared along two opposing sides. Tsukamoto and Minematsu (1987) isolated the perimeter of small Sugi trees and sheared them along their bases. All of these tests show that the shear strength of the soil-root mass increases with the weight (or number) of the roots present in the soil mass. (This is consistent with equations B.1, B.2 and B.5.) When the shear strength of soil specimens with roots is compared to the shear strength of soil without roots, the roots appear to provide cohesion but not an increase in the friction angle of the soil (O'Loughlin and Ziemer 1982). (That is, the increase in strength is not dependent on normal or confining stress.)

Direct shear tests may better account for pull-out resistance and for the fact that maximum tensile strength is not mobilized by all of the roots simultaneously, but there are still problems with measuring root reinforcement in this way; specifically, at high strains, the soil block tends to be torn apart by the roots. Also, with Ziemer's device, roots can pass completely through the soil block, which may not correctly model the failure mode of the soil-root mass in nature. However, results of direct shear tests generally have been comparable to root strength per soil unit area computed from individual root tensile strength tests, except in the cases described above in which the pull-out resistance of the roots was very low (such as Waldron and Dakessian 1981 and Gray and Ohashi 1983).

## Pull Tests on Large Root Systems and Whole Trees

This method may be the most reliable for measuring the effective tensile strength and pull-out resistance of root systems, because it simulates more closely what occurs during slope failure. Tests of this type have been attempted by Abe and Iwamoto (1985) and Tsukamoto and Kusakabe (1984). Endo and Tsuruta (1969b) performed tensile strength tests on blocks of soil and roots by attempting to pull the soil-root blocks apart. Tensile strength values measured were close to the shear strength values reported for the two methods described above.

## Back-Analysis of Existing Failures

By estimating or measuring prefailure values for all other parameters needed in a stability analysis, root strength values can be back-calculated using information on existing failures. The assumption is that the factor of safety equals 1 at failure. This method does give approximate values, but unless the values for the other variables can be estimated confidently, this becomes a mathematical number exercise for which there are several possible combinations of values that give a factor of safety of 1. Back-calculated values reported in the literature were not used in estimating distributions for use in LISA. However, they do support that  $t_R$  values calculated with equation B.1 or B.2 are realistic even with all of the uncertainty about progressive root failure and pull-out resistance. For example, Reistenberg and Sovonick-Dunford (1983) counted the number of roots found on both the scarp and slip surface of an existing failure and computed

root strength using equation B.1. They computed a greater root strength per unit soil area in the scarp than on the slip surface because there were a greater number of roots in the scarp. When the appropriate root strength values were used in a method-of-slices stability analysis, they were able to calculate a factor of safety close to 1 for the prefailure conditions, indicating the values used for root strength were realistic, even though pull-out resistance and progressive root failure were not considered.

## APPENDIX C—RATIONALE FOR SELECTING ROOT STRENGTH PDF'S

To estimate probability distributions for each root morphology type, we used the data tabulated in table 5.2, along with the following observations and assumptions to select PDFs for root strength.

- We assumed that the measured values of root strength reported in the literature and summarized in table 5.2 and figure 5.6 apply to soil-root morphology types B and C, where roots intersect the entire failure plane. As mentioned in appendix B, many of the root strengths reported were computed from tensile strength tests on individual roots and from root numbers, which probably overestimate root strength because not all roots would be loaded to failure simultaneously during a slope failure, and because of root slippage and pull out. However, none of the methods of measuring root strength described includes soil buttressing and arching. Gray and Megahan (1981) present a formula for calculating buttressing and arching resistance. However, they do not present any typical values nor indicate how the values should be used in a stability analysis. We have assumed that buttressing and arching would be significant enough in types B and C to offset any overestimating of root strength that would result from individual root tensile strength measurements. There also may be some increase in strength due to increased stress on the failure plane as calculated by equation B.4.
- Because the infinite slope equation assumes that root strength acts along the entire failure surface, the measured values of root strength must be reduced to some *apparent* values for types A and D where root strength acts only along the failure perimeter. To estimate reasonable values for apparent root strength, a comparison was made between the root strength values that give the same factor of safety for the infinite slope equation and for a three-dimensional block model (Burroughs 1984). The three-dimensional block model considers root strength to act only in the top 2 feet of soil, thereby increasing shear resistance along the block sides and tensile resistance along the block headwall. Roots are assumed not to penetrate the stable substrate, so there is no increase in shear resistance along the block base even when the soil is less than 2 feet thick. This is consistent with the type A and D conditions.

The first step in the comparison was to find block lengths and widths that produced factors of safety equal to those calculated by the infinite slope equation for several combinations of slope and soil depth, and with root strength equal to zero. Length-to-width ratios of 1.1:1 or 1.2:1 at 45 percent slope, to 1.5:1 at 75 percent slope satisfied this step. Next, the factors of safety for each block were calculated using the three-dimensional model with root strength values of 50 to 400 psf. The apparent root strength values required to give

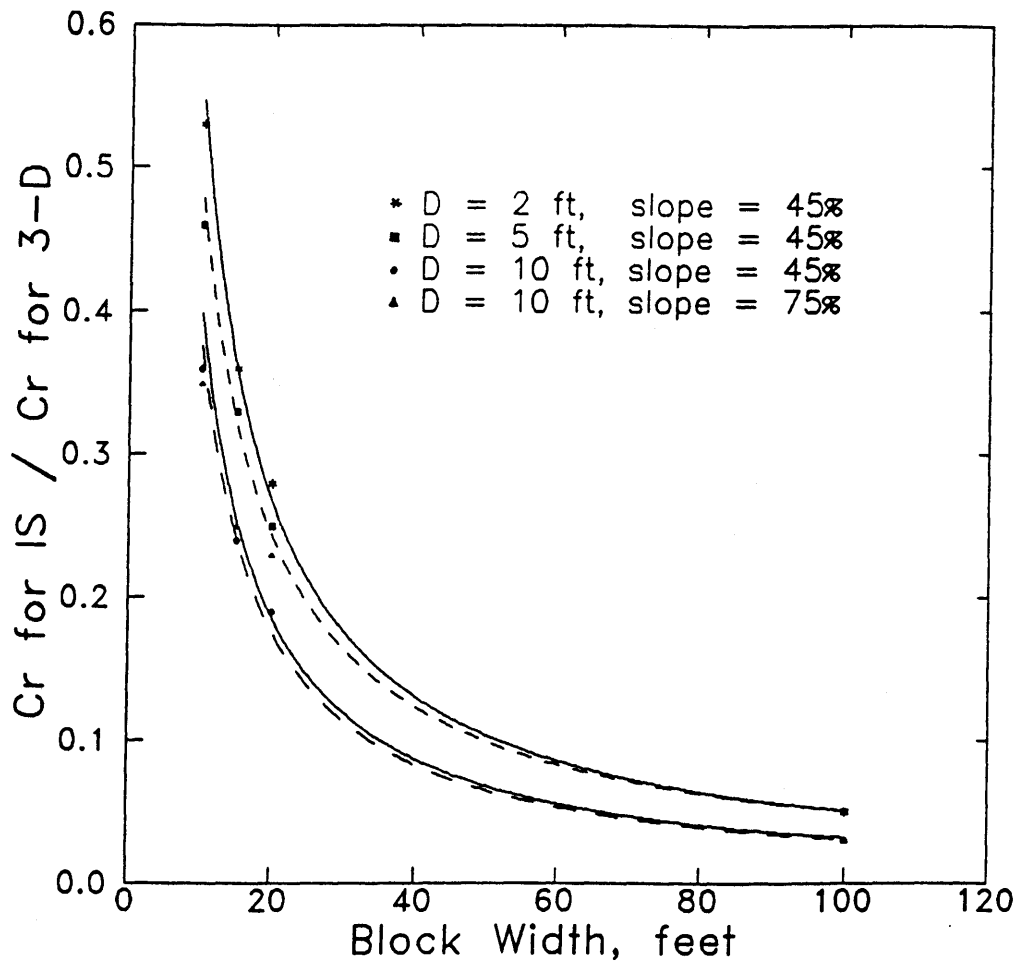


Figure C.1—Ratios of apparent root strength needed for the infinite slope model to root strength used in the three-dimensional block model to give the same  $FS$ .

the same factors of safety using the infinite slope equation then were back-calculated.

The results are shown in figure C.1. Two trends are observed. First, the apparent root strength decreases as the block width increases. For block widths of 100 feet, apparent root strength values are about 5 percent of the values used in the block model. This is consistent with what would be expected in relatively shallow soil conditions; as the size of the failure mass increases, the side and headwall resisting forces, and therefore root strength, have proportionately less influence on the stability of the soil mass.

The second trend is that for a given block width, the apparent root strength decreases as the soil depth increases. For instance, the apparent root strength values for a 20-foot-wide block are 28 percent (0.28) of the values used in the block model when the soil is 2 feet deep, and 18 percent (0.18) when the soil is 10 feet deep.

These trends were used to develop distributions for soil-root morphology types A and D from the distributions developed for types B and C.

- The criteria used to select distributions for each root morphology type are:
  1. We assumed the mode of the probability distribution describing type B to be about 100 psf, which is equal to the mode of the histogram in figure 5.6. For the type C distribution, we assumed a mode of about 150 psf to account for greater tree buttressing and root penetration along the base of the failure plane. We assumed modes of 40 psf for type A and 20 psf for type D based on the three-dimensional modeling of failures less than about 20 feet in width as described above.
  2. We assumed that all distributions should have large standard deviations to account for the great variability and uncertainty in reported values.
  3. We selected lognormal probability distributions to reflect the tendency for right skew in the data (as shown in fig. 5.6), thereby giving a low (but non-zero) probability of simulating relatively high values.

Based on these criteria, the suggested distributions for root strength in dense timber stands are shown in figure 5.8. Height differences in the plots are due to the fact that the area under each plot must equal 1.0. Important things to note are the range in values, the mode, and the shape of the distributions.

The rationale for selecting PDF's for minimum root strength following clearcut timber harvest is discussed in section 5.3.4.3.

## APPENDIX D—USING INFILTRATION EVENT RETURN PERIODS WITH PROBABILITIES OF FAILURE FROM LISA

As is stated in section 1.4, the probability of failure estimated using LISA is a *conditional* probability of failure that is valid only if the infiltration event, with the resulting groundwater ( $D_w/D$ ) distribution used in the analysis, occurs. Time can be incorporated into the probability of failure estimate by weighting the conditional probability of failure with the probability of the groundwater distribution occurring during a specified time interval. This method considers the return periods of the rainfall or snowmelt infiltration events. Because return periods commonly are used in many professional fields and are understood by land managers, their use may improve understanding of LISA results. This method also improves an assessment of the likelihood of a major landslide event occurring during the 3 to 10 years of minimum root strength following timber harvest (see section 5.3.4.3). The method will show that as the length of time considered increases, the probability that a major infiltration event occurs increases and, therefore, the expected probability of failure increases. The expected probability of failure can be thought of as the *average* likelihood of failures (or the *average* land area in failure) over *many*  $N$ -year trial periods.

Unfortunately, neither precipitation (or snowmelt) data nor groundwater response data typically are available to do a detailed time-history analysis. Therefore, the method suggested here must still be based on subjective estimates of groundwater response in average or major infiltration events, and as such is only a tool to help illustrate how event return periods might be handled. This method makes two assumptions—that the infiltration events are independent, and that the probabilities remain constant from year to year. The steps of the method are outlined below.

1. Make subjective estimates for the distribution of peak groundwater ( $D_w/D$ ) levels in response to a minor infiltration event, an average event, and a major event. (Although three events are illustrated here, the method does not require three events.)
2. Use LISA to estimate the conditional probability of failure ( $P[FS \setminus \text{event } i]$ ) for each of the three infiltration events  $i$  — make three LISA runs changing only the groundwater distributions to obtain the corresponding probabilities of failure.
3. Assume a return period ( $RP_i$ ) for each event, and for each event compute the probability that at least one event with that return period (or greater) will occur during the next  $N$  years ( $P[\text{event } i]$ ). This probability can be computed using the equation

$$P[\text{event } i] = 1 - \left(1 - \frac{1}{RP_i}\right)^N . \quad (D.1)$$

4. Compute the probabilities that the maximum event during an  $N$ -year period will be smaller than the average event, equal to or greater than the average event but less than the major event, and equal to or greater than the major event ( $P[\max i]$ ) by taking the difference between pairs of probabilities computed in step 3. These probabilities should sum to 1.
5. Calculate the weighted probability of failure ( $P[FS \cap \max i]$ ) by multiplying the conditional probability of failure estimated using LISA by the probability that the corresponding event will be the maximum event in  $N$  years; that is,

$$P[FS \cap \max i] = P[FS \setminus \text{event } i] \times P[\max i]$$

6. Compute the expected probability of failure for the specified time period by summing the weighted probabilities of failures.

An example will illustrate the method. Groundwater distributions for the minor, average, and major events have been evaluated, and conditional probabilities of failure of 0.002, 0.034, and 0.582 have been estimated with LISA. The return periods for the average and major events are assumed to be 2 years and 20 years, respectively; the minor event is assumed to be any event with less than a 2-year return. The exceedance probabilities for a 10-year period are desired because of concern about a 10-year postharvest period of minimum root strength.

Equation D.1 is used to compute the probabilities of at least one 2-year (or greater) event and of one 20-year (or greater) event occurring during a 10-year period:

$$P[\text{event} \geq 2 \text{ years}] = 1 - \left(1 - \frac{1}{2}\right)^{10} = 0.999$$

$$P[\text{event} \geq 20 \text{ years}] = 1 - \left(1 - \frac{1}{20}\right)^{10} = 0.401$$

The probability of at least one minor event occurring during the 10 years is 1.

The probability that the maximum event during that period will be minor, average and major is given below.

Maximum event	Calculation	
minor	$P[\text{max} < 2 \text{ years}] = 1 - 0.999$	= 0.001
average	$P[2 \text{ years} \leq \text{max} < 20 \text{ years}] = 0.999 - 0.401$	= 0.598
major	$P[\text{max} \geq 20 \text{ years}]$	= 0.401
		Total = 1.000

The weighted and expected probabilities of failure are shown in table D.1. Table D.2 summarizes the computations including 1-year and 25-year periods for comparison. Note that the probability of the maximum event being a major event increases as the length of time considered increases. Therefore, as the time increases, the groundwater distribution corresponding to a major infiltration event is more likely to occur, as is the probability of failure resulting from that groundwater distribution, causing the expected probability of failure to increase. This increase in expected probability of failure with longer analysis periods was also found by Miller (1988).

**Table D.1**—Computations of weighted and expected probability of failure for  $N = 10$  years

Event	$P[FS \setminus \text{event } i] \times P[\text{max } i] = P[FS \cap \text{max } i]$		
	$P[FS \leq 1]$ from LISA	$P[\text{max } i]$	Weighted $P[FS \leq 1]$
Minor (event < 2 years)	0.002	0.001	0.000002
Average (2 years ≤ event < 20 years)	.034	.598	.0203
Major (event ≥ 20 years)	.582	.401	.2334
	Expected probability of failure		= .254

**Table D.2**—Expected probability of failure with analysis periods of 1, 10, and 25 years

Event	$R_{pi}$	LISA $P_f$	$P[\text{event } i]$			$N = 1$		$N = 10$		$N = 25$	
			$N = 1$	$N = 10$	$N = 25$	$P[\text{event } i]$	Weighted $P_f$	$P[\text{event } i]$	Weighted $P_f$	$P[\text{event } i]$	Weighted $P_f$
Minor	< 2	0.002	1.00	1.000	1.000	0.50	0.001	0.001	0.000	0.000	0.000
Average	2	.034	.50	.999	1.000	.45	.015	.598	.020	.277	.009
Major	20	.582	.05	.401	.723	.05	.045	.401	.233	.723	.421
Expected $P_f$							0.061		0.254		0.430

# INDEX

3DLISA, 32

## A

analysis

- center of gravity–infinite slope (C.G.I.S.) method, 30, 51
- deterministic, 7–8, 11
- probabilistic, 7–9
- sensitivity, 10, 32–36, 47, 80, 83
- three-dimensional, 32
- two-dimensional, 32

angle of shear distortion, 119  
apparent cohesion ( $C_{app}$ ), 68, 78–80  
apparent soil depth, 53  
arching resistance, 122  
artesian pressure, 44

## B

back analysis, 47, 55, 59, 68, 76, 80, 83, 121–122  
beta distribution, 23–25, 39, 49  
bivariate normal distribution, 28–29, 39, 40–41, 80  
bulk density ( $D_b$ ), 69

## C

capillary pressure, see *capillary suction*  
capillary suction, 44, 68, 78–81  
CDF (cumulative distribution function), 14–15  
  definition of, 15  
central tendency, 11, 16–17  
classes, recommended number for histogram, 26  
  unequal width, 26–28  
clay, shear strength, 69–77  
  normally consolidated, 69–74  
  overconsolidated, 74–77  
coefficient of determination ( $r^2$ ), 20, 81  
coefficient of friction ( $\mu$ ), 64  
coefficient of variation ( $C_v; c_v$ ), 19, 22, 45, 49, 63–64  
  definition of, 19  
cohesion  
  apparent, 68, 78–80  
  apparent, due to capillary suction, clays, 78–80  
  apparent, due to capillary suction, sands and gravels, 68  
  intercept, 68  
  true, 68, 76, 80  
compass, Brunton, 51  
conditional PDF, definition of, 18  
conditional probability of failure, 9, 44  
constant value, 39  
  misuse of, 49  
correlation  
  between variables, 39–44  
  coefficient ( $r$ ), 20, 29, 40, 80–81  
  coefficient, definition of, 19  
  linear, 19, 28  
  spurious, 19  
covariance, definition of, 17  
cumulative distribution function, definition of, 15  
current *in situ* stress, 76

## D

data files, 48  
debris avalanche, 30  
debris flow, 30  
definitions, 14–20  
dependence, linear, 19  
  stochastic, 17  
deterministic analysis, 7–8, 11  
digital elevation models (DEM's), 51  
direct shear test for root strength, 118  
distribution  
  beta, 23–25, 39, 49  
  bivariate normal, 28–29, 76–77  
  conditional, 18  
  frequency density, 27  
  Gaussian (normal), 20–22, 39, 49  
  histogram, 25–28, 39, 49  
  input, 10  
  lognormal, 22–23, 39, 49  
  marginal, 17, 28–29  
  normal, 20–22, 39, 49  
  relative-frequency histogram, 25–28, 39, 49  
  selection of, see *distribution type, selection of*  
  triangular, 20, 39, 49  
  uniform, 20, 39, 49  
distribution type, selection of  
  friction angle, 59–81  
  ground slope, 51  
  groundwater–soil depth ratio, 82–86  
  moisture content, 81–82  
  root strength, 54–61  
  soil depth, 51–53  
  soil shear strength, 59–81  
  soil unit weight, 59–81  
  tree surcharge, 53–54  
DLISA, 47, 82, 83  
dry unit weight ( $\gamma_d$ ), 62, 67, 69, 77

## E

effective stress analysis, 68, 69, 76  
environmental assessment reports (EAR's), 7  
estimating input values, see *distribution type, selection of*  
event, definition of, 14  
expectation ( $E[X]$ ), 11, 16  
expected monetary value (EMV), 10

## F

flow, subsurface, 82–83  
flowlines, 83  
frequency density distribution, 27  
friction angle  
  apparent ( $\phi'_a$ ), 76  
  peak ( $\phi'_p$ ), 68, 69, 74, 76

residual ( $\phi_r'$ ), 68, 77–78  
selecting distribution, 61–81  
ultimate ( $\phi_{ult}$ ), 68, 77–78  
value estimation, normally consolidated clay, 69–74  
value estimation, overconsolidated clay, 74–77  
value estimation, sands and gravels, 67–69

## G

Gaussian distribution, see *normal distribution*  
Geographic Information System (GIS), 51  
Geologic Resources and Conditions (GRC), 47, 49, 87  
ground slope  
  estimating values, 51  
  selecting distribution, 51  
  sensitivity of infinite slope equation to, 32  
groundwater, 9  
  data file, 48  
  height, 44  
  values, 44  
groundwater–soil depth ratio  
  estimating values, 82–86  
  selecting distribution, 82–86  
  sensitivity of infinite slope equation to, 32

## H

hazard, 7, 8, 10  
  assessment, 10  
  definition of, 8  
histogram distribution, 25–28, 39, 49  
hydrostatic suction, 80

## I

inclinometer, 51  
inequality data, 53  
infinite slope model, 8, 30–38  
  assumptions of, 30–32  
  sensitivity to input values 32–38  
input value estimation, see *distribution type, selection of*  
interdependence of input variables 32–36  
internal angle of friction, see *friction angle*

## J

Janbu's simplified method of analysis, 30  
joint probability density function, 28  
  definition of, 17

## L

Land System Inventory (LSI), 47, 49  
landslide  
  hazard, 7, 8  
  inventory, 9–10  
Level I stability analysis, definition of, 47  
Level II analysis, 7, 10, 62, 87, 89–94  
Level III analysis, 10, 62, 94  
limit equilibrium equations, 7  
limitations of LISA, 11  
limits  
  of lognormal distribution, 23

  of normal distribution, 21–22  
linear  
  correlation, 19, 28  
  dependence, 19  
  regression, 62, 80  
lognormal distribution, 22–23, 39, 49  
longitudinal stiffness modulus, 120

## M

map unit, definition of, 48  
marginal distribution, 17, 28–29  
marginal probability density function, definition of, 17  
material data file, 48  
matric suction, see *capillary suction*  
mean, 11, 16, 17, 18–19  
save definition of, 16  
  factor of safety, 8, 11  
  of a population, 19  
  of a statistical sample, 18–19  
measurement uncertainty, 7, 9  
median, 11, 16, 17  
  definition of, 16  
mobilized tensile root strength, 121  
mode, 11, 16, 17  
  definition of, 16  
Mohr-Coulomb failure envelope, 39, 41, 68, 69, 76  
moisture content  
  estimating values, 81–82  
  sensitivity of infinite slope equation to, 32, 82  
Monte Carlo simulation, 8–9, 30, 32

## N

negative values from normal distribution, 22  
normal distribution, 20–22, 39, 49

## O

outcome, 14  
overburden pressure, 120

## P

parallel seepage assumption, 30  
PDF (probability density function), 14  
  definition of, 15  
  mean, mode, and median of, 16–17  
performance function, 8  
piezometer, 83  
planning  
  forest, 7  
  land management, 10  
  transportation, 7  
planning-level decisionmaking, 47  
plasticity index, 69, 78  
polygon  
  definition of, 47  
  delineation of, 47, 89–94  
preconsolidated stress, 76  
probabilistic analysis, 7–9  
probability concepts, 14–29  
probability density function (PDF), 14  
  definition of, 15

- mean, mode, and median of, 16–17
- probability distribution, 20–29
  - definition of, 15
- probability of failure, 9–12
  - definition of, 9
  - meaning of, 9–10
  - reproducibility of, 44–45
  - use of, 10
- pull test, 118, 121
- pull-out resistance, 121

## R

- random number seed, 10, 80
- random variable, 14, 21–22, 26
  - definition of, 14
- range, definition of, 17
- regression, linear, 62, 80
- relationships, important, 20
- relative density ( $D_r$ ), 59, 64–65, 67, 68
- relative-frequency histogram, 25–28, 39, 49
- reproducibility of probability of failure, 44–45
- residual friction angle ( $\phi_r$ ), 68, 77–78
- resource allocation, 7
- return period, 125
- risk analysis, 7, 8, 10
- risk, definition of, 8
- road location, 48
- root morphology, 56–58
- root strength
  - estimating values, 30
  - models, 118–120
  - selecting distribution, 54–61, 122–124
  - sensitivity of infinite slope equation to, 32
- rotational slope failure, 30

## S

- sample, definition of, 18
- sample vs specimen, 18–19
- SARA (Stability Analysis for Road Access) program, 48, 94
- scatter plot, 39
- seismic refraction, 53
- sensitivity analysis, 10, 32–38, 47, 80, 83
- sensitivity of model to input variables, 32–38
- shear resistance, 79–80
- shear strength, see *soil shear strength*
- site data file, 48
- skin friction stress, 120
- soft data, 53
- soil buttress, 124
- soil
  - hydraulic conductivity, 51, 84
  - layers, multiple, 30
  - mantle, 30
  - penetrometer, 51
- soil depth
  - estimating values, 51–53
  - selecting distribution, 51–53
  - sensitivity of infinite slope equation to, 32–33
- Soil Resource Inventory (SRI), 47, 49, 91
- soil shear strength, 30, 40, 59–81
  - estimating values, clays, 30, 69–77

- estimating values, sands, 30, 67–69
- residual, of sands and clays, 68, 77–78
- selecting distribution, clays, 69–77
- selecting distribution, sands, 67–69
- sensitivity of infinite slope equation to, 32
- soil-root
  - classification, 56–58
  - morphology types, 56–58
- spatial variability, 7, 9
- specific gravity ( $G_s$ ), 67, 69
- specimen, 14
  - definition of, 18
  - vs sample, 18–19
- spurious correlation, 19
- Stability Analysis for Road Access (SARA), 48, 95
- standard deviation
  - definition of, 17
  - estimation for normal distribution, 21
  - of a population, 19
  - of a statistical sample, 18–19
- standpipe piezometer, 83
- stochastic dependence, 17
- stratified random sampling, 51, 53
- stress, current *in situ*, 76
  - preconsolidated, 76
- stress-strain curves, 77
- subsurface flow, 82–83

## T

- tensile strength measurements of roots, 118–120
- three-dimensional analysis, 31–32
- three-dimensional block model, 31–32
- through flow, 83
- timber harvest, effect on groundwater levels, 84–86
  - effect on root strength, 58–61
- time, accounting for in analysis, 125–127
- tree surcharge
  - estimating values, 53–54
  - selecting distribution, 53–54
  - sensitivity of infinite slope equation to, 32
- triangular distribution, 20, 39, 49
- triaxial compression test, 62, 78, 80
- triggering mechanism, 82
- true cohesion, 68, 76, 80
- two-dimensional analysis, 31–32

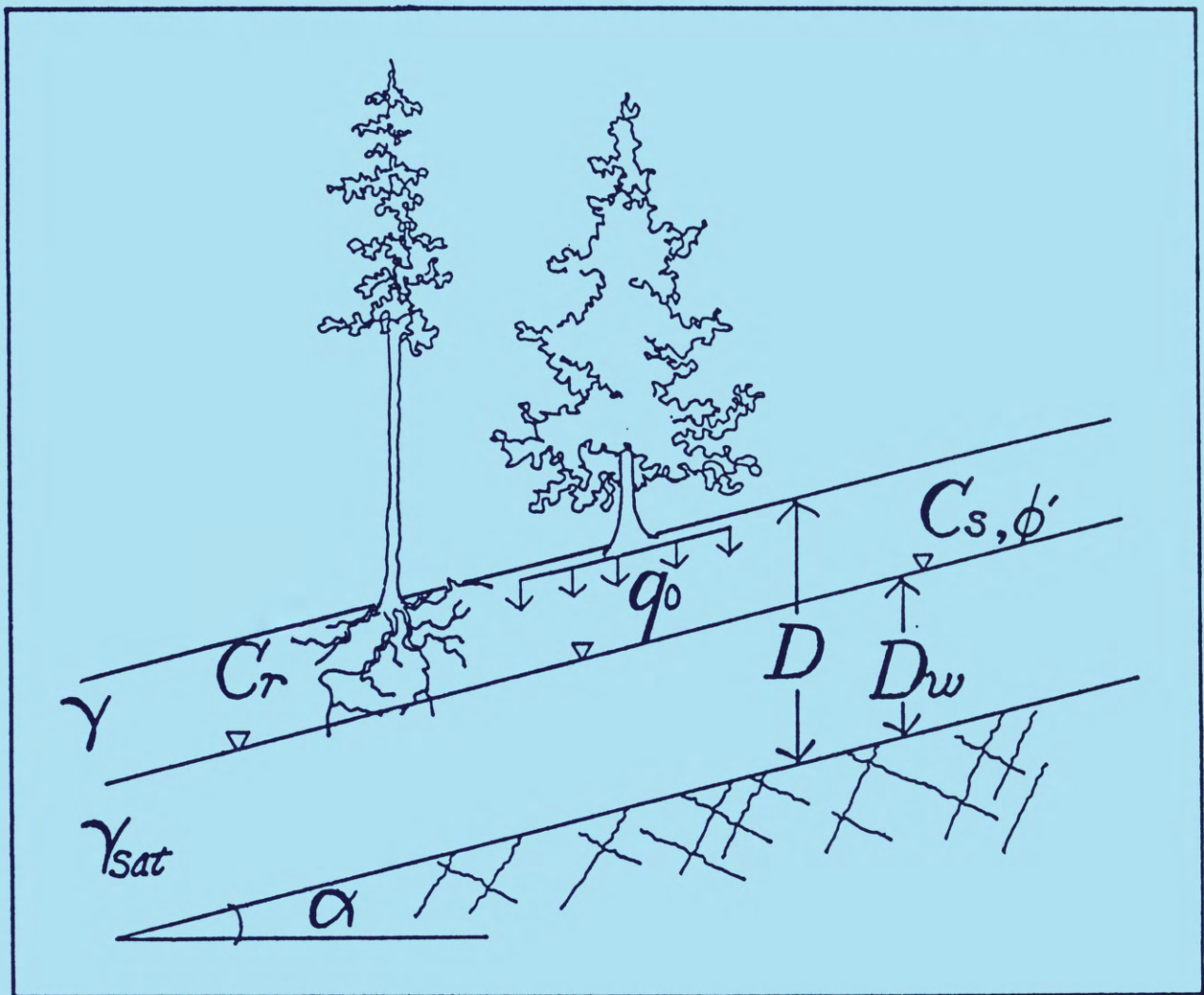
## U

- ultimate friction angle ( $\phi_{ult}$ ), 68, 77–78
- uncertainty of estimation, 7
- uniform distribution, 20, 39, 49
- unit weight, 59–81
  - estimating values, clay, 77
  - estimating values, sand and gravel, 69
  - sensitivity of infinite slope model to, 32

## V

- variability, 17–20
  - spatial, 7, 9
- variance, 17
  - definition of, 17
- void ratio, 65, 67, 74, 77

## Part 2—Program Operation



# CHAPTER 1 — INSTALLATION INSTRUCTIONS

We have assumed in writing these instructions that users know basic DOS tasks (such as how to format a floppy disk, make and change directories on a hard disk, copy files, and view or print disk directories and the contents of ASCII files), and that users are familiar with DOS filename syntax. If the user is unfamiliar with these tasks, some assistance may be required.

## 1.1 Hardware Requirements

To use LISA, the user will require:

- An IBM PC or near compatible, with at least 444 kilobytes of *available* random access memory (RAM).
- Preferably one floppy disk drive (of at least 360 kilobytes capacity) and a hard disk drive or equivalent; or two floppy disk drives, one of which must be of at least 720 kilobytes capacity. (No floppy disk drives are required if LISA is acquired through the computer's serial port, as it would be if it were RISed from the Data General computer as described in appendix A. One is still recommended, however.)
- MS-DOS or PC-DOS disk operating system 2.0 or later.

The following are highly recommended, but not essential:

- A floating-point math coprocessor (8087, 80287, or 80387). LISA will take advantage of the coprocessor if one is installed.
- An IBM-compatible VGA, EGA, or CGA graphics adapter and an appropriate monitor. Without graphics capability, you will not be able to view plots of the input distributions or scatter plots of simulated values, but LISA will still function.
- An IBM-compatible printer for hardcopy output.

## 1.2 LISA Installation

LISA version 2.00 is distributed as one “self-extracting” file<sup>1</sup> called **LISA200.EXE**.<sup>2</sup> When you run **LISA200**, it will generate several files, which are described in section 1.3.

### TO INSTALL LISA ONTO A HARD DISK

- Create an appropriate subdirectory on the hard disk for the program, and change to that subdirectory. For example, type

```
MD C:\SS\LISA 
```

```
CD C:\SS\LISA 
```

- Place the disk containing **LISA200.EXE** into a floppy drive (say, drive A) and run **LISA200** by typing, for example,

```
A:LISA200 
```

### TO INSTALL LISA ONTO A DUAL-FLOPPY SYSTEM

- Format a floppy disk for at least 720 kilobytes capacity, and copy the DOS file **COMMAND.COM** onto the disk. Place this disk in an appropriate disk drive, and make that drive the current drive.

---

<sup>1</sup>PKWARE's PKZIP and ZIP2EXE version 1.1 were used. The USDA Forest Service has a site license for use of PKZIP.

<sup>2</sup>The name of the self-extracting file will change with future updates. For example, if a version 2.05 of LISA were released, it would be called **LISA205.EXE**.

- Place the disk containing `LISA200.EXE` into the other drive, and run `LISA200` by typing, for example,

`B:LISA200` 

### 1.2.1 Data File Location

LISA saves its data files in subdirectories corresponding to map unit names specified by the user when running LISA. The subdirectories may reside on the hard disk under either the program directory or a separate directory, or on a floppy disk. The user specifies the path to the data subdirectories from within LISA, and LISA creates the data subdirectories as needed, giving them filename extensions of `.MPU`, as discussed in section 3.4. The path may be changed any time LISA is run. This method allows great flexibility in the use of LISA, and allows the disk operating system to handle data file management.

### 1.2.2 Running LISA From Any Subdirectory

You can run LISA from any subdirectory, as long as DOS's `PATH` includes the subdirectory in which LISA is stored. LISA will create in each subdirectory from which it is started a configuration file, `CONFIG.L1`, specifying the location of data files and the screen color selection. Thus, each user can customize LISA simply by running LISA from his or her own subdirectory.

### 1.2.3 Running LISA from Windows 3.0

LISA can be run as a “nonwindow” (full screen) or a “window” application under WINDOWS 3.0. The plots of input distributions and the scatter plots of simulated values cannot be displayed while running LISA in a window, because they use EGA graphics, but they can be viewed by switching from a window to a full screen application using  and .

LISA can be run as a background task if you create a WINDOWS PIF file and turn the background option on. For more information on running DOS applications under WINDOWS, see the WINDOWS 3.0 documentation.

### 1.2.4 Customizing LISA With Environment Variables

LISA is aware of two DOS environment variables. `LISALIST` tells LISA what program to use for viewing the output files `RESULTS.OUT` and `SIMULATE.OUT`, and `LISAGRAPH` affects the content of the output file `RESULTS.OUT` created in the simulation.

Environment variables are `SET` from the DOS prompt before invoking LISA. If they are to be set consistently, you may want to put the `SET` command in either your `AUTOEXEC.BAT` file (near the bottom of the file, but before any calls to hard disk management programs) or the `LISA.BAT` file (anywhere before the `LISARA /L` line).

You may list the values of all current DOS environment variables by typing `SET`  at the DOS prompt.

#### 1.2.4.1 Specifying Your Own File Viewer

Unless it is told otherwise, LISA uses a program called `BROWSE`<sup>3</sup> to view the `RESULTS` and `SIMULATED DATA` files. If you tell LISA to use a file editor, you can format the output files as you desire before printing them, without leaving LISA.<sup>4</sup>

To specify a different viewing or editing program, use the DOS `SET` command to create an environment variable called `LISALIST` and give as its value the name of the viewing or editing program as it would be called from DOS. The file viewer or editor that you specify must meet the following requirements:

<sup>3</sup>Petzold (1986). `BROWSE` may be freely copied and used for noncommercial use only.

<sup>4</sup>Another way to edit the `RESULTS` and `SIMULATED DATA` files is to save them and edit them after leaving LISA. Editors not directly compatible with LISA may be used in this way.

- It can be invoked from the DOS command line with the name (including the path) of the file to be loaded.
- It reads ASCII files.
- It can be called from any subdirectory.
- It is not a “memory hog”; if LISA is being run on a machine with 640 kilobytes of RAM, about 250 kilobytes will be available for the viewer or editor.

PC-WRITE is one program that meets these requirements, and it will be used here to illustrate how to specify a viewer or editor. If the PC-WRITE editor ED is stored on the C drive in subdirectory \WP\PCW, you would type

```
SET LISALIST=C:\WP\PCW\ED 
```

#### 1.2.4.2 Specifying IBM Graphics Characters

When LISA saves histogram plots in the output file RESULTS.OUT, it assumes that you need standard ASCII characters rather than the IBM line graphics characters that are displayed on the screen. If you would prefer to have the graphics characters stored in the file, set the DOS environment variable LISAGRAPH to the value IBM. To do this, type the following at the DOS prompt before you start LISA:

```
SET LISAGRAPH=IBM 
```

You must not have any spaces around the = sign or after IBM, and IBM must be in uppercase letters.

### 1.3 LISA Program Files

The following files will be generated when LISA200 is run:

- |    |                                  |  |
|----|----------------------------------|--|
| 1. | LISARA.EXE                       | Executable code for LISA and SARA                          |
| 2. | LISA.BAT                         | Starts LISA  |
| 3. | BRUN45.EXE                       | Runtime library for LISA and SARA                          |
| 4. | BROWSE.COM                       | File viewing utility                                       |
| 5. | DEMO.BAT                         | Creates DEMO.MPU and copies demonstration data files to it |
| 6. | DEMO.SIT<br>DEMO.MTL<br>DEMO.HYD | Data files for the demonstration problem                   |
| 7. | DLISA.EXE                        | Executable code for Deterministic LISA                     |
| 8. | README                           | Describes program or manual revisions                      |

LISARA.EXE, LISA.BAT, and BRUN45.EXE are required to run the LISA program. BROWSE.COM is also required, unless the SET LISALIST command has been used to specify another file-viewing utility (see section 1.2.4.1). The DOS file COMMAND.COM must also be available on one of the floppy disks for a dual-floppy system or on the hard disk; see section 1.2. The DEMO files are optional and are used for working through the demonstration problem in this manual. The README file, if it exists, discusses program changes or manual revisions, or both, and should be reviewed before you proceed. The single file DLISA.EXE is required to run the deterministic version of LISA, DLISA. Chapter 4 discusses installation and use of DLISA.

## CHAPTER 2 — GENERAL EXECUTION INSTRUCTIONS

- **Just knowing how to run LISA is not enough.** We *strongly* recommend that you read Part 1 before attempting any LISA runs for project work. *Part 1 gives the background needed to understand what LISA is doing and how to properly use and interpret the results.* However, you may find it helpful in understanding Part 1 to be familiar with the operation of LISA first.

### 2.1 Screen Structure of LISA

Several screens in the LISA program aid the user in option selection and data entry (see fig. 2.1). These screens are designed to be self-explanatory so that little reference need be made to this manual. However, detailed descriptions of each screen and the options available are presented in chapter 3, “Detailed Execution Instructions”, should they be needed.

### 2.2 Data File Structure

Three types of data files are used in LISA. They are:

<b>Site</b>	Specifies the probability distributions for soil depth, ground surface slope, tree surcharge, and root cohesion.
<b>Material</b>	Specifies the probability distributions for friction angle, soil cohesion, dry unit weight, and moisture content of soil above the phreatic surface, and the value of specific gravity of solids.
<b>Groundwater</b>	Specifies the probability distribution for groundwater–soil depth ratio.

The data files have file extensions of **.SIT**, **.MTL**, and **.HYD**, respectively. Data files are separated in this manner to allow easy use of one material file with several site files. This makes file editing and selection more convenient when the site conditions change but the soil type remains fairly uniform over an area, or when the same soil type is found in numerous locations across a forest.

For each input variable, a constant value or a distribution type is specified by the user. The available distributions are uniform, normal, lognormal, triangular, beta, histogram, and, for  $C'_s$  and  $\phi'$ , bivariate normal. Groundwater–soil depth ratio is limited to constant, uniform, triangular, beta, and histogram distribution types. Only a constant value can be entered for specific gravity.

Data files are grouped into *map units* (subdirectories on disk with an extension of **.MPU**). A map unit can be thought of as a study or analysis area, or as a geomorphic landtype. The map unit serves as a bookkeeping mechanism under which data files are organized (see sections 1.2.1 and 3.4 for more information). Data files can be created, modified, and saved from within LISA, but they cannot be erased.

### 2.3 General Principles

Some general principles to keep in mind when creating data files and running LISA are listed below.

- LISA makes extensive use of highlighted menus and options in its user interface. The highlight is moved by pressing **SPACE** or the arrow keys (**←** **→** **↑** **↓**). Pressing **ENTER** selects the highlighted file name or option.

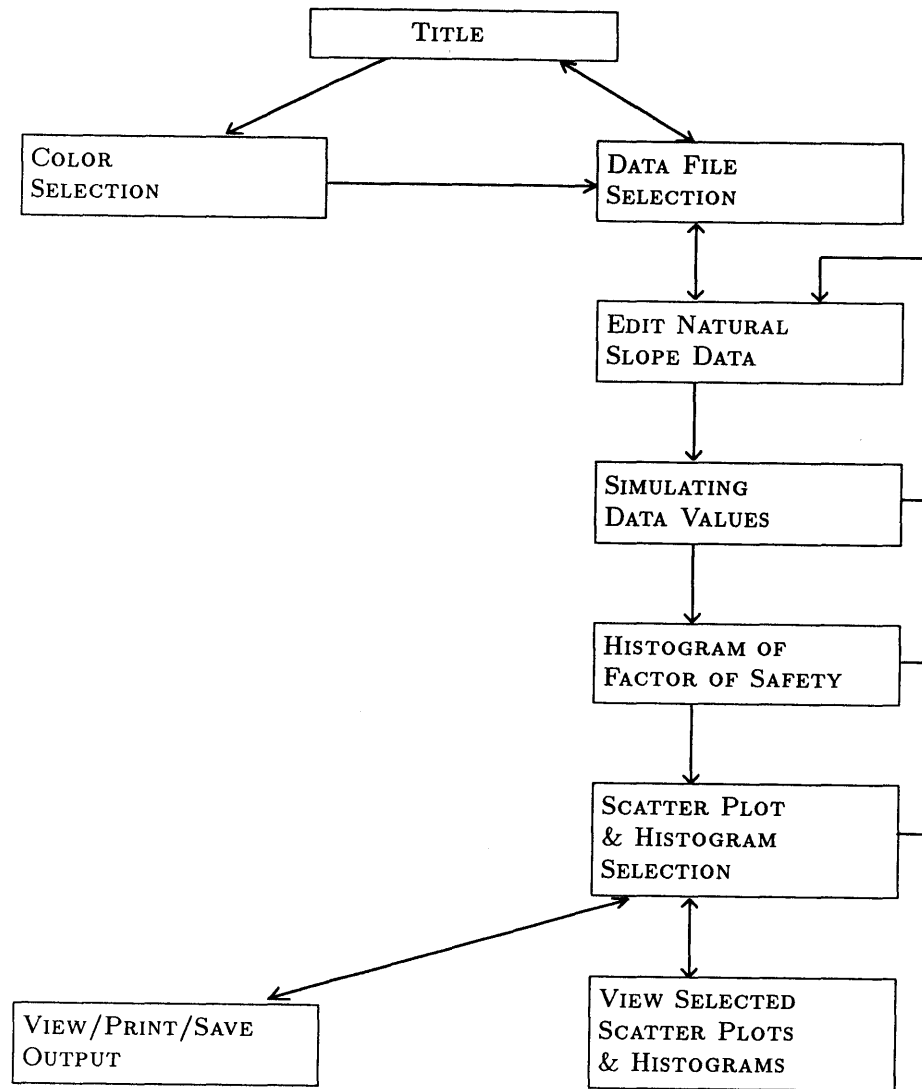


Figure 2.1—LISA screen structure.

- Single-character responses require that you press only that character, *without* pressing **ENTER**. Examples include selecting distribution **Plot** or file **Save** functions and answering yes-no questions. Single-character responses are displayed by a highlighted character. A default response for a yes-no question will be given and may be accepted by pressing **ENTER**. Either uppercase or lowercase is acceptable for single-character letter responses.
- An input that requires or allows more than a single-character response is typed into a highlighted input field and accepted by pressing **ENTER**. The length of the highlight indicates the maximum number of characters allowed for that entry. Invalid keystrokes are ignored. The previous response used is usually displayed in the highlighted field. Generally, this response may be edited by first pressing the backspace key,<sup>5</sup> thereby delet-

<sup>5</sup>The destructive backspace key looks similar to the nondestructive cursor left key. In this manual, we will reserve the symbol **←** for the nondestructive cursor left key.

ing the character to the left of the cursor. Pressing a valid number or letter key first erases what had been in the highlight. Pressing **ENTER** at any time enters the response in the highlight at that time. An exception to the above behavior occurs when saving RESULTS or SIMULATED DATA files. Here valid characters are appended to the path shown in the highlighted field without the need to first press the backspace key, and **ESC** clears the highlighted field (see section 3.20).

- Pressing **ESC** will back you up to the previous prompt, input field, or screen. Generally, pressing **ESC** while editing a highlighted input field will cancel any changes made for that input. If you have made changes to values of the input variables from the EDIT NATURAL SLOPE DATA screen and then press **ESC** to return to the DATA FILE SELECTION screen, you will be asked whether you want to save the changes.
- The bottom line or two on each screen display the currently available options that are selected by single keystrokes. Warning and error messages are displayed in windows in the middle of the screen and require pressing any key to continue program operation.
- **F10** is a quick exit to DOS. If any of the three data files has been modified, all three will be saved automatically, as **QUICK.SIT**, **QUICK.MTL**, and **QUICK.HYD**, in the appropriate map unit subdirectory. You may rename or erase these files from DOS. Pressing **ESC** from the TITLE screen will also return you to DOS.

## CHAPTER 3 — DETAILED EXECUTION INSTRUCTIONS

This chapter is a detailed user guide for executing LISA. It shows screen images and describes program prompts, valid responses, and messages. In addition, demonstration entries are shown to illustrate some of the features of the program. To run the demonstration, you must first run **DEMO.BAT** from the LISA subdirectory. **DEMO.BAT** will create a subdirectory called **DEMO.MPU** under the LISA directory and copy the demonstration data files (**DEMO.SIT**, **DEMO.MTL**, and **DEMO.HYD**) to it.

### 3.1 Executing LISA

The system date and time should be set properly before invoking LISA, because LISA records the date and time of the simulation in the output files. In addition, system time is used to generate a seed (starting number) for the random number generator.

If you are running LISA from floppy disks, put the program disk in drive A and a formatted disk for data in drive B, make drive A the current drive, and at the DOS prompt, type **LISA** and press **ENTER**. If LISA is installed on a hard disk, change to the subdirectory containing the program, type **LISA** and press **ENTER**. (As discussed in section 1.2.2, you may run LISA from any directory as long as the DOS **PATH** statement includes the path to the subdirectory containing **LISARA.EXE**, **LISA.BAT**, and **BRUN45.EXE**.)

LISA will display the **TITLE** screen (fig. 3.1). From the **TITLE** screen, you may select the colors used in LISA by pressing **C** (see section 3.2), return to DOS by pressing **ESC**, or proceed to the **DATA FILE SELECTION** screen by pressing any other key.

#### DEMONSTRATION

Execute **LISA** from the LISA subdirectory or another subdirectory as desired.

#### ERROR MESSAGE

Input run-time module path:

DOS issues this message upon trying to load LISA if it cannot find the file **BRUN45.EXE**. Press **CTRL-C** to return to the DOS prompt, and ensure that **BRUN45.EXE** is in the current directory or in DOS's **PATH**.

### 3.2 Selecting Colors

Pressing **C** from the **TITLE** screen brings up the **COLOR SELECTION** screen (fig. 3.2). From this screen you can select the colors for LISA to use for its menus, general text, prompts, and warnings by repeatedly pressing **M**, **T**, **P**, and **W**. This screen is an exception to the general rule—it is case-sensitive. Each of menu,

LISA

Level I Stability Analysis  
of natural slopes using  
infinite slope equation

Version 2.00  
January 1991

Carol Hammond, David Hall, Scott Kendall, Paul Swetik  
U S Forest Service, Intermountain Research Station, Moscow ID 83843

The authors assume no liability or responsibility for the use of LISA, the interpretation of LISA results, or the consequences of management decisions which are based upon LISA results. Efforts have been made to see that LISA is reliable, but it is a model of reality, not reality itself. The user should have a thorough understanding of the model, and should compare results to actual field conditions.

No person, whether an employee of the Federal government or any outside agency, corporation or individual, may sell the LISA program for profit.

[Runtime library (c) Microsoft Corp. 1982-1987]

Press C) to select colors, ESC) to exit, or anything else to continue

Figure 3.1—TITLE screen.

text, and prompts has two associated colors; by pressing the uppercase letter you change one of the colors, and by pressing the lowercase letter, you change the other. **C** causes the colors to cycle one direction, and **c** causes them to cycle the other way; the current direction is displayed highlighted in the lower right corner of the screen. The keys **C** and **c**, the unshifted counterparts to **C** and **c**, also work.

Press **Z** to select colors appropriate for monochrome display systems. Press **U** or **ENTER** to use the displayed colors for the current session only, or press **S** to save the color selection in the LISA configuration file **CONFIG.L1** in the subdirectory from which LISA was started. Press **ESC** to cancel any changes made and use the last set of colors saved. LISA will display the **DATA FILE SELECTION** screen after **U**, **ENTER**, **S**, **Z**, or **ESC** has been pressed.

### 3.3 Entering a User Name

The first prompt on the **DATA FILE SELECTION** screen is for a user name (fig. 3.3). A user name may be from 1 to 20 characters in length, and almost any character will be accepted. The name entered is stored in any site files the user saves and in the output files created during simulation. Type your name or initials and press **ENTER**. Pressing **ESC** from the **User name** prompt will return you to the **TITLE** screen.

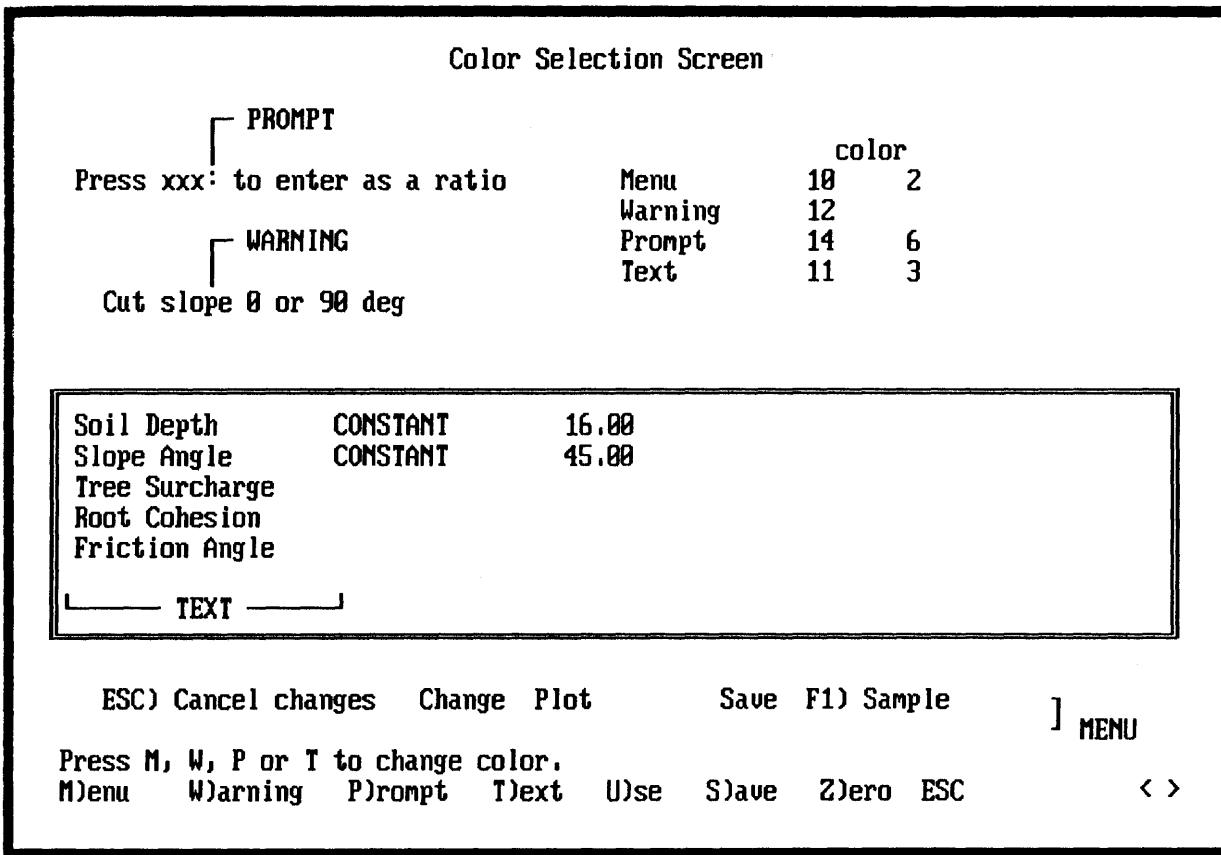


Figure 3.2—COLOR SELECTION screen.

### ERROR MESSAGES

A name is required  
Press any key to continue

LISA will not let you proceed without entering a name.

### DEMONSTRATION

Type your name and press .

### 3.4 Selecting the Path to Data (Map Unit) Subdirectories

After the user name is entered, LISA will display the current path to the data (.MPU) subdirectories and will prompt for the name of the map unit you want to use. It is under this path that any map units created and data files saved will be placed. All of the available map units will be shown in a window below the prompt.

### Data File Selection Screen

User name: C.Hammond

Enter name to be saved in results file  
ESC) Quit

Figure 3.3—Entering a user name.

The first time LISA is started from a particular subdirectory, the path will be to that subdirectory. If you want to save data files to another disk or subdirectory, press **ESC** or **↑** to move the highlight up to the current path, and type the new path. As with any highlight, the current path can be edited by first pressing the backspace key. Pressing any other valid key first erases the current path. Pressing **ENTER** accepts the path in the highlight. The path to the data subdirectories may be changed any time LISA is executed, and the last path used will be displayed the next time LISA is run from the same directory.

### ERROR MESSAGES

Invalid Path - drive or directory does not exist.  
Press any key to continue

This message occurs when an invalid path is entered. Be sure that you conform to DOS's naming convention for subdirectories and that the path that you specify names an existing subdirectory.

## DEMONSTRATION

To have access to the data files for the demonstration, the path must point to the LISA program subdirectory, where **DEMO.MPU** was created and the demonstration data files stored. **DEMO.MPU** will be displayed in the window of available map units if the path is correct. Change the data path if necessary.

### 3.5 Selecting an Existing Map Unit

At the **Map unit to analyze:** prompt, the user has four choices:

1. Press **ENTER** or **↓** before entering a name at the map unit prompt, and the highlight will move into the window displaying the available map units. Use **SPACE** or the cursor-control keys (**←** **→** **↑** **↓** **PG UP** **PG DN** **HOME** and **END**) to move the highlight to the desired map unit and press **ENTER** to select it. The available map units are listed in alphabetical order from left to right, top to bottom. If you press **ENTER** at the map unit prompt when there are no available map units listed in the window, LISA will ask you to create a new map unit by displaying the message

Please create a new map unit by entering a name  
Press any key to continue

There will be no available map units if the current path points to a subdirectory with no **.MPU** subdirectories. Either enter a name for a new map unit subdirectory, or press **ESC** to enter a different data path.

2. Type the name of the desired map unit and press **ENTER** (fig. 3.4). If the map unit entered does not exist, you will be asked whether you want to create it (see section 3.6).
3. Use DOS's wildcard convention to limit the list of available map units displayed in the window. Use **?** to match exactly one character, or **\*** to match 1 or more characters. For example, an entry of **NEW\*** would display all available map units whose names start with the letters **new** (as is shown in fig. 3.5); an entry of **NEW?1** would match such map unit names as **NEW11**, **NEW21**, and **NEW31**, but not **NEW231**. The desired map unit then may be selected by moving the highlight and pressing **ENTER**.
4. Press **ESC** or **↑** to specify a different map unit path, as described in section 3.4.

## ERROR MESSAGES

More than 100 map units found.  
Press any key to continue

LISA can display no more than 100 map unit names at once. If more are found, only the first 100, in the order that they are stored in the disk directory, will be displayed as available map units. You should

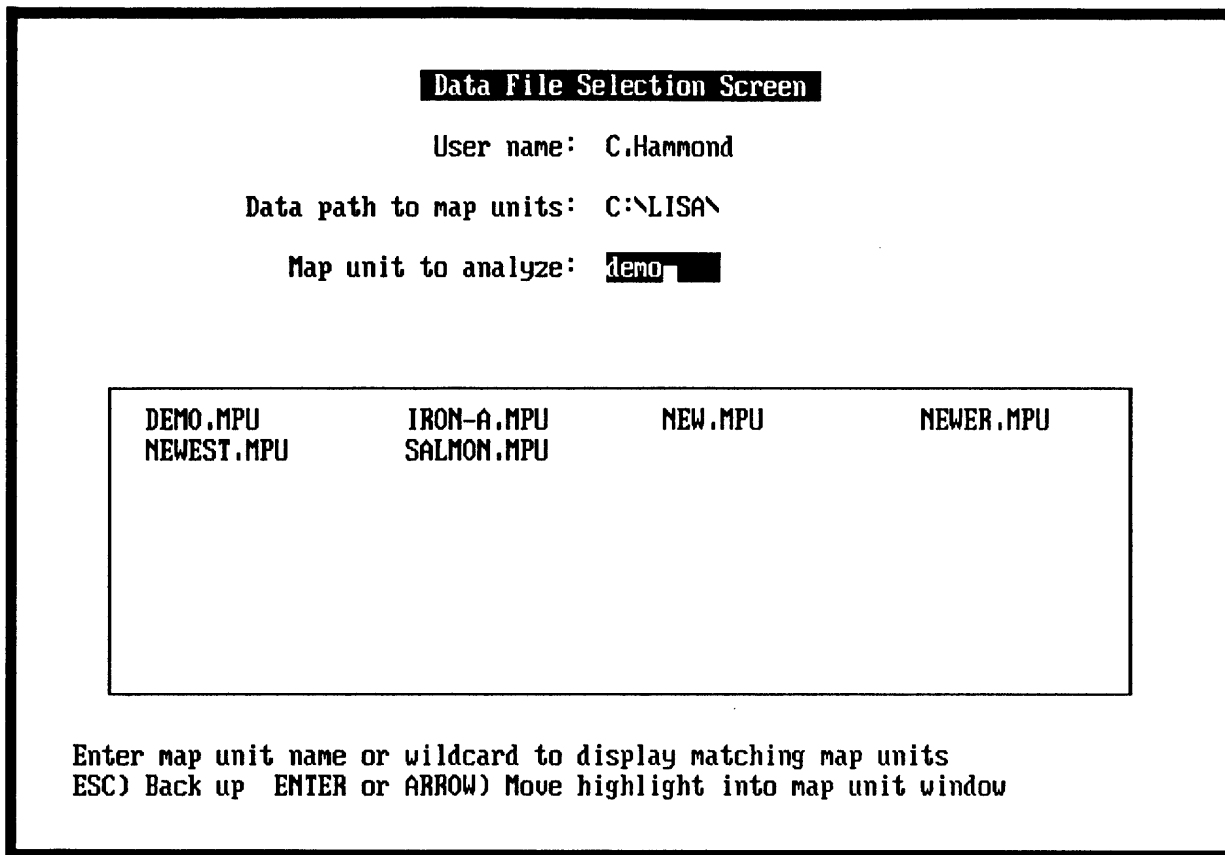


Figure 3.4—Selecting the DEMO map unit.

either move some of the .MPU subdirectories and their data files into another subdirectory, which cannot be done within LISA, or use the wildcard feature to limit the number of map units displayed.

More than 50 *type* data files found  
Press any key to continue

LISA can display no more than 50 data files of any file type at one time (sections 2.2 and 3.8 explain file types). If more files are found when the map unit is selected, this message (with *type* being SITE, MATERIAL, or GROUNDWATER) will be displayed, and you will be able to access only the first 50 files in the map unit, in alphabetical order by file name. In order to access the rest of the files, you will have to delete some data files or move them into another map unit subdirectory. Section 3.9 describes how to delete data files from within LISA.

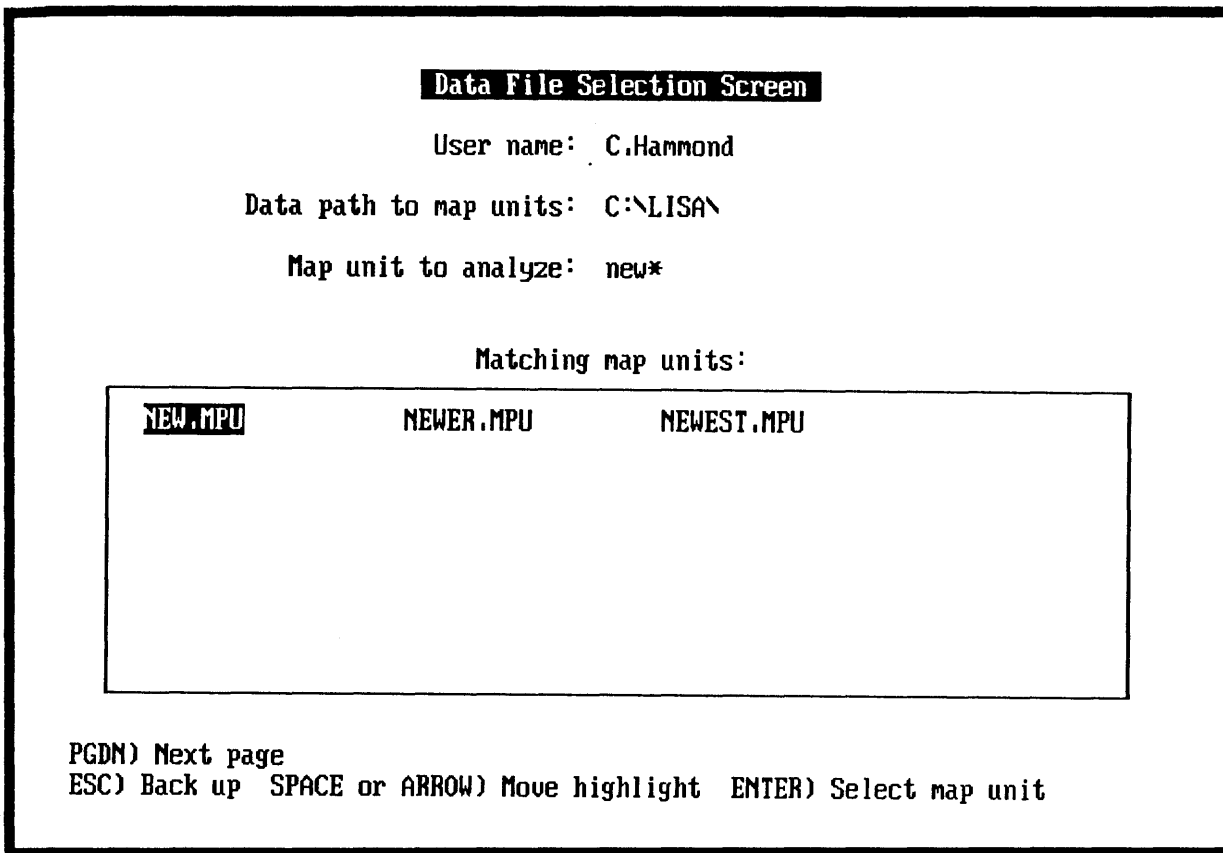


Figure 3.5—Displaying names of map units matching NEW\*.

**DEMONSTRATION**

Select the DEMO map unit, as shown in figure 3.4, by typing `demo` at the Map unit to analyze: prompt.

### 3.6 Creating a New Map Unit

To create a new map unit, type a new name into the highlight at the Map unit to analyze: prompt and press **ENTER**. LISA will respond with:

Create: *drive:\datapath\map-unit-name.MPU?* (Y/n)

where the applicable drive, data path, and map unit name are shown. Yes is the default. Press **Y** or **ENTER** to create the map unit. Press **ENTER** again to select the new map unit, and LISA will go to the EDIT NATURAL SLOPE DATA screen where you can begin entering data. Because a map unit is actually a DOS subdirectory, the name you use must conform to DOS filename standards; that is, it must be one to eight characters long without blanks or punctuation. The program will ignore invalid characters in the input field, and an extension of `.MPU` is automatically added to the name.

### 3.7 Deleting an Existing Map Unit

Map units cannot be removed from within LISA. To delete a map unit subdirectory using DOS, the data files within that map unit must first be deleted and then the subdirectory removed.

### 3.8 Selecting Existing Data Files

LISA stores data in three types of files — site, material, and groundwater files. After a map unit has been selected, a window for each file type listing the names of available data files will be displayed, as shown in figure 3.6. You may proceed directly to the EDIT DATA screen to start a new problem, or you may select one or more existing data files to use or modify.

To select a data file, use **SPACE** or **←** or **→** to first select a file type, and then **↑** or **↓** to highlight the desired file name, and press **ENTER**. **PG UP** and **PG DN** will display more file names if the window is full. After a file has been selected, its name will be displayed above the window. To “unselect” a selected data file, highlight the name of the selected file in the window and press **ENTER**.

#### DEMONSTRATION

Select the **DEMO** data file for each file type and press **F1**.

### 3.9 Deleting an Existing Data File

You may delete any LISA data file by highlighting the name of the file when it is displayed in the DATA FILE SELECTION screen and pressing **DEL**. LISA will ask you for confirmation with the message

Delete drive:\datapath\filename (y/N)?

Press **Y** to delete the file or any other key to keep the file.

### 3.10 Entering or Editing Data

Press **F1** from the DATA FILE SELECTION screen to go to the EDIT NATURAL SLOPE DATA screen (fig. 3.7). If existing data files have been selected, the name of the file will be shown next to the file type title, and the distribution type and the values for the distribution parameters will be displayed next to each input variable name.

To enter or edit data, move the highlight to the desired variable and press **ENTER**. A window listing the available distribution types will be displayed, with the current distribution type highlighted (fig. 3.8). The current distribution is indicated also by a highlighted letter after the **Choose distribution (C-V)**: prompt at the bottom of the window. Select a distribution type either by moving the highlight to the desired type and pressing **ENTER** or by pressing the letter indicated next to the distribution type.

The available distribution types are uniform, normal, lognormal, triangular, beta, histogram, and, for  $C'_s$  and  $\phi'$ , bivariate normal. Groundwater-soil depth ratio is limited to uniform, triangular, beta, and histogram to avoid simulation of  $D_w/D$  values that are negative or greater than 1. A constant value may also be specified for any variable.

**Data File Selection Screen**

User name: C.Hammond

Data path to map units: C:\LISA\

Current map unit: DEMO.MPU

Current LISA Files:

Site:

Material:

Groundwater:

DEMO.SIT	DEMO.MTL	DEMO.HYD
----------	----------	----------

F1) Enter or Edit Data

ESC) Back up SPACE or ARROW) Move highlight ENTER) Select LISA file

Figure 3.6—Windows listing the available files for each file type.

After selecting a distribution type, highlighted input fields prompting for values for the appropriate distribution parameters will appear to the right of the variable name. Figure 3.9 illustrates data entry for a triangular distribution. Any nonnegative number up to six characters in length, including an optional decimal point, may be entered into the input field. The backspace key may be used to edit the value in the highlight before pressing **ENTER**. **ESC** will return you to the previous prompt.

If you select the same distribution type for a variable as is currently specified (or, for soil cohesion and friction angle, you switch between normal and bivariate normal), the current values will be shown in the highlights. You may use these values by pressing **ENTER**, edit them by using the backspace key, or replace them by typing a new number.

**F4** will take you to the DOS shell, which is handy for running DLISA or for issuing DOS commands, such as deleting or moving files, while LISA remains in memory. You must type **EXIT** at the DOS prompt to return to LISA. **F4** is active only in the EDIT DATA and SCATTER PLOT AND HISTOGRAM screens.

To return to the DATA FILE SELECTION screen, press **ESC**. The names of the data files originally selected will be kept as the current files even if new data files have been saved. If you press **ESC** to return to the DATA FILE SELECTION screen without saving modified data files, the following message will be displayed:

**EDIT NATURAL SLOPE DATA**

		<b>SITE</b>	File: DEMO.SIT
<b>Soil depth, ft.</b>	Uniform	Min.: 1.5	Max.: 12.0
<b>Ground slope, %</b>	Histogram	9 classes:	5 11 22 28 13 8 4 7 2 %
<b>Tree surchrg, psf</b>	Uniform	Min.: 10.0	Max.: 20.0
<b>Root cohes., psf</b>	Beta	Min.: 10.0	Max.: 155.0 P : 1.50 Q : 5.00
		<b>MATERIAL</b>	File: DEMO.MTL
<b>Friction angle, °</b>	Normal	Mean: 33.0	Std.: 1.0
<b>Soil cohesion, psf</b>	Uniform	Min.: 10.0	Max.: 50.0
<b>Dry unit wt., pcf</b>	Normal	Mean: 105.0	Std.: 1.5
<b>Moist content, %</b>	Normal	Mean: 18.0	Std.: 2.0
<b>Specific gravity</b>		2.66	
		<b>WATER</b>	File: DEMO.HYD
<b>Groundwater (Du/D)</b>	Triangular	Min.: 0.1	Apex: 0.5 Max.: 0.9
<b>Save simulated values:</b>		No	Random seed: 1502678690
<b>ID: EXAMPLE DATA SET</b>			# iterations: 1000

**Data Directory: C:\LISA\DEMO.MPUS**

ESC) Cancel changes Plot Save Files F1) Execute ENTER) Change

Figure 3.7—The content of the DEMO data files displayed on the ENTER NATURAL SLOPE DATA screen.

About to exit EDIT NATURAL SLOPE DATA  
 Changes Made  
 Save changes? (Y/n)  
 Esc) Cancel request

If you press **N**, any changes made will be lost. Section 3.13 explains how to save data files.

In sections 3.10.1 through 3.10.8, we comment on each distribution type and explain the required inputs and the error messages that might occur during data entry.

### DEMONSTRATION

To illustrate editing data (as shown in fig. 3.9):

- Move the highlight to **Soil depth** and press **ENTER**.
- Move the highlight to **Triangular** and press **ENTER**, and the prompt for the minimum value for the distribution will appear next to **Soil depth**.
- Press **1 . 5 ENTER**, and the prompt for the apex value will appear.
- Press **4 ENTER**, and the prompt for the maximum value will appear.
- Press **1 2 ENTER**, and the changed distribution will be shown for soil depth. The highlight will move down automatically to the next variable (ground slope).

### DEMONSTRATION

To illustrate changing values with the same distribution type:

- Move the highlight to **Friction angle** and press **ENTER**.
- Press **ENTER** again to select **Normal**, which is the current distribution type. The prompt for the mean value will have the current value (33°) as the default.
- Press the backspace key, then **4 ENTER** to change the mean value from 33° to 34°.
- Press **ENTER** to accept the default (current) value for the standard deviation.

#### 3.10.1 Constant Value

Any input variable may be given a constant value. No error message is issued.

#### 3.10.2 Uniform Distribution

The uniform distribution is specified by a minimum value and a maximum value.

### ERROR MESSAGES

Maximum must be greater than minimum  
Press any key to continue

#### 3.10.3 Normal Distribution

The normal distribution is specified by the mean and standard deviation. The normal distribution used in LISA is a "constrained" distribution—no values less than the mean minus 3.09 standard deviations nor greater than the mean plus 3.09 standard deviations are returned. In addition, you are not allowed to specify a distribution that would return negative values within this range.

**EDIT NATURAL SLOPE DATA**

		SITE	File: DEMO.SIT
Soil depth, ft.	Uniform	Min.: 1.5	Max.: 12.0
Ground slope, %	Histogram	9 classes: 5 11 22 28 13 8 4 7 2 %	
Tree surchrg, psf	Uniform	Min.: 10.0	Max.: 20.0
Root cohes., psf	Beta	Min.: 10.0	Max.: 155.0 P : 1.50 Q : 5.00
<b>Available Distributions</b>			
Friction angle, °	Normal	C) Constant	
Soil cohesion, psf	Uniform	U) <u>Uniform</u>	
Dry unit wt., pcf	Normal	N) Normal	
Moist content, %	Normal	L) Lognormal	
Specific gravity		T) Triangular	
		B) Beta	
Groundwater (Dw/D)	Triangul	H) Histogram	
Save simulated values: No		ax.: 0.9	
ID: EXAMPLE DATA SET		: 1502678690	
Data D		s: 1000	
		Choose distribution (C-U): J	

(ESC) Cancel changes Plot Save Files F1) Execute ENTER) Change

Figure 3.8—Selecting a probability distribution type.

### ERROR MESSAGES

Values < 0 possible (mean - 3.09s <= 0)  
Press any key to continue

To prevent the sampling of negative values, LISA checks to ensure that the mean ( $\mu$ ) minus 3.09 times the standard deviation ( $s$ ) is positive. If it is not, this message will be displayed. After pressing a key, enter either a larger mean or a smaller standard deviation such that  $\mu - 3.09s > 0$ .

Standard deviation must be greater than zero  
Press any key to continue

LISA will not allow you to specify a normal distribution with a standard deviation of zero.

EDIT NATURAL SLOPE DATA

SITE		File: DEMO.SIT	
Soil depth, ft.	Triangular	Min : 1.5	Apex: 4 Max : 12
Ground slope, %	Histogram	9 classes:	5 11 22 28 13 8 4 7 2 %
Tree surchrg, psf	Uniform	Min.: 10.0	Max.: 20.0
Root cohes., psf	Beta	Min.: 10.0	Max.: 155.0 P : 1.50 Q : 5.00
MATERIAL		File: DEMO.MTL	
Friction angle, °	Normal	Mean: 33.0	Std.: 1.0
Soil cohesion, psf	Uniform	Min.: 10.0	Max.: 50.0
Dry unit wt., pcf	Normal	Mean: 105.0	Std.: 1.5
Moist content, %	Normal	Mean: 18.0	Std.: 2.0
Specific gravity		2.66	
WATER		File: DEMO.HYD	
Groundwater (D <sub>w</sub> /D)	Triangular	Min.: 0.1	Apex: 0.5 Max.: 0.9
Save simulated values:	No	Random seed:	1502678690
ID:	EXAMPLE DATA SET	# iterations:	1000
Data Directory: C:\LISA\DEMO.MPU			

ESC) Cancel changes Plot Save Files F1) Execute ENTER) Change

Figure 3.9—Editing the triangular distribution for soil depth.

**3.10.4 Lognormal Distribution**

The lognormal distribution is specified by the mean and standard deviation of the distribution, in the units of the variable to be simulated (*not* in the logarithm of the units of the variable).

**ERROR MESSAGES**

Zero mean not allowed  
Press any key to continue

LISA will not allow you to specify a lognormal distribution with a mean of zero.

Standard deviation must be greater than zero  
Press any key to continue

LISA will not allow you to specify a lognormal distribution with a standard deviation of zero.

### 3.10.5 Triangular Distribution

The triangular distribution is specified by a minimum value, a most likely (apex) value, and a maximum value.

#### ERROR MESSAGES

Apex must not be less than minimum  
Press any key to continue

Maximum must not be less than apex  
Press any key to continue

Maximum must be greater than minimum  
Press any key to continue

### 3.10.6 Beta Distribution

The beta distribution is specified by a minimum value, a maximum value, and two shape parameters,  $P$  and  $Q$ .  $P$  and  $Q$  may be any positive real number, but values greater than 1 produce distribution shapes that better model the typical spatial distributions of the physical factors in the infinite slope model.

It takes approximately 2.5 minutes on an 8086 machine, 70 seconds on an 80286 machine, 15 seconds on an 80386 machine, and 7 seconds on an 80486 machine to simulate 1,000 values from a typical beta distribution if the machine has a math co-processor; without one, expect to wait about 10 times as long. Beta distributions with one shape parameter ( $P$  or  $Q$ ) less than 1 take somewhat longer to simulate. Because the beta distribution takes longer to simulate than do the other distributions, LISA displays the message

Simulating Beta nnnn

and displays the iteration number to assure the user that the program is operating.

#### ERROR MESSAGES

Maximum must be greater than minimum  
Press any key to continue

$P$  must be greater than zero  
Press any key to continue

$Q$  must be greater than zero  
Press any key to continue

### 3.10.7 Histogram Distribution

The histogram distribution is specified by the number of classes to be used, the minimum and maximum value for each class, and the percentage of observations in each class. LISA allows at most 10 classes to be used, and the classes are assumed to be contiguous (therefore, the minimum for one class is the maximum of the preceding class); however, any class may have zero observations specified.

Only the number of classes and the percentage of observations in each class are displayed on the EDIT NATURAL SLOPE DATA screen. To see the minimum and maximum values for each class, you must either plot or edit the distribution. Figure 3.10 shows a nearly completed entry for a nine-class histogram distribution for ground slope.

**EDIT NATURAL SLOPE DATA**

SITE    File: DEMO.SIT

Soil depth, ft.    Triangular Min.: 1.5    Apex: 4.0    Max.: 12.0

**Ground slope, %**    Histogram Specification for    Q : 5.00

Tree surchr, psf    Ground slope

Root cohes., psf    9 classes

Class	Min	Max	% of values
1	10.0	20.0	5.0
2	20.0	30.0	11.0
3	30.0	40.0	22.0
4	40.0	50.0	28.0
5	50.0	60.0	13.0
6	60.0	70.0	8.0
7	70.0	80.0	4.0
8	80.0	90.0	7.0
9	90.0	100.0	<b>2</b>

Friction angle, °

Soil cohesion, ps

Dry unit wt., pcf

Moist content, %

Specific gravity

Groundwater (Dw/D

Save simulated va    total= 98.0% ( 2.0% remaining)    98

ID: EXAMPLE DATA

ESC) Cancel changes    Plot    Save Files F1) Execute    ENTER) Change

Figure 3.11—Entering values for the histogram distribution.

When entering a new histogram, LISA assumes that the histogram is to have classes of equal width. If this is the case, you need enter only the minimum and maximum for the first class, and the percentage in each class. As you step through the input, the correct minimum (the previous class's maximum) and a suggested maximum (for a class of the same width as the first class) are displayed. You may change the class widths as you go. In addition, a running sum of the percentages from each class and the value needed to make the total equal 100 percent are displayed at the bottom of the window. The default value for percentage for the last class will make the total 100 percent.

## ERROR MESSAGES

# of classes must be between 1 and 10  
Press any key to continue

The number of classes must be between 1 and 10, inclusive.

Maximum must be greater than minimum  
Press any key to continue

Classes of zero or negative width are not allowed.

% must be between 0 and 100  
Press any key to continue

No class may have more than 100 percent of the observations.

Total percentage exceeds 100%  
Press any key to continue

Total percentage less than 100%  
Press any key to continue

One of these messages is displayed if the total percentage of all classes in the histogram does not equal 100 percent.

### 3.10.8 Bivariate Normal Distribution

In LISA version 2.0, linear correlation between  $C'_s$  and  $\phi'$  can be considered only with the bivariate normal distribution. When bivariate normal is selected for either  $C'_s$  or  $\phi'$ , you will be prompted for the mean and standard deviation for each variable, and the correlation coefficient ( $r$ ) between the two.

Although the lower limit of the marginal normal is checked to see that the mean minus 3.09 times the standard deviation is greater than or equal to zero, it is still possible to get a negative value using the bivariate normal if the lower limit is equal to (or very close to) zero. If this occurs, the negative value will be shown on the STATISTICS OF SIMULATED DATA screen. The user should then adjust the mean or standard deviation to give a slightly larger minimum value for the marginal distribution, or run the simulation again with a new random number seed until no negative values are simulated.

## WARNING AND ERROR MESSAGES

Friction angle will be changed to normal  
Press any key to continue

If  $C'_s - \phi'$  is specified as bivariate normal and you change  $C'_s$  to a univariate distribution, LISA automatically changes  $\phi'$  to a univariate normal with the same mean and standard deviation it had in the bivariate normal.

**Soil cohesion will be changed to normal**  
**Press any key to continue**

If  $C'_s - \phi'$  is specified as bivariate normal and you change  $\phi'$  to a univariate distribution, LISA automatically changes  $C'_s$  to a univariate normal with the same mean and standard deviation it had in the bivariate normal.

**Values < 0 possible (mean - 3.09s <= 0)**  
**Press any key to Continue**

As with the normal distribution, LISA will not allow you to enter a mean ( $\mu$ ) and standard deviation ( $s$ ) that would cause  $\mu - 3.09s$  to be negative. This reduces the likelihood of returning negative values for  $C'_s$  or  $\phi'$ . Enter a larger mean value or a smaller standard deviation such that  $\mu - 3.09s > 0$ .

**Make phi bivariate also**  
**Press any key to continue**

If you select the bivariate normal distribution for soil cohesion and enter all of the values for  $C'_s$ , then press **[ESC]** while entering the mean for  $\phi'$ , LISA will display this message. You must enter a mean and standard deviation value for  $\phi'$ .

**Make Cs bivariate also**  
**Press any key to continue**

If you select the bivariate normal distribution for friction angle and enter all of the values for  $\phi'$ , then press **[ESC]** while entering the mean for  $C'_s$ , LISA will display this message. You must enter a mean and standard deviation value for  $C'_s$ .

**r must be between -1 and 1**  
**Press any key to continue**

The correlation coefficient  $r$  must be between -1 and 1, inclusive.

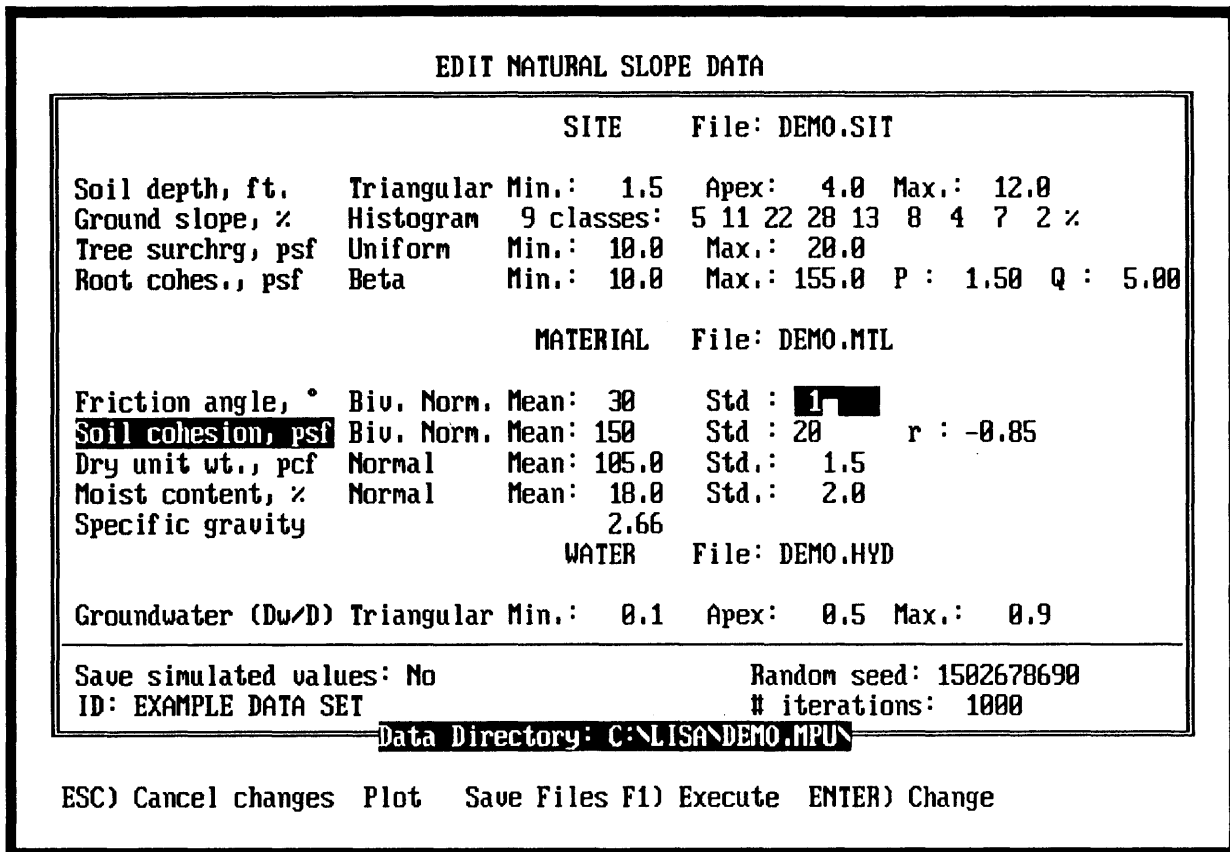


Figure 3.11—Entering values for a bivariate normal distribution for  $C'_s$  and  $\phi'$ .

**DEMONSTRATION**

The highlight should be on soil cohesion after making changes to friction angle. To illustrate the use of the bivariate normal distribution for  $C'_s$  and  $\phi'$  (see fig. 3.11):

- Press  (ENTER), move the highlight to **Bivariate Normal**, and press  (ENTER) (or simply press  (V)).
- Enter 150 for the mean, 20 for the standard deviation, and -0.85 for  $r$ .
- A prompt for the mean friction angle will appear. Enter 30 for the mean and 1 for the standard deviation.

The bivariate normal distribution is now shown as the current distribution for both soil cohesion and friction angle, with the value for  $r$  shown once for each variable.

## DEMONSTRATION

We will now change friction angle to be a uniform distribution:

- Move the highlight to **Friction Angle** and press **ENTER**.
- Select **Uniform**.
- Enter **20** for the minimum and **30** for the maximum.
- Notice the message in the center of the screen. Press any key, and the cohesion specification will change to a normal distribution with a mean of 150 and a standard deviation of 20.

### 3.11 Plotting Distributions

To plot the shape of the specified probability density function (PDF) for any variable (except  $G_s$ ) from the EDIT DATA screen, highlight the desired variable and press **F**. Plotting the PDF is particularly helpful for previewing the shape of the beta and lognormal distributions; the limits of data simulation for the normal, bivariate normal, and lognormal distributions; the effect of the correlation coefficient for the bivariate normal distribution; and the classes and limits for the histogram distribution. If unequal class widths are used, the plot of the histogram PDF might appear different from the relative-frequency histogram (see part 1, section 2.18); the PDF is true to what will be sampled. A plot of the bivariate normal distribution (for  $C'_s$  and  $\phi'$ ) shows a rough contour plot of the probability surface. The limits of the bivariate normal plot are  $\mu \pm 3s$  (the mean plus or minus three times the standard deviation) for each variable; sampled values generally fall within this range, but a few outliers may be expected. Figure 3.12 shows an example of a plot of a normal distribution.

If the **Plot** option is not shown on the bottom line of the screen, then LISA does not recognize that your system supports graphics and it will ignore your plot request. In some cases, LISA may not recognize that your system supports graphics when it actually does; for example, if you are using a video board that emulates CGA graphics on a monochrome monitor. In this case, try switching the active display adapter to the Color/Graphics Monitor Adapter by typing **MODE C080** from DOS before invoking LISA.

To return to the EDIT DATA screen after viewing the plot of a uniform, triangular, or histogram distribution, press any key. These three distributions cannot be modified while viewing the plot. Section 3.12 discusses how to return after viewing the other distribution types.

## ERROR MESSAGES

Zero standard deviation  
Press any key to continue

This message is displayed when you try to plot a normal, bivariate normal, or lognormal distribution with a standard deviation of zero. It should never be displayed unless the input data files have been modified outside of LISA.



the others, the changes are not as obvious. To help in selecting proper values, you can change some parameter values while viewing the plot of the normal, lognormal, beta, and bivariate normal distributions and observe the change in shape or endpoints or both. LISA does not allow you to change parameter values for the uniform, triangular, or histogram distribution while viewing the plot; you will have to return to the DATA ENTRY screen to modify these distribution types.

For the beta distribution, the mode and skewness change as you change the values of the shape parameters  $P$  and  $Q$ . LISA does not allow you to change the endpoints of the beta while displaying the plot. If you make multiple changes to the beta distribution parameters, each curve will be shown on the same plot until you press **SPACE** to erase previous plots. For the lognormal distribution, the mode, skewness, and limiting values can all change as you change the values of mean and standard deviation. The current lognormal distribution plot will be erased before a new one is displayed. Only the sampling endpoints change as the mean and standard deviation of the normal distribution change. The values for the new endpoints will be displayed. The normal distribution routine will not return values outside the displayed range. The endpoints and surface shape of the bivariate normal PDF will change as the standard deviations and correlation coefficient change. (LISA does not allow you to change the mean values while displaying the bivariate normal plot.) Unlike the normal distribution routine, the bivariate distribution routine does not limit the range of returned values, so a small percentage of values may be expected to fall outside the indicated range.

To change the distribution values while viewing the plot, press **C** and the cursor (a small block) will appear in the display of distribution values in the upper right corner of the screen. The input field is not in reverse video, as it is in most other LISA screens; as always, however, the current value may be edited by pressing the backspace key, accepted with **ENTER**, or replaced by a new value. Figure 3.13 shows an example of a plot of two beta distributions.

You may return to the EDIT DATA screen in one of two ways—by pressing **ESC** to return with the original distribution parameter values, or by pressing **ENTER** to return with the current distribution parameter values.

## ERROR MESSAGES

Zero mean not allowed.

Non-positive standard deviation.

LISA allows only strictly positive values for the mean and standard deviation for normal, lognormal, and bivariate normal distributions.

Values  $< 0$  possible (mean-3.09s  $\leq 0$ ).

LISA truncates the normal distribution at the mean plus and minus 3.09 times the standard deviation, and checks the lower limit to see that it is not negative. The bivariate normal distribution is not truncated, but the check is still made to reduce the likelihood of sampling negative values.



### 3.13 Saving Data Files

To save the current data to disk, press **S** from the EDIT DATA screen, and a window listing the three file types and the current file name, if any, for each will be displayed. Using **↑** and **↓**, move the highlight to the type of file that you want to save, and enter a file name using the standard LISA approach. File names must conform to DOS's filenaming conventions (one to eight characters long without spaces or punctuation). Do not include a file extension. You do not need to save all three types of files nor use the same file name for each file type.

If you enter the name of an existing file, LISA will respond with "Overwrite File (y/N)?". To keep from losing the existing file of that name, press **N** or **ENTER** or **ESC** and LISA will allow you to enter another file name. To save the current parameter specifications under the same file name, thereby losing the previous contents of the file, press **Y**.

You do not have to save the data to disk before you start the simulation. This allows you to run LISA in an iterative manner, making several LISA runs and saving to disk only those datasets you feel are important for future use. To prevent unintentional loss of data, you will be asked when you leave the EDIT DATA screen by pressing **ESC** whether you want to save the current data (see section 3.9). In addition, if any changes have been made to the data, the datasets will be saved as files **QUICK.SIT**, **QUICK.MTL**, and **QUICK.HYD** in the current map unit subdirectory when you exit LISA using **F4**, as explained in section 3.21.

#### DEMONSTRATION

- Press **S** from the EDIT DATA screen.
- Type **NEW** and press **ENTER** for the site file name, and the site data will be saved as file **NEW.SIT**. (Note that if someone has already run through the demonstration, file **NEW.SIT** may already exist and LISA will ask whether to overwrite it. Press **Y** or press **N** and enter a different name.) The material file name will now be highlighted.
- Press **ENTER** to save the modified material data as file **DEMO.MTL**. Because file **DEMO.MTL** already exists, LISA will ask whether you want to overwrite it (see figure 3.14). Press **N**, and enter a different name.
- Press **ESC** to return to the EDIT DATA screen, since we do not want to save the groundwater data to disk.

### 3.14 Saving Simulated Values

You may ask LISA to save the sampled (simulated) values of all of the input variables and the calculated factors of safety in a file called **SIMULATE.OUT** in the current map unit subdirectory. **SIMULATE.OUT** will be sorted from lowest to highest value of factor of safety, facilitating examination of the combinations of input variables that generated the lowest factors of safety to determine whether those combinations actually exist in nature. If they do not, the simulation results may be unrealistic. Because histograms of the simulated values for any variable and scatter plots of any pairing of variables are available from within LISA, you may rarely need this option. However, we feel that it is important to

Simulating Natural Slope Parameters					
	Minimum	Maximum	Mean	Std. Dev.	P[FSS<=1]
Soil depth (ft)	1.64	11.87	5.85	2.24	
Ground slope (%)	10.55	98.38	47.01	19.05	
Tree surcharge (psf)	10.01	20.00	14.97	2.86	
Root cohesion (psf)	10.47	125.58	43.64	21.27	
Friction angle (deg)	20.01	30.00	25.02	2.87	
Soil cohesion (psf)	88.20	211.80	151.23	20.23	
Dry unit weight (pcf)	100.36	109.64	105.00	1.50	
Moisture content (%)	11.82	24.18	17.98	1.94	
Moist unit weight (pcf)	116.95	130.78	123.85	2.63	
Saturated unit weight (pcf)	125.83	130.82	127.93	0.93	
Groundwater ratio (Dw/D)	0.12	0.89	0.50	0.17	
Factor of safety	0.61	0.77	1.86	0.98	0.111
ESC) Edit Natural Data		Any other key to continue			

Figure 3.14—Screen for saving data files. The user has just saved the site data as file NEW and has asked to save the material data as file DEMO, which already exists.

have available the actual numbers used. SIMULATE.OUT will be about 80 kilobytes long for a simulation of 1,000 iterations. Section 3.21 shows part of an example SIMULATE.OUT file and describes how to view, print, and rename it.

To tell LISA whether to save the sampled values, highlight the **Save simulated values:** prompt on the EDIT DATA screen and press . You will then be asked to press  if you want to save the values, or  if not.

### DEMONSTRATION

Move the highlight to **Save simulated values:** and press  followed by .

### 3.15 Entering a Descriptive Comment ("ID")

You may add a descriptive comment of up to 40 characters in length for the run. The comment will be stored in the results file (RESULTS.OUT), and stored in the site file and simulated data file if they are saved. To edit the existing comment or enter a new comment, move the highlight to the ID: prompt and press . The existing comment will be displayed in an input field for you to edit.

### 3.16 Changing the Random Seed

LISA uses a pseudorandom number generator in sampling values for each input variable from the probability distribution specified by the user. The *random number seed* specifies a starting point for sampling. At the beginning of each session, LISA generates a suggested seed value based on the date and time found in the computer system clock. Each variable has its own seed value, hidden from the user and based on the main random number seed, from which its values are sampled. This ensures that sampling is repeatable and allows the user to see the effect of changing the values of a variable without introducing the effect of sampling using a different seed.

LISA will sample values for all variables the first time you press **F1** from the EDIT DATA screen. Thereafter, to increase the execution speed of LISA, only those variables that you have modified will be resampled. You may force LISA to resample all variables by changing either the random number seed or the number of iterations. *We recommend that, once you are satisfied with all of the input distributions, you run LISA several times with different seed values to observe the variation in simulation results due to random variation (see part 1, section 4.4).*

To change the random seed, highlight **Random seed:** and press **ENTER**. LISA will generate a new seed value and display it in an input field. You may press **ENTER** to accept it, press **ESC** to cancel the change request and keep the old seed, or type a number between 1 and 2,147,483,646 inclusive and press **ENTER**. Entering your own seed value allows you to duplicate exactly a previous run.

The seed number used for a simulation is reported in the results file **RESULTS.OUT** and, if it is created, in **SIMULATE.OUT**.

#### ERROR MESSAGE

Seed must be between 1 and 2,147,483,646  
Press any key to continue

The seed you enter must be an integer greater than 0 and less than 2,147,483,647.

#### DEMONSTRATION

To duplicate the results for the demonstration exercise exactly, enter 1502678690 as the random seed.

### 3.17 Entering the Number of Iterations

We recommend that 1,000 iterations be used for all final LISA runs to increase repeatability between runs (see part 1, section 4.4). However, you may want to use a smaller number for initial runs to speed execution. To change the number of iterations, move the highlight to the **# iterations** option, press **ENTER**, and enter a number between 1 and 1,000 (inclusive) into the highlight.

## ERROR MESSAGES

No more than 1000 iterations allowed.  
Press any key to continue

At least 1 iteration required.  
Press any key to continue

One of these messages is displayed if you ask for 0 or more than 1,000 iterations. Enter a number between 1 and 1,000 inclusive.

## DEMONSTRATION

To duplicate the results of the demonstration exactly, use 1000 iterations.

### 3.18 Starting the Simulation

Press **F1** from the EDIT DATA screen to begin sampling a set of possible input values for each variable. Each input variable must be given a distribution type or a constant value before LISA will start the simulation. All of the variables will be sampled only the first time you press **F1**, or when the random number seed or number of iterations have changed; otherwise, only those variables you have modified will be resampled. After each variable is sampled, the minimum, maximum, mean, and standard deviation of the sampled values will be displayed on the SIMULATING DATA VALUES screen. If the variable being sampled has a beta distribution, LISA will display the message **Simulating beta** and count the number of completed iterations, because sampling from the beta distribution takes noticeably longer than does sampling from the other distribution types (see section 3.9.6). You may stop the simulation and return to the EDIT DATA screen by pressing **ESC**. LISA will complete sampling of the current parameter before it responds.

After all input values have been sampled, the factors of safety will be calculated and the probability of failure ( $P[FS \leq 1]$ ) will be displayed. The message

One Moment Please

will be displayed while LISA sorts the factor of safety values and writes output files to disk.

After the simulation is complete, press any key (except **F1** and **ESC**) to examine the results, as described in the next three sections.

Alternatively, it may be easier when doing many runs to simply write down the probability of failure value or press **F1/ESC** to print a copy of the results shown on the screen, and then return directly to the EDIT DATA screen by pressing **ESC**; however, you will lose access to the results files (**RESULTS.OUT** and **SIMULATE.OUT**).

## ERROR MESSAGES

Not all variables have been specified  
Press any key to continue

This message is displayed when **F1** is pressed before distributions have been specified for all input variables.

### DEMONSTRATION

Press **F1**, and observe the values being sampled. For this example, the  $P[FS \leq 1]$  should be 0.111 unless you made changes other than those described in the demonstration or you did not use the same random number seed. Figure 3.15 shows the simulation screen for the demonstration.

### EDIT NATURAL SLOPE DATA

	SITE	File: DEMO.SIT
Soil depth, ft.	Triangular Min.:	1.5 Apex: 4.0 Max.: 12.0
Ground slope, %	Histogram	9 classes: 5 11 22 28 13 8 4 7 2 %
Tree surchrg, psf		
Root cohes., psf		
Friction angle, °	Save Files	: 1.50 Q : 5.00
Soil cohesion, ps	New Site File : new	
Dry unit wt., pcf	Saved	
Moist content, %	New Material File : DEMO	
Specific gravity	Overwrite File? (y/N) _	
Groundwater (Dw/D	New Groundwater File : DEMO	
	ESC) Return to Edit Enter) Save	ax.: 0.9
	Arrows) Move Highlight	
Save simulated values: No		Random seed: 1502678690
ID: EXAMPLE DATA SET		# iterations: 1000
Data Directory: C:\LISA\DEMO.MPUN		

Figure 3.15—The minimum, maximum, mean, and standard deviation of the sampled values and of the factors of safety, and the probability of failure,  $P[FS \leq 1]$ , are displayed.

### 3.19 Viewing and Modifying the Factor of Safety Histogram

Upon pressing a key from the SIMULATING DATA VALUES screen, the histogram of the factor of safety values will appear.<sup>6</sup> The factor of safety histogram is stored automatically in the results file; it also may be printed directly by using the **PRINT** key. (Note: a screen print will not show the same characters as are displayed on the screen if your printer does not print the IBM graphics characters.)

You may press **ESC** to return to the EDIT DATA screen; **C** to change the minimum and maximum values for the histogram; or any other key (except **F4**) to continue on to the SCATTER PLOT AND HISTOGRAM screen. Viewing a histogram of a portion of the factor of safety values can be useful for removing the tail of highly skewed histograms and for looking more closely at the distribution of values less than or equal to 1. The minimum and maximum values calculated during the simulation will remain as the defaults to make it easy to recall the original histogram.

If you want to save any modified histogram in the results file, press **S**. If the DOS environment variable LISAGRAPH has been set to IBM before LISA was started, then the characters as displayed on the screen will be saved in the results file; otherwise, the graphics characters will be converted to standard ASCII characters. The LISAGRAPH environment variable is discussed further in section 1.2.4.2.

#### DEMONSTRATION

Press any key to view the histogram of the factor of safety values (shown in fig. 3.16). Since the histogram for this example is highly skewed, we want to remove part of the tail from the plot. To change the maximum value of the histogram to be displayed:

- Press **C**.
- Press **ENTER** to accept the minimum value displayed.
- Enter 3.5 for the maximum value and view the partial distribution of factor of safety values. The distribution is still skewed right, but with the tail removed, the distribution of the majority of the values is better displayed (as shown in fig. 3.17).
- Press **S** to store the modified histogram in the results file.
- Press **SPACE** (or any key other than **C**, **S**, **F4**, and **ESC**) to go to the SCATTER PLOT AND HISTOGRAM screen.

### 3.20 Viewing Scatter Plots and Variable Histograms

The SCATTER PLOT AND HISTOGRAM screen has two functions:

- To display a scatter plot of the sampled or calculated values of any of the listed variables against any other variable, and to display a histogram of the sampled or calculated values for any of the variables, as discussed below.
- To display, print, and save the LISA results and simulation output files, as discussed in section 3.20.

<sup>6</sup>If you specified 1 iteration, or all input variables were set to constants, LISA will display the message **Cannot display histogram of constant or 1 value**. In this case, a keypress takes you to the SCATTER PLOT AND HISTOGRAM screen, described in section 3.19.

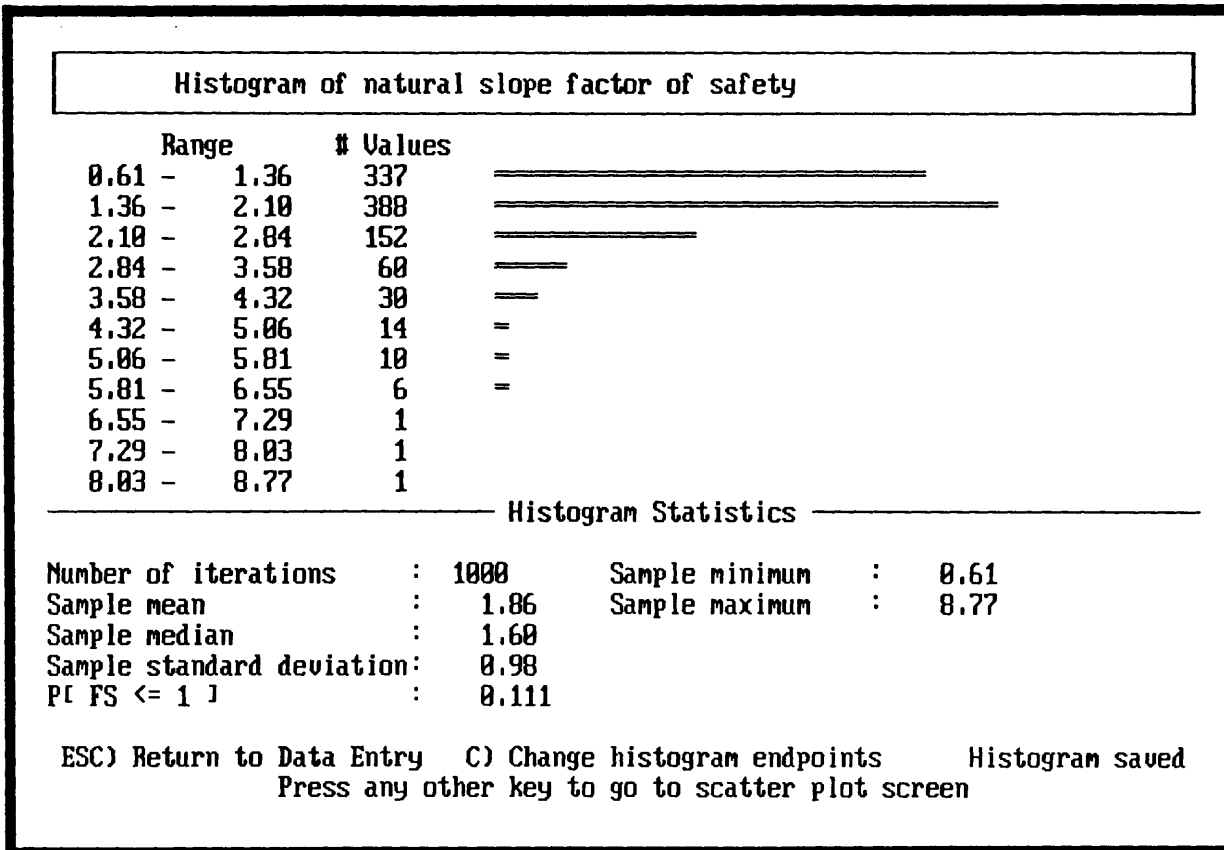


Figure 3.16—Histogram of the factor of safety values for the demonstration problem.

Neither scatter plots nor histograms may be generated for constant-value variables. The variables that were assigned a constant value are indicated by a different color on the SCATTER PLOT AND HISTOGRAM screen.

To view the histogram of any of the listed variables, highlight the variable name and press **ENTER** twice. Viewing the histogram of the input variables is helpful in comparing the sampled values to the distribution specified in the EDIT DATA screen. The minimum and maximum values for the displayed histogram may be changed by pressing **C**. Any of the histograms may be stored in the results file by pressing **S** while the histogram is displayed. The character set used in the file depends upon the value of the DOS environment variable LISAGRAPH, as explained in sections 1.2.4.2 and 3.18.

To view the scatter plot of any two variables (values of one variable plotted against values of another variable), highlight the name of the first (X-axis) variable and press **ENTER**, then highlight the name of the second (Y-axis) variable and press **ENTER**. The scatter plot will be displayed, and LISA will calculate the correlation coefficient,  $r$ , which measures *linear* dependence between two variables. If the factor of safety is selected as the second variable, a horizontal line representing a factor of safety of 1.00 will be displayed (if it falls within the range of the plot).

In general, scatter plots between two input variables will show little correlation. Exceptions are the positive correlation between friction angle and dry,

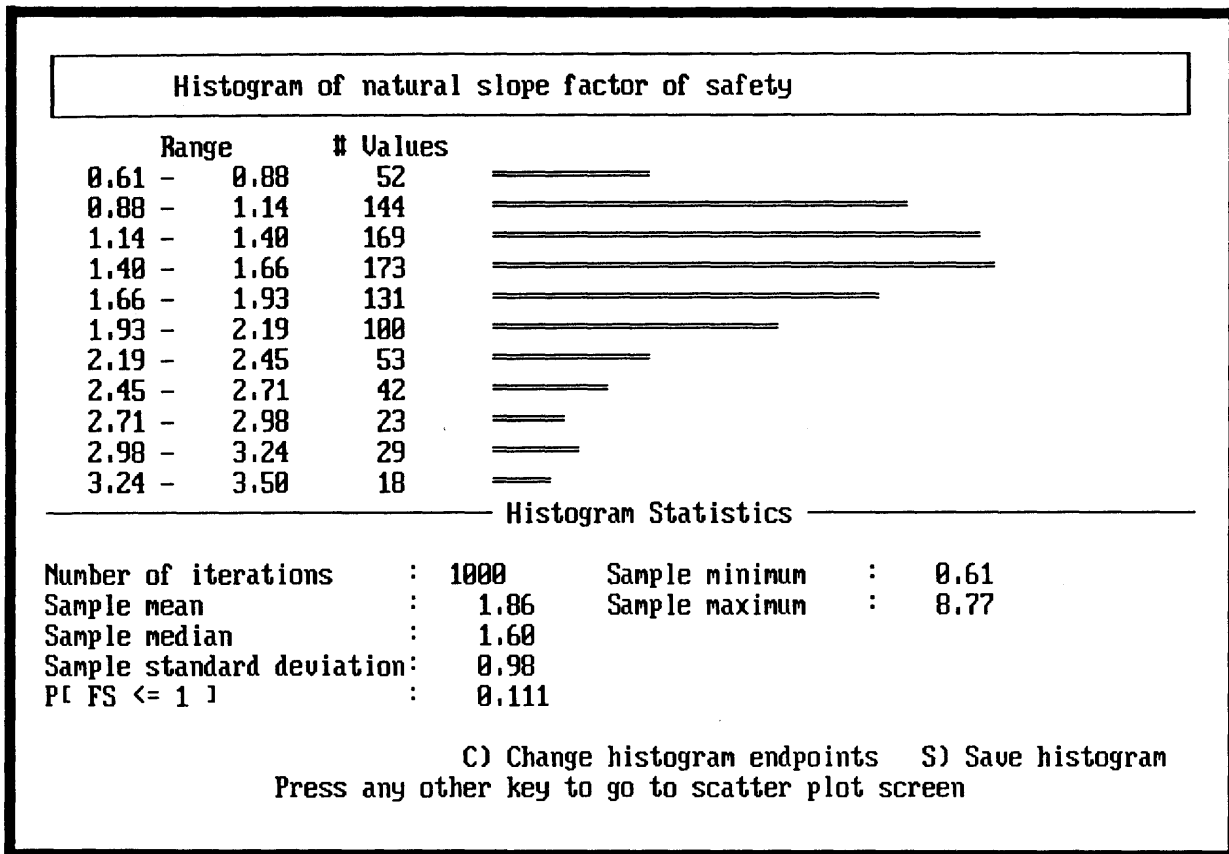


Figure 3.17—Histogram of the factor of safety values less than 3.5.

moist, and saturated unit weight; and the (inverse) correlation between soil cohesion and friction angle if a bivariate normal distribution is used. Scatter plots are particularly useful for examining the dependence of the factor of safety on individual input variables. Variables to which factor of safety is insensitive will show little or no correlation, while variables to which factor of safety is sensitive should show a fairly high (although not necessarily linear) correlation, depending on the range of values used.

A scatter plot of shear strength ( $\tau$ ) against effective normal stress ( $\sigma'$ ) is useful in illustrating the effects of a  $C'_s$ - $\phi'$  correlation on the simulation results; a larger negative value for  $r$  between  $C'_s$  and  $\phi'$  will increase the correlation (reduce the scatter) between  $\tau$  and  $\sigma'$  (see discussion in part 1, section 4.2).

Scatter plots are also useful for showing the scatter of the values sampled for two variables you might consider somewhat correlated in nature (such as surface slope and soil depth). If there are many points that seem like unreasonable pairings, you may want to restrict the range of one or both variables (see discussion in part 1, section 4.2).

The scatter plot is displayed at EGA resolution, and cannot be displayed as a windowed application in Windows 3.0. See section 1.2.3 for some hints if you are running LISA under Windows 3.0.

When you have finished viewing plots and viewing, printing, and saving output files, press **[ESC]** to return to the EDIT NATURAL SLOPE DATA screen.

## ERROR MESSAGES

Cannot display histogram of a constant or 1 value  
Press any key to continue

This message is displayed when you try to view a histogram of a variable that was specified as a constant or when one iteration was specified.

X is constant, cannot make scatterplot  
Press any key to continue

Y is constant, can't make scatterplot  
Press any key to continue

One of these messages is displayed when you request a scatter plot when one or both of the variables has a constant value.

### DEMONSTRATION

- Highlight **Groundwater ratio** and press **ENTER** twice. The histogram shown in figure 3.18 will appear in a moment. It should resemble the triangular distribution that was entered.
- Press **SPACE** to return to the SCATTER PLOT OR HISTOGRAM screen.
- Highlight **Ground slope** and press **ENTER**, then highlight **Factor of safety** and press **ENTER**. The scatter plot shown in figure 3.19 will appear, demonstrating the dependence of the factor of safety on ground slope.
- Press **SPACE** to return to the SCATTER PLOT OR HISTOGRAM screen.

### 3.21 Viewing, Saving, and Printing the Output Files

LISA automatically saves temporary output files from each run in the current map unit subdirectory. The distributions for input variables, the summary of sampled data values, the probability of failure, and the histogram of the factor of safety values, along with any other histograms you may have stored, are saved in a file called **RESULTS.OUT**. The sampled data values are saved in a file called **SIMULATE.OUT**, if you requested that they be saved. These output files can be viewed, printed, or saved from the SCATTER PLOT AND HISTOGRAM screen.

To view a results or simulated data file, move the highlight to the **View** prompt next to the desired file type and press **ENTER**. By default, LISA uses a program called **BROWSE** to let you view the output files (this can be changed; see section 1.2.4). When **BROWSE** is called, the top 25 lines of the selected file are displayed on the screen. **BROWSE** allows you to look at different parts of the file by using the cursor-control keys (**↑** **→** **↓** **←** **PG UP** **PG DN** **HOME** and **END**). To return to the SCATTER PLOT AND HISTOGRAM screen, press **ESC**.

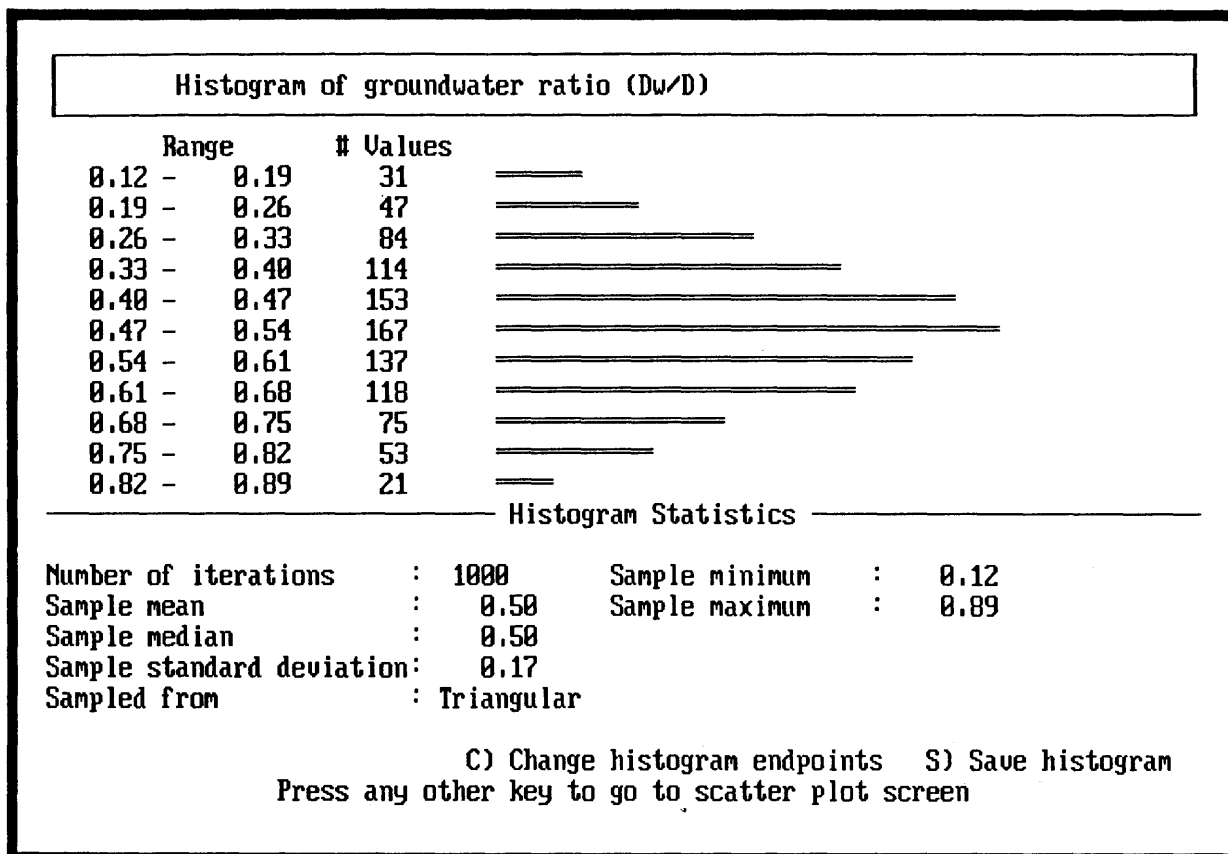


Figure 3.18—Histogram of the groundwater–soil depth ratio values sampled in the demonstration problem.

To print a results or simulated data file, move the highlight to the **Print** prompt beside the desired file type and press **ENTER**.

Because the output files **RESULTS.OUT** and **SIMULATE.OUT** will be overwritten the next time a LISA simulation is run within the same map unit, they must be saved under a different name if you want to keep a copy permanently. To save a results or simulated data file, move the highlight to the **Save** prompt beside the desired file type, and press **ENTER**. The current path for the results or simulated data file will be displayed in a highlighted input field. Type a legal file-name (to save the file in the current map unit subdirectory as given in the highlight), or edit the entry to specify another drive, existing path, and file name (fig. 3.20). *Note that this input field works differently than do the other input fields in LISA.* Here, typed characters will be appended to the path in the input field; **ESC** clears the input field; the backspace key deletes characters to the left; and **ESC**, when pressed in a clear input field, backs you out of the save request.

Once you press **ESC** to leave the **SCATTER PLOT AND HISTOGRAM** screen, you can no longer save the output files from within LISA. If you return to the **EDIT DATA** screen prematurely, you can save the output files by pressing **F4** to go to the DOS shell to copy or rename the files and then return to LISA by typing **EXIT** at the DOS prompt when you are done. You may also press **F4** from the **SCATTER PLOT AND HISTOGRAM** screen to change output file format, or to perform other file management tasks (see section 3.22).

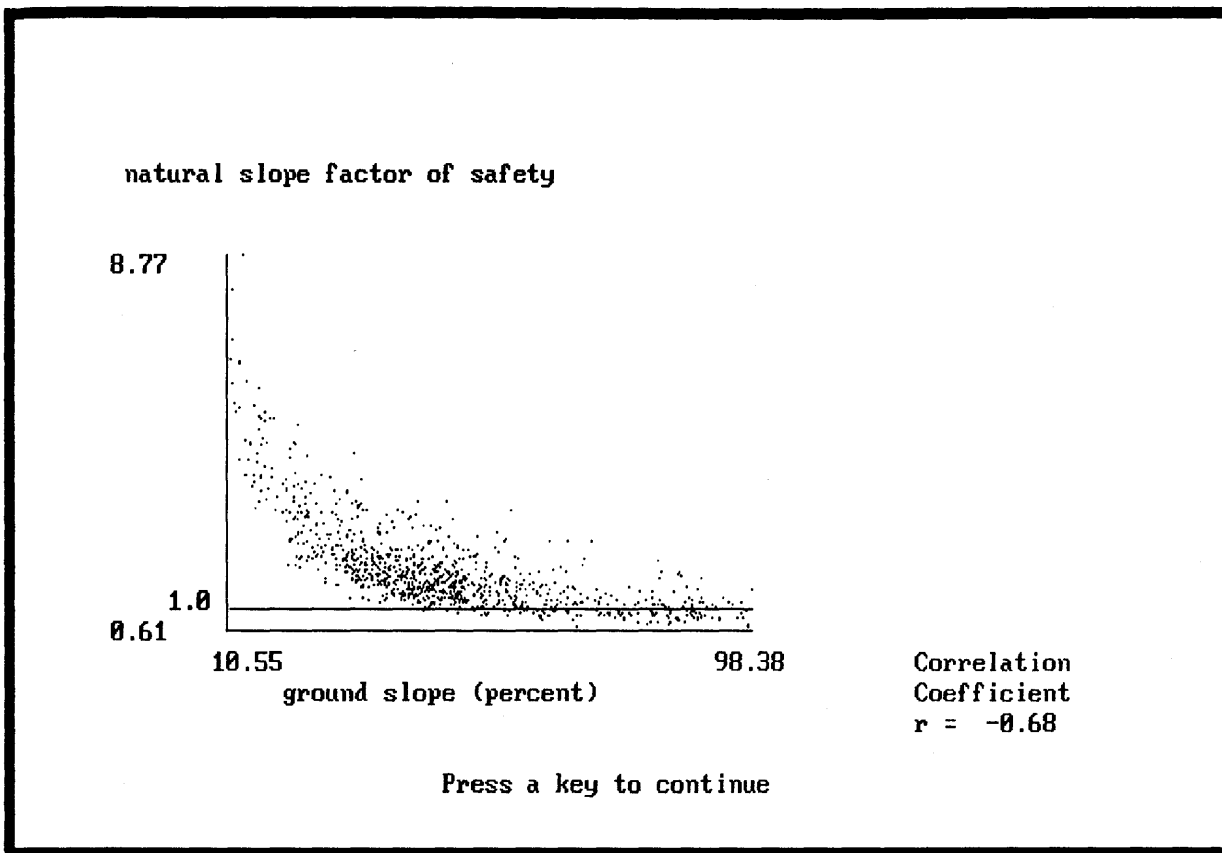


Figure 3.19—Scatter plot of factor of safety against ground slope illustrating a non-linear dependence.

## ERROR MESSAGES

Simulated data not saved  
Press any key to continue

This message is displayed when you ask to view, print, or save the simulated values but did not ask LISA to save them.

Printer needs attention. Fix problem, or <ESC> to cancel.

When you ask LISA to print a file, it checks to see that the printer is ready before trying to print the file. If the printer is turned off, is off-line, is out of paper, or is not connected to the computer, this message will be displayed on the top line of the screen, and LISA will wait for you to either fix the problem or press **ESC** to cancel the print request and return to the SCATTER PLOT AND HISTOGRAM screen. If you have a print spooler installed, the print request may be executed normally without an error message even when the printer is off-line; the hard copy will be produced when the printer is turned on-line or activated by your local procedures.

## SCATTER PLOT and HISTOGRAM

Soil depth	Natural factor of safety
Ground slope	
Tree surcharge	
Root cohesion	
Friction angle	
Soil cohesion	
Dry unit weight	
Moisture content	
Moist unit weight	
Saturated unit weight	
Groundwater ratio (Dw/D)	
Effective normal stress	
Shear strength	

---

View Print Save results as: **C:\LISA\DEMO.MPU\DEMO.OUT**  
View Print Save simulated data

For a scatter plot, select X variable and then Y variable.  
For a histogram, highlight the variable and press ENTER twice.  
ESC) Edit Natural Slope Data                      ENTER) Select option or variable

Figure 3.20—Saving the results file from the demonstration problem to disk as DEMO.OUT.

### Bad command or file name

This DOS message may be displayed momentarily when you select the **view** option if DOS cannot find the file viewer (either **BROWSE.COM** or the program specified by environment variable **LISALIST**). You may exit to the DOS shell by pressing **F4**, type **SET** to have DOS display the current values of environment variables, find the file viewer and copy it into the LISA subdirectory or another subdirectory in the DOS path, and type **EXIT** to return to LISA. You cannot effectively change the values of the environment variables while in the DOS shell, because the changes will be lost when you return to LISA.

### Invalid directory

This DOS message may be displayed momentarily if you give an invalid file name in the **save** option. The file *has not* been saved. Select **save** again, and enter a valid file name.

## DEMONSTRATION

The results file, **RESULTS.OUT**, for the demonstration exercise is shown in figure 3.21. A portion of the simulated data file, **SIMULATE.OUT**, is shown in figure 3.22. View your results and simulated data files and compare them to those in the figures.

### 3.22 Exiting LISA

There are two ways to exit LISA. One is to repeatedly press **ESC** until you back out of LISA. As is discussed in section 3.9, when you press **ESC** from the EDIT DATA screen and any changes have been made to the data since the datasets have been saved, you will be asked whether you want to save the data.

There is also a quick exit from LISA—from almost anywhere, you may press **F4** and be returned directly to DOS. If any dataset has been modified but not saved, all three datasets will be saved automatically in the current map unit subdirectory under the names **QUICK.SIT**, **QUICK.MTL**, and **QUICK.HYD**. The **QUICK** files will be overwritten the next time you quick-exit from the same map unit in LISA. Therefore, if you want to keep the data from the **QUICK** files, they should be renamed (either from DOS or from within LISA by loading the three **QUICK** files and saving them with different names *before* you quick-exit again).

LISA allows you to enter a DOS shell from the EDIT DATA screen and the SCATTER PLOT AND HISTOGRAM screen by pressing **F4**. LISA will remain in memory, leaving approximately 250,000 to 300,000 bytes of RAM free on a 640 kilobyte machine to perform other tasks. You must type **EXIT** at the DOS prompt, preferably from the subdirectory from which you started LISA, to return to LISA.

Level One Stability Analysis  
LISA Version 2.00

=====

ID: EXAMPLE DATA SET

User name                   C.Hammond  
Time of simulation         05-22-1991 09:16:57  
Map unit                    DEMO.MPU  
Number of iterations       1000  
Random number seed        1502678690  
Probability of failure      .111

INPUT DATA

NATURAL DATA

Soil depth                   (ft) Triangular Min.: 1.50   Apex: 4.00   Max.: 12.00  
Ground slope                (%) Histogram 9 classes

Class	Minimum	Maximum	Percent
1	10.00	20.00	5.00
2	20.00	30.00	11.00
3	30.00	40.00	22.00
4	40.00	50.00	28.00
5	50.00	60.00	13.00
6	60.00	70.00	8.00
7	70.00	80.00	4.00
8	80.00	90.00	7.00
9	90.00	100.00	2.00

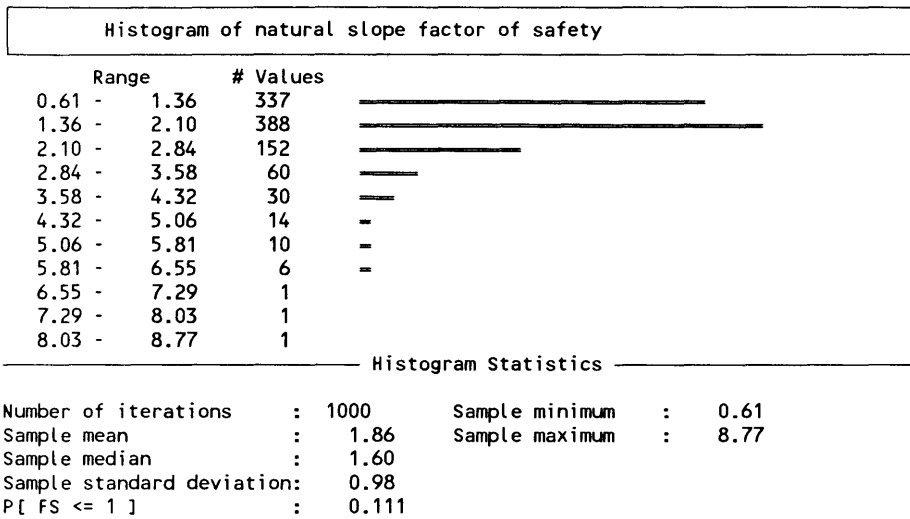
Tree surcharge           (psf) Uniform   Min.: 10.00   Max.: 20.00  
Root cohesion           (psf) Beta       Min.: 10.0    Max.: 155.0   P: 1.5   Q: 5.0  
Friction angle           (deg) Uniform   Min.: 20.00   Max.: 30.00  
Soil cohesion           (psf) Normal     Mean: 150.00   Std.: 20.00  
Dry unit weight          (pcf) Normal     Mean: 105.00   Std.: 1.50  
Moisture content         (%) Normal       Mean: 18.00    Std.: 2.00  
Specific gravity          Constant        Value: 2.66  
Groundwater ratio (Dw/D) Triangular Min.: 0.10   Apex: 0.50   Max.: 0.90

LISA Version 2.00  
EXAMPLE DATA SET

DESCRIPTIVE STATISTICS OF SIMULATED VALUES -- NATURAL SLOPE

	MINIMUM	MAXIMUM	MEAN	S.D.
Soil depth                (ft)	1.64	11.87	5.85	2.24
Ground slope             (%)	10.55	98.38	47.01	19.05
Tree surcharge           (psf)	10.01	20.00	14.97	2.86
Root cohesion           (psf)	10.47	125.58	43.64	21.27
Friction angle           (deg)	20.01	30.00	25.02	2.87
Soil cohesion           (psf)	88.20	211.80	151.23	20.23
Dry unit weight          (pcf)	100.36	109.64	105.00	1.50
Moist unit weight        (pcf)	116.95	130.78	123.85	2.63
Saturated unit wt.       (pcf)	125.03	130.82	127.93	0.93
Moisture content         (%)	11.82	24.18	17.98	1.94
Groundwater ratio (Dw/D)	0.12	0.89	0.50	0.17
Factor of safety	0.61	8.77	1.86	0.98

**Figure 3.21**—Results file (RESULTS .OUT) from the demonstration, printed at 16.67 characters per inch, 80 lines per page (con.)



LISA Version 2.00  
EXAMPLE DATA SET

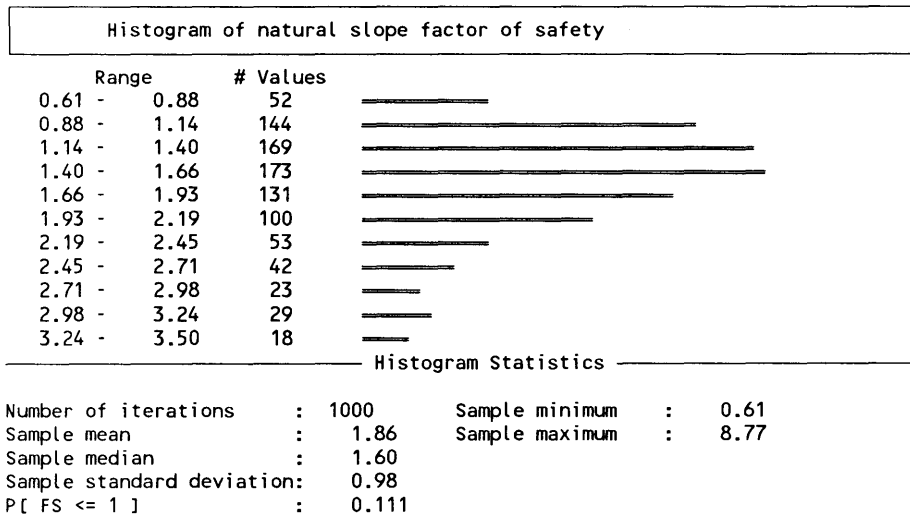


Figure 3.21—(con.)

Level One Stability Analysis  
LISA Version 2.00

=====

ID: EXAMPLE DATA SET

```

User name           C.Hammond
Time of simulation  05-22-1991 09:16:52
Map unit           DEMO.MPU
Number of iterations 1000
Random number seed 1502678690
Probability of failure .111
  
```

soil depth	ground slope	tree surch.	root cohes.	frict. angle	soil cohes.	dry un. wt.	moist un. wt.	Dw/D	FS
11.40	97.71	14.84	25.24	21.87	157.63	103.67	19.80	0.26	0.61
9.10	68.86	18.11	19.04	20.21	112.18	101.96	17.40	0.63	0.62
8.85	84.45	10.36	15.91	21.70	153.34	103.57	13.67	0.58	0.65
10.04	80.88	10.51	43.54	24.82	157.16	104.93	17.94	0.77	0.68
8.78	97.75	19.88	55.48	21.78	154.15	103.62	16.72	0.56	0.68
8.09	84.67	11.97	18.83	21.05	171.12	103.12	16.74	0.64	0.69
8.36	82.63	14.18	37.77	26.19	127.98	105.45	18.48	0.75	0.69
9.42	87.18	19.41	19.73	27.10	134.08	105.83	16.27	0.52	0.70
7.95	79.17	16.89	32.98	22.51	161.80	103.99	16.16	0.81	0.71
11.55	81.45	19.37	43.81	28.22	170.69	106.38	18.29	0.72	0.72
8.53	85.92	19.30	29.93	24.65	181.27	104.87	15.96	0.71	0.74
6.33	76.92	14.46	26.34	21.95	134.58	103.71	17.87	0.76	0.75
9.14	92.88	16.84	55.86	22.52	176.54	104.00	16.04	0.49	0.75
8.28	86.22	19.57	40.66	29.21	150.09	107.11	19.11	0.81	0.75
10.24	68.44	17.93	54.77	22.69	145.53	104.08	16.42	0.62	0.76
7.49	89.32	17.25	16.57	29.29	140.29	107.20	16.45	0.65	0.76
8.58	63.12	18.08	51.62	21.82	134.40	103.64	17.20	0.78	0.77
6.58	89.92	16.58	40.92	20.41	172.27	102.39	18.41	0.73	0.78
7.98	91.76	16.37	66.79	23.23	159.35	104.31	20.13	0.57	0.79
7.89	89.42	12.28	20.61	26.61	161.81	105.62	14.18	0.52	0.79
6.45	88.72	15.48	35.89	29.40	119.73	107.33	19.41	0.73	0.79
10.00	85.73	18.84	23.33	27.97	173.54	106.24	18.00	0.46	0.79
9.34	85.84	11.01	63.18	25.44	166.10	105.16	18.45	0.54	0.80
7.81	95.99	19.87	32.51	22.11	185.29	103.79	15.47	0.37	0.80
6.12	93.03	15.42	17.64	20.98	152.00	103.06	15.12	0.33	0.80
8.47	84.56	19.11	36.60	29.80	144.26	108.10	18.93	0.64	0.80
6.64	75.41	17.69	20.81	22.94	136.26	104.19	19.17	0.50	0.81
8.12	62.80	16.70	11.53	20.54	114.45	102.59	16.17	0.22	0.82
5.89	76.76	10.34	24.96	24.07	129.63	104.65	18.50	0.66	0.82
6.96	96.74	10.37	29.17	25.29	175.03	105.11	18.91	0.51	0.83
10.33	82.17	14.94	57.12	29.50	158.86	107.46	18.06	0.56	0.83
9.84	87.43	15.32	76.46	29.92	166.98	108.60	18.89	0.66	0.83
9.11	73.49	12.05	98.46	20.02	151.68	100.77	18.67	0.52	0.84
8.06	84.28	17.91	62.31	26.55	142.47	105.60	20.26	0.56	0.84
10.95	52.76	12.41	32.30	22.07	164.35	103.78	18.33	0.72	0.84
11.04	63.06	13.13	59.87	25.82	173.25	105.31	19.43	0.77	0.84
11.27	64.05	19.00	18.51	26.52	155.19	105.59	18.41	0.53	0.84
6.52	88.49	17.74	23.71	29.63	143.10	107.69	22.05	0.63	0.85
7.66	69.03	13.52	46.87	20.08	135.73	101.41	19.69	0.35	0.85
9.15	74.33	12.67	90.81	26.86	149.63	105.72	17.81	0.77	0.85
10.31	69.51	10.67	10.47	26.51	179.72	105.58	17.68	0.49	0.86
9.88	53.43	17.39	31.20	21.13	138.82	103.18	20.79	0.55	0.86
5.32	62.73	14.50	15.63	21.91	117.15	103.69	18.01	0.70	0.86
6.22	73.68	18.76	29.08	23.02	142.03	104.22	21.79	0.59	0.86
8.35	76.13	18.99	43.81	26.02	147.97	105.39	20.44	0.48	0.86

Figure 3.22—A portion of the simulated data file (SIMULATE.OUT) from the demonstration.

# CHAPTER 4 — DLISA EXECUTION INSTRUCTIONS

## 4.1 Introduction

The deterministic slope stability program DLISA can solve the infinite slope equation for:

- soil depth
- surface slope
- root cohesion
- groundwater height
- friction angle
- soil cohesion
- factor of safety

If you supply a single value for each of the other variables, DLISA will return one value for the solution variable, along with the associated dry, moist, and saturated unit weights; saturated moisture content; and moisture content of the soil above the groundwater surface. Alternatively, you may give a range of values for any one variable and a single value for the rest, and DLISA will display a table of results. The automatic calculation of several results is useful in performing sensitivity analyses and back-analyses. Appendix C gives the equations used for each of the solution variables.

Figure 4.1 illustrates the use of DLISA to calculate combinations of  $C'_s$  and  $\phi'$  which yield a factor of safety of 1.00. Figure 4.2 shows an output file illustrating solution of groundwater heights in order to find the critical groundwater height that gives a factor of safety of 1.00. These types of back-analyses performed on the estimated prefailure conditions of existing failures can aid in selecting ranges of values to use in LISA.

## 4.2 Installation

DLISA is an executable program compiled with the Microsoft QUICKBASIC compiler for microcomputers running the MS-DOS operating system. Although DLISA is supplied with LISA, it is a separate, stand-alone program. One file, **DLISA.EXE**, is required for running DLISA; it may be placed on any available subdirectory on any disk. DLISA does not need any special installation and does not read or write any data files. The optional output report may be written to disk or printed directly. DLISA uses EGA-resolution graphics if it is available, but graphics capability is not necessary. A math coprocessor is not required. DLISA uses the DOS environment variable **DLPRINTER** to tell it whether to include the output plot in the printed or filed report.

## 4.3 Starting DLISA

To start DLISA, change to the drive and subdirectory that contains the DLISA program and, at the DOS prompt, type **DLISA** . As with LISA, if the DOS **PATH** includes the path to the drive and subdirectory in which DLISA is stored, then you may start DLISA from any subdirectory on your system. After a moment, the DLISA title screen will be displayed; press any key to proceed to the **DATA ENTRY** screen. You may bypass the title screen by including an argument on the command line when you start DLISA; the argument can be any string of characters that DOS won't misinterpret (as file redirection commands, for example).

DETERMINISTIC LEVEL I STABILITY ANALYSIS

Infinite Slope Equation

```

Soil depth (ft)           7.00
Surface slope (%)         55.00
Tree surcharge (psf)     15.00
Root cohesion (psf)      40.00
VARY  Groundwater height (ft)  0.00 To 7.00 By 0.70
Friction angle (deg)     32.00
Soil cohesion (psf)      50.00
Dry unit weight (pcf)    105.00
Moisture content (%)     20.00
Specific gravity          2.65
SOLVE FOR  Factor of safety
    
```

Groundwater ratio (ft)	Factor of safety	Dry unit wt. (pcf)	Moist unit wt. (pcf)	Saturated unit wt. (pcf)	Saturated moist. cont. (pcf)	Moisture content (%)
0.00	1.37	105.00	126.00	127.78	21.69	20.00
0.70	1.32					
1.40	1.26					
2.10	1.21					
2.80	1.15					
3.50	1.10					
4.20	1.04					
4.90	0.99					
5.60	0.93					
6.30	0.88					
7.00	0.82					

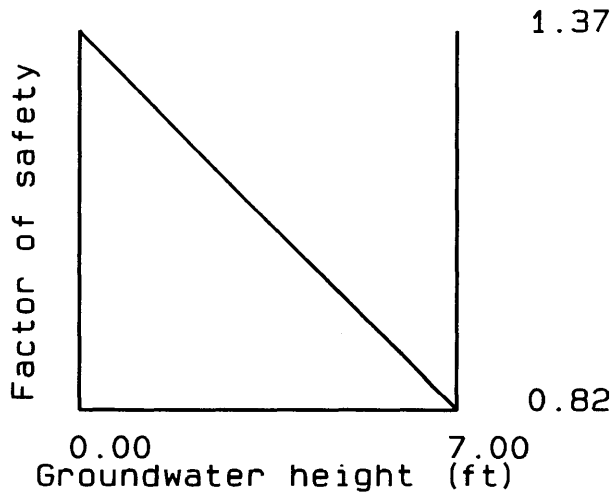


Figure 4.1—Calculation of critical combinations of  $C'_s$  and  $\phi'$  for the prefailure conditions of an existing failure.

To print an X-Y plot of the solutions, you must use a LaserJet III or any other printer which understands Hewlett Packard's HP-GL/2 language, and you must tell DLISA that you are using such a printer by defining a DOS environment variable DLPRINTER. To do so, type SET DLPRINTER=HPLJ3 at the DOS prompt before starting DLISA(see section 4.6). Similarly, you can change the colors that DLISA uses on screen by defining the DOS environment variable DLCOLOR. The color of the six screen objects given in the following table may be specified. The syntax is SET DLCOLOR= $n_1/n_2/n_3/n_4/n_5/n_6$  where the  $n_i$  are integers between 1 and 15 representing the color to use, and  $i$  is the number for the screen element in the table.

DETERMINISTIC LEVEL I STABILITY ANALYSIS

Infinite Slope Equation

```

Soil depth (ft)          5.00
Surface slope (%)        75.00
Tree surcharge (psf)    15.00
Root cohesion (psf)     40.00
Groundwater height (ft) 3.00
VARY                      Friction angle (deg) 30.00 To 40.00 By 1.00
SOLVE FOR                Soil cohesion (psf)
Dry unit weight (pcf)    105.00
Moisture content (%)     20.00
Specific gravity         2.65
Factor of safety         1.00
    
```

Friction angle (deg)	Soil cohesion (psf)	Dry unit wt. (pcf)	Moist unit wt. (pcf)	Saturated unit wt. (pcf)	Saturated moist. cont. (pcf)	Moisture content (%)
30.00	101.03	105.00	126.00	127.78	21.69	20.00
31.00	94.06					
32.00	86.95					
33.00	79.67					
34.00	72.23					
35.00	64.61					
36.00	56.81					
37.00	48.80					
38.00	40.58					
39.00	32.14					
40.00	23.45					

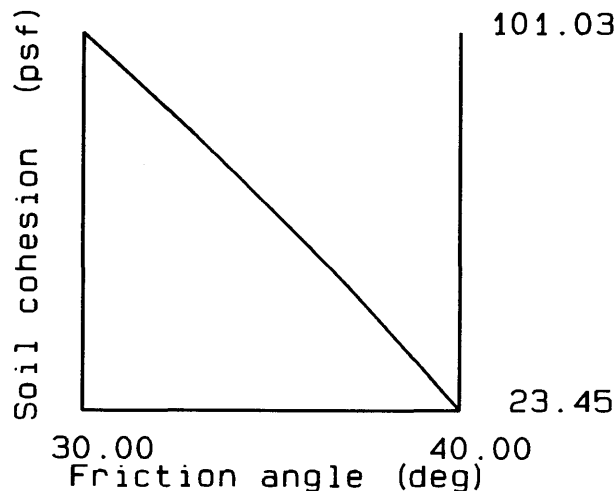


Figure 4.2—DLISA output file illustrating solution for the critical groundwater height to give a factor of safety of 1.00

<i>i</i>	Screen object	<i>i</i>	Screen object
1	menu text	4	X-Y plot axis titles
2	report heading	5	X-Y plot axis labels
3	report body	6	X-Y plot axes

The colors represented by the integers 1 to 15 will vary somewhat among monitors and graphics cards. Any  $n_i$  may be omitted, leaving the color unchanged for that object. Thus, you would type `SET DLCOLOR=12//3` at the DOS prompt to have DLISA use color 12 (red) for menu text and color 3 (cyan) for the report body.

## 4.4 Data Entry

All of the variables in the infinite slope equation are listed in the DATA ENTRY screen. You may move the highlight bar freely among the variables (using the space bar and cursor-control keys) and give them values in any order. With the name of the desired variable highlighted, you may press

- ENTER** to specify a single value
- V** to specify a range of values
- S** to specify the solution variable

After you press **ENTER** or **V**, you will be asked to enter a single value or range of values for the variable, using the standard LISA method. If you already have a variable marked as *varying* (or one to *solve for*), and then you select **V** (or **S**) for another variable, the previously marked variable will revert to a single value. To clear the current problem so that all variables are undeclared, press **C**.

You may load a demonstration problem for learning how DLISA works by pressing **D**. *Note that the values used in the demonstration problem are not recommended for any particular purpose other than becoming familiar with the operation of the program.*

A one-line menu

ESC) Exit	ENTER) Constant	V) Vary	S) Solve for	F1) Execute	C) Clear
-----------	-----------------	---------	--------------	-------------	----------

is displayed on the bottom line of the screen. The menu will not show the **S) Solve for** option when dry unit weight, moisture content, specific gravity, or tree surcharge is highlighted because DLISA cannot solve for these variables.

### ERROR MESSAGES

Cannot solve for Dry unit weight Press any key to continue
---

Cannot solve for Moisture content Press any key to continue
--

Cannot solve for Specific gravity Press any key to continue
--

Cannot solve for Tree surcharge Press any key to continue
--

DLISA cannot solve the infinite slope equation for these four variables.

## 4.5 Entering Values

To specify a single value for a variable, highlight that variable's name and press **ENTER**. If that variable currently has a value, DLISA will display it in an input field. You may use the displayed value by pressing **ENTER** or **SPACE**, edit it by

pressing the backspace key, or replace it by pressing a numeric key. Pressing **[ESC]** cancels the request to specify a single value.

To specify a range of values for a variable, highlight the variable's name, press **[V]**, and enter the minimum and maximum value for the variable. DLISA solves the infinite slope equation for 11 values of the variable equally spaced between the minimum and maximum specified.

Ground surface slope may be specified either in degrees or as a slope percentage. To enter slope in degrees, type the value followed by **[D]**. To enter slope as a percentage, type the value followed by **[Z]**. If you type a value and press **[ENTER]** or **[SPACE]**, DLISA will use degrees or percentage slope as was used previously. If you are solving for surface slope and the units displayed for surface slope are not the units you want, set the correct unit by entering a single value for surface slope, and then set surface slope as the solution variable.

Similarly, groundwater may be specified as a groundwater-soil depth ratio ( $D_w/D$ ) or as a groundwater height ( $D_w$ ). To enter a groundwater-soil depth ratio, type the value followed by **[R]**. To enter a groundwater height, type the value followed by **[']** (the apostrophe key). Use caution in specifying groundwater as a height when soil depth is allowed to vary.

The only error checking done as values are entered is to ensure that the range given for a variable is proper; all other error checking is deferred until you press **[F]** to tell DLISA to solve the specified problem (see section 4.6).

## ERROR MESSAGES

Maximum must be greater than minimum.

Press any key to continue

This message is displayed when the value entered for the minimum of a range is larger than or equal to the value entered for the maximum.

## 4.6 Execution

When you are satisfied with the problem as specified on the DATA ENTRY screen, press **[F]**. You must have one variable marked for solution, and all variables must be declared. If either of these conditions is not met when **[F]** is pressed, an error message will be displayed.

If a solution was found for the problem, DLISA will display a table of results, including values for moist unit weight, saturated unit weight, and moisture content. If more than one solution has been found and DLISA recognizes that your computer is capable of displaying EGA-resolution graphics, it also will draw a small plot of the results. This plot is useful for observing whether there is a positive or negative, and a linear or nonlinear relationship between the  $X$  variable and the  $Y$  variable. The slope of the line does not indicate the sensitivity of the  $Y$  variable to the  $X$  variable, because the maximum and minimum values of each variable are always placed at the extremes of the axis; thus, even a tiny change in one with respect to the other can result in a line with a 45-degree slope.

After the results are shown, you may press **[P]** to print the results, **[S]** to save the results to disk, or any other key to return to the DATA ENTRY screen. When you press **[S]**, you will be asked for file name. Enter any valid DOS filename, or press **[ESC]** to cancel the request. The  $X$ - $Y$  plot of the solutions will be printed

and saved in the output file only if the DOS environment variable **DLPRINTER** has the value **HPLJ3** (as explained in section 4.3). The plot will consist of printer instructions in the HP-GL/2 language.

## ERROR MESSAGES

**variable not specified!**  
**Press any key to continue**

This message will be displayed if a variable has neither been declared as having a single value or a range of values, nor specified as the solution variable. The first undeclared variable (in the order in which they are displayed on the screen) will be named.

**You must solve for one variable.**  
**Press any key to continue**

This message is displayed if you have not specified a variable for which to solve.

**Groundwater ht. greater than soil depth**  
**Press any key to continue**

This message is displayed if the maximum groundwater height value specified for a range is greater than the single soil depth value, or the single groundwater height value is greater than either the single soil depth value or the minimum soil depth specified for a range.

**Groundwater ratio greater one**  
**Press any key to continue**

This message is displayed if you have entered a value for groundwater-soil depth ratio that is greater than 1.00.

**Printer needs attention. Fix problem, or <ESC> to cancel.**

This message is displayed when you ask to print the results, but the printer is turned off, is off-line, is out of paper, or is not connected to the computer. As soon as the problem is fixed, the results will be printed. If you cannot or do not want to solve the problem, you may press **[ESC]** to cancel the print request. If you have a print spooler installed, the print request may be executed normally without an error message even when the printer is off-line; the hard copy will be produced when the printer is turned on-line or activated by your local procedures.

### 4.7 Back-calculation Error

DLISA cannot find a solution for every possible combination of input values. Some problems lead to a solution with a negative value, and others lead to a solution with a value of infinity, neither of which DLISA will accept. Other problems, specifically those problems for which surface slope is to be solved, have no

solution because the curve of the relationship between surface slope and any of the other variables can be U-shaped or  $\cap$ -shaped, and no solution can be found for values below the minimum or above the maximum. DLISA uses an iterative algorithm (as given in appendix C) to find a value for surface slope, and it returns a value for the flatter of the two surfaces that would solve the problem.

Figure 4.3 shows a run in which DLISA could find no solutions for soil cohesion when friction angle is greater than  $34^\circ$  and factor of safety is 1.00. For this set of input values, the factor of safety will be greater than 1.00 when the friction angle is greater than  $34^\circ$ , even when there is no soil cohesion. Thus, DLISA has been asked to solve for a combination of soil cohesion, friction angle, and factor of safety values that cannot physically exist.

#### WARNING MESSAGES

**No solution found.  
Press any key to continue**

This message is displayed if no solution could be found for the specified problem.

**No solution found  
for *n* values.**

This message is displayed if DLISA could find at least one solution to the problem, but could not find all of the solutions. The solutions that could be found will be displayed.

#### 4.8 Leaving DLISA

You leave DLISA by pressing **ESC** from the DATA ENTRY screen. You will be asked to verify your request by the message

**ESC) Confirm exit      any other key) remain in DLISA**

Press **ESC** again to return to DOS or any other key to continue running DLISA.

DETERMINISTIC LEVEL I STABILITY ANALYSIS

Infinite Slope Equation

	Soil depth (ft)	7.00			
	Surface slope (%)	65.00			
	Tree surcharge (psf)	15.00			
	Root cohesion (psf)	40.00			
	Groundwater height (ft)	2.00			
VARY	Friction angle (deg)	30.00	To	40.00	By 1.00
SOLVE FOR	Soil cohesion (psf)				
	Dry unit weight (pcf)	105.00			
	Moisture content (%)	20.00			
	Specific gravity	2.65			
	Factor of safety	1.00			

Friction angle (deg)	Soil cohesion (psf)	Dry unit wt. (pcf)	Moist unit wt. (pcf)	Saturated unit wt. (pcf)	Saturated moist. cont. (pcf)	Moisture content (%)
30.00	56.65	105.00	126.00	127.78	21.69	20.00
31.00	43.82					
32.00	30.73					
33.00	17.35					
34.00	3.66					

No solution found for 6 values.

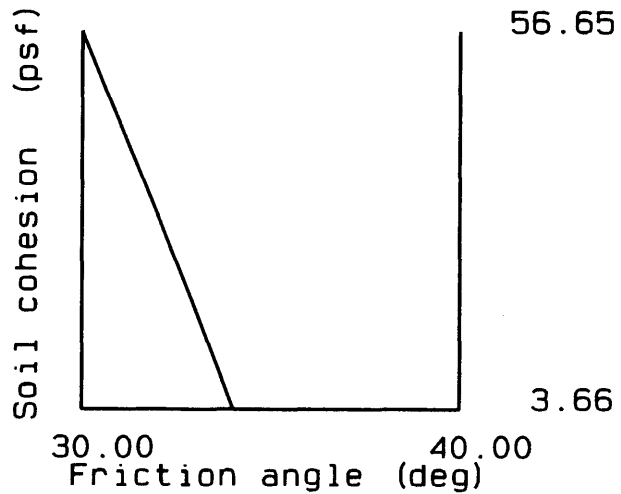


Figure 4.3—DLISA cannot find a solution to this set of values if  $\phi'$  is greater than about 34 degrees without soil cohesion becoming negative.

## REFERENCE

Petzold, C. 1986. Programming/Utilities column. PC Magazine. March 25: 253-267.

## APPENDIX A — DOWNLOADING FROM THE DG

LISA can be downloaded from the Forest Service Data General computer network to your PC. Once you get it onto your PC, you will have to unarchive it.

### Transfer LISA to Your DG

The procedure for retrieving LISA varies depending upon which release of IS is operating on the DG computer at your end. To transfer (RIS) a copy of LISA from the Forest Service computer at Moscow, ID, to the Forest Service computer at your site, follow the appropriate set of steps given below.

#### IS Versions Prior to 6.42

- Log onto the DG and go to IS.
- Find an IS drawer and folder to hold LISA temporarily on the DG system. LISA200.EXE is 217,126 bytes (2587 blocks) long.
- From the INFORMATION SYSTEM main menu, select 3--Utilities.
- Select 6--Retrieval and DCC Access.
- Select 1--Retrieval.
- Fill in the IS RETRIEVAL UTILITY screen as follows:

```
LOCATION OF FILE TO BE RETRIEVED
HOST NAME:  S22L04A
LEVEL (1. PUBLIC, 2. STAFF):  2
STAFF NAME:  4702
DRAWER NAME:  REMOTE
FOLDER NAME:  LISA
FILE NAME:  LISA200.EXE
```

Then fill in the appropriate information for the file destination, giving the level, drawer, and folder you selected for LISA200. This file is large, so you might want to delay transfer until evening to save money.

- CANCEL/EXIT out of the IS RETRIEVAL UTILITY screen to the IS main menu, and then CANCEL/EXIT out of CEO. You should get a DG mail message from "information system" or the equivalent on your system when the file has been transferred.

#### IS Version 6.42 or Later

- Log onto the DG and go to IS.
- Find an IS drawer and folder to hold LISA temporarily on the DG system. LISA200.EXE is 217,126 bytes (2587 blocks) long.
- From the INFORMATION SYSTEM main menu, select 3--Utilities.
- Select 6--Transfer (Information transfer and DCC Access).
- Select 1--Info transfer.
- Fill in INFORMATION TRANSFER UTILITY screen 1 as follows:

TRANSFER TYPE (1. SEND, 2. RETRIEVE): 2

LOCAL INFORMATION STRUCTURE

LEVEL (1. PUBLIC, 2. STAFF): *as appropriate*

DRAWER NAME: *drawer on your system*

FOLDER NAME: *folder on your system*

FILE NAME: LISA200.EXE

LOCAL TRANSFER ACTION (Y/N)? N

- Fill in INFORMATION TRANSFER UTILITY screen 2 as follows:

HOST NAME: S22L04A

REMOTE INFORMATION STRUCTURE

LEVEL (1. PUBLIC, 2. STAFF): 2

STAFF NAME: 4702

DRAWER NAME: REMOTE

FOLDER NAME: LISA

FILE NAME: LISA200.EXE

REMOTE INFORMATION (Y/N)? N

Answer the two remaining questions, “Do YOU WANT TO OMIT CEO MAIL NOTIFICATION (Y/N)?” and “Do YOU WANT TO SUBMIT TRANSFER REQUEST NOW (Y/N)?”, as you want. This file is large, so you might want to delay transfer until evening to save money.

- CANCEL/EXIT out to the INFO SYSTEM main menu, and then CANCEL/EXIT out of CEO. You should get a DG mail message from “information system” or the equivalent on your system when the file has been transferred.

### Download LISA from IS to a PC

We recommend putting the LISA200 archive file on a floppy disk so that you will have a backup copy for future use. You will need a formatted disk with about 300,000 bytes or more available. The method for downloading LISA from the DG to a PC is as follows:

- Log onto the Data General from a personal computer using CEO-CONNECTION software, and go to IS.
- From the IS main menu, select 1--Access Information and navigate to the IS drawer and folder containing file LISA200.EXE.
- From the COMMAND: prompt, press **CTRL**-**SPACE** to return to the CEO-CONNECTION main menu.
- Select 5--Retrieve a file and enter the HOST PATHNAME and MS-DOS PATHNAME for the LISA200 file. For example,

HOST PATHNAME: :STAFF:xxx:drawer:folder:LISA200.EXE

MS-DOS PATHNAME: A:LISA200.EXE

- Select 3--Terminal, to return to IS. If the DG does not respond, press **CTRL**-**D** three times.
- Delete LISA200.EXE from IS.
- Log off of the DG and leave CEO-CONNECTION.

## APPENDIX B — USING THE SOFTWARE REFERENCE CENTER

Information about the slope stability computer programs available from this Research Work Unit will be stored in the Software Reference Center (SRC) located on the Forest Service's Washington Office computer. The information stored there will include a description of the program, the date and revision number of the current version, the name and DG address of whom to contact for more information, and instructions for retrieving the latest version of the program. The computer programs themselves will be stored on, and can be retrieved from, the Data General computer at the Forestry Sciences Laboratory in Moscow, ID, as described in appendix A.

The Software Reference Center can be accessed by the following steps:

- While you are in CEO on the Data General, press **FS** (the CEO interrupt key).
- Select **7--User Applications** from the INTERRUPT menu.
- Type **INFO\_CENTER** after the **Application you want to run** prompt on the **SELECT AN APPLICATION** menu. (Note that some systems may use a different application name for the **INFORMATION CENTER ACCESS** menu. To find out what it is called on your system, press **shift-F2** to obtain a list of available applications.)
- Select **1--Standard** from the **SELECT AN APPLICATION** menu.
- Select **1--SRC** from the **FOREST SERVICE INFORMATION CENTERS** menu. You should get a message on the bottom line of your terminal saying that your system is **Calling Information Center...**, followed by a list of the folders in the SRC drawer. Be patient, responses are slow over the telephone lines.
- Select **1--List Documents** and folder **Engineering**<sup>1</sup> and the system will display a list of documents including those from this Research Work Unit matching the names of its slope stability programs **LISA**, **DLISA**, **SARA**, **DSARA**, and **XSTABL**. View or mail to yourself the document with the name of the program you are interested in.
- Back out of the SRC by pressing the **Cancel/Exit** key several times. You will pass through the **DOCUMENT LIST**, the **FOLDER LIST**, and the **FILING FUNCTIONS** menu, to the **MAIN** menu on the Washington Office computer. Press the **Cancel/Exit** key once more and answer **Y** to the **Do you want to exit (Y/N)?** question to log off the Washington computer and return to your regular CEO session.

---

<sup>1</sup>We hope to be able to create a folder called **Geotechnical Engineering**. If that folder is listed, select it, instead.

## APPENDIX C — DLISA EQUATIONS

### Factor of Safety

$$FS = \frac{C + [q_0 + \gamma d + (\gamma_{\text{sat}} - \gamma_w - \gamma)D_w] \cos^2 \alpha \tan \phi}{[q_0 + \gamma d + (\gamma_{\text{sat}} - \gamma)D_w] \cos \alpha \sin \alpha}$$

### Total Cohesion

$$C = [q_0 + \gamma d + (\gamma_{\text{sat}} - \gamma)D_w] \cos \alpha \sin \alpha FS - [q_0 + \gamma d + (\gamma_{\text{sat}} - \gamma_w - \gamma)D_w] \cos^2 \alpha \tan \phi$$

### Friction Angle

$$\phi = \tan^{-1} \left\{ \frac{[q_0 + \gamma d + (\gamma_{\text{sat}} - \gamma)D_w] \cos \alpha \sin \alpha FS - C}{[q_0 + \gamma d + (\gamma_{\text{sat}} - \gamma_w - \gamma)D_w] \cos^2 \alpha} \right\}$$

### Soil Depth

$$d = \frac{\frac{C}{\cos \alpha} + [q_0 + (\gamma_{\text{sat}} - \gamma_w - \gamma)D_w] \cos \alpha \tan \phi - [q_0 + (\gamma_{\text{sat}} - \gamma)D_w] \sin \alpha FS}{\gamma \sin \alpha FS - \gamma \cos \alpha \tan \phi}$$

### Groundwater Height

$$D_w = \frac{(q_0 + \gamma d)(\sin \alpha FS - \cos \alpha \tan \phi) - \frac{C}{\cos \alpha}}{(\gamma_{\text{sat}} - \gamma_w - \gamma) \cos \alpha \tan \phi - (\gamma_{\text{sat}} - \gamma) \sin \alpha FS}$$

### Ground Surface Slope

$$\begin{aligned} &\alpha \leftarrow 0 \\ &D_o \\ &\alpha' \leftarrow \alpha \\ &\alpha \leftarrow \sin^{-1} \left\{ \frac{C + [q_0 + \gamma d + (\gamma_{\text{sat}} - \gamma_w - \gamma)D_w] \cos^2 \alpha' \tan \phi}{[q_0 + \gamma d + (\gamma_{\text{sat}} - \gamma)D_w] \cos \alpha' FS} \right\} \\ &\text{Loop until } \alpha \approx \alpha' \end{aligned}$$

### Tree Surcharge

$$q_0 = \frac{\frac{C}{\cos \alpha} + [\gamma d + (\gamma_{\text{sat}} - \gamma_w - \gamma)D_w] \cos \alpha \tan \phi - [\gamma d + (\gamma_{\text{sat}} - \gamma)D_w] \sin \alpha FS}{\sin \alpha FS - \cos \alpha \tan \phi}$$

## APPENDIX D — ERROR AND WARNING MESSAGES

### LISA

# of classes must be between 1 and 10	152
% must be between 0 and 100	152
A name is required	139
About to exit EDIT NATURAL SLOPE DATA...Save changes?	146
Apex must not be less than minimum	150
At least 1 iteration required	162
Bad command or file name	170
Cannot display histogram of a constant or 1 value	164, 167
Friction angle will be changed to normal	152
Input run-time module path	137
Invalid directory	170
Invalid path - drive or directory does not exist	137
Make Cs bivariate also	153
Make phi bivariate also	153
Maximum must not be less than apex	150
Maximum must be greater than minimum	147, 150, 152
More than 100 map units found.	141
More than 50 <i>typedata</i> files found	142
No more than 1000 iterations allowed	162
Non-positive standard deviation	157
Not all variables have been specified	163
P must be greater than zero	150, 158
Please create a new map unit by entering a name	141
Printer needs attention. Fix...to cancel	169
Q must be greater than zero	150, 158
r must be between -1 and 1	153
Seed must be between 1 and 2,147,483,646	161
Selected parameter is a constant	156
Simulated data not saved	169
Simulating Beta <i>nnnn</i>	150, 162
Soil cohesion will be changed to normal	153
Standard deviation must be greater than zero	148, 149
Total percentage exceeds 100%	152
Total percentage less than 100%	152
Values < 0 possible (mean - 3.09s <= 0)	148, 153, 157
X is constant, can't make a scatterplot	167
Y is constant, can't make a scatterplot	167
Zero mean not allowed	149, 157
Zero standard deviation	155

## DLISA

Cannot solve for Dry unit weight 178  
Cannot solve for Moisture content 178  
Cannot solve for Specific gravity 178  
Cannot solve for Tree surcharge 178  
Dry unit weight not specified! 180  
Factor of safety not specified! 180  
Friction angle not specified! 180  
Groundwater ht. greater than soil depth 180  
Groundwater height not specified! 180  
Groundwater ratio greater than one 180  
Maximum must be greater than minimum 179  
Moisture content not specified! 180  
No solutions found 181  
No solution found for  $n$  values 181  
Printer needs attention. Fix problem, or <ESC> to cancel 180  
Root cohesion not specified! 180  
Soil cohesion not specified! 180  
Soil depth not specified! 180  
Specific gravity not specified! 180  
Surface slope not specified! 180  
Tree surcharge not specified! 180  
You must solve for one variable 180

# INDEX

# iterations prompt, 161–162

## A

ASCII characters, 161  
AUTOEXEC.BAT file, 132

## B

back-analysis, 175  
back-calculation error in DLISA, 179–181  
beta distribution, 134, 144, 150, 155, 157  
bivariate normal distribution, 134, 144, 152–153, 155, 157  
BROWSE file viewer, 132, 133, 167  
BROWSE.COM file viewer, 132, 133, 170  
BRUN45.EXE runtime library, 133, 137

## C

Choose distribution (C-V) prompt, 144  
clear current problem, 178  
color selection  
    DLISA, 176–177  
    LISA, 137–138  
    command-line switch, 175  
COMMAND.COM, 131, 133  
CONFIG.L1 (LISA configuration file), 132, 138  
constant value, 134, 147  
correlation  
    between  $C'_s$  and  $\phi'$ , 152, 166  
    between  $\phi'$  and  $\gamma$ , 165–166  
    between  $\tau$  and  $\sigma'$ , 166  
correlation coefficient ( $r$ ), 152, 153, 165, 166  
Create... .MPU? prompt, 143  
customization  
    DLISA, 175–177  
    LISA, 132–133

## D

data entry, 144–155, 178  
data files  
    deleting, 144  
    demonstration, 133, 137  
    groundwater (.HYD), 134, 142  
    location, 132, 139–140  
    material (.MTL), 134, 142  
    saving, 159  
    selecting, 144  
    site (.SIT), 134, 142  
    unselecting, 144  
date, 137, 161  
DEMO.\* files, 133, 137  
demonstration  
    data files, 133, 137  
    problem, DLISA, 178  
descriptive comment, 160  
distribution  
    beta, 134, 144, 150, 155, 157  
    bivariate normal, 134, 144, 152–153, 155, 157

    histogram, 134, 144, 151–152, 155, 157  
    lognormal, 134, 144, 149, 155, 157  
    marginal, 152  
    modifying while plotting, 156–158  
    normal, 134, 144, 147–148, 155, 157  
    plotting shape of input, 155–156  
    triangular, 134, 144, 150, 157  
    uniform, 134, 144, 147, 157  
DLCOLOR environment variable, 176–177  
DLISA, 133, 145, 175–181  
    installation, 175  
DLISA.EXE, 133, 175  
DLPRINTER environment variable, 175, 176, 180  
DOS shell, 145, 168, 171  
downloading LISA and DLISA, 183–184

## E

effective normal stress, 166  
environment variables, 132–133, 164, 165, 170, 175, 176, 180  
equations, DLISA, 186  
error messages, 136, 187–188  
execute  
    DLISA, 179–180  
    LISA, 137  
exit  
    DLISA, 181  
    LISA, 136, 171  
    quick, 136, 171

## F

factor of safety histogram, 164  
    modifying, 164  
    saving to disk, 164  
    viewing, 164  
file viewer, 132–133, 167, 170

## G

graphics characters, IBM, 133, 164  
graphics adapter, 131, 155, 166, 179  
groundwater data files, 134, 142  
groundwater, entered as soil depth ratio or height, 179

## H

hardware  
    recommended, 131  
    required, 131  
Hewlett Packard HP-GL/2 printer language, 176, 180  
histogram  
    distribution, 134, 144, 151–152, 155, 157  
    factor of safety, 164  
    variable, 159, 164–167  
HP-GL/2 printer language, 176, 180

## I

ID prompt, 160  
infinite slope equation, 175, 178, 179

installation  
DLISA, 175  
LISA, 131–133  
iterations, number of, 161–162  
iterative operation of LISA, 159, 162

## L

linear dependence, 165  
LISA200, 131–132, 133  
LISA.BAT, 133, 137  
LISAGRAPH environment variable, 132, 133, 164, 165  
LISALIST environment variable, 132–133, 170  
LISARA.EXE, 133, 137  
lognormal distribution, 134, 144, 149, 155, 157

## M

map unit, 132, 134  
creating, 143  
deleting, 144  
selecting, 141–142  
Map unit to analyze prompt, 141, 143  
material data files, 134, 142  
math coprocessor, 131, 175  
MODE CO80, 155  
mode, change in by varying parameter values, 157  
modifying distributions while plotting, 157–158  
monochrome monitor, 138, 155  
.MPU subdirectories, 132, 134, 139–140

## N

negative values from bivariate normal, 152, 153  
normal distribution, 134, 144, 147–148, 155, 157  
normal stress, effective, 166  
number of iterations, 161–162

## O

output files, viewing, saving, and printing, 167–170  
Overwrite File (y/N) prompt, 159

## P

PATH, 132, 137, 175  
path to map units, 139–140  
PKZIP file compression program, 131  
plot of results, 176, 179–180  
plotting shape of input distributions, 155–156  
Print prompt, 168  
print spooler, 169, 180  
printer, 131, 169, 176  
printing output files, 167–170, 179–180  
probability of failure, 162

## Q

quick exit, 136, 171  
QUICK.\* files, 136, 159, 171

## R

random number seed, 137, 152, 161

Random seed prompt, 161  
random variation, 161  
repeatability  
of results, 161  
of sampling, 161  
RESULTS.OUT output file, 132, 160, 161, 167  
Results  
printing DLISA, 179  
saving DLISA, 179  
saving LISA, 136

## S

save  
data files, 159  
output files, 167  
simulated values, 159–160  
Save prompt, 168, 170  
Save simulated values prompt, 160  
scatter plot, 131, 159, 164–167  
SCATTER PLOT AND HISTOGRAM screen, colors in, 165  
screen structure, 134  
sensitivity analysis, using DLISA for, 175, 179  
sensitivity of factor of safety to input variables, 166  
shear strength ( $\tau$ ), 166  
shell, 145, 167, 171  
SIMULATE.OUT output file, 132, 159–160, 161, 162, 167  
simulated values, saving, 159–160  
simulation  
starting, 162  
stopping, 162  
site data files, 134, 142  
skewness, change in by changing parameter values, 157  
Software Reference Center, 185  
Solve for prompt, 178  
specific gravity, 134  
surface slope, entered as degrees or percent, 179  
system date and time, 137, 161

## T

time, 137, 161  
triangular distribution, 134, 144, 150, 157

## U

uniform distribution, 134, 144, 147, 157  
unit weights displayed by DLISA, 175  
User name, 138–139  
User name prompt, 138–139

## V

Vary prompt, 178  
View prompt, 167, 170  
viewing output files, 171–174

## W

warning messages, 136, 187–188  
wildcard (DOS filename), 141, 142  
WINDOWS 3.0, 132, 166

---

Hammond, Carol; Hall, David; Miller, Stanley; Swetik, Paul. 1992. Level I Stability Analysis (LISA) documentation for version 2.0. Gen. Tech. Rep. INT-285. Ogden, UT: U. S. Department of Agriculture, Forest Service, Intermountain Research Station. 190 p.

LISA uses Monte Carlo simulation of the infinite slope equation to estimate a probability of slope failure for use in relative stability hazard assessment of natural slopes or landforms. The manual discusses probabilistic concepts, the mathematical basis of the model, suggestions for estimating input probability distributions, and an example application, as well as instructions for program operation.

---

**KEYWORDS:** probabilistic stability analysis, landslide hazard analysis, Monte Carlo simulation, infinite slope equation, probability of failure, probabilistic computer model

---





The Intermountain Research Station provides scientific knowledge and technology to improve management, protection, and use of the forests and rangelands of the Intermountain West. Research is designed to meet the needs of National Forest managers, Federal and State agencies, industry, academic institutions, public and private organizations, and individuals. Results of research are made available through publications, symposia, workshops, training sessions, and personal contacts.

The Intermountain Research Station territory includes Montana, Idaho, Utah, Nevada, and western Wyoming. Eighty-five percent of the lands in the Station area, about 231 million acres, are classified as forest or rangeland. They include grasslands, deserts, shrublands, alpine areas, and forests. They provide fiber for forest industries, minerals and fossil fuels for energy and industrial development, water for domestic and industrial consumption, forage for livestock and wildlife, and recreation opportunities for millions of visitors.

Several Station units conduct research in additional western States, or have missions that are national or international in scope.

Station laboratories are located in:

Boise, Idaho

Bozeman, Montana (in cooperation with Montana State University)

Logan, Utah (in cooperation with Utah State University)

Missoula, Montana (in cooperation with the University of Montana)

Moscow, Idaho (in cooperation with the University of Idaho)

Ogden, Utah

Provo, Utah (in cooperation with Brigham Young University)

Reno, Nevada (in cooperation with the University of Nevada)

USDA policy prohibits discrimination because of race, color, national origin, sex, age, religion, or handicapping condition. Any person who believes he or she has been discriminated against in any USDA-related activity should immediately contact the Secretary of Agriculture, Washington, DC 20250.